The naturalness criterion for supersymmetric scenarios

Sandra Robles

Supervisors: Prof. J. Alberto Casas
Prof. Jesús M. Moreno

Instituto de Física Teórica UAM-CSIC

This dissertation is submitted for the degree of
Doctor of Philosophy

June 2017

Facultad de Ciencias
Departamento de Física Teórica

Instituto de Física Teórica
IFT UAM-CSIC

The naturalness criterion for supersymmetric scenarios

Tesis doctoral presentada por

Sandra Clarisa Robles Portilla

para optar al título de Doctora en Física Teórica

Tesis doctoral dirigida por:

J. Alberto Casas y Jesús M. Moreno

Madrid, Junio de 2017

To the loving memory of my mother, who had the arduous task of raising me, supported me in all my endeavours and inherited me her love for mathematics, but unfortunately not her teaching skills.

To my father, who encouraged my curiosity for science, technology and history since a very young age, and has always challenged me to be a better person.

Declaration

I hereby declare that except where specific reference is made to the work of others, the contents of this dissertation are original and have not been submitted in whole or in part for consideration for any other degree or qualification in this, or any other university. This dissertation is my own work and contains nothing which is the outcome of work done in collaboration with others published in refs. [1–4], except as specified in the text. Additional research in the field of particle physics carried out while in candidature for the Ph.D. degree, not included in this dissertation, was published in refs. [5–8].

Sandra Robles
June 2017

Abstract

Supersymmetry (SUSY) has been considered since long ago the leading paradigm of beyond the Standard Model (SM) physics as a framework that tackles the SM hierarchy problem, provides gauge coupling unification and a well-behaved cold dark matter (DM) candidate. Nevertheless, current experimental searches for new physics seem to have cornered the minimal versions of these models in unnatural regions of their parameter space, according to the *standard* Natural SUSY scenario. With the aim of formulating a general naturalness criterion for minimal supersymmetric scenarios, we have carefully re-examined the *standard* fine-tuning measure, which only deals with the cancellations needed to obtain the electroweak symmetry breaking (EWSB) scale, introducing several improvements such as the mixing of the fine-tuning conditions and the dependence on the low and high-energy (HE) scales. Furthermore, we have outlined a method that allow to straightforwardly derive naturalness bounds on the initial parameters and mass spectrum of any minimal supersymmetric standard model (MSSM) defined at any HE scale. We have applied this method to specific scenarios to compute a complete set of naturalness bounds. and also employed it to find the most natural gauge-mediated SUSY breaking model. Contrary to what was expected, we show that Natural SUSY, in general, does not demand light stops. The most stringent upper bound from naturalness is that of the gluino mass, which typically sets the level of fine-tuning, but strongly depends on the HE scale. The most robust result of Natural SUSY is by far that Higgsinos should be rather light. Besides, we have investigated other potential sources of fine cancellations in the MSSM, that if present, must be combined with that of the EWSB scale. The most important being the tuning to obtain the experimental Higgs mass and that required to reproduce the correct DM relic abundance. We have quantified them with p-value like measures that allow us to multiplicatively combine them with the electroweak (EW) fine-tuning. Regarding DM, we have considered the lightest neutralino as the DM particle and explored the various possibilities for its mass, composition and interactions that could give rise to accurate arrangements of the initial parameters to achieve the observed DM relic density. Finally, to illustrate the utility of the above stated criteria to estimate the global degree of naturalness, we have applied all of them to a specific model that features low-mass neutralinos and sleptons at low-energy. We find that these scenarios are rather unnatural when taking into account the aforementioned sources of tuning, which would have gone unnoticed, if we have only considered the EW fine-tuning.

Resumen

Durante mucho tiempo la supersimetría (SUSY) ha sido considerada el principal paradigma de los modelos de física más allá del modelo estándar (ME), como un marco de trabajo que aborda el problema de las jerarquías del ME, produce acoplos gauge unificados y proporciona un buen candidato a materia oscura fría. Sin embargo, las búsquedas actuales de nueva física parecerían haber arrinconado a las versiones mínimas de estos modelos en zonas antinaturales de su espacio de parámetros, según el escenario estándar de Natural SUSY. Con el objetivo de formular un criterio general de naturalidad para los modelos supersimétricos mínimos, hemos revisado meticulosamente la medida estándar del fine-tuning, la cual sólo se ocupa de las cancelaciones necesarias para obtener la escala de rompimiento de la simetría electrodébil. Hemos realizado varias mejoras tales como la mezcla de las condiciones del fine-tuning y las dependencias de las escalas de alta y baja energía. Es más, hemos descrito un método que permite derivar directamente límites de naturalidad sobre los parámetros iniciales y el espectro de masas de cualquier modelo estándar supersimétrico mínimo (MSSM), definido a un valor cualquiera de alta energía. Hemos aplicado este método a escenarios específicos para calcular un conjunto completo de límites. También hemos utilizado dicho método para encontrar el modelo con rompimiento de supersimetría por mediación gauge con el fine-tuning mínimo. Contrariamente a lo esperado, hemos demostrado que modelos de SUSY naturales no exigen en general stops ligeros. El límite de naturalidad más riguroso es el de la masa del gluino, el cual típicamente determina el nivel de fine-tuning, pero depende fuertemente de la escala de alta energía. El resultado más robusto de Natural SUSY es de lejos que los Higgsinos deben ser bastante ligeros. Además, hemos analizado otras fuentes potenciales de ajustes finos, que si están presentes, tienen que ser combinados con el de la escala electrodébil. Los más importantes son el requerido para obtener la masa experimental del Higgs y el necesario para reproducir la abundancia correcta de materia oscura. Hemos cuantificado estos fine-tunings con medidas basadas en el p-value, lo que permite combinarlos multiplicativamente con el de la escala electrodébil. Con respecto a la materia oscura, hemos considerado que el neutralino más ligero es la partícula de materia oscura y hemos explorado las diferentes posibilidades de masa, composición e interacciones que pueden dar lugar a delicados ajustes de los parámetros iniciales para conseguir la densidad reliquia observada. Finalmente, con el propósito de ilustrar la utilidad de los criterios antes enunciados para estimar el grado global de naturalidad, los hemos aplicado a un modelo específico que cuenta con neutralinos de baja masa y sleptones ligeros a baja energía. Encontramos que estos escenarios son bastante antinaturales, cuando consideramos las antes mencionadas fuentes de ajustes finos, lo que hubiera pasado desapercibido si solamente hubiéramos considerado el fine-tuning electrodébil.

Table of contents

List of publications

1. **Low-mass neutralino dark matter in supergravity scenarios: phenomenology and naturalness**
   Miguel Peiró and Sandra Robles
   JCAP **1705** (2017) 010 [arXiv:1612.00460]

2. **Local Quantum Thermometry using Unruh-De Witt detectors**
   Sandra Robles and Javier Rodríguez-Laguna
   J.Stat.Mech. **1703** (2017) 033105 [arXiv:1609.01154]

3. **Naturalness of MSSM dark matter**
   María Eugenia Cabrera, J. Alberto Casas, Antonio Delgado, Sandra Robles and Roberto Ruiz de Austri
   JHEP **1608** (2016) 058, [arXiv:1604.02102].

4. **Reducing the fine-tuning of gauge-mediated SUSY breaking**
   J. Alberto Casas, Jesús M. Moreno, Sandra Robles and Krzysztof Rolbiecki
   Eur. Phys. J. **C76** (2016) 450, [arXiv:1602.06892].

5. **Enhanced lines and box-shaped features in the gamma-ray spectrum from annihilating dark matter in the NMSSM**
   David G. Cerdeño, Miguel Peiró and Sandra Robles
   JCAP **1604** (2016) 011, [arXiv:1507.08974].

6. **On the importance of direct detection combined limits for spin independent and spin dependent dark matter interactions**
   Cristina Marcos, Miguel Peiró and Sandra Robles
   JCAP **1603** (2016) 019, [arXiv:1507.08625].

7. **Fits to the Fermi-LAT GeV excess with RH sneutrino dark matter: Implications for direct and indirect dark matter searches and the LHC**
   David G. Cerdeño, Miguel Peiró and Sandra Robles
   Phys. Rev. **D91** (2015) 123530, [arXiv:1501.01296].

List of figures

List of tables

Nomenclature

Greek Symbols

$\Delta^{(\mathrm{DM})}$	Fine-tuning to reproduce the DM relic density
$\Delta^{(\mathrm{EW})}$	Electroweak fine-tuning measure
$\Delta^{(m_h)}$	Fine-tuning to obtain the experimental Higgs mass
Λ_{SM}	Standard model cutoff
$\tilde{\Delta}$	Standard electroweak fine-tuning measure
$\Delta^{(\mathrm{tot})}$	Total fine-tuning

Acronyms / Abbreviations

AMSB	Anomaly-Mediated Supersymmetry Breaking
BSM	Beyond the Standard Model
CLIC	Compact Linear Collider
CMSSM	Constrained Minimal Supersymmetric Standard Model
DM	Dark matter
dSphs	Dwarf Spheroidal Galaxies
EW	Electro-Weak
EWSB	Electro-Weak Symmetry Breaking
FCNC	Flavour changing neutral currents
GMSB	Gauge-Mediated Supersymmetry Breaking
GUT	Grand Unification Theory
HE	High-energy

HL-LHC	High luminosity LHC
ILC	International Linear Collider
LAT	Large Area Telescope
LE	Low-energy
LEP	Large Electron-Positron collider
LHC	Large Hadron Collider
LH	Left-handed
LL	Leading log
LSP	Lightest Supersymmetric Particle
MCMC	Markov chain Monte Carlo
MSSM	Minimal Supersymmetric Standard Model
NMSSM	Next-to-Minimal Supersymmetric Standard Model
NP	New Physics
NUHM	Non-Universal Higgs Masses
REWSB	Radiative Electroweak Symmetry Breaking
RGE	Renormalization Group Equation
RG	Renormalization Group
RH	Right-handed
SD	Spin dependent
SI	Spin independent
SM	Standard Model
SUGRA	Supergravity
SUSY	Supersymmetry
VEV	Vacuum expectation value
WIMP	Weakly Interacting Massive Particle

Chapter 1

Introduction

The Standard Model (SM) of particle physics [9–11], the collective achievement of both, theoretical and experimental physicists, is by far a well established theory that comprises electroweak (EW) and strong interactions. Over the last fifty years, this self-consistent and predictive theory has been put it to the test, and it has successfully explained almost all experimental findings ranging from low to high energies. Furthermore, it has also precisely predicted a wide variety of phenomena. Its most recent success being the discovery of the Higgs boson at the Large Hadron Collider (LHC) [12–15]. However, we know that the SM is not the ultimate theory of Nature, since it does not include gravity, for which a high-energy (HE) description is still missing. Phenomenological reasons to extend the SM are the lack of a mechanism to provide neutrino masses and a good candidate for dark matter (DM). In view of the foregoing, the SM can be regarded as an effective theory which describes with impressive precision the phenomenology of particle physics up to energies around the TeV scale.

The SM also suffer from theoretical issues that arise from naturalness arguments such as the strong CP problem and the main concern of beyond the SM (BSM) physics, the hierarchy problem [16–21], i.e. the question of why the EW scale is so far below the reduced Planck scale $M_{\rm Pl} = (8\pi G_{\rm N})^{-1/2} = 2.4 \times 10^{18}$ GeV. A question with deep implications, as we will see below.

In the SM, the Higgs boson is the responsible for the electroweak symmetry breaking (EWSB) [22–27], which gives masses to the fermions and the heavy bosons. The Higgs field, H, is a complex doublet scalar with potential

$$V = m_{h_0}^2 |H|^2 + \lambda |H|^4 \,, \tag{1.1}$$

where m_{h_0} is the Higgs mass bare parameter and λ the Higgs quartic coupling. Since the discovery of the Higgs boson with a physical mass $m_h = 125.09$ GeV [28–30], the values of the running parameters m_{h_0} and λ are determined, $\lambda \simeq 0.13$ and $m_{h_0} \simeq 88.8$ GeV [31]. Nevertheless, without a symmetry to protect it, the Higgs mass parameter m_{h_0} is subject to receive large radiative corrections coming from new physics (NP) that we know it must exist at a scale above the SM cutoff $\Lambda_{\rm SM}$, requiring fine cancellations to keep m_{h_0} small. This is the essence of the hierarchy problem. For instance, the leading one-loop

contribution to the Higgs mass (first diagram of figure 1.1) can be approximated as

$$\delta m_{h_0}^2 \simeq -\frac{3y_t^2}{8\pi^2}\int^{\Lambda_{\rm SM}} \frac{d^4p}{p^2} \simeq -\frac{3y_t^2}{8\pi^2}\Lambda_{\rm SM}^2 \,. \tag{1.2}$$

Indeed, a more accurate expression for quadratic divergences due to the SM cutoff includes one-loop quantum corrections from top, gauge and Higgs bosons (see figure 1.1)

$$\delta m_{h_0}^2 \simeq \frac{3\Lambda_{\rm SM}^2}{16\pi^2 v^2}\left(m_h^2 + m_Z^2 + 2m_W^2 - 4m_t^2\right) \,, \tag{1.3}$$

where $v =< H >$ is the vacuum expectation value (VEV) of the Higgs field. In the same way, any new particle that directly or indirectly couples to the Higgs will also induce additional terms to $\delta m_{h_0}^2$, increasing the amount of required cancellations.

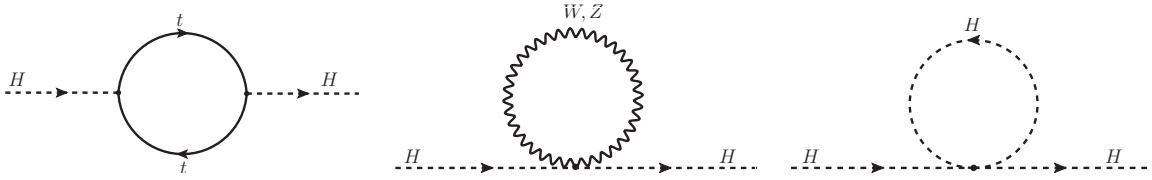

Figure 1.1: One-loop leading corrections to the Higgs mass parameter.

Another approach to interpret this is using the following fine-tuning measure [32]

$$\tilde{\Delta} = \left|\frac{\delta m_{h_0}^2}{m_{h_0}^2}\right| = \frac{2|\delta m_{h_0}^2|}{m_h^2}, \tag{1.4}$$

where the physical Higgs mass is $m_h^2 = 2|m_{h_0}^2|$. If $\Lambda_{\rm SM}$ is of the order of the grand unification scale, $M_X \simeq 2\times 10^{16}$, then using eq. (1.3) in eq. (1.4), $\tilde{\Delta} \simeq 10^{27}$, i.e. a precision of one in 10^{27} is needed in order to reproduce the smallness of m_{h_0}. In other words, if we want to avoid large cancellations and demand e.g. $\tilde{\Delta} \leq 10$, that is, we allow at most only one digit cancellation is required, we find that the scale of BSM physics is around $\Lambda \simeq 1.75$ TeV. This simple argument has been the main motivation to expect signals of new physics within the reach of the LHC and the hierarchy problem the main reason for theorists to formulate BSM models that cope with this issue.

Two kind of solutions has been proposed to solve the hierarchy problem: anthropics and dynamics. In the former, the electroweak scale is fixed by the anthropic principle, then the aforementioned fine-tuning is allowed, but a multiverse is presumed to exist (see e.g. [33]). On the other hand, dynamical solutions address this problem with new interactions beyond $\Lambda_{\rm SM}$ that deal with the quadratic divergences such as supersymmetry (SUSY) [34–41], composite Higgs models [42–47] and extra dimensions [48] or without NP at the weak scale like the recently proposed cosmological relaxation [49, 50] and clockwork [51] models.

Out of these proposals, we will focus on the SUSY framework, where the hierarchy problem is alleviated by introducing a boson-fermion symmetry that cancel the quadratic divergences in all orders

of perturbation theory, while the Higgs boson remains a fundamental particle [52–57]. It is worth emphasising that the naturalness of the EWSB scale is not the only motivation for SUSY and without a doubt not the only reason for which SUSY has been considered for many years the paradigm of BSM physics. Aside from its solid mathematical foundations, SUSY also provides for free gauge coupling unification and a well-behaved candidate for cold dark matter, the lightest supersymmetric particle (LSP) as long as DM is made of weakly interacting massive particles (WIMPs).

Despite all these distinctive features, since the discovery of the Higgs boson, the LHC has been imposing increasingly stringent bounds on the existence of new particles, challenging models of new physics, among them SUSY scenarios have been pushed back to fine-tuned regions of their parameter space, at least for the minimal models. This is owing to the fact that null results from the LHC imply superpartner masses around the TeV scale. Besides, in the minimal supersymmetric Standard Model (MSSM) to concoct a Higgs mass of 125 GeV requires a heavy SUSY spectrum, in particular large stop and gluino masses, which generally entail a rather severe fine-tuning to obtain the correct EW scale. Then, it seems we have traded one fine-tuning for another or perhaps we need to re-evaluate previous assumptions on natural SUSY scenarios.

Due to these facts and remaining SUSY a well-motivated framework for BSM physics, the ultimate aim of this dissertation is to define a naturalness criterion that could serve as a guide to explore SUSY phenomenology, been able to identify regions of the parameter space where the fine-tuning is as mild as possible in light of current and forthcoming experimental results.

To this end, we start re-examining the 'standard' Natural SUSY scenario in the context of the MSSM in chapter 2, including several improvements, such as the mixing of the fine-tuning conditions for different soft terms. In addition, we identify potential extra tunings, that if found, must be combined with that of the electroweak scale. We provide tables and plots that allow to easily evaluate the fine-tuning and the corresponding naturalness bounds for any theoretical model defined at any high-energy scale. Then, we apply the preceding result to derive a complete set of fine-tuning bounds for the unconstrained MSSM and scenarios with different correlations of the soft terms, defined at any HE scale.

In spite of their appealing features such as preventing dangerous flavour changing neutral current effects, models with gauge-mediated supersymmetry breaking (GMSB) typically present a high degree of fine-tuning. This is due to the initial absence of the top trilinear scalar couplings, mainly $A_t(HE) = 0$, which forces the stop masses to be quite large in order to generate sizeable enough radiative corrections to the Higgs mass. In chapter 3, we evaluate the tuning of the minimal GMSB model using the method developed in the previous chapter, showing that is worse than the per mil level. With the goal of finding the optimum GMSB setup (with minimal matter content), concerning the fine-tuning issue, we examine some of the existing proposals in the literature to generate $A_t(HE) \neq 0$ at one-loop and tree level. Furthermore, we propose a conceptually simplified version of the latter; which is arguably the least fine-tuned GMSB scenario. We also explore the interplay between the so-called 'little A_t^2/m^2 problem' and the EW fine-tuning.

As mentioned before, there exist experimental facts that claim for extensions of the SM. Dark matter is the leading empirical evidence for new particles beyond the SM. A wide variety of evidence at galactic,

extra-galactic and cosmological scales has been accumulated in support of its existence, since first pointed out by Fritz Zwicky in 1933 [58–73]. Nevertheless, the presence of DM has been inferred uniquely through its gravitational influence, then its particle nature remains still unknown. WIMPs are among the best motivated candidates for explaining the cold dark matter in the Universe, because they naturally have the correct thermal relic density and may be detected in several ways. In R-parity preserving SUSY models, the LSP is stable, since sparticles can only be produced or annihilate in pairs, rendering the LSP an excellent WIMP candidate. Consequently, if we aim that a given SUSY scenario accounts for the DM in the Universe, the observed DM relic density must be fulfilled, which may also entail another source of tuning.

There exists a vast literature examining the EW fine-tuning problem in supersymmetric scenarios, but little concerned with that related to the DM relic abundance, which should be combined with the former. In chapter 4, we study this problem in an, as much as possible, exhaustive and rigorous way. We have considered the MSSM framework, assuming that the LSP is the lightest neutralino, χ_1^0, and exploring the various possibilities for its mass and composition, as well as different mechanisms for neutralino annihilation in the early Universe, namely well-tempering, funnels and co-annihilation scenarios. We also discuss the statistical meaning of the fine-tuning and how it should be computed for the DM abundance, and combined with the EW fine-tuning. Our results are very robust and model-independent and favour some scenarios (like the h-funnel when $M_{\chi_1^0}$ is not too close to $m_h/2$) with respect to others (such as the pure wino case). These features should also be taken into account when investigating 'Natural SUSY' scenarios and their possible signatures at the LHC and DM detection experiments.

In order to illustrate the usefulness of the criteria to measure the potential fine-tunings of the MSSM studied in chapters 2 and 4, we apply them to a specific MSSM model in chapter 5. As mentioned above, the latest experimental results from the LHC and DM searches suggest that the parameter space allowed in supersymmetric theories is subject to strong reductions. These bounds are especially constraining for scenarios entailing light DM particles. Previous studies have shown that light neutralino DM in the MSSM, with parameters defined at the EW scale, is still viable when the low-energy spectrum of the model features light sleptons, in which case, the relic density constraint can be fulfilled. In view of this, we investigate the viability of light neutralinos as DM candidates in the MSSM, with parameters defined at the grand unification scale. First, we analyse the phenomenology of this scenario and find the configurations of the parameter space that overcome the stringent experimental constraints from colliders and DM direct and indirect experiments. Next, we investigate the naturalness of these solutions, carefully evaluating every possible tuning to lastly yield a total estimation of the fine-tuning.

Finally, a summary of the findings of the dissertation, conclusions and final remarks are presented in chapter 6.

Chapter 2

What is a Natural SUSY scenario?

The idea of 'Natural SUSY' has become very popular in the last times, especially as a framework that justifies that e.g. the stops should be light (much lighter than the other squarks), say $m_{\tilde{t}} \lesssim 600$ GeV. This is an attractive scenario since it gives theoretical support to searches for light stops and other particles at the LHC, a hot subject from the theoretical and the experimental points of view.

In a few words, the idea is to lie in a region of the MSSM parameter space where the electroweak symmetry breaking is not (or not too much) fine-tuned. This is reasonable since, as usually argued, the main phenomenological virtue of supersymmetry (SUSY) is precisely to avoid the huge fine-tuning associated with the hierarchy problem.

Then, the main argument is in brief the following: 'Stops produce the main radiative contributions to the Higgs potential, in particular to the Higgs mass bare parameter $m^2_{h_0}$. To avoid fine-tunings, these contributions should be reasonably small, not much larger than $m^2_{h_0}$ itself. Since they are proportional to the stop masses, the latter cannot be too large'. Other supersymmetric particles, like gluinos, are also constrained by the same reason; in particular the gluino mass is bounded from above due to its important contribution to the running of the stop masses, which implies a significant two-loop contribution to $m^2_{h_0}$. In addition, Higgsinos should be light, as their masses are controlled by the $\mu-$parameter, which contributes to $m^2_{h_0}$. These statements sound reasonable and have been often used to quantify the 'naturalness' upper bounds on stop masses, gluino masses, etc.

Aside from theoretical arguments, the ATLAS and CMS experiments at the LHC, have performed a large number of SUSY searches, covering a significant region of the parameter space [74–81]. From the point of view of Natural SUSY models, the most interesting bounds are those imposed on stops, gluinos and Higgsinos. The lower limits from direct production of stops reach as far as 650 GeV [82], but they are sensitive to the stop physics, in particular the mass difference between the stop and the LSP. Much lighter stops are still allowed by the current experimental bounds once certain conditions on their decays are fulfilled [83–85]. Concerning the gluino, current experimental bounds have a strong dependence on the masses of light squarks. Assuming that the stops are the only squarks lighter than the gluino (as suggested by the very 'Natural SUSY' rationale), the latter decays through a chain $\tilde{g} \to t\bar{t}\tilde{\chi}^0_1$, and the lower limit reaches $m_{\tilde{g}} \lesssim 1.4$ TeV [86]. Again, with some additional assumptions on the decay chains

this limit can be somewhat relaxed. Finally, the μ parameter is the least constrained at the LHC. Because of the low electroweak production cross section and the large model dependence, it is entirely possible to have Higgsinos just above the current LEP limit, $\mu \gtrsim 95$ GeV [87, 88]. On the other hand, the LEP limit is rather model independent, even if the Higgsino is the LSP with three almost mass degenerate states around 100 GeV. All these bounds are relevant to establish the present degree of fine-tuning in different SUSY scenarios.

Another important experimental ingredient in clear connection with Natural SUSY is the physics of the Higgs boson [12, 13]. In particular, the Higgs mass plays a prominent role in naturalness arguments. According to the most recent analyses, $m_h = 125.09 \pm 0.21(\text{stat.}) \pm 0.11(\text{sys.})$ GeV [28–30] (ATLAS & CMS combined analysis). It is interesting to note that the current measurements are already more accurate than the theoretical predictions, which have a $\sim 2-3$ GeV uncertainty [89–91]. Furthermore, all observed Higgs properties are remarkably close to the SM predictions [92], which, within the SUSY context, points to the decoupling limit [93].

In this chapter, we revisit the arguments leading to the previous Natural SUSY scenario, showing that some of them are weak or incomplete. In section 2.1, we review the 'standard' Natural SUSY scenario, pointing out some weaknesses in the usual evaluation of its electroweak fine-tuning, i.e. the tuning to obtain the correct electroweak scale. We also address the existence of two potential extra fine-tunings that cannot be ignored in the discussion, namely the tuning to obtain $m_h = m_h^{\text{exp}}$ when stops are too light and the tuning to achieve a large $\tan\beta$. In section 2.2, we discuss the electroweak fine-tuning of the MSSM, showing its statistical meaning and its generic expression for any theoretical framework. We provide in appendix A tables and plots that allow to easily evaluate the fine-tuning for any theoretical model within the MSSM framework, at any value of the high-energy scale. In section 2.3, we describe our method to rigorously extract bounds on the initial (high-energy) parameters and on the supersymmetric spectrum, from the fine-tuning conditions. In section 2.4, we apply this method to obtain the numerical values of the various naturalness bounds for specific MSSM scenarios, defined at arbitrary high-energy scales, in a systematic way. In section 2.5, we evaluate the impact of the potential extra fine-tunings mentioned above, discussing also the correlation between soft terms that the experimental Higgs mass imposes on the MSSM and its consequences for the electroweak fine-tuning. Finally, in section 2.6 we present the summary and conclusions of the chapter, outlining the main characteristics of Natural SUSY and their level of robustness against changes in the theoretical framework or the high-energy scale at which the soft parameters appear.

2.1 The Natural SUSY scenario. A critical review

2.1.1 The 'standard' Natural SUSY

Naturalness arguments have been used since long ago [94] to constrain from above supersymmetric masses[1]. Already in the LHC era, they were re-visited in ref. [144] to formulate the so-called Natural

[1] For a partial list of references on naturalness in SUSY, see [32, 95–125] (before LHC) and [126–143].

SUSY scenario. For the purpose of later discussion, we summarise in this subsection the argument of ref. [144], which have been invoked in many papers.

Assuming that the extra (supersymmetric) Higgs states are heavy enough, the Higgs potential can be written as in the SM (see eq. 1.1), where the SM-like Higgs doublet, H, is a linear combination of the two supersymmetric Higgs doublets, $H \sim \sin\beta H_u + \cos\beta H_d$. Then, the absence of fine-tuning can be expressed as the requirement of not-too-large contributions to the Higgs mass parameter, $m^2_{h_0}$. Since the physical Higgs mass is $m_h^2 = 2|m^2_{h_0}|$, a sound measure of the fine-tuning is eq. (1.4) [32]. [2] For large $\tan\beta$, the value of $m^2_{h_0}$ is given by $m^2_{h_0} = |\mu|^2 + m^2_{H_u}$, so we immediately note that both μ and m_{H_u} should be not-too-large in order to avoid fine-tuning (as has been well-known since many years ago). For the $\mu-$parameter this implies

$$\mu \lesssim 200\,\text{GeV}\left(\frac{m_h}{120\,\text{GeV}}\right)\left(\frac{\tilde{\Delta}^{-1}}{20\%}\right)^{-1/2}. \tag{2.1}$$

This sets a constraint on Higgsino masses. Constraints for other sparticles come from the radiative corrections to $m^2_{H_u}$. The most important contribution comes from the stops. Following ref. [144]

$$\delta m^2_{H_u}|_{\text{stop}} = -\frac{3}{8\pi^2} y_t^2 \left(m^2_{Q_3} + m^2_{U_3} + |A_t|^2\right) \log\left(\frac{\Lambda}{\text{TeV}}\right), \tag{2.2}$$

where Λ denotes the scale of the transmission of SUSY breaking to the observable sector and the one-loop leading-log (LL) approximation was used to integrate the renormalization-group equations (RGEs). Then, the above soft parameters $m^2_{Q_3}$, $m^2_{U_3}$ and A_t are to be understood at low-energy, and thus they control the stop spectrum. This sets an upper bound on the stop masses. In particular, we have

$$\sqrt{m^2_{\tilde{t}_1} + m^2_{\tilde{t}_2}} \lesssim 600\,\text{GeV}\frac{\sin\beta}{(1+x^2)^{1/2}}\left(\frac{\log\left(\Lambda/\,\text{TeV}\right)}{3}\right)^{-1/2}\left(\frac{\tilde{\Delta}^{-1}}{20\%}\right)^{-1/2}, \tag{2.3}$$

where $x = A_t/\sqrt{m^2_{\tilde{t}_1} + m^2_{\tilde{t}_2}}$. Eq. (2.3) imposes a bound on the lightest stop. Besides the stops, the most important contribution to m_{H_u} is that of the gluino, due to its large one-loop renormalization group (RG) correction to stop masses. Again, in the one-loop LL approximation used in ref. [144], we obtain

$$\delta m^2_{H_u}|_{\text{gluino}} \simeq -\frac{2}{\pi^2} y_t^2 \left(\frac{\alpha_s}{\pi}\right)|M_3|^2 \log^2\left(\frac{\Lambda}{\text{TeV}}\right), \tag{2.4}$$

where M_3 is the gluino mass. From the previous equation,

$$M_3 \lesssim 900\,\text{GeV}\sin\beta\left(\frac{\log\left(\Lambda/\,\text{TeV}\right)}{3}\right)^{-1}\left(\frac{m_h}{120\,\text{GeV}}\right)\left(\frac{\tilde{\Delta}^{-1}}{20\%}\right)^{-1/2}. \tag{2.5}$$

Altogether, the summary of the minimal requirements for a natural SUSY spectrum, as given in ref. [144], is:

[2] This measure yields similar results to the somewhat standard parametrization of the fine-tuning, see eq. (2.14) below.

- two stops and one (left-handed) sbottom, both below $500 - 700$ GeV.
- two Higgsinos, *i.e.*, one chargino and two neutralinos below $200 - 350$ GeV. In the absence of other [lighter] chargino/neutralinos, their spectrum is quasi-degenerate.
- a not too heavy gluino, below 900 GeV $- 1.5$ TeV.

In the next subsections, we will identify the weak points of the above arguments that support the 'standard' Natural SUSY scenario. Part of those points have been addressed in the literature after ref. [144] (see ref. [145] for a recent and sound presentation of the naturalness issue in SUSY and references therein.)

2.1.2 The dependence on the initial parameters

The one-loop LL approximation used to write eqs. (2.3, 2.4), from which the naturalness bounds were obtained, is too simplistic in two different aspects.

First, it is not accurate enough since the top Yukawa-coupling, y_t, and the strong coupling, α_s, are large and vary a lot along the RG running. As a result, the soft masses evolve greatly and cannot be considered as constant, even as a rough estimate. This effect can be incorporated by integrating numerically the RGE, which corresponds to summing the leading-logs at all orders [146–149].

Second, and even more important, the physical squark, gluino and electroweakino masses are not initial parameters, but rather a low-energy consequence of the initial parameters at the high-energy scale. This means that we should evaluate the cancellations required among those initial parameters in order to obtain the correct electroweak scale. This entails two subtleties. First, there is not one-to-one correspondence between the initial parameters and the physical quantities, since the former are mixed along their coupled RGEs. Consequently, it is not possible in general to determine individual upper bounds on the physical masses, not even on the initial parameters. Instead, we should expect to obtain contour-surfaces with equal degree of fine-tuning in the parameter space and, similarly, in the 'space' of the possible supersymmetric spectra. The second subtlety is that the results depend (sometimes critically) on what we consider as initial parameters.

The most dramatic example of the last statements is the dependence of $m^2_{H_u}$ on the stop masses in the constrained MSSM (CMSSM). In the CMSSM, we assume universality of scalar masses at the GUT scale, M_X. This is a perfectly reasonable assumption that takes place in well-motivated theoretical scenarios, such as minimal supergravity. Then, we have to evaluate the impact of the initial parameters on $m^2_{H_u}$, and see whether or not the requirement of no-fine-tuning implies necessarily light stops. A most relevant analytic study concerning this issue is the well-known work by Feng et al. [122], where they studied the focus point [104, 122, 123] region of the CMSSM. In the generic MSSM, the (one-loop) RG

evolution of a shift in the initial values of $m^2_{H_u}, m^2_{U_3}, m^2_{Q_3}$ reads

$$\frac{d}{dt}\begin{bmatrix} \delta m^2_{H_u} \\ \delta m^2_{U_3} \\ \delta m^2_{Q_3} \end{bmatrix} = \frac{y_t^2}{8\pi^2}\begin{bmatrix} 3 & 3 & 3 \\ 2 & 2 & 2 \\ 1 & 1 & 1 \end{bmatrix}\begin{bmatrix} \delta m^2_{H_u} \\ \delta m^2_{U_3} \\ \delta m^2_{Q_3} \end{bmatrix}, \tag{2.6}$$

where $t \equiv \ln Q$, with Q the renormalization-scale, and y_t is the top Yukawa coupling. Hence, starting with the CMSSM universal condition at M_X: $m^2_{H_u} = m^2_{U_3} = m^2_{Q_3} = m^2_0$, we find

$$\delta m^2_{H_u} = \frac{\delta m^2_0}{2}\left\{3\exp\left[\int_0^t \frac{6y_t^2}{8\pi^2}dt'\right] - 1\right\}. \tag{2.7}$$

Provided $\tan\beta$ is large enough, $\exp\left[\frac{6}{8\pi^2}\int_0^t y_t^2 dt'\right] \simeq 1/3$ for the integration between M_X and the electroweak scale, so the value of $m^2_{H_u}$ depends very little (in the CMSSM) on the initial scalar mass, m_0. However, the average stop mass is given by (see eq. (2.50) below)

$$\overline{m}^2_{\tilde{t}} \simeq 2.97M_3^2 + 0.50m_0^2 + \cdots, \tag{2.8}$$

where M_3 is the gluino mass at M_X. Therefore, if the stops are heavy *because* m_0 is large, this does *not* imply fine-tuning. This is a clear counter-example to the need of having light stops to ensure naturalness.

From the previous discussion it turns out that the most rigorous way to analyse the fine-tuning is to determine the full dependence of the electroweak scale (and other potentially fine-tuned quantities) on the initial parameters, and then derive the regions of constant fine-tuning in the parameter space. These regions can be (non-trivially) translated into constant fine-tuning regions in the space of possible physical spectra. This goal is enormously simplified if we determine in the first place the analytical dependence of low-energy quantities on the high-energy initial parameters, a task which will be carefully addressed in subsection 2.2.3.

2.1.3 Fine-tunings left aside

In a MSSM scenario, there are two implicit potential fine-tunings that have to be taken into account to evaluate the global degree of fine-tuning. They stem from the need of having a physical Higgs mass consistent with $m_h^{\rm exp} \simeq 125$ GeV and from the requirement of rather large $\tan\beta$. Let us comment on them in order.

Fine-tuning to obtain $m_h^{\rm exp} \simeq 125$ GeV

As is well known, the tree-level Higgs mass in the MSSM is given by $(m_h^2)_{\rm tree-level} = M_Z^2\cos^2 2\beta$, so radiative corrections are needed in order to reconcile it with the experimental value. A simplified expression of such corrections, obtained at the leading-log approximation [150–152], useful for the sake

of discussion, is

$$\delta m_h^2 = \frac{3G_F}{\sqrt{2}\pi^2} m_t^4 \left(\log\left(\frac{\overline{m}_{\tilde{t}}^2}{m_t^2}\right) + \frac{X_t^2}{\overline{m}_{\tilde{t}}^2}\left(1 - \frac{X_t^2}{12\overline{m}_{\tilde{t}}^2}\right)\right) + \cdots , \tag{2.9}$$

with $\overline{m}_{\tilde{t}}$ the average stop mass and $X_t = A_t - \mu \cot\beta$. The X_t-contribution arises from the threshold corrections to the quartic coupling at the stop scale. This correction is maximised for $X_t = \sqrt{6}\overline{m}_{\tilde{t}}$ ($X_t \simeq 2\overline{m}_{\tilde{t}}$ when higher orders are included). Notice that if the threshold correction were not present we would need heavy stops (of about 3 TeV once higher order corrections are included) for large $\tan\beta$ (and much heavier as $\tan\beta$ decreases, see ref. [153, 154]); which is inconsistent with the requirements of Natural SUSY in its original formulation. However, taking X_t close to the 'maximal' value, it is possible to obtain the correct Higgs mass with rather light stops, even in the $500-700$ GeV range; a fact frequently invoked in the literature to reconcile the Higgs mass with Natural SUSY.

On the other side, requiring $X_t \sim$ maximal, amounts also to a certain fine-tuning if we need to lie close to such value with great precision. The precision (and thus the fine-tuning) required depends in turn on the values of $\tan\beta$ and the stop masses. Therefore, when analysing the naturalness issue we should take into account, besides the fine-tuning associated with the electroweak breaking, that associated with the precise value required for X_t. In subsection 2.5.1 we will discuss the size of this fine-tuning in further detail.

Fine-tuning to obtain large $\tan\beta$

The value of $\tan\beta \equiv \langle H_u\rangle/\langle H_d\rangle$ is given, at tree level, by

$$\frac{2}{\tan\beta} \simeq \sin 2\beta = \frac{2B\mu}{m_{H_d}^2 + m_{H_u}^2 + 2\mu^2} = \frac{2B\mu}{m_A^2} , \tag{2.10}$$

where m_A is the mass of the pseudoscalar Higgs state; all the quantities above are understood to be evaluated at the low-scale. Clearly, in order to obtain large $\tan\beta$ we need small $B\mu$ at low-energy. However, even starting with vanishing B at M_X we find a large radiative correction due to the RG running. Consequently, very large values of $\tan\beta$ are very fine-tuned[3], as they require a cancellation between the initial value of B and the radiative contributions. On the other hand, moderately large values may be non-fine-tuned, depending on the size of the RG contribution to $B\mu$ and the value of m_A. Hence, a complete analysis of the MSSM naturalness has to address this potential source of fine-tuning.

[3]The existence of this fine-tuning was first observed in ref. [155, 156] and has been discussed, from the Bayesian point of view in ref. [157].

2.2 The electroweak fine-tuning of the MSSM

In the MSSM, the vacuum expectation value of the Higgs, $v^2/2 = |\langle H_u \rangle|^2 + |\langle H_d \rangle|^2$, is given, at tree-level, by the minimization relation

$$-\frac{1}{8}(g^2+g'^2)v^2 = -\frac{M_Z^2}{2} = \mu^2 - \frac{m_{H_d}^2 - m_{H_u}^2 \tan^2\beta}{\tan^2\beta - 1} \ . \tag{2.11}$$

As is well known, the value of $\tan\beta$ must be rather large, so that the tree-level Higgs mass, $(m_h^2)_{\rm tree-level} = M_Z^2 \cos^2 2\beta$, is as large as possible, $\simeq M_Z^2$; otherwise, the radiative corrections needed to reconcile the Higgs mass with its experimental value, would imply gigantic stop masses [153, 154] (see subsection 2.1.3 above) and thus an extremely fine-tuned scenario. Notice here that the focus-point regime is not useful to cure such fine-tuning since it only works if $\tan\beta$ is rather large and stop masses are not huge. Therefore, for Natural SUSY the relevant limit is the large $\tan\beta$ regime. Then, eq. (2.11) can be approximated as

$$-\frac{1}{8}(g^2+g'^2)v^2 = -\frac{M_Z^2}{2} = \mu^2 + m_{H_u}^2 \ . \tag{2.12}$$

The two terms on the r.h.s have opposite signs and their absolute values are typically much larger than M_Z^2, thereby giving rise to a potential fine-tuning associated with the electroweak symmetry breaking.

It is well-known that the radiative corrections to the Higgs potential reduce the fine-tuning to a certain extent [95]. This effect can be honestly included taking into account that the effective quartic coupling of the SM-like Higgs runs from its initial value at the SUSY threshold[4], which hereafter we identify with the low-energy (LE) scale, $\lambda(Q_{\rm LE}) = \lambda(Q_{\rm threshold}) = \frac{1}{8}(g^2+g'^2)$, until its final value at the electroweak scale, $\lambda(Q_{EW})$. The effect of this running is equivalent to include the radiative contributions to the Higgs quartic coupling in the effective potential, which increase the tree-level Higgs mass, $(m_h^2)_{\rm tree-level} = 2\lambda(Q_{\rm threshold})v^2 = M_Z^2$, up to the experimental value, $m_h^2 = 2\lambda(Q_{EW})v^2$. Consequently, replacing $\lambda_{\rm tree-level}$ by the radiatively-corrected quartic coupling is equivalent to replace $M_Z^2 \to m_h^2$ in eq. (2.12) above, i.e.

$$-\frac{m_h^2}{2} = \mu^2(LE) + m_{H_u}^2(LE) \ , \tag{2.13}$$

which is the expression from which we will evaluate the electroweak fine-tuning in the MSSM. We emphasise here that in this expression μ^2 and $m_{H_u}^2$ are to be understood at low energy. As mentioned above, the radiative corrections slightly alleviate this fine-tuning, since $m_h > M_Z$.

[4] A convenient choice of the SUSY-threshold is the average stop mass, since the one-loop correction to the Higgs potential is dominated by the stop contribution. Hence, choosing $Q_{\rm threshold} \simeq m_{\tilde{t}}$, the one-loop correction is minimised and the Higgs potential is well approximated by the tree-level expression.

2.2.1 The measure of the fine-tuning

It is a common practice to quantify the amount of fine-tuning using the parametrization first proposed by Ellis et al. [158] and Barbieri and Giudice [94], which in our case reads

$$\frac{\partial m_h^2}{\partial \theta_i} = \Delta_{\theta_i} \frac{m_h^2}{\theta_i} \ , \qquad \Delta \equiv \text{Max } |\Delta_{\theta_i}| \ , \tag{2.14}$$

where θ_i is an independent parameter that defines the model under consideration and Δ_{θ_i} is the fine-tuning parameter associated with it. Very often in the literature (see e.g. [145]), the initial (high-energy) values of the soft terms and the μ parameter are considered as the independent θ_i parameters in the previous expression. Nevertheless, for specific scenarios of SUSY breaking and transmission to the observable sector, the initial parameters might be particular theoretical parameters that define the scenario and hence determine the soft terms, e.g. a Goldstino angle in scenarios of moduli-dominated SUSY breaking. We will comment further on this issue in subsection 2.2.2.

It is worth briefly commenting on the statistical meaning of Δ_{θ_i}. In ref. [97], it was argued that (the maximum of all) $|\Delta_{\theta_i}|$ represents the inverse of the probability of a cancellation among terms of a given size to obtain a result which is $|\Delta_{\theta_i}|$ times smaller. This can be intuitively inferred as follows. Expanding $m_h^2(\theta_i)$ around a point in the parameter space that gives the desired cancellation, say $\{\theta_i^0\}$, up to first order in the parameters, we find that only a small neighbourhood $\delta\theta_i \sim \theta_i^0/\Delta_{\theta_i}$ around this point gives a value of m_h^2 equal or smaller than the experimental value [97]. Therefore, if we assume that θ_i could reasonably have taken any value of the order of magnitude of θ_i^0, then only for a small fraction $\left|\delta\theta_i/\theta_i^0\right| \sim \Delta_{\theta_i}^{-1}$ of this region we obtain $m_h^2 \lesssim (m_h^{\rm exp})^2$, hence the rough probabilistic meaning of Δ_{θ_i}. Thus, the value of Δ can be interpreted as the inverse of the p-value to obtain m_h^2 from eq. (2.13) equal or smaller than the experimental m_h^2. If θ is the parameter that gives the maximum fine-tuning and $\delta\theta$ represents the θ-interval for which $m_h^2 \lesssim (m_h^{\rm exp})^2$, then[5]

$$p-\text{value} \simeq \left|\frac{\delta\theta}{\theta_0}\right| \equiv \Delta^{-1} \ . \tag{2.15}$$

It is noteworthy that for the previous arguments it was implicitly assumed that the possible values of a θ_i-parameter are distributed, with approximately flat probability, in the $[0,\theta_i^0]$ range. In a Bayesian language, the prior on the parameters was assumed to be flat, within the mentioned range. If the assumptions are different (either because the allowed ranges of some parameters are restricted by theoretical consistency or experimental data, or because the priors are not flat), then the probabilistic interpretation has to be consistently modified. These issues become more transparent using a Bayesian approach.

[5]Notice that in the particular case when θ^0 minimises the value of m_h, then $\partial m_h/\partial\theta|_{\theta=\theta_0} = 0$. This lack of sensitivity at first order when θ_0 is close to a stationary point, would seemingly imply no fine-tuning, according to the 'standard criterion'. However, from the above discussion, it is clear that in this case the expansion at first order is meaningless; we should start at second order, and then it becomes clear that the fine-tuning is really very high since only when θ is close to θ_0, we obtain $m_h^2 \lesssim (m_h^{\rm exp})^2$. In other words, the associated p-value would be very small.

In a Bayesian analysis, the goal is to generate a map of the relative probability of the different regions of the parameter space of the model under consideration (MSSM in our case), using all the available (theoretical and experimental) information. This is the so-called *posterior* probability, $p(\theta_i|\text{data})$, where 'data' stands for all the experimental information and θ_i represent the various parameters of the model. The posterior is given by the Bayes' theorem

$$p(\theta_i|\text{data}) \;=\; p(\text{data}|\theta_i)\; p(\theta_i)\; \frac{1}{p(\text{data})}\;, \tag{2.16}$$

where $p(\text{data}|\theta_i)$ is the likelihood (sometimes denoted by $\mathscr{L}$), i.e. the probability density of observing the given data if nature has chosen to be at the $\{\theta_i\}$ point of the parameter space (this is the quantity used in frequentist approaches); $p(\theta_i)$ is the prior, i.e. the 'theoretical' probability density that we assign a priori to the point in the parameter space; and, finally, $p(\text{data})$ is a normalisation factor which plays no role unless we wish to compare different classes of models.

For the sake of concreteness, let us focus on a particular parameter defining the MSSM, namely the $\mu-$parameter[6]. Now, instead of solving μ in terms of M_Z and the other supersymmetric parameters using the minimization conditions (as usual), we can (actually should) treat M_Z^{exp}, i.e. the electroweak scale, as experimental data on a similar footing with the other observables, entering the total likelihood, $\mathscr{L}$. Approximating the M_Z likelihood as a Dirac delta,

$$p(\text{data}|M_1, M_2, \cdots, \mu) \;\simeq\; \delta(M_Z - M_Z^{\text{exp}})\; \mathscr{L}_{\text{rest}}\;, \tag{2.17}$$

where $\mathscr{L}_{\text{rest}}$ is the likelihood associated with all the physical observables except M_Z, we can marginalise the $\mu-$parameter

$$\begin{aligned} p(M_1, M_2, \cdots|\;\text{data}) &= \int d\mu\; p(M_1, M_2, \cdots, \mu|\text{data}) \\ &\propto\; \mathscr{L}_{\text{rest}} \left|\frac{d\mu}{dM_Z}\right|_{\mu_Z} p(M_1, M_2, \cdots, \mu_Z)\;, \end{aligned} \tag{2.18}$$

where we have used eqs. (2.16, 2.17). Here μ_Z is the value of μ that reproduces M_Z^{exp} for the given values of $\{M_1, M_2, \cdots\}$, and $p(M_1, M_2, \cdots, \mu)$ is the prior in the initial parameters (still undefined). Note that the above Jacobian factor in eq. (2.18) can be written as[7]

$$\left|\frac{d\mu}{dM_Z}\right|_{\mu_Z} \propto \left|\frac{\mu}{\Delta_\mu}\right|_{\mu_Z}\;, \tag{2.19}$$

where the constant factors are absorbed in the global normalisation factor of eq. (2.16). The important point is that the relative probability density of a point in the MSSM parameter space is multiplied

[6] Indeed, we could have taken here another parameter and the argument would be the same (actually, in some theoretical scenarios μ may not be an initial parameter). On the other hand, μ is a convenient choice since it is the parameter usually solved in terms of M_Z in phenomenological analyses.

[7] Notice that the dependence of M_Z on μ is through eq. (2.13), which determines the Higgs VEV. Thus $\frac{dM_Z^2}{d\mu} \propto \frac{dm_h^2}{d\mu}$.

by Δ_μ^{-1}, which is consistent with the above probabilistic interpretation of Δ [114, 157, 159, 160]. Actually, the equivalence is exact if we assume that the prior in the parameters is factorizable, i.e. $p(M_1, M_2, \cdots, \mu) = p(M_1)p(M_2)\cdots p(\mu)$, *and* $p(\mu_Z) \propto 1/\mu_Z$, so that the numerator in the r.h.s of (2.19) is cancelled when plugged in eq. (2.18). This assumption can be realised in two different ways. First, if μ has a flat prior in the range $\sim [0, \mu_Z]$, then the normalisation of the $\mu-$prior goes like $\propto 1/\mu_Z$. This is exactly the kind of implicit assumption discussed above. Alternatively, if μ has a logarithmically flat prior, then $p(\mu) \propto 1/\mu$, with the same result (this is probably the most sensible prior to adopt since it means that all magnitudes of the SUSY parameters are equally probable).

In summary, the standard measure of the fine-tuning (2.14) is reasonable and can be rigorously justified using Bayesian methods. In consequence, we will use it throughout this chapter. Nevertheless, it should be kept in mind that the previous Bayesian analysis also provides the implicit assumptions for its validity. If a particular theoretical model does not fulfil them, the standard criterion is inappropriate and should be consistently modified.

2.2.2 Generic expression for the fine-tuning

Clearly, in order to use the standard measure of the fine-tuning (2.14) it is necessary to write the r.h.s. of the minimization equation (2.13) in terms of the initial parameters of the model. This in turn implies to write the low-energy values of $m_{H_u}^2$ and μ in terms of the initial, high-energy, soft-terms and $\mu-$term (for specific SUSY constructions, these parameters should themselves be expressed in terms of the genuine initial parameters of the model). Low-energy (LE) and high-energy (HE) parameters are related by the RGEs, which normally have to be integrated numerically. However, it is extremely convenient to express this dependence in an exact, analytical way. Fortunately, this can be straightforwardly done, since dimensional and analytical consistency dictates the form of the dependence,

$$\begin{aligned} m_{H_u}^2(LE) &= c_{M_3^2} M_3^2 + c_{M_2^2} M_2^2 + c_{M_1^2} M_1^2 + c_{A_t^2} A_t^2 + c_{A_t M_3} A_t M_3 + c_{M_3 M_2} M_3 M_2 + \cdots \\ &\quad \cdots + c_{m_{H_u}^2} m_{H_u}^2 + c_{m_{Q_3}^2} m_{Q_3}^2 + c_{m_{U_3}^2} m_{U_3}^2 + \cdots \qquad (2.20) \\ \mu(LE) &= c_\mu \mu \ , \qquad (2.21) \end{aligned}$$

where M_i are the $SU(3) \times SU(2) \times U(1)_Y$ gaugino masses, A_t is the top trilinear scalar coupling; and $m_{H_u}, m_{Q_3}, m_{U_3}$ are the masses of the H_u-Higgs, the third-generation squark doublet and the stop singlet respectively, all of them understood at the HE scale. The numerical coefficients, $c_{M_3^2}, c_{M_2^2}, \ldots$ are obtained by fitting the result of the numerical integration of the RGEs to eqs. (2.20, 2.21), a task that we perform carefully in subsection 2.2.3.

The above equations (2.20, 2.21) replace the one-loop LL expressions (2.2, 2.4) used in the standard Natural-SUSY treatment. If we consider the initial values of the soft parameters and μ as the independent parameters that define the MSSM, then we can easily extract the associated fine-tuning by applying eq. (2.14) to (2.13), and replacing $m_{H_u}^2$ by expression (2.20). Note that the above definition of Δ, eq. (2.14), is actually not very different from the definition (1.4) used in ref. [144]; actually they are

identical for the parameters that enter as a single term in the sum of eq. (2.20), e.g. $m^2_{\tilde{U}_3}$. Nevertheless, eq. (2.14) differs from eq. (1.4) when the parameter enters in several terms, e.g. M_3.[8] On the other hand, definition (2.14), besides being statistically more meaningful, allows to study scenarios where the initial parameters are not soft masses.

From eqs. (2.13, 2.20, 2.21), it is easy to derive the different $\{\Delta_{\theta_i}\}$ (2.14) for any MSSM scenario. A common practice is to consider the (HE) soft terms and the $\mu-$term as the independent parameters, say

$$\Theta_\alpha = \left\{\mu, M_3, M_2, M_1, A_t, m^2_{H_u}, m^2_{H_d}, m^2_{U_3}, m^2_{Q_3}, \cdots\right\}, \tag{2.22}$$

which is equivalent to the so-called 'Unconstrained MSSM'[9]. Then, we easily compute Δ_{Θ_α}

$$\Delta_{\Theta_\alpha} = \frac{\Theta_\alpha}{m_h^2}\frac{\partial m_h^2}{\partial \Theta_\alpha} = -2\frac{\Theta_\alpha}{m_h^2}\frac{\partial m^2_{H_u}}{\partial \Theta_\alpha}\,. \tag{2.23}$$

E.g. Δ_{M_3} is given by

$$\Delta_{M_3} = -2\frac{M_3}{m_h^2}\left(2c_{M_3^2}M_3 + c_{A_tM_3}A_t + c_{M_3M_2}M_2 + \cdots\right)\,. \tag{2.24}$$

The identification $\frac{\partial m_h^2}{\partial \Theta_\alpha} \simeq -2\frac{\partial m^2_{Hu}}{\partial \Theta_\alpha}$ in eq. (2.23) comes from eq. (2.13) and thus is valid for all the parameters except μ, for which we simply have

$$\Delta_\mu = \frac{\mu}{m_h^2}\frac{\partial m_h^2}{\partial \mu} = -4c_\mu^2\frac{\mu^2}{m_h^2} = -4\left(\frac{\mu(LE)}{m_h^2}\right)^2\,. \tag{2.25}$$

Besides, the term proportional to $m^2_{H_d}$ in eq. (2.11), which was subsequently neglected, can give relatively important contributions to $\Delta_{m^2_{H_d}}$ if $\tan\beta$ is not too large ($\lesssim 10$), namely

$$\Delta_{m^2_{H_d}} \simeq -2\frac{m^2_{H_d}}{m_h^2}\left(c_{m^2_{H_d}} - c'_{m^2_{H_d}}\,(\tan^2\beta - 1)^{-1}\right)\,, \tag{2.26}$$

where $c'_{m^2_{H_d}} \simeq 1$ denotes the $c-$coefficient of $m^2_{H_d}$ in the expression of the LE value of $m^2_{H_d}$ itself, see table A.1 in appendix A. In any case, the contribution of $m^2_{H_d}$ to the fine-tuning is always marginal.

[8] Indeed, if eq. (1.4) were refined to incorporate the M_3-dependent contributions to m^2, e.g. through their impact on the stop mixing, the result would be very similar to that of eq. (2.14).

[9] The name 'Unconstrained MSSM' could be a bit misleading in this context, since it would seem to imply that we are not making any assumption about the soft terms. Although, there is in fact an assumption, namely that they are not correlated. Note in particular that even if the parameter space of the Unconstrained MSSM includes any MSSM, e.g. the 'Constrained MSSM', the calculation of the fine-tuning for the latter requires to take into account a specific correlation between various soft-terms. Still, we are showing in this section that the results for the Unconstrained MSSM allow to easily evaluate the fine-tuning in any other MSSM scenario.

Note that for any other theoretical scenario, the Δs associated with the genuine initial parameters, say θ_i, can be written in terms of Δ_{Θ_α} using the chain rule

$$\Delta_{\theta_i} \equiv \frac{\partial \ln m_h^2}{\partial \ln \theta_i} = \sum_\alpha \Delta_{\Theta_\alpha} \frac{\partial \ln \Theta_\alpha}{\partial \ln \theta_i} = \frac{\theta_i}{m_h^2} \sum_\alpha \frac{\partial m_h^2}{\partial \Theta_\alpha} \frac{\partial \Theta_\alpha}{\partial \theta_i} \,. \tag{2.27}$$

Finally, in order to obtain fine-tuning bounds on the parameters of the model we demand $|\Delta_{\theta_i}| \lesssim \Delta^{\max}$, where $\Delta^{\max}$ is the maximum amount of fine-tuning we are willing to accept. E.g.

$$\Delta^{\max} = 100 \,, \tag{2.28}$$

represents a fine-tuning of $\sim 1\%$.

2.2.3 Fit to the low-energy quantities

Fits of the kind of eq. (2.20) can be found in the literature, see e.g.[161, 162]. However, though useful, they should be refined in several ways in order to perform a precise fine-tuning analysis. The most important improvement is a careful treatment of the various threshold scales. In particular, the initial MSSM parameters (i.e. the soft terms and the $\mu-$parameter) are defined at a high-energy (HE) scale, which is usually identified as M_X, i.e. the scale at which the gauge couplings unify. Although, this is a reasonable assumption, it is convenient to consider the HE scale as an unknown; e.g. in gauge-mediated scenarios it can be in principle any scale. The low-energy (LE) scale at which we set the SUSY threshold and the supersymmetric spectrum is computed, is also model-dependent. A reasonable choice is to take $M_{\rm LE}$ as the averaged stop masses. As discussed above, at this scale the one-loop corrections to the effective potential are minimised, so that the potential is well approximated by the tree-level expression; thus eq. (2.20) should be understood at this scale. Nevertheless, in many fits from the literature $M_{\rm LE}$ is identified with M_Z. Finally, some parameters are inputs at M_Z, e.g. the gauge couplings, while others, like the soft $B-$parameter (the coefficient of the bilinear Higgs coupling), have to be evaluated in order to reproduce the correct electroweak breaking with the value of $\tan\beta$ chosen. Similarly, the value of the top Yukawa-coupling has to be settled at high energy in such a way that it reproduces the value of the top mass at the electroweak scale (which is below the LE scale). All this requires to divide the RG-running into two segments, $[M_{\rm EW}, M_{\rm LE}]$ and $[M_{\rm LE}, M_{\rm HE}]$. Besides this refinement, we have integrated the RGEs at two-loop order, using `SARAH 4.1.0` [163].

The results of the fits for all the LE quantities for $\tan\beta = 10$ and $M_{\rm HE} = M_X$ are given in appendix A, tables A.1, A.2, A.3, A.4, A.5, A.6, and A.7. The value quoted for each $c-$coefficient has been evaluated at $M_{\rm LE} = 1$ TeV. The dependence of the $c-$coefficients on $M_{\rm LE}$ is logarithmic and can be well approximated by

$$c_i(M_{\rm LE}) \simeq c_i(1 \ \text{TeV}) + b_i \ln \frac{M_{\rm LE}}{1 \ \text{TeV}} \,. \tag{2.29}$$

The value of the b_i coefficients is also given in tables A.1–A.7 (for $M_{\rm HE} = M_X$). Certainly, the value of $M_{\rm LE} \sim \overline{m_{\tilde{t}}}$ is itself a (complicated) function of the initial soft parameters. Nevertheless, it is typically dominated by the (RG) gluino contribution, $M_{\rm LE} \sim \overline{m_{\tilde{t}}} \sim \sqrt{3}|M_3|$ for $M_{\rm HE} = M_X$. This represents an additional dependence of $m^2_{H_u}$ on M_3, which should be taken into account when computing Δ_{M_3}. Actually, this effect diminishes the fine-tuning associated with M_3 (which is among the most important ones) because the impact of an increase of M_3 on the value of $m^2_{H_u}$ becomes (slightly) compensated by the increase of the LE scale and the consequent decrease of the $c_{M_3^2}$ coefficient in eq. (2.20). We have incorporated this fact in the computations of the fine-tuning.

Let us now turn to the dependence of the fine-tuning on the high-energy scale, $M_{\rm HE}$. The absolute values of all the $c-$coefficients in the fits decrease with $M_{\rm HE}$, except perhaps the coefficient that multiplies the parameter under consideration (e.g. $c_{m^2_{H_u}}$ in eq. (2.20)). In the limit $M_{\rm HE} \to M_{\rm LE}$ the latter becomes 1, and the others go to zero. Obviously, the fine-tuning decreases as $M_{\rm HE}$ decreases. The actual dependence of the $c-$coefficients on $M_{\rm HE}$ is related to the loop-order at which it arises. If it does at one-loop, the dependence is logarithmic-like, e.g. for $c_{M_2^2}$ in eq. (2.20); if it does at two-loop, the dependence goes like $\sim (\log M_{\rm HE})^2$, e.g. for $c_{M_3^2}$. These dependences are shown in figures A.1, A.2, A.3, A.4 and A.5.

Summing up, with the help of tables A.1–A.7 and figures A.1–A.5 it is straightforward to evaluate the fine-tuning parameters of any MSSM scenario.

2.3 Naturalness bounds

2.3.1 Bounds on the initial (high-energy) parameters

Let us explore further the size and structure of the fine-tuning, and the corresponding bounds on the initial parameters, in the unconstrained MSSM, i.e. taking as initial parameters the HE values of the soft terms and the μ-term: $\Theta_\alpha = \left\{\mu, M_3, M_2, M_1, A_t, m^2_{H_u}, m^2_{H_d}, m^2_{U_3}, m^2_{Q_3}, \cdots\right\}$. This is interesting by itself, and, as discussed above, it can be considered as the first step to compute the fine-tuning in any theoretical scenario. For any of those parameters we demand

$$|\Delta_{\Theta_\alpha}| \lesssim \Delta^{\rm max} \,, \tag{2.30}$$

where Δ_{Θ_α} are given by eq. (2.23). Now, for the parameters that appear just once in eqs. (2.20, 2.21) the corresponding naturalness bound (2.30) is trivial and has the form of an upper limit on the parameter size. For dimensional reasons this is exactly the case for dimension-two parameters in mass units, e.g. for the squared stop masses

$$\left|\Delta_{m^2_{Q_3}}\right| = \left|-2\frac{m^2_{Q_3}}{m^2_h}\, c_{m^2_{Q_3}}\right| \lesssim \Delta^{\rm max} \quad \longrightarrow \quad m^2_{Q_3} \lesssim 1.36\, \Delta^{\rm max}\, m^2_h \tag{2.31}$$

$$\left|\Delta_{m^2_{U_3}}\right| = \left|-2\frac{m^2_{U_3}}{m^2_h}\, c_{m^2_{U_3}}\right| \lesssim \Delta^{\max} \quad \longrightarrow \quad m^2_{U_3} \lesssim 1.72\, \Delta^{\max}\, m^2_h\,, \tag{2.32}$$

where we have plugged , $c_{m_{Q_3}} = -0.367$, $c_{m_{U_3}} = -0.29$, which correspond to $M_{\rm HE} = M_X$ and $M_{\rm LE} =$ 1 TeV, see table A.1. For $\Delta^{\max} = 100$, we find $m_{Q_3} \lesssim 1.46$ TeV, $m_{U_3} \lesssim 1.64$ TeV, substantially higher than the usual quoted bounds [145]. This is mainly due to the refined RG analysis and the use of the radiatively upgraded expression eq. (2.13), rather than eq. (2.12), to evaluate the fine-tuning. We stress that these are the bounds on the high-energy soft masses, the bounds on the physical masses will be worked out in subsection 2.3.3. The naturalness bounds for the other (HE) dimension-two parameters ($m^2_{D_3}, m^2_{Q_{1,2}}, m^2_{U_{1,2}}, m^2_{D_{1,2}}, m^2_{L_3}$, ...) have a form similar to eqs. (2.31, 2.32) and are also higher than usually quoted. Due to its peculiar RGE, this is also the case of the $\mu-$parameter, see eq. (2.25).

On the other hand, for dimension-one parameters (except μ) the naturalness bounds (2.30) appear mixed. In particular, this is the case for the bounds associated with M_3, M_2, A_t. From eqs. (2.23) and (2.20)

$$|\Delta_{M_3}| = \frac{1}{m^2_h}\left|6.41 M_3^2 - 0.57 A_t M_3 + 0.27 M_3 M_2\right| \lesssim \Delta^{\max} \tag{2.33}$$

$$|\Delta_{M_2}| = \frac{1}{m^2_h}\left|-0.81 M_2^2 - 0.14 A_t M_2 + 0.27 M_3 M_2\right| \lesssim \Delta^{\max} \tag{2.34}$$

$$|\Delta_{A_t}| = \frac{1}{m^2_h}\left|0.44 A_t^2 - 0.57 A_t M_3 - 0.14 A_t M_2\right| \lesssim \Delta^{\max}\,, \tag{2.35}$$

where, again, we have plugged the values of the $c-$coefficients corresponding to $M_{\rm HE} = M_X$ and $M_{\rm LE} = 1$ TeV. Other parameters, like M_1, A_b, are also mixed with them in the bounds, but their coefficients are much smaller, so we have neglected them. We show in figure 2.1 the region in the $\{M_2, M_3, A_t\}$ space that fulfils the inequalities for $\Delta^{\max} = 100$. The figure is close to a prism. Their faces are given by the following approximate solution to eqs. (2.33–2.35)

$$M_3^{\max} \simeq \pm m_h \sqrt{\frac{\Delta^{\max}}{6.41}} + \frac{1}{12.82}(0.57 A_t - 0.27 M_2) \tag{2.36}$$

$$M_2^{\max} \simeq \pm m_h \sqrt{\frac{\Delta^{\max}}{0.81}} + \frac{1}{1.62}(0.27 M_3 - 0.14 A_t) \tag{2.37}$$

$$A_t^{\max} \simeq \pm m_h \sqrt{\frac{\Delta^{\max}}{0.44}} + \frac{1}{0.88}(0.57 M_3 + 0.14 M_2)\,, \tag{2.38}$$

where the superscript 'max' denotes the, positive and negative, values of the parameter that saturate inequalities (2.33–2.35). Thus eqs. (2.36–2.38) represent the naturalness bounds to M_3, M_2, A_t. Each individual bound depends on the values of the other parameters due to the presence of the mixed terms. Depending on the relative signs of the soft terms, the bounds can be larger or smaller than those obtained

when neglecting the mixed terms. However, the presence of the latter stretches each individual *absolute* upper bound in a non-negligible way, by doing an appropriate choice of the other soft terms (compatible with their own fine-tuning condition).

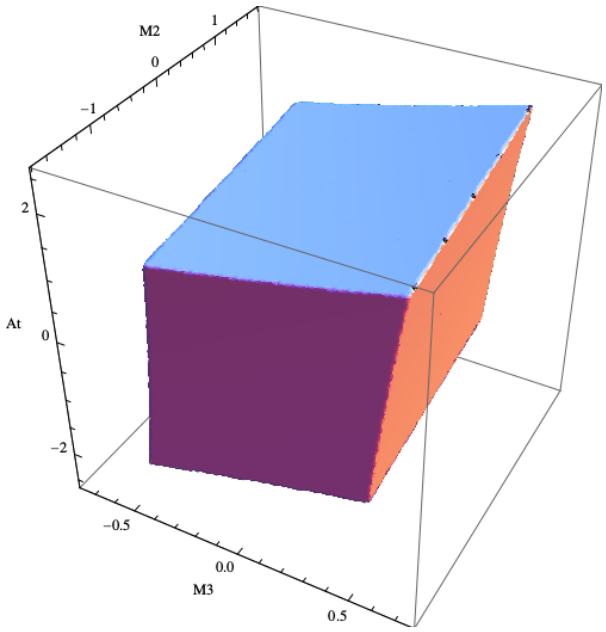

Figure 2.1: Region in the $\{M_2, M_3, A_t\}$ space that fulfils eqs. (2.33–2.35) for $\Delta^{\max} = 100$ (axes units: TeVs). For other values, a $\sqrt{\Delta^{\max}/100}$ scaling factor has to be applied.

A generic, approximate, expression for the absolute upper bound on a dimension-one parameter, i.e. $\mathscr{M}_i$ ($\mathscr{M}_i = M_3, M_2, M_1, A_t, A_b ...$) can be obtained by replacing the other dimension-one parameters, $\mathscr{M}_{j\neq i}$, by the values that saturate their zeroth-order fine-tuning bounds, $\pm\mathscr{M}_j^{\max} \simeq m_h\sqrt{\Delta^{\max}/4|c_{\mathscr{M}_j^2}|}$, with the appropriate sign; namely

$$|\mathscr{M}_i| < \frac{m_h}{2}\sqrt{\frac{\Delta^{\max}}{|c_{\mathscr{M}_i^2}|}}\left(1+\sum_{j\neq i}\frac{1}{4}\frac{|c_{\mathscr{M}_i\mathscr{M}_j}|}{\sqrt{|c_{\mathscr{M}_i^2}c_{\mathscr{M}_j^2}|}}\right) . \tag{2.39}$$

In practice, in order to obtain the absolute upper bounds on M_3, M_2, A_t we have ignored the presence of additional parameters ($M_1, A_b, \cdots$) in (2.39). Its inclusion would stretch even further the absolute bounds, but quite slightly and artificially since this would imply a certain conspiracy between soft parameters. As a matter of fact, even playing just with the three parameters which show a sizeable correlation, i.e. $\{M_3, M_2, A_t\}$, implies a certain degree of conspiracy to achieve the maximum value quoted in (2.39). This means that the bound (2.39) is conservative. A more restrictive and rigorous bound can be obtained by demanding that the addition in quadrature of the Δ_i parameters never exceeds the reference value, $\Delta^{\max}$. In any case, since the fine-tuning conditions of M_3, M_2, A_t are correlated, as shown in eqs. (2.33–2.35), the most meaningful approach is to determine the regions of the parameter space simultaneously consistent with all the fine-tuning conditions. This will be done in detail in section

2.5.2 below. The numerical modification of eqs.(2.33–2.38) for different values of $M_{\rm LE}$, $M_{\rm HE}$ can be straightforwardly obtained from table A.1 and figure A.1.

Choosing $\Delta^{\rm max} = 100$, eqs. (2.36–2.38) give $|M_3| \lesssim 610$ GeV, $|M_2| \lesssim 1630$ GeV, $|A_t| \lesssim 2430$ GeV. The limit on M_3 is similar to that found by Feng [145], although this is in part a coincidence. In ref. [145] it was chosen M_3^2, rather than M_3, as an independent parameter; which reduces the associated Δ_{M_3} by a factor of 2. So, their bound on M_3 was increased (quite artificially in our opinion) by $\sqrt{2}$. On the other hand, in ref. [145] the RG running was not done in two steps, but simply running all the way from M_X till M_Z. Furthermore, they did not consider the mixed terms of eq. (2.33). And finally they used eq. (2.12) instead of eq. (2.13) to evaluate the fine-tuning. It turns out that, all together, these three approximations increase the estimate of the fine tuning, thus decreasing the upper bound on M_3 by a factor which happens to be $\sim 1/\sqrt{2}$.

Actually, for the particular case of the M_3-parameter this is not the end of the story. As discussed in subsection 2.2.2, the $c_{M_3^2}$ coefficient has a dependence on $M_{\rm LE}$ approximately given by eq. (2.29). Since $M_{\rm LE} \simeq \overline{m_{\tilde t}}$ and typically $\overline{m}_{\tilde t}^2 \simeq \frac{1}{2}(c_{M_3^2}^{(Q_3)} + c_{M_3^2}^{(U_3)})^2 M_3^2$, where $c_{M_3^2}^{(Q_3)}$, $c_{M_3^2}^{(U_3)}$ are the coefficients of M_3^2 in the LE expression of $m_{Q_3}^2$, $m_{U_3}^2$ (given in table A.2 and figures A.2, A.3 for any HE scale), we have an additional contribution to the computation of Δ_{M_3} in eq. (2.23). The corresponding correction to $M_3^{\rm max}$ can be estimated by expanding the new inequality around the previous value of $M_3^{\rm max}$. We find

$$\delta M_3^{\rm max} \simeq \frac{1}{2}\frac{b_{M_3}}{|c_{M_3^2}|}\left(\frac{\sqrt{\frac{1}{2}\left(c_{M_3^2}^{(Q_3)} + c_{M_3^2}^{(U_3)}\right)}\, M_3^{\rm max}}{1\ \text{TeV}} - \frac{1}{2}\right) M_3^{\rm max}\,, \tag{2.40}$$

where we have neglected subdominant terms[10]. For $M_{\rm HE} = M_X$ and $M_{\rm LE} = 1$ TeV we have $c_{M_3^2} \simeq -1.6$, $c_{M_3^2}^{(Q_3)} + c_{M_3^2}^{(U_3)} \simeq 6$, so the previous correction becomes

$$\delta M_3^{\rm max} \simeq \frac{2.06 M_3^{\rm max} - 0.6\ \text{TeV}}{10\ \text{TeV}}\, M_3^{\rm max}\,. \tag{2.41}$$

This increases further $M_3^{\rm max}$ from 610 GeV to ~ 660 GeV, i.e. $m_{\tilde g} \lesssim 1440$ GeV which is about the present experimental lower limit on the gluino mass. Recall that this bound has been obtained assuming $\Delta^{\rm max} = 100$, thus we conclude that the unconstrained MSSM is fine-tuned at about 1%. We emphasise that these results have been obtained in the framework of the 'unconstrained MSSM', so that M_3, M_2, A_t are treated as independent, non-theoretically-correlated, parameters; and under the assumption $M_{\rm HE} = M_X$.

2.3.2 Correlations between soft terms

Using the chain rule (2.27), we can easily evaluate the fine-tuning bounds when the initial soft terms are related in any way determined by the theoretical framework chosen. For instance, it is reasonable to

[10] Note that this correction is applicable as long as $M_{\rm HE}$ is large ($\gtrsim 10^{10}$ GeV); otherwise, it is quite small, the stop mass is not determined anymore by M_3.

assume that the soft masses at HE come from the same source, and therefore they are related, even if they are not equal. E.g. suppose that at HE

$$\{m_{H_u}^2, m_{Q_3}^2, m_{U_3}^2\} = \{a_{H_u}, a_{Q_3}, a_{U_3}\} m_0^2 \,. \tag{2.42}$$

Then, plugging eq. (2.20) into eq. (2.27) we immediately derive the fine-tuning condition for m_0^2

$$\left|\Delta_{m_0^2}\right| = \left|-2\frac{m_0^2}{m_h^2}\left(c_{m_{H_u}^2} a_{H_u} + c_{m_{Q_3}^2} a_{Q_3} + c_{m_{U_3}^2} a_{U_3}\right)\right| \lesssim \Delta^{\max} \,, \tag{2.43}$$

which entails an upper bound on m_0^2, and hence on the stop masses at high energy. E.g.

$$m_{U_3}^2 \lesssim \frac{1}{2}\left|\frac{\Delta^{\max}}{-0.29 + 0.631\frac{a_{H_u}}{a_{U_3}} - 0.367\frac{a_{Q_3}}{a_{U_3}}}\right| m_h^2 \,, \tag{2.44}$$

where we have used the $c-$coefficients corresponding to $M_{\rm LE} = 1$ TeV, $M_{\rm HE} = M_X$ (table A.1). This bound can be compared with the bound for the unconstrained MSSM, eq. (2.32). Depending on the relative values between the as, the bound on $m_{U_3}^2$ increases (the usual case) or decreases. For the universal case, $a_{H_u} = a_{Q_3} = a_{U_3}$, we find $m_{U_3} \lesssim \sqrt{\Delta^{\max}}\ 550$ GeV, which allows for quite heavy stops with very little fine-tuning.

The same game can be played with the gaugino masses and the trilinear couplings. E.g. suppose that

$$\{M_1, M_2, M_3, A_t\} = \{a_1, a_2, a_3, a_t\} M_{1/2} \,. \tag{2.45}$$

Then, the fine-tuning condition for $M_{1/2}$ reads $\left|\Delta_{M_{1/2}}\right| \lesssim \Delta^{\max}$, with

$$\Delta_{M_{1/2}} = -4\frac{M_{1/2}^2}{m_h^2}\left(c_{M_3^2} a_3^2 + c_{M_2^2} a_2^2 + c_{A_t^2} a_t^2 + c_{M_3 M_2} a_3 a_2 + c_{M_3 A_t} a_3 a_t + c_{M_2 A_t} a_2 a_t\right) \,. \tag{2.46}$$

E.g. the bound on M_3 becomes

$$M_3^2 \lesssim \frac{a_3^2}{4}\left|\frac{\Delta^{\max}}{1.6a_3^2 - 0.203a_2^2 + 0.109a_t^2 + 0.134a_3 a_2 - 0.285a_3 a_t - 0.068a_2 a_t}\right| m_h^2 \,, \tag{2.47}$$

where, once more, we have used the $c-$coefficients corresponding to $M_{\rm LE} = 1$ TeV, $M_{\rm HE} = M_X$. For the universal case, $a_3 = a_2 = a_t$, the bound on M_3 becomes similar to that of the unconstrained MSSM. However, for other combinations the bound can be much larger. E.g. for $\frac{a_2}{a_3} = 3.16, -2.50$ and $a_t = 0$ the denominator would cancel.[11] This represents a different kind of focus-point, in this case for gauginos.

[11] See [128, 129, 134] for some studies about non-universal gaugino masses and fine-tuning.

Other correlations between soft parameters and the appearance of alternative focus-point regimes can be explored in a similar way starting at any HE scale, by using the tables and figures in appendix A. See refs. [142, 143] for recent works on this subject.

2.3.3 Bounds on the supersymmetric spectrum

So far, in this section we have explained in detail how to extract the naturalness limits on the initial (HE) soft terms and $\mu-$term in generic MSSM scenarios. The next step is to translate those bounds into limits on the physical supersymmetric spectrum. Therefore, we have to go back from the high-energy scale to the low-energy one, using the RG equations. Once more, this can be immediately done using the analytical expressions discussed in subsection 2.2.3 and appendix A for any value of the HE and the LE scales.

Unfortunately, there is no a one-to-one correspondence between the physical masses, and the soft-parameters and $\mu-$term at high-energy. The only approximate exception are the gaugino and Higgsino masses. Namely, from tables A.5, A.7

$$\begin{aligned} M_{\tilde{g}} &\simeq M_3(M_{\rm LE}) \simeq 2.22 M_3 \\ M_{\tilde{W}} &\simeq M_2(M_{\rm LE}) \simeq 0.81 M_2 \\ M_{\tilde{B}} &\simeq M_1(M_{\rm LE}) \simeq 0.43 M_1 \\ M_{\tilde{H}} &\simeq \mu(M_{\rm LE}) \simeq 1.002\mu \ , \end{aligned} \tag{2.48}$$

where the above numbers correspond to $M_{\rm LE} = 1$ TeV, $M_{\rm HE} = M_X$. Of course, these are not yet the physical masses, except, approximately, for the gluino. For a more precise calculation of the physical (pole) gluino mass, we must incorporate radiative corrections which depend on the size of the squark masses and that can be rather significant for more than one squark generation with $m_{\tilde{q}} \gg M_3$ [164]. The other gauginos and the Higgsinos are mixed in the chargino and neutralino mass matrices. However, since we are considering upper limits on these masses, the mixing entries in those matrices are subdominant and do not appreciably affect the bounds. On the other hand, as discussed in subsection 2.3.1, the naturalness limits on (the HE values of) M_3, M_2 are more involved than for other parameters, since the respective fine-tuning inequalities are not independent of each other and also are mixed with A_t. Using the ($M_{\rm LE} = 1$ TeV, $M_{\rm HE} = M_X$) limits on M_3, M_2, M_1 and μ, obtained for the unconstrained MSSM (see sections 2.3.1 and 2.4.1), we find $M_{\tilde{g}} \lesssim 1440$ GeV, $M_{\tilde{W}} \lesssim 1300$ GeV, $M_{\tilde{B}} \lesssim 3370$ GeV and $M_{\tilde{H}} \lesssim 627$ GeV.

On the contrary, the physical masses of the sparticles, $m^2_{\tilde{t}_1}$, $m^2_{\tilde{t}_2}$, $m^2_{\tilde{Q}_{1,2}}$ $m^2_{\tilde{U}_{1,2}}$, $m^2_{\tilde{D}_{1,2}}$, $m^2_{H^\pm}$, etc., are non-trivial combinations of the various initial soft terms and products of them. The case of the stops is particularly important, since it is a common assumption that Natural SUSY demands light stops. E.g. using $M_{\rm LE} = 1$ TeV, $M_{\rm HE} = M_X$, we see from table A.1 that the values of $m^2_{Q_3}$, $m^2_{U_3}$ at LE are given by:

$$\begin{aligned} m^2_{Q_3}(M_{\rm LE}) &= 3.191 M_3^2 + 0.333 M_2^2 + 0.871 m^2_{\tilde{Q}_3} - 0.095 m^2_{\tilde{U}_3} - 0.118 m^2_{H_u} + 0.072 A_t M_3 + \cdots \\ m^2_{U_3}(M_{\rm LE}) &= 2.754 M_3^2 - 0.151 M_2^2 - 0.192 m^2_{\tilde{Q}_3} + 0.706 m^2_{\tilde{U}_3} - 0.189 m^2_{H_u} + 0.159 A_t M_3 + \cdots \end{aligned} \tag{2.49}$$

These are not yet the physical stop masses. We have to take into account the top contribution, m_t^2, and the off-diagonal entries in the stop mass matrix, $\sim m_t X_t$ where $X_t = A_t + \mu \cot\beta \simeq A_t$. Finally, we have to extract the mass eigenvalues, $m_{\tilde{t}_1}^2$ and $m_{\tilde{t}_2}^2$. A representative, and easier to calculate, quantity is the average stop mass,

$$\begin{aligned} \overline{m}_{\tilde{t}}^2 &\equiv \frac{1}{2}(m_{\tilde{t}_1}^2 + m_{\tilde{t}_2}^2) = \frac{1}{2}(m_{Q_3}^2(M_{\rm LE}) + m_{U_3}^2(M_{\rm LE})) + m_t^2 \\ &\simeq (2.972 M_3^2 + 0.339 m_{Q_3}^2 + 0.305 m_{U_3}^2 + 0.091 M_2^2 - 0.154 m_{H_u}^2 \cdots) + m_t^2 \ . \end{aligned} \tag{2.50}$$

The average stop mass is also an important quantity to evaluate the threshold correction to the Higgs mass, and thus it plays an important role in the evaluation of the potential fine-tuning associated with it, see eq. (2.9) and subsection 2.5.1. Setting M_3, m_{Q_3}, m_{U_3} and M_2 at their upper bounds (and neglecting additional terms in the parenthesis of eq. (2.50)), we obtain an upper bound for $\overline{m}_{\tilde{t}}$, namely $\overline{m}_{\tilde{t}} \lesssim 1.7$ TeV. However, this is somehow too optimistic since it requires that all these HE parameters are simultaneously at their upper bounds, which is unlikely. A way to deal with this problem is to slightly modify the fine-tuning measure (2.14), in a (more restrictive) fashion, which counts all the contributions to the fine-tuning. Namely, instead using $\Delta \equiv \text{Max } |\Delta_{\theta_i}|$, we define $\Delta \equiv \{\sum_i |\Delta_{\theta_i}|^2\}^{1/2}$, which, as has been argued [165], it is a more meaningful quantity. If the fine-tuning is dominated by one of the HE parameters (which is the usual case) both definitions are equivalent, but if there are several parameters contributing substantially to the fine-tuning, the second definition is more sensible (and restrictive). Then, it is easy to show that the maximum value of $\overline{m}_{\tilde{t}}^2$ subject to the condition $\Delta \leq \Delta_{\rm max}$, with Δ defined in this modified way, is

$$\overline{m}_{\tilde{t}}^2 = \left[2.972^2 (M_3^{\rm max})^4 + 0.339^2 (m_{Q_3}^{\rm max})^4 + 0.305^2 (m_{U_3}^{\rm max})^4 + 0.091^2 (M_2^{\rm max})^4 + \cdots\right]^{1/2} + m_t^2 \ .$$

Using just the dominant terms appearing explicitly above, we find (for $M_{\rm HE} = M_X$) $\overline{m}_{\tilde{t}} \leq 1320$ GeV.

From these results, it is clear that for the unconstrained MSSM, with $M_{\rm HE} = M_X$, the naturalness bound on the gluino mass is much more important for LHC detection than that of the stop masses. Next, we show the numerical values of the various naturalness bounds in a systematic way.

2.4 Application to specific scenarios

2.4.1 Unconstrained MSSM

The unconstrained MSSM, where the soft-terms and $\mu-$term at the HE scale are taken as the independent parameters, has been already considered in the previous subsections as a guide to discuss the various naturalness bounds. However, we have so far restricted ourselves to the case $M_{\rm LE} = 1$ TeV, $M_{\rm HE} = M_X$. It is interesting to show the limits, both on the initial parameters and on the supersymmetric spectrum, for other choices of $M_{\rm HE}$. Following the procedure explained in subsections 2.3.1 and 2.3.3, we have computed the fine-tuning constraints for three representative values of $M_{\rm HE}$, namely $M_{\rm HE} = 2 \times 10^{16}$ GeV,

10^{10} GeV and 10^4 GeV, keeping $M_{\rm LE} = 1$ TeV. Using the plots shown in appendix A the reader can evaluate the bounds for any other choice of $M_{\rm HE}$.

The absolute upper bounds on the most relevant HE parameters, obtained from eq. (2.39), with the additional correction (2.40) for M_3, are shown in table 2.1. Similarly, the corresponding bounds on supersymmetric masses at low energy, evaluated as in subsection 2.3.3, are shown in table 2.2. All the bounds have been obtained by setting $\Delta^{\rm max} = 100$, they simply scale as $\sqrt{\Delta^{\rm max}/100}$.

	$M_{\rm HE} = 2\times 10^{16}$ GeV	$M_{\rm HE} = 10^{10}$ GeV	$M_{\rm HE} = 10^4$ GeV
$M_3^{\rm max}(M_{\rm HE})$	660	1 162	5 376
$M_2^{\rm max}(M_{\rm HE})$	1 646	1 750	3 500
$M_1^{\rm max}(M_{\rm HE})$	8 002	6 100	11 048
$A_t^{\rm max}(M_{\rm HE})$	2 504	2 227	3 094
$m_{H_u}^{\rm max}(M_{\rm HE})$	1 038	1 046	913
$m_{H_d}^{\rm max}(M_{\rm HE})$	6 945	14 472	9 784
$\mu^{\rm max}(M_{\rm HE})$	624	640	630
$m_{Q_3}^{\rm max}(M_{\rm HE})$	1 458	1 687	3 527
$m_{U_3}^{\rm max}(M_{\rm HE})$	1 640	1 828	3 710
$m_{D_3}^{\rm max}(M_{\rm HE})$	5 682	7 812	20 277
$m_{Q_{1,2}}^{\rm max}(M_{\rm HE})$	5 601	7 693	19 288
$m_{U_{1,2}}^{\rm max}(M_{\rm HE})$	3 818	5 254	13 975
$m_{D_{1,2}}^{\rm max}(M_{\rm HE})$	5 613	7 722	19 764
$m_{L_{1,2,3}}^{\rm max}(M_{\rm HE})$	5 557	7 664	20 278
$m_{E_{1,2,3}}^{\rm max}(M_{\rm HE})$	5 524	7 607	20 278

Table 2.1: Upper bounds on some of the initial (HE) soft terms and $\mu-$term for three different values of $M_{\rm HE}$, in the unconstrained MSSM scenario. All quantities are given in GeV.

	$M_{\rm HE} = 2\times 10^{16}$ GeV	$M_{\rm HE} = 10^{10}$ GeV	$M_{\rm HE} = 10^4$ GeV
$M_{\tilde g}^{\rm max}$	1 440	1 890	5 860
$M_{\tilde W}^{\rm max}$	1 303	1 550	3 435
$M_{\tilde B}^{\rm max}$	3 368	4 237	10 565
$M_{\tilde H}^{\rm max}$	627	627	627
$\overline{m}_{\tilde t}^{\rm max}$	1 320	1 590	3 190
$m_{H^0}^{\rm max}$	7 252	14 510	9 900

Table 2.2: Upper bounds on some of the physical masses for three different values of $M_{\rm HE}$, in the unconstrained MSSM scenario. All quantities are given in GeV.

From the previous tables we can notice some generic facts.

- Taking into account the present and future LHC limits, the upper bound on the gluino mass is typically the most stringent, being at the reach of the LHC (for $\Delta^{\rm max} = 100$), unless the high-energy scale is rather low. On the other hand, the gluino bound is the most sensitive to the value of $M_{\rm HE}$,

since it is a two-loop effect. For $M_{\rm HE} \simeq 10^7$ GeV, it is as already beyond the future LHC limit (~ 2.5 TeV, see e.g. [166]) and it increases rapidly as $M_{\rm HE}$ approaches the electroweak scale.

- The upper bound on the wino mass, $M_{\tilde{W}}$, is similar to that of the gluino. Note here that (unless $M_{\rm HE}$ is quite small) the weight of M_2^2 in the value of $m_{H_u}^2(M_{\rm LE})$ is certainly smaller than that of M_3^2; but this effect is compensated, when computing the physical masses, by the large increase in M_3 when running from $M_{\rm HE}$ to $M_{\rm LE}$ (see figures A.1 and A.4). On the other hand, the bound on $M_{\tilde{W}}$ is much less restrictive than that of $M_{\tilde{g}}$, given the LHC discovery potential. The upper bound on the bino, as expected, is quite mild and always beyond the reach of the next LHC run. This is just a consequence of the little impact that M_1 has on $m_{H_u}^2(LE)$.

- Concerning electroweakinos, the most relevant upper bounds are those on Higgsinos, $M_{\tilde{H}}$. Not only they are the strongest (hopefully at the reach of the LHC for $\Delta^{\rm max} = 100$), but also, by far, the most stable of all bounds. This is a consequence of the fact that μ runs proportional to itself, so their fine-tuning parameter is insensitive to the HE scale, see eq. (2.25). Apart from that, the running of μ is very little. It is worth-mentioning that for $\Delta^{\rm max} = 100$ the upper bound on $M_{\tilde{H}}$ is not far from $M_{\tilde{H}} \simeq 1$ TeV, which is the value required if dark matter is made of Higgsinos [167, 168].

- The upper bounds on stops are not as stringent as that of the gluino mass unless $M_{\rm HE}$ is pretty close to the electroweak scale, in which case none of them is relevant. In general, it is not justified to say that Natural SUSY prefers light stops, close to the LHC limits. Actually, for $\Delta^{\rm max} = 100$ the upper bounds on stops are beyond the LHC reach [166]. Taking lighter stops does not really improve the fine-tuning since there are other contributions to it which are dominant, in particular that of the gluino mass.

- Given the present LHC limits, the contribution of the gluino to the $m_{H_u}^2$ is bigger than that of stops, then it is not useful to have light stops. This conclusion is reinforced when other aspects are considered, see subsection 2.5.1 below. Unless $M_{\rm HE}$ is very small, the gluino mass sets the level of EW fine-tuning of the unconstrained MSSM, which is $\mathcal{O}(1\%)$.

  If $M_{\rm LE}$ becomes close to the electroweak scale, the supersymmetric fine-tuning becomes much less severe. This fact is strengthened by the fact that additional soft dimension-4 Higgs operators may start to become relevant, increasing the tree-level Higgs mass and thus decreasing further the fine-tuning. These aspects were noted in ref. [169–171].

- Concerning the squarks of the first two generations and all the generations of sleptons, their bounds are, as expected, far beyond the reach of the LHC; the reason being that their contribution to $m_{H_u}^2$ is very small.

- Lastly, we can see the large upper bounds on $m_{H_d}^2$. When $M_{\rm LE}$ is very large, its contribution to the fine-tuning is very small. However, for low values of $M_{\rm LE}$, the term proportional to

$m_{H_d}^2(\tan^2\beta - 1)^{-1}$ (neglected for simplicity in expression (2.13)) actually becomes the dominant one, causing a larger impact of $m_{H_d}^2$ on the EW fine-tuning and, as consequence, decreasing the respective upper bound. This can be seen from table (2.1), where the bound on m_{H_d} is lower for $M_{\rm LE} = 10^4$ GeV. Being the largest bounds as compared to the those of μ and $m_{H_u}^2$, the term $m_{H_d}^2$ dominates the bounds on the masses of the heavy Higgses (see table 2.2).

2.4.2 CMSSM and Non-Universal Higgs Masses (NUHM)

We now proceed to analyse popular scenarios that assume some correlations on the soft parameters, namely the constrained MSSM (CMSSM) and MSSM with non-universal Higgs masses (NUHM). In both of them, gaugino masses and trilinear terms are universal (denoted by $m_{1/2}$ and A_0, respectively). However, in the NUHM the two Higgses H_u and H_d are allowed to have different masses, moreover, different from the scalar mass m_0. This difference between the two scenarios is going to play an important role when computing the fine-tuning of the stops, as we will comment below.

Taking $M_{\rm HE} = M_X$ and, as usual, $M_{\rm LE} = 1$ TeV and using the coefficients of the fit for $m_{H_u}^2(LE)$ in table A.1, we obtain for the CMSSM

$$m_{H_u}^2(LE)|_{\rm CMSSM} = -1.54m_{1/2}^2 - 0.02m_0^2 - 0.11A_0^2 + 0.36A_0 m_{1/2}\,, \tag{2.51}$$

and for the NUHM

$$m_{H_u}^2(LE)|_{\rm NUHM} = -1.54m_{1/2}^2 - 0.68m_0^2 - 0.11A_0^2 + 0.36A_0 m_{1/2} + 0.03m_{H_d}^2 + 0.63m_{H_u}^2\,. \tag{2.52}$$

Analogous expressions are obtained for other values of $M_{\rm HE}$. We note the big difference in the coefficient of m_0 for both cases, which reflects the fact that for the CMSSM, the impact of m_0 on $m_{H_u}^2$ (in the $M_{\rm HE} = 2\times 10^{16}$ GeV) is much milder due to the focus point effect discussed in section 2.1.2. The upper bounds on these soft parameters are shown in table 2.3. We see that the difference in m_0 is around a factor 5 for the same amount of fine-tuning, $\Delta_{\rm max} = 100$.

	$M_{\rm HE} = 2\times 10^{16}$ GeV		$M_{\rm HE} = 10^{10}$ GeV		$M_{\rm HE} = 10^4$ GeV	
	CMSSM	NUHM	CMSSM	NUHM	CMSSM	NUHM
$m_{1/2}^{\rm max}$	633	633	1 295	1 295	4 422	4 422
$m_0^{\rm max}$	4 337	765	1 345	874	697	1 807
$A_0^{\rm max}$	2 377	2 377	2 271	2 271	3 070	3 070
$m_{H_u}^{\rm max}$	-	793	-	740	-	651
$m_{H_d}^{\rm max}$	-	3 915	-	5 402	-	14 453

Table 2.3: Upper bounds on the soft parameters in the CMSSM and NUHM scenarios. All quantities are given in GeV.

These imply the following bounds on the mass spectrum

	$M_{\rm HE} = 2\times10^{16}$ GeV		$M_{\rm HE} = 10^{10}$ GeV		$M_{\rm HE} = 10^{4}$ GeV	
	CMSSM	NUHM	CMSSM	NUHM	CMSSM	NUHM
$M^{\rm max}_{\tilde{g}}(LE)$	1 408	1 408	2 124	2 124	4 823	4 823
$M^{\rm max}_{\tilde{W}}(LE)$	498	498	1 146	1 146	4 348	4 347
$M^{\rm max}_{\tilde{B}}(LE)$	268	268	900	900	4 229	4 229
$M^{\rm max}_{\tilde{H}}(LE)$	890	890	911	911	897	897
$\overline{m}^{\rm max}_{\tilde{t}}(LE)$	4 302	1 216	2 079	1 733	2 096	2 849

Table 2.4: Upper bounds on low energy masses in the CMSSM and NUHM scenarios. All quantities are given in GeV.

2.4.3 Gauge-mediated SUSY breaking (GMSB)

A popular scenario for supersymmetry breaking is the GMSB. There, SUSY is broken in a hidden sector and transmitted at loop-level to the visible sector via heavy chiral supermultiplets (messengers) that are charged under the very same gauge interactions of the MSSM. These messengers couple to the superfield X which breaks SUSY in the hidden sector once its scalar and auxiliary components obtain non-zero VEVs ($\langle X\rangle$ and $\langle F_X\rangle$, respectively).

Gauginos and sparticles acquire mass due to one and two loop diagrams involving those messengers fields, respectively. In the limit $\Lambda \equiv \langle F_X\rangle/\langle X\rangle \ll M_{\rm HE}$

$$M_i = \frac{\alpha_i}{4\pi}\Lambda N_5 \,, \tag{2.53}$$

$$m^2_{\tilde{f}} = 2\Lambda^2 N_5 \sum_{i=1}^{3} C_i^{\tilde{f}} \left(\frac{\alpha_i}{4\pi}\right)^2 \,, \tag{2.54}$$

where Λ has dimension of mass and α_i and $C_i^{\tilde{f}}$ are the corresponding gauge couplings and Casimir coefficients, respectively. Besides, the messenger sector comprise N_5 copies of the fundamental representation, $5+\bar{5}$. Notice that in this scenario, sfermion soft masses are distinct for different species, although they are identical for different families.

The high scale in this case is fixed by the messenger scale, $M_{\rm HE} = M_{\rm mess}$, we will consider three typical values of this scale for the sake of illustration (see table 2.5 below). Trilinear terms arise also at two-loop level but are even more suppressed, so that we can safely approximate them to zero at the $M_{\rm mess}$ scale. We hence have all the soft masses as a function of a unique parameter Λ.

With the $m^2_{H_u}$ fit and the EW fine-tuning criterion as before, for $\Delta_{\rm max} = 100$, we obtain,

$$\Lambda_{\rm max} = \sqrt{\frac{m_h^2 \Delta_{\rm max}}{2N_5|c_{\rm sfer} + c_{\rm gau}N_5|}} \,, \tag{2.55}$$

where $c_{\rm sfer}$ is the sum of coefficients for sfermions and Higgses, and $c_{\rm gau}$ the sum of gaugino coefficients. For instance, for $M_{\rm HE} = 2\times10^{16}$ GeV we have $c_{\rm sfer} = -1.36\times10^{-5}$, $c_{\rm gau} = -1.57\times10^{-5}$.

We show our results in table 2.5 for three different values of $M_{\rm HE}$ (i.e. $M_{\rm mess}$ in this case), and two values of the N_5 parameter characterising the messenger sector.

	$M_{\rm HE} = 2\times10^{16}$ GeV		$M_{\rm HE} = 10^{10}$ GeV		$M_{\rm HE} = 10^{5}$ GeV	
	$N_5 = 1$	$N_5 = 4$	$N_5 = 1$	$N_5 = 4$	$N_5 = 1$	$N_5 = 4$
$\Lambda_{\rm max}$ (GeV)	1.2×10^5	3.6×10^4	1.6×10^5	5×10^4	2.5×10^5	3×10^5

Table 2.5: Upper bounds from the EW fine-tuning on the Λ scale in the GMSB scenario.

We note that for $M_{\rm HE} = 10^4$ GeV, the bound on Λ is lower for $N_5 = 4$ than for $N_5 = 1$, contrary to what happens for the other $M_{\rm HE}$ choices. This is due to a particular cancellation in the coefficients of eq.(2.55). Indeed, for this case $c_{\rm sfer} = 7.9\times10^{-6}$ and $c_{\rm gau} = 1.7\times10^{-6}$, so that $N_5 = 4$ produces a fine cancellation.

The previous bounds on Λ are translated in bounds on gluinos and stops, which we show in table 2.6.

	$M_{\rm HE} = 2\times10^{16}$ GeV		$M_{\rm HE} = 10^{10}$ GeV		$M_{\rm HE} = 10^{5}$ GeV	
	$N_5 = 1$	$N_5 = 4$	$N_5 = 1$	$N_5 = 4$	$N_5 = 1$	$N_5 = 4$
$M_{\tilde g}^{\rm max}(LE)$	819	1 015	1 135	1 372	1 827	8 639
$M_{\tilde W}^{\rm max}(LE)$	289	357	411	497	628	2 970
$M_{\tilde B}^{\rm max}(LE)$	156	193	221	268	338	1 599
$M_{\tilde H}^{\rm max}(LE)$	1.2×10^5	3.6×10^4	1.6×10^5	4.8×10^4	2.5×10^5	2.9×10^5
$\overline{m}_{\tilde t}^{\rm max}(LE)$	733	474	1 028	636	1 556	3 662

Table 2.6: Upper bounds on gluinos and average stop mass in the GMSB scenario, from EW fine-tuning. All quantities are given in GeV.

The current experimental bound on gluinos[12] is about 1.4 TeV, beyond the above values obtained for the case $M_{\rm HE} = 2\times10^{16}$ GeV assuming a fine-tuning of 1%. Conversely, such an experimental bound implies that the fine-tuning of the GMSB scenarios we have considered here are at the per mil level.

2.4.4 Anomaly-mediated SUSY breaking (AMSB)

In this scenario, soft masses come from the violation of local conformal invariance at loop level, whereas the theory at tree level preserves supersymmetry. This is valid for models with dimensionless couplings in the SUSY limit like the Next-to-Minimal Supersymmetric Standard Model (NMSSM).[13] As in gauge mediation, the breaking is transmitted through gauge loops, so that soft terms are flavour-blind. In particular, gaugino masses read [41]

$$M_i = \frac{b_i g_i^2}{16\pi^2}\langle F_\phi\rangle, \quad b_i = (33/5, 1, -3)\ , \tag{2.56}$$

[12] See for instance [CMS-SUS-13-20].

[13] Remember that the only dimensionful coupling of the MSSM is the μ term, whereas in the NMSSM this term comes from the VEV of a new singlet S.

where g_i are the corresponding gauge couplings, and $\langle F_\phi \rangle$ the VEV of the auxiliary field inside the superfield [14] ϕ which is responsible for the super-conformal symmetry breaking. Here, SUSY breaking is transmitted at the Planck scale. The masses of the sfermions and trilinear terms do also depend only on $\langle F_\phi \rangle$. [15] So the trilinear terms read

$$a^{ijk} = -\langle F_\phi \rangle \beta_{y^{ijk}} \,, \tag{2.57}$$

with $\beta_{y^{ijk}}$ the beta function of the corresponding Yukawa. One striking feature of AMSB is that the above relations are independent of the scale. Thus, they constitute not only boundary conditions at every scale, but solutions themselves. Given this fact, we could evaluate the EW fine-tuning from the corresponding expression of $m^2_{H_u}$ resulting in this scenario [172]

$$m^2_{H_u} = -\alpha_{H_u} \langle F^2_\phi \rangle + m^2_0 \approx -1.3 \times 10^{-5} \langle F^2_\phi \rangle + m^2_0 \,, \tag{2.58}$$

where the coefficient α_{H_u} has been evaluated at 1 TeV scale. Therefore, the bound on $\langle F_\phi \rangle$ from fine-tuning arguments is

$$\langle F_\phi \rangle \lesssim \left| \frac{1}{4(-1.3 \times 10^{-5})} \right|^{1/2} \sqrt{\Delta_{\max} m^2_h} \approx 175 \text{ TeV} \,. \tag{2.59}$$

Even if, it appears to be a very high value -certainly higher than those obtained for the CMSSM, $\mathcal{O}$(1 TeV)-, note that the standard lore for AMSB is to have $\langle F_\phi \rangle$ around 100 TeV, in order to have soft masses around the TeV scale. This is due to the suppression given by the loop factors, as in (2.56). Just for comparison with the GMSB scenario, the gluino mass predicted here is around $m_{\tilde{g}}(\Delta_{\max}) \approx 4.2$ TeV, much beyond the current LHC limits.

2.4.5 Dilaton-dominated scenario

Another popular scenario among the string community is to consider the presence of moduli superfields, while some of them have non-vanishing VEVs for their auxiliary components. This implies that SUSY is spontaneously broken in the moduli sector. Regardless the specific mechanism causing the supersymmetry breaking, the soft mass terms are predicted to be [173]

$$m^2_0 = m^2_{3/2}, \quad m_{1/2} = -A_0 = \sqrt{3}\, m_{3/2} \,, \tag{2.60}$$

where we have considered that the VEV of the auxiliary component of the moduli superfield Φ, $\langle F_\Phi \rangle$, which breaks SUSY, is related to the gravitino mass $m_{3/2}$. In this very constrained (thereby predictive)

[14] More rigorously, ϕ is a non-dynamical superfield called the 'conformal compensator', which is dimensionless (thus dim(F_ϕ)=[mass].)

[15] However, it is known that in this minimal set up, sleptons masses are negative, so that the model ends up with tachyonic states. A workaround to this is to add a mass contribution m^2_0 to all the scalar soft masses at some scale, which is large enough to compensate for the negative slepton masses (see e.g. [172]).

scenario, we find the following bound on the gravitino mass coming from fine-tuning arguments

$$m_{3/2} \lesssim \left|\frac{1}{4(-6.1)}\right|^{1/2} \sqrt{\Delta_{\max} m_h^2} \approx 255 \text{ GeV} . \tag{2.61}$$

This implies the following bound on the physical masses

$$\begin{aligned} &m_{\tilde{g}}^{\max} = 980 \text{ GeV}, \quad m_{\tilde{W}}^{\max} = 346 \text{ GeV}, \quad m_{\tilde{B}}^{\max} = 186 \text{ GeV}, \\ &m_{\tilde{H}}^{\max} = 890 \text{ GeV}, \quad \overline{m}_{\tilde{t}}^{\max} = 775 \text{ GeV} . \end{aligned} \tag{2.62}$$

This value for the gluino is already excluded by LHC searches. Conversely, the present exclusion limits on the gluinos implies that in this scenario the fine-tuning to obtain such a gluino mass is 5 per mil.

2.5 Impact of other potential fine-tunings of the MSSM

2.5.1 Fine-tuning to obtain the experimental Higgs mass

From the results of the previous section it is clear that, concerning naturalness, little is gained by going to light stops, say < 800 GeV. Actually, such light stops could entail, as already mentioned in section 2.1.3, an additional fine-tuning since the condition $m_h^{\text{exp}} \simeq 125$ GeV may require the threshold contribution to the Higgs mass to be maximal with high accuracy. The relevant equation is

$$m_h^2 = (m_h^2)_{\text{tree-level}} + \delta_{\text{rad}} m_h^2 + \delta_{\text{thr}} m_h^2 , \tag{2.63}$$

where $\delta_{\text{rad}} m_h^2$ ($\delta_{\text{thr}} m_h^2$) is the radiative (threshold) contribution to m_h^2, approximately given by the X_t-independent (dependent) part of eq. (2.9). We recall that for moderately large $\tan\beta$ we can approximate $X_t = A_t(M_{\text{LE}}) - \mu \cot\beta \simeq A_t(M_{\text{LE}})$. Figure 2.2 shows the dependence of m_h vs $A_t(M_{\text{LE}})$ for different values of the (LE) soft stop-masses, taken as degenerate for simplicity, $m_{Q_3} = m_{U_3} = 500, 1000, 2000$ GeV. If the stops are light, ~ 500 GeV, the correct value of the Higgs boson mass, $m_h = 125 \pm 2$ GeV (the uncertainty is mainly due to the theoretical calculation), requires $A_t(M_{\text{LE}})$ to be precisely fine-tuned[16] at ± 1000 GeV. On the other hand, if the stop masses are ~ 1000 or 2000 GeV, a broad range of values is allowed, $A_t(M_{\text{LE}}) = \pm(2000 \pm 1000)$ GeV, which entails no fine-tuning.

We emphasise that this potential fine-tuning is independent of that required to obtain the correct electroweak scale, which has been analysed in the previous section. Therefore, if both fine-tunings are present we should combine them, i.e. multiply the two small probabilities of obtaining both the correct electroweak scale and the correct Higgs mass. This requires to quantify the fine-tuning associated with the Higgs mass in a fashion which has similar statistical meaning as the measure used for the electroweak fine-tuning. Taking into account the discussion of subsection 2.2.1, we adopt here a fine-tuning measure

[16] Note that in this case the 'standard criterion' to evaluate the fine-tuning, i.e. $\Delta = \partial \log m_h / \partial \log A_t$ is not applicable (indeed, we would conclude from it that there is no fine-tuning at all), since A_t is close to an stationary point, see footnote 5.

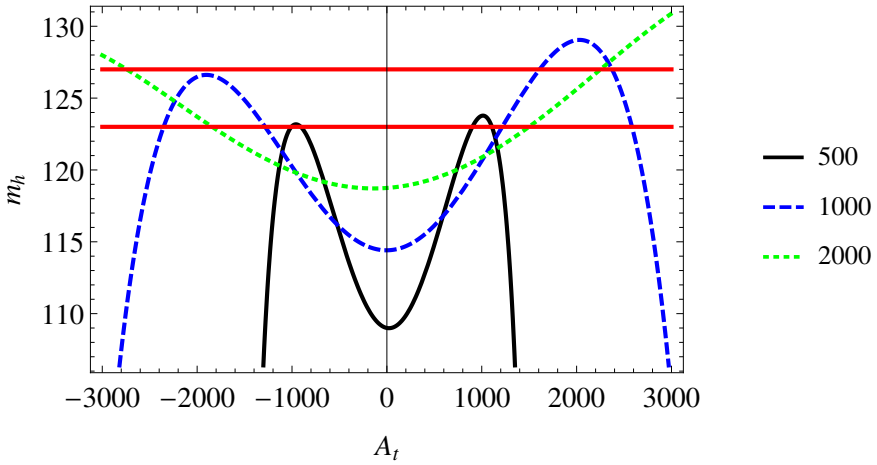

Figure 2.2: The Higgs boson mass, m_h, as a function of the third generation squark masses, $m_{Q_3} = m_{U_3}$. The black-solid line is for $m_{Q_3} = 500$ GeV, blue-dashed for $m_{Q_3} = 1000$ GeV, and green-dotted for $m_{Q_3} = 2000$ GeV. The red horizontal lines denote $m_h = 125 \pm 2$ GeV band. The Higgs boson mass has been calculated using `FeynHiggs 2.10.1` [90, 174–177].

that is also consistent with an interpretation in terms of p-value. In particular, if the stops are light, the fine-tuning is well reflected by the $p-$value of achieving a m_h as large as $m_h^{\rm exp}$ or larger

$$p-\text{value} = \int_{m_h \geq m_h^{\rm exp}} dm_h \; \mathscr{P}(m_h) \; . \tag{2.64}$$

Here $\mathscr{P}(m_h)$ is the probability of a Higgs mass value, given by

$$\mathscr{P}(m_h) = \left| \frac{dX_t}{dm_h} \right| \mathscr{P}(X_t(m_h)) \; , \tag{2.65}$$

where $\mathscr{P}(X_t)$ is the probability distribution of X_t-values.[17] The final step is to assume a shape for $\mathscr{P}(X_t)$. Note here that $X_t \simeq A_t(M_{\rm LE})$ is a low-energy quantity, so it is not much sense to adopt a prior for it. Strictly speaking, the prior should be assumed for the initial, high-energy parameters that determine the value of $A_t(M_{\rm LE})$, (i.e. A_t, M_3, M_2), in a similar fashion as that followed to establish the electroweak fine-tuning in the previous sections. Nevertheless, it is clear from figure 2.2 that, roughly speaking, for $\overline{m}_{\tilde{t}} \gtrsim 1000$ GeV and any sensible theoretical scenario for the soft terms, the $p-$value will be $\sim 20\%$ or larger, which means that there is not really a fine-tuning associated with $m_h \simeq 125$ GeV. Living in this range, the only important fine-tuning is that associated with the electroweak scale. On the other hand, if stops are very light, both fine-tunings should be simultaneously considered. Then, we should multiply the $\Delta_{\rm electroweak}$ parameter by the inverse of the above p-value, which necessarily leads to a per-mil (or

[17] For a range of m_h values, there are four X_t solutions for which $m_h = m_h^{(\rm exp)}$ (see figure 2.2), so $\mathscr{P}(m_h)$ is the sum of four terms, corresponding to those solutions.

even more severe) global fine-tuning. So, interestingly, if the average stop mass is light, say $\lesssim 800$ GeV, the situation is typically more fine-tuned than for heavier stops, $\sim \mathcal{O}(1\ \text{TeV})$.

2.5.2 The Higgs mass and the parameter space selected by naturalness

On the other hand, even if there is no fine-tuning to reproduce the experimental Higgs mass, the requirement $m_h = m_h^{\text{exp}}$ implies a balance between $\delta_{\text{rad}} m_h^2$ and $\delta_{\text{thr}} m_h^2$ in eq. (2.63), which in turn implies a correlation between the initial parameters, especially M_3 (the main responsible for the size of the stop masses) and A_t. This correlation has non-trivial consequences for the electroweak fine-tuning.

To see this, consider Δ_{M_3}, which is usually the most significant fine-tuning parameter. As discussed in subsection 2.3.1, Δ_{M_3} is a function, not only of M_3, but also of M_2 and A_t. E.g. for $M_{\text{HE}} = M_X, M_{\text{LE}} = 1$ TeV, Δ_{M_3} is given by eq. (2.24), where we can note that it will be partially suppressed as long as M_3 and A_t are of the same sign. Therefore, fixing $M_3 > 0$ we would expect the lowest electroweak fine-tuning for $A_t > 0$. On the other side, it is evident from table A.6 that the RG running pushes such A_t towards rather low and possibly negative values. However, low values of A_t at LE are in conflict with the measured Higgs boson mass, as can be seen in figure 2.2. This will result in a tension between low fine tuning of the electroweak scale and the Higgs mass.

This situation is depicted in figure 2.3 where we show the contours of constant Higgs boson mass (black) and fine tuning (red), together in the (high-energy) M_3–A_t plane, for different choices of M_{HE}. For simplicity we have chosen $M_2 = M_3$ and $m_{Q_3}^2 = m_{U_3}^2 = 0$ at HE. Note here that, unless the HE stop masses are very large, their LE values are essentially determined by M_3 (unless M_{HE} is small), so the results of the figures are quite general. The fine-tuning shown corresponds to the largest Δ among the parameters. Usually it is given by Δ_{M_3}, especially when there is a significant amount of running, although for large $|A_t|$ it may be given by Δ_{A_t} (then the red lines become horizontal in the plots). As expected from the above discussion, when the fine-tuning is dominated by Δ_{M_3}, it tends to be lower for $A_t > 0$; however, $m_h \sim 125$ GeV prefers $A_t < 0$. For $M_{\text{HE}} = 2 \cdot 10^{16}$ GeV (upper-left panel of figure 2.3), the Higgs boson mass requires $A_t \sim -2000$ GeV, resulting in a large fine tuning, $\Delta \sim 250$. Moreover, M_3 is required to be larger than ~ 750 GeV which implies that the gluino mass should be (at least) slightly above current exclusion limits. Of course larger values of M_3 result in a more severe fine-tuning, as is clear from the figure. The tension between different low energy requirements is clearly visible in the upper-right panel, $M_{\text{HE}} = 10^{10}$ GeV, where the correct Higgs mass is obtained for $A_t \sim -1500$ GeV with $\Delta \sim 100$ or even smaller, which corresponds to $M_3 \sim 900$ GeV and, again, a physical gluino mass just above the current exclusion limits. Once more, higher values of the gluino mass imply higher fine-tuning, but the increase is not as dramatic as for $M_{\text{HE}} = 2 \cdot 10^{16}$ GeV. On the other hand, for positive A_t a much higher value is required, $A_t \sim 3000$ GeV, which results in a significant increase in fine tuning due to A_t, namely $\Delta_{A_t} \sim 300$. Only for a very low choice of the high-energy scale, $M_{\text{HE}} = 10^4$ GeV, the positive A_t is preferred. In this case the fine-tuning becomes substantially smaller, $\Delta \lesssim 50$. The result is rather independent of M_3 which only enters at two-loops in the Higgs mass and has a very limited impact on other SUSY parameters due to RGE running.

We can therefore conclude that, unless the scale of SUSY breaking transmission is quite low, the least fine-tuned scenarios (i.e. the most 'natural') generically demand negative A_t, a requirement driven by the measured Higgs mass. The corresponding fine-tuning is $\mathcal{O}(100)$, with gluinos only slightly heavier than the current limits, promising interesting discovery prospects at the second run of the LHC with increased centre-of-mass energy.

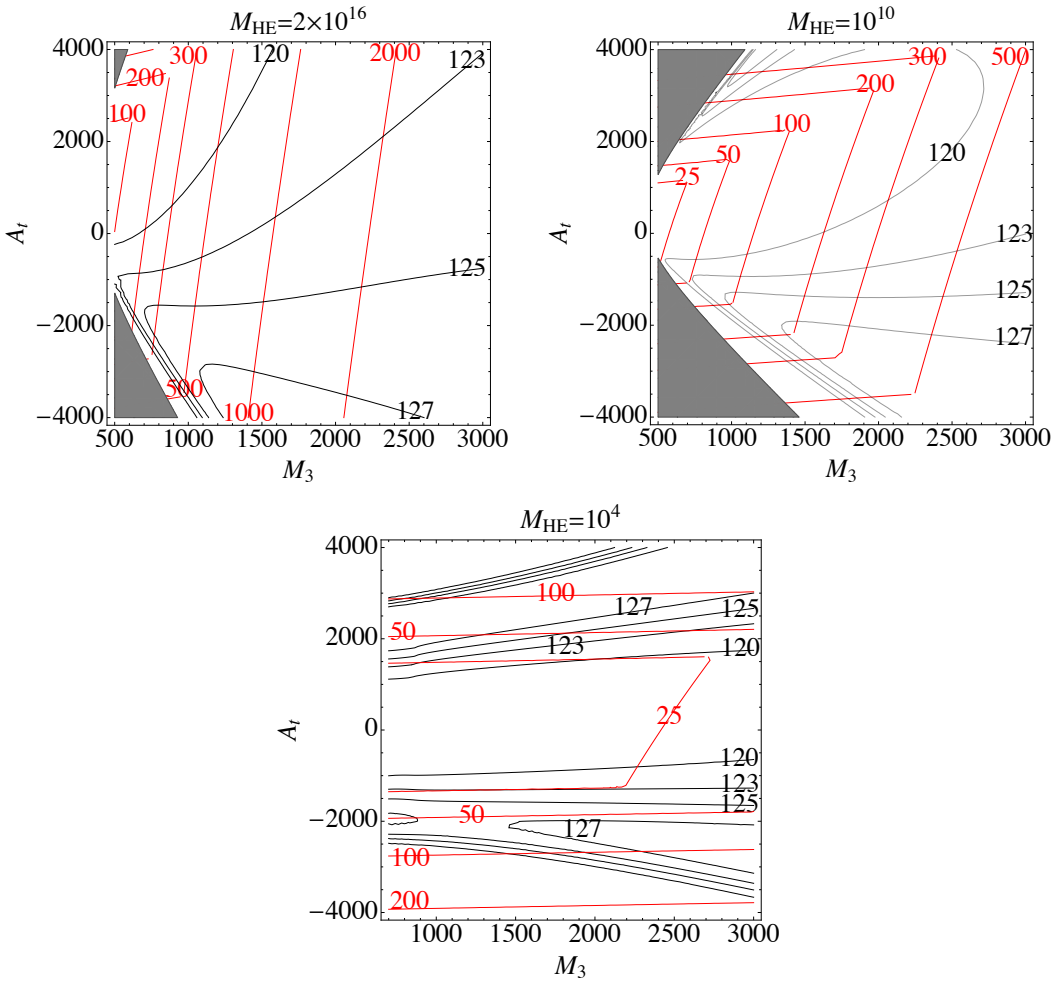

Figure 2.3: Contours of constant Higgs boson mass (black, contours for $m_h = 120, 123, 125, 127$ GeV) and fine-tuning (red), eq. (2.23), in the M_3–A_t plane. We have chosen $M_2 = M_3$ and $m^2_{Q_3} = m^2_{U_3} = 0$ at HE. From left to right to bottom, $M_{\rm HE} = 2 \cdot 10^{16}, 10^{10}, 10^4$ GeV. The unphysical region with tachyonic stops is shaded in grey.

2.5.3 Fine-tuning to obtain large $\tan\beta$

As pointed out in section 2.1.3, a large value of $\tan\beta$ generically requires a small value of $B\mu$ at low energy, which requires a cancellation between the initial value and the radiative contribution from the RG-running. Here, we quantify this fine-tuning and discuss its consequences.

From eq. (2.10), we can write, for $\tan\beta \gg 1$,

$$\tan\beta \simeq \frac{m_{H_d}^2 + m_{H_u}^2 + 2\mu^2}{B\mu} = \frac{m_A^2}{B\mu} \,, \tag{2.66}$$

where m_A is the mass of the pseudoscalar Higgs and all the quantities are understood at the low-energy (LE) scale. As discussed in subsection 2.1.3, the fine-tuning to obtain large $\tan\beta$ can be reasonable quantified using the standard criterion. Namely, for any initial parameter of the theory, θ, we define the associated fine-tuning, $\Delta_\theta^{(\tan\beta)}$

$$\Delta_\theta^{(\tan\beta)} = \frac{\theta}{\tan\beta}\frac{d\tan\beta}{d\theta} = \frac{\theta}{m_A^2}\left[\frac{dm_A^2}{d\theta} - \tan\beta\,\frac{d(B\mu)}{d\theta}\right] \,, \tag{2.67}$$

where we have used eq. (2.66). For large $\tan\beta$, $\Delta_\theta^{(\tan\beta)}$ is normally dominated by the second term within brackets in (2.67)

$$\left|\Delta_\theta^{(\tan\beta)}\right| \simeq \tan\beta \left|\frac{\theta}{m_A^2}\frac{d(B\mu)}{d\theta}\right| \,. \tag{2.68}$$

The next step is to express the LE value of $B\mu$ in terms of the initial (HE) parameters. E.g. assuming $M_{\rm HE} = M_X$, $M_{\rm LE} = 1$ TeV, from table A.7

$$B\mu(LE) \simeq B\mu + 0.46 M_3\mu - 0.35 M_2\mu - 0.34 A_t\mu - 0.03 M_1\mu + \cdots \,, \tag{2.69}$$

where the quantities on the r.h.s. are at the HE scale. Then, the corresponding fine-tuning Δs for the relevant parameters[18], B, M_3, M_2, A_t, read

$$\left|\Delta^{(\tan\beta)}_{\{B,M_3,M_2,A_t\}}\right| \simeq \tan\beta \left|\frac{\mu}{m_A^2}\{B,\ 0.46M_3,\ 0.35M_2,\ 0.34A_t\}\right| \,, \tag{2.70}$$

where we recall that r.h.s. parameters at the HE-scale. Going to particular models, we clearly expect some of the $\{\mu B,\ \mu M_3,\ \mu M_2,\ \mu A_t\}$ quantities to be of the order of m_A^2. Indeed, the HE value of B could be zero, but M_3, M_2 cannot. This means that a certain fine-tuning, $\Delta^{(\tan\beta)} \gtrsim 5-10$ occurs if $\tan\beta \gtrsim 15-30$. Since this fine-tuning has a different nature from that of the electroweak scale (discussed in detail in the previous sections), and given the probabilistic meaning of the fine-tuning parameters, this implies that the two Δs have to be multiplied, $\Delta = \Delta^{(\rm EW)}\Delta_\theta^{(\tan\beta)}$, which generically results in an exaggerated fine-tuning ($> 500-1000$). Notice that these conclusions are alleviated if the HE scale is smaller, since the numerical coefficients in (2.69) decrease. On the other hand, for $\Delta^{(\tan\beta)} \lesssim 5$ there is no really fine-cancellation to obtain the value of $\tan\beta$ and we can ignore the $\Delta^{(\tan\beta)}$ fine-tuning factor.

The conclusion is that very large $\tan\beta$, say $\tan\beta \gtrsim 15-30$, implies a high fine-tuning price, unless the special characteristics of the model lead to a small r.h.s. in (2.68), e.g. if m_A^2 is abnormally large.

[18] Note that $\Delta_\mu^{(\tan\beta)} \simeq 1$.

Let us conclude this section pointing out that for $\tan\beta \gtrsim 30$ the impact of the bottom and tau Yukawa couplings in the RGEs become non-negligible, so the previous numerical values would be modified, but the general conclusion would be the same.

2.6 Conclusions: The most robust predictions of a Natural SUSY scenario

The idea of 'Natural SUSY', understood as a supersymmetric scenario where the fine-tuning is as mild as possible, is a reasonable guide to explore supersymmetric phenomenology, since, as usually argued, the main phenomenological virtue of SUSY is precisely to avoid the huge fine-tuning associated with the hierarchy problem. Much work has been done in the literature to quantify the fine-tuning of a generic MSSM and to extract the features of Natural SUSY. However, these analyses often ignore relevant aspects, such as the 'mixing' of the fine-tuning conditions or the presence of other potential fine-tunings.

In this chapter, we have addressed the supersymmetric fine-tuning in a comprehensive way, including a discussion of the fine-tuning measure and its probabilistic meaning, the mixing of the fine-tuning conditions, the method to extract fine-tuning bounds on the initial parameters and the low-energy supersymmetric spectrum, as well as the role played by extra potential fine-tunings. We have provided tables and plots that allow to easily evaluate the fine-tuning and the corresponding naturalness bounds for any theoretical model defined at any high-energy (HE) scale. Finally, we have analysed in detail the complete fine-tuning bounds for different MSSM scenarios, defined at any HE scale, including the impact that the experimental Higgs mass imposes on the soft terms.

From the results of the previous sections, in what follows we summarise the most important implications of fine-tuning arguments on the MSSM; or, in other words, the features of a Natural-SUSY scenario.

1. For the fine-tuning evaluation, it is crucial to define: i) the initial (independent) parameters of the theoretical setup, ii) the high-energy (HE) scale at which they are defined and iii) the criterion to quantify the fine-tuning.

   We have found that the 'standard' fine-tuning criterion (2.14) normally has a sound statistical meaning, though we should be careful about the implicit assumptions of the prior for the initial parameters (if they do not hold, the standard criterion must be consistently modified). Besides, we have provided tables and plots (see appendix A) that allow to straightforwardly evaluate the fine-tuning for any theoretical setup at any HE-scale.

2. Concerning the electroweak fine-tuning of the MSSM (i.e. that required to obtain the correct electroweak scale), the most robust result is by far that Higgsinos should be rather light, certainly below 700 GeV for $\Delta < 100$, i.e. to avoid a fine-tuning stronger than 1% (all the bounds on SUSY masses scale as $\sqrt{\Delta^{\rm max}}$). This result is enormously stable against changes in the HE scale since the $\mu-$parameter runs proportional to itself (besides the very little running from HE to LE). The

only way of substantially relaxing this limit would be that the $\mu-$parameter were theoretically related to the soft masses in such a way that there occurred a cancellation at LE between μ^2 and $m^2_{H_u}$ (see eq. (2.13)). This is difficult to conceive and, certainly, it is not realised in the known theoretical SUSY frameworks. Incidentally, this upper bound is not far from $M_{\tilde{H}} \simeq 1$ TeV, which is the value required if dark matter is made only of Higgsinos.

3. The most stringent naturalness upper bound, from the phenomenological point of view, is that of the gluino mass. If $M_{\rm HE} \simeq M_X$, we find $M_{\tilde{g}} \lesssim 1.5$ TeV for $\Delta^{\rm max} = 100$, i.e. just around the corner at the LHC. In other words, the gluino mass typically sets the level of the electroweak fine-tuning of the MSSM, which at present is $\mathcal{O}(1\%)$.

   However, this limit is not as robust as that of Higgsinos. First, it presents a strong dependence on the HE-scale (due to the two-loop dependence of the electroweak scale on the gluino mass). Actually, for $M_{\rm HE} \lesssim 10^7$ GeV and $\Delta^{\rm max} = 100$ the upper bound on $M_{\tilde{g}}$ (about 2.7 TeV) goes beyond the present LHC reach. In addition, it could be relaxed if the initial soft parameters (e.g. the gaugino masses) were theoretically related in a favourable way.

4. The upper limit on the wino mass, $M_{\tilde{W}}$, is slightly smaller than that of the gluino, but less relevant for LHC phenomenology. It also has a similar degree of robustness, though it is less dependent on $M_{\rm HE}$. The upper bound on the bino mass, $M_{\tilde{B}}$ is weaker and beyond the LHC reach.

5. A remarkable conclusion is that light stop masses are *not* really a generic requirement of Natural SUSY. Actually, stops could be well beyond the LHC limits without driving the electroweak fine-tuning of the MSSM beyond 1%. Even more, in some scenarios, like universal scalar masses with $M_{\rm HE} = M_X$, stops above 1.5 TeV are consistent with a quite mild fine-tuning of $\sim 10\%$. Hence, the upper bounds on stops are neither stringent nor stable under changes of the theoretical scenario.

   In contrast, as mentioned above, the gluino mass is required to be light with much more generality, although its impact on the fine-tuning depends crucially on the size of $M_{\rm HE}$ (reaching its maximum value for $M_{\rm HE} = M_X$). Consequently, the electroweak scale is typically fine-tuned at 1% in most cases, and having light stops does not help, since the electroweak fine-tuning stems from a single cancellation between terms, essentially between those proportional to M_3^2 and μ^2 in eq. (2.13).

6. In addition to the conventional fine-tuning to obtain the correct electroweak scale, there are two potential extra tunings, namely that of the threshold correction to reproduce $m_h = m_h^{\rm exp}$ when stops are too light, and the tuning of $B\mu$ (at low-energy) to achieve a large $\tan\beta$. It is convenient to avoid these additional fine-tunings, otherwise they have to be combined with (i.e. multiplied by) the electroweak fine-tuning, normally resulting in a gigantic global tuning. Typically, this requires a not-too-light average stop mass, i.e. $\overline{m}_{\tilde{t}} \gtrsim 800$ GeV; and not-too-large $\tan\beta$, i.e. $\tan\beta \lesssim 15-30$. The precise conditions to avoid these tunings are discussed in section 2.5. Note that a small average stop mass is disfavoured, but the mass of the lightest stop could be light or very light.

7. Unless the high-energy scale is quite low, the less fine-tuned scenarios generically demand negative A_t, a requirement driven by the measured Higgs mass. The corresponding fine-tuning is $\mathcal{O}(100)$, with gluinos only slightly heavier than the current limits, which offers interesting prospects for the second run of the LHC.

8. Lastly, the fine-tuning bounds on all the sleptons, the first two generations of squarks and the heavy Higgs states, are, as expected, far beyond the reach of LHC. This is a consequence of the little effect these parameters have on the value of $m_{H_u}^2$ at low energy.

Chapter 3

Reducing the fine-tuning of Gauge-Mediated SUSY Breaking

3.1 GMSB models

Models with gauge-mediated supersymmetry breaking (GMSB) [178–188], have become one of the most popular supersymmetric scenarios. In these models the breakdown of supersymmetry (SUSY) takes place in a hidden sector and is radiatively transmitted to the visible sector via heavy particles (messengers) that are charged under the standard gauge interactions. The main merit of GMSB models is that they automatically imply universality of soft terms (associated with fields with the same quantum numbers), thus avoiding dangerous flavour changing neutral currents (FCNC) effects. On the other hand, these models typically present a high degree of fine-tuning, a problem which is accentuated by the rather high Higgs mass and by the initial absence of (stop) scalar trilinear coupling. In this chapter, we carefully compute this fine-tuning and explore the possibilities to reduce it as much as possible, keeping the minimal matter content.

Let us briefly review the formulation of GMSB models. We start with a set of messenger superfields coupled to the superfield X which breaks SUSY in the hidden sector, thanks to a non-vanishing VEV of its auxiliary component, $\langle F_X \rangle \neq 0$. Typically, the scalar component of X obtains a VEV as well, contributing to the masses of the messengers. Schematically, the relevant superpotential reads

$$W_{\text{mess}} = kX\bar{\Phi}\Phi + \hat{M}_{\text{mess}}\bar{\Phi}\Phi \,, \tag{3.1}$$

where Φ and $\bar{\Phi}$ collectively denote the messenger superfields, k is a dimensionless coupling and $\hat{M}_{\text{mess}}$ is a messenger mass term. In general, there can be different couplings and masses for the various messengers, though usually they are taken universal for simplicity. Then, without loss of generality, we can re-define the scalar component of X either to make $\hat{M}_{\text{mess}} = 0$ or $\langle X \rangle = 0$. The masses of the fermionic components of the messengers are simply $M_{\text{mess}} = \hat{M}_{\text{mess}} + k\langle X \rangle$, while the masses of the

scalar partners arise from the mass-squared matrix

$$\begin{pmatrix} M^2_{\rm mess} & (kF_X)^\dagger \\ (kF_X) & M^2_{\rm mess} \end{pmatrix} . \tag{3.2}$$

Consequently, the requirement of positive masses demands

$$x < 1 , \tag{3.3}$$

where

$$x \equiv \frac{\Lambda}{M_{\rm mess}} , \quad \Lambda \equiv \frac{kF_X}{M_{\rm mess}} . \tag{3.4}$$

If the messengers form complete $SU(5)$ representations, then gauge unification is preserved. Hence, a usual (and somehow minimal) choice is that the messenger sector consists of N_5 copies of fundamental representation, $5+\bar{5}$. With this minimal content, the gauginos and sfermions of the MSSM acquire masses at one-loop and two-loops respectively, namely [189–191]

$$M_i = \frac{\alpha_i}{4\pi}\Lambda N_5 \left[1+\mathscr{O}(x^2)\right] , \tag{3.5}$$

$$m^2_{\tilde{f}} = 2\Lambda^2 N_5 \sum_{i=1}^{3} C_i^{\tilde{f}} \left(\frac{\alpha_i}{4\pi}\right)^2 \left[1+\mathscr{O}(x^2)\right] . \tag{3.6}$$

Here $\alpha_i = g_i^2/4\pi$ stand for the usual gauge couplings, C_i are the corresponding quadratic Casimir (see B.1 for further details). The above expressions are to be understood at the high scale, $M_{\rm HE}$, where the effects of SUSY breaking are transmitted to the observable sector, which coincides with the messenger mass, $M_{\rm HE} = M_{\rm mess}$. Altogether the *minimal* GMSB scenario has only four independent parameters,

$$\{\Lambda, M_{\rm mess}, \mu, B\} \tag{3.7}$$

(plus the discrete $\mathscr{O}(1)$ number N_5), in contrast with the 5 parameters of the constrained MSSM: $\{m_0, M_{1/2}, A, \mu, B\}$. Hence, the GMSB is a highly predictive and well-motivated MSSM, and thus with extremely interesting phenomenology. In this sense, a distinctive feature of GMSB models is that, unlike the constrained MSSM, the soft masses are different for particles with different quantum numbers, although they are independent of the family. This partial universality is enough to avoid dangerous FCNC effects, which is an important success of GMSB.

On the other hand, there is no clear mechanism to generate neither a μ-term for the two Higgses in the superpotential ($W \supset \mu H_u H_d$), nor the corresponding soft bilinear scalar coupling, B. A usual procedure is to assume that μ and B have appropriate values at low energy in order to produce the required VEVs for the two Higgses, $\langle H_u\rangle^2 + \langle H_d\rangle^2 = \langle H_{\rm SM}\rangle^2$, and a reasonable value of $\tan\beta \equiv \langle H_u\rangle/\langle H_d\rangle$. Incidentally, this is exactly the strategy followed in the constrained MSSM.

One of the most problematic aspects of the GMSB scenario is the initial absence of trilinear scalar couplings, $A_i = 0$, in particular that associated with the top, A_t. Although a non-vanishing A_t is generated

along the renormalization group (RG) running from high to low energy, its final value is rather small. The consequence is that the threshold correction to the Higgs mass, m_h, is far from its maximal value, and thus the stop masses must be quite large in order to generate sizeable radiative corrections to m_h, able to reconcile it with its experimental value. Such large stop masses (around 10 TeV) imply in turn a severe fine-tuning in order to obtain the right electroweak (EW) breaking scale. The reason is that, along the RG running, the soft masses of the Higgses (in particular $m^2_{H_u}$) receive important contributions proportional to the stop masses. Then a tuning of parameters (essentially between $m^2_{H_u}$ and μ^2) is necessary to achieve the correct expectation values of the Higgses. As shown in the previous chapter, typically such large stops lead to fine-tunings of one per mil or per ten thousand.

This problem has been addressed in the literature following different strategies [192–217]. Keeping a minimal matter content, the only way out is to devise some mechanism able to generate the desired A-terms ab initio. This requires non-trivial couplings between the messengers and the MSSM superfields in the superpotential. The most studied scenarios involve the generation of A-terms through loops. This idea was first considered in ref. [192] and further developed in ref. [193] and in many other papers [194–199, 201–205, 209, 210]. In ref. [209], Evans and Shih performed an extensive survey of this type of models, finding out those that are the most favourable for the fine-tuning. Also, in ref. [210], Calibbi et al. studied in depth a model of this kind, showing explicitly how a maximal A_t can be generated, allowing for much lighter stops.

Later, a mechanism for tree-level generation of an A_t-term has been explored in ref. [217], where the authors stress the so-called "little A_t^2/m^2 problem" [201], i.e. the fact that a large A_t-term is normally accompanied by a similar or larger sfermion mass-squared, which typically implies an increase in the fine-tuning.

In this chapter, we re-visit the computation and the prospects of the fine-tuning associated with GMSB models and propose a simple scenario, which alleviates this problem as much as it is possible (at least playing with minimal matter content). In section 3.2, we expound the strategy for the computation of the fine-tuning in the MSSM, particularising to the GMSB scenario. We also comment on the importance of a reliable computation of the Higgs mass, especially when the stops are heavy (which is the usual case in GMSB). In this sense, we use the most recent codes for the Higgs mass computation, showing that previous analyses underestimated the fine-tuning of GMSB. In section 3.3, we compute the fine-tuning of the minimal GMSB set up, showing that it is a few per ten thousand. Section 3.4 is devoted to models with radiatively generated A-terms. We refine the fine-tuning calculation for the most favourable case, according to Evans and Shih [209], and compute it for the scenario proposed by Calibbi et al. [210]. We show that, in the latter case, even though the stop masses become smaller than in the minimal GMSB, the fine-tuning does not improve; actually, it becomes more severe. In section 3.5, we consider the tree-level generation of A-terms, in the spirit of ref. [217]. We explore this scenario, simplifying it to some extent and looking for the version that optimises the fine-tuning (which does not necessarily coincides with the one that minimises the little A_t^2/m^2 problem). In the best case scenario, the fine-tuning can be better than one per mil. This is still a severe fine-tuning, but much milder than

other versions of gauge-mediation (at least with minimal observable matter content), and of the same order as in other MSSM scenarios. Finally, in section 3.6 we present our conclusions.

3.2 Computing the electroweak fine-tuning

3.2.1 Fine-tuning of GMSB models

In the previous chapter, section 2.2.1 and appendix A, we have derived the low-energy (LE) values of μ^2 and $m_{H_u}^2$ entering eq. (2.13) as a function of the initial high-energy (HE) values of *all* the soft masses and μ through the RG-equations. Nevertheless, the independent parameters of GMSB are not the HE soft parameters, but Λ, μ, $M_{\rm mess}$ and B, as in eq. (3.7). In particular, for the simplest GMSB, the gaugino and scalar masses are given by eqs. (3.5) and (3.6), while $A_i = 0$. Therefore, neglecting the higher-order corrections in x in eqs. (3.5) and (3.6), i.e. for $x \ll 1$, the r.h.s. of eq. (2.20) is proportional to Λ^2, as well as $\mu(\mathrm{LE})$ is proportional to its initial value at HE. Plugging these expressions in eqs. (2.13) and (2.14) we find that the fine-tuning in Λ and μ simply read

$$|\Delta_\Lambda| = \left| \frac{\Lambda}{m_h^2} \frac{\partial m_h^2}{\partial \Lambda} \right| = 4 \left| \frac{m_{H_u}^2(\mathrm{LE})}{m_h^2} \right| , \tag{3.8}$$

$$|\Delta_\mu| = \left| \frac{\mu}{m_h^2} \frac{\partial m_h^2}{\partial \mu} \right| = 4 \frac{\mu^2(\mathrm{LE})}{m_h^2} . \tag{3.9}$$

Since $\left|m_{H_u}^2(\mathrm{LE})\right| \simeq \left|\mu^2(\mathrm{LE})\right|$, the fine-tuning associated with Λ and μ are almost exactly the same. Actually, they are somehow redundant since the value of m_h^2 arises as a cancellation between both quantities, eq. (2.13).

Of course, for a particular value of Λ, the corresponding $m_{H_u}^2(\mathrm{LE})$ depends on the initial HE scale at which eqs. (3.5) and (3.6) should be evaluated. Therefore, the EW fine-tuning depends on $M_{\rm mess}$. Actually, by continuity we expect a value of $M_{\rm mess}$ for which $m_{H_u}^2(\mathrm{LE}) = 0$, since for large $M_{\rm mess}$, say $M_{\rm mess} = M_X$, $m_{H_u}^2(\mathrm{LE})$ is negative, while for $M_{\rm mess} = M_{\rm LE}$ it is positive. So, there is a particular choice of $M_{\rm mess}$ between these two scales for which $m_{H_u}^2(\mathrm{LE}) = 0$, and therefore the fine-tuning disappears! In other words, for some clever choice of the high-energy scale the simplest GMSB scenario presents a global focus point. We will see soon which scale is that. But, in any case, notice that this is not the end of the story. $M_{\rm mess}$ is an independent parameter itself, so if we allow ourselves to choose it at convenience there is a fine-tuning parameter associated with $M_{\rm mess}$,

$$|\Delta_{M_{\rm mess}}| = \left| \frac{M_{\rm mess}}{m_h^2} \frac{\partial m_h^2}{\partial M_{\rm mess}} \right| \simeq 2 \left| \frac{M_{\rm mess}}{m_h^2} \frac{\partial m_{H_u}^2(\mathrm{LE})}{\partial M_{\rm mess}} \right| . \tag{3.10}$$

This fine-tuning is normally smaller than that associated to Λ, since the dependence of $m_{H_u}^2(\mathrm{LE})$ on $M_{\rm mess}$ is only logarithmic.

Finally, if we go beyond the minimal GMSB model, e.g. by including non-trivial couplings between the messengers and the chiral fields in the superpotential, as mentioned in the Introduction, then there are additional independent parameters (the values of those couplings), whose associated fine-tuning should be computed and taken into account in eq. (2.14). All these issues will be illustrated in the following sections.

3.2.2 The Higgs mass issue

As is well known, radiative corrections to the Higgs mass are needed in the MSSM in order to reconcile it with the experimental value. In order to obtain a reliable expression for the Higgs mass, especially when the stops are heavier than 1 TeV, higher-order corrections are crucial. There exist in the literature several codes that cope with this problem. Among the most recent ones are the last versions of `FeynHiggs` [90, 174–177] and `SusyHD` [218]. It turns out that, typically, previous codes overestimated the Higgs mass in the large-stop-mass regime. This is quite relevant for the computation of the GMSB fine-tuning. In these models, the absence of an initial A_t soft term implies that the threshold correction is far from maximal, hence $m_h \simeq 125$ GeV requires large stop masses. The fact that the latter were underestimated in previous codes implies that the required value of Λ, and thus the fine-tuning, was also underestimated.

In order to illustrate the Higgs mass dependence on the (averaged) stop mass and A_t at the LE scale, we show in figure 3.1 contour lines of constant m_h in the $\overline{m}_{\tilde{t}}$–A_t plane. We have calculated the Higgs mass with `FeynHiggs 2.11.3` [90, 174–177] (dashed cyan lines) and `SusyHD 1.0.2` [218] (solid blue lines) with parameters in the OS-scheme, taking the soft stop masses as degenerate for simplicity, $\mu = 200$ GeV and $\tan\beta = 10$. Note that for a moderately large value of $\tan\beta$, as usual, $X_t \simeq A_t(\mathrm{LE})$.

For a given value of the Higgs mass, the minimum stop mass occurs for the two values of $A_t(\mathrm{LE})$ that maximise the threshold correction, $A_t(\mathrm{LE}) - \mu\cot\beta \simeq \pm 2\overline{m}_{\tilde{t}}$ (note that this value slightly departs from the previous leading-order one, $\pm\sqrt{6}\overline{m}_{\tilde{t}}$). As long as $A_t(\mathrm{LE})$ departs from the maximising value, larger stop masses are required to reproduce the Higgs mass. Typically, for the same stop mass, the `FeynHiggs` result for m_h is ~ 2 GeV larger than that obtained with `SusyHD`. This has a non-negligible impact in the calculation of the fine-tuning. In the next sections, we present our results using both codes.

3.3 The fine-tuning of the minimal GMSB

The minimal GMSB scenario, as it was defined in the Introduction (see eq. (3.7)), has only four independent parameters, $\{\Lambda, M_{\mathrm{mess}}, \mu, B\}$. The tuning associated with Λ is given by eq. (3.8), which is equivalent to that of μ, eq. (3.9). As discussed in section 3.2.1, we expect some value of M_{mess} for which $m^2_{H_u}(\mathrm{LE}) = 0$. This is illustrated in figure 3.2, which shows $m^2_{H_u}(\mathrm{LE})$ vs. M_{mess} for fixed Λ and $N_5 = 3$. Since all gaugino (sfermion) masses are proportional to Λ (Λ^2), then $m^2_{H_u}(\mathrm{LE}) \propto \Lambda^2$, so the corresponding curves for different choices of Λ are easy to draw. The important point is that

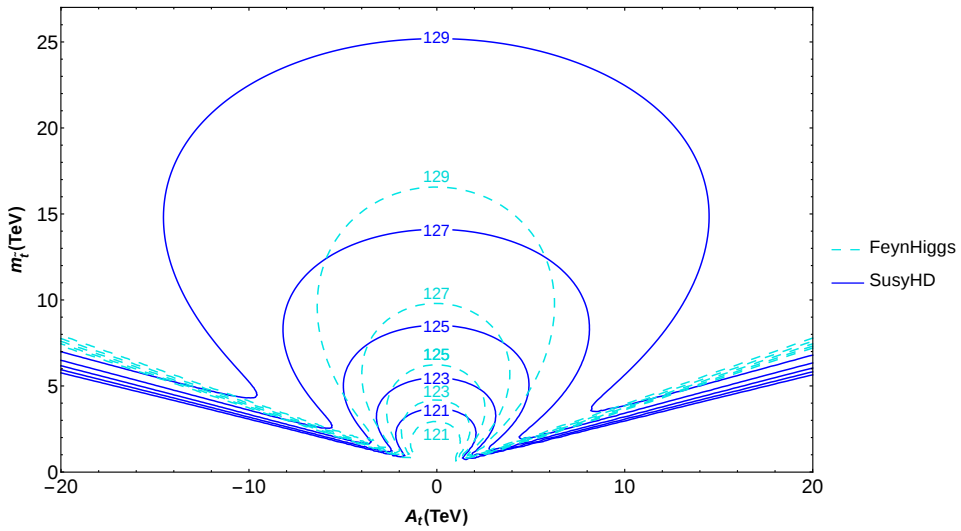

Figure 3.1: Contour lines of constant m_h in the $\overline{m}_{\tilde{t}}$–A_t plane. The dashed cyan lines and the solid blue lines correspond to the Higgs mass calculated with `FeynHiggs` and `SusyHD`, respectively.

for $M_{\rm mess} \simeq 10^5$ GeV we obtain $m^2_{H_u}(\mathrm{LE}) = 0$, independently of the value of Λ, exhibiting a global fixed-point. Thus, for that choice of $M_{\rm mess}$, the electroweak fine-tuning associated with Λ vanishes!

However, there is a drawback that make this solution unworkable. As is clear from the right panel of figure 3.3, the value of Λ required to produce heavy enough stops, so that the Higgs mass is consistent with the experimental measurement, is rather large, $\Lambda \simeq \mathscr{O}(10^6)$ GeV. Consequently, the focus-point solution occurs for $\Lambda > M_{\rm mess}$, which leads to negative mass-squared for some (scalar components of) messengers, that is not acceptable (it would lead to charge and colour breaking).

Figures 3.3, 3.4 and 3.5 show $\overline{m}_{\tilde{t}}$, Δ_Λ and $\Delta_{M_{\rm mess}}$ respectively, in the acceptable region (which does not include the focus-point for the above-mentioned reason), for two choices of the number of messengers, namely $N_5 = 1$ and $N_5 = 3$, and $\tan\beta = 10$. The figures have been obtained using the complete expressions for the initial values of the soft masses given in B.1. The two fine-tunings were evaluated along the lines of subsection 3.2.1, with the RG-parameters computed as in chapter 2. [1]

Notice that the fine-tuning associated with $M_{\rm mess}$, which is an independent parameter in this context, is always lower than Δ_Λ.

The bottom line is that the electroweak fine-tuning for the minimal GMSB is very large, $\mathscr{O}(10^4)$ for $m_h = 125$ GeV, evaluated with `SusyHD`, although it can be below 10^3 if we compute m_h with `FeynHiggs` and allow $m_h = 123$ GeV, to account for theoretical uncertainties. From now on we will take this conservative value for m_h to compare the fine-tuning of different scenarios, independently of the code used to compute m_h. The main cause of the large fine-tuning is the small value of A_t, which leads to large stop masses in order to reproduce the experimental Higgs mass. Those stop masses require in turn a large value of Λ, increasing the value of $m^2_{H_u}(\mathrm{LE})$ and thus the fine-tuning. The latter is actually more

[1] The only difference is the LE scale that was now chosen to be 10 TeV.

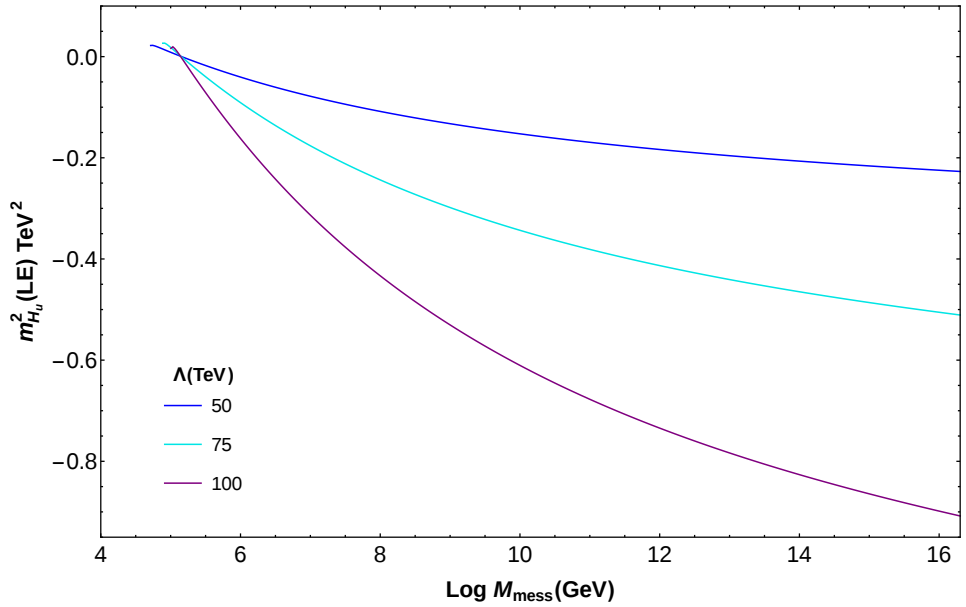

Figure 3.2: $m^2_{H_u}(\text{LE})$ vs. M_{mess} for $N_5 = 3$ and different choices of Λ. Note the focus-point behaviour around $M_{\text{mess}} \simeq 10^5$ GeV.

severe than previous estimates in the literature since previous codes used to evaluate the Higgs mass did not work with enough accuracy for large stop masses.

Consequently, in order to make the GMSB scenario less fine-tuned we have to go beyond this minimal setup, exploring mechanisms to incorporate a non-vanishing A_t. This is the subject of the next two sections.

3.4 Models with radiatively generated A-terms

The possibility of generating A-terms through loops thanks to messenger-MSSM interactions has been investigated in many papers; see refs. [194–199, 201–205, 209, 210]. In ref. [209], Evans and Shih performed an extensive survey of this type of models. Namely, they considered both, scenarios with cubic MSSM-MSSM-messenger or MSSM-messenger-messenger operators in the superpotential. Besides, they distinguished between cases where the relevant messengers are squark-like or Higgs-like. They concluded that all scenarios had fine-tunings to the sub-percent level. Actually, all scenarios analysed had tunings at the sub-per-mil level, except one, based on the coupling

$$\Delta W = \lambda\, U H_u \phi_{10,Q}, \tag{3.11}$$

which had $\Delta \simeq 850$. Here, $\phi_{10,Q}$ denotes the Q-like component of a messenger in the 10 representation of $SU(5)$ (for further details see ref. [209]). The corresponding one-loop-generated A-term can be read from B.2. The mentioned fine-tuning represents an appreciable improvement over the minimal GMSB

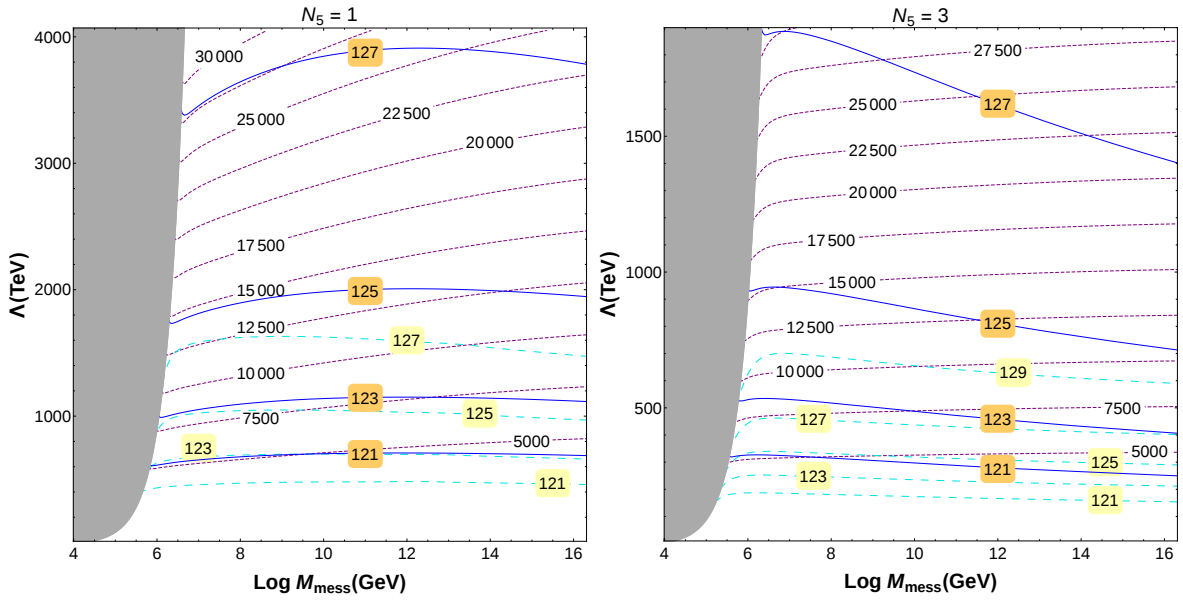

Figure 3.3: Contours of the average stop mass (purple lines) and the Higgs mass in the $M_{\rm mess}$–Λ plane for the minimal GMSB and different choices of N_5. The dashed cyan lines and the solid blue lines correspond to the Higgs mass calculated with `FeynHiggs` and `SusyHD`, respectively. The $\Lambda \geq M_{\rm mess}$ region is shaded in grey.

model, analysed in the previous section, where the minimal fine-tuning was slightly above 1000, and typically was $\gtrsim 2500$.

Nevertheless, in order to compare the performance of both models, the tuning must be evaluated with the same criteria. Here, we re-analysed the Evans and Shih model defined by eq. (3.11) in an improved fashion, consistent with the analysis of the minimal case (section 3.3). First of all, we include the exact two-loop corrections to the scalar masses, whereas in ref. [209] these corrections were approximated by the first term in their x-expansion (x has been defined in eq. (3.4)); see B.2 for further details. Second, as discussed in previous sections, in order to calculate the Higgs mass we have used the more recent versions of `FeynHiggs` and `SusyHD`, while the authors of ref. [209] used the `SOFTSUSY` code [219]. It is known that, for given supersymmetric parameters, `SOFTSUSY` produces a larger value for m_h especially when the stops are heavy [218, 220], which is the typical case in GMSB. Consequently, their results are more optimistic than ours. On the other hand, we have allowed the theoretical value of m_h to be as low as 123 GeV to account for theoretical uncertainties, whereas in ref. [209] m_h was fixed at 125 GeV. Finally, the fine-tuning criterion in ref. [209] was also (slightly) different. Instead of considering Λ as an independent parameter, and thus evaluating Δ_Λ, they considered a bunch of independent parameters: $\Lambda_i = \{g_i^2\Lambda^2, y_i^2\Lambda, \lambda\Lambda, \Lambda_{1-loop}\}$ (see ref. [209] for the precise definition of Λ_{1-loop}). Certainly, the various contributions to $m_{H_u}^2$(LE) are proportional to the various (squared) couplings in the theory (gauge couplings, Yukawa couplings and the λ-coupling) times Λ. In this sense, their criterion captures the level of "conspiracy" between different terms. However, all those couplings (except λ) are fixed by experiments, and it is contrived to examine variations of parameters which are fixed [97, 165, 221].

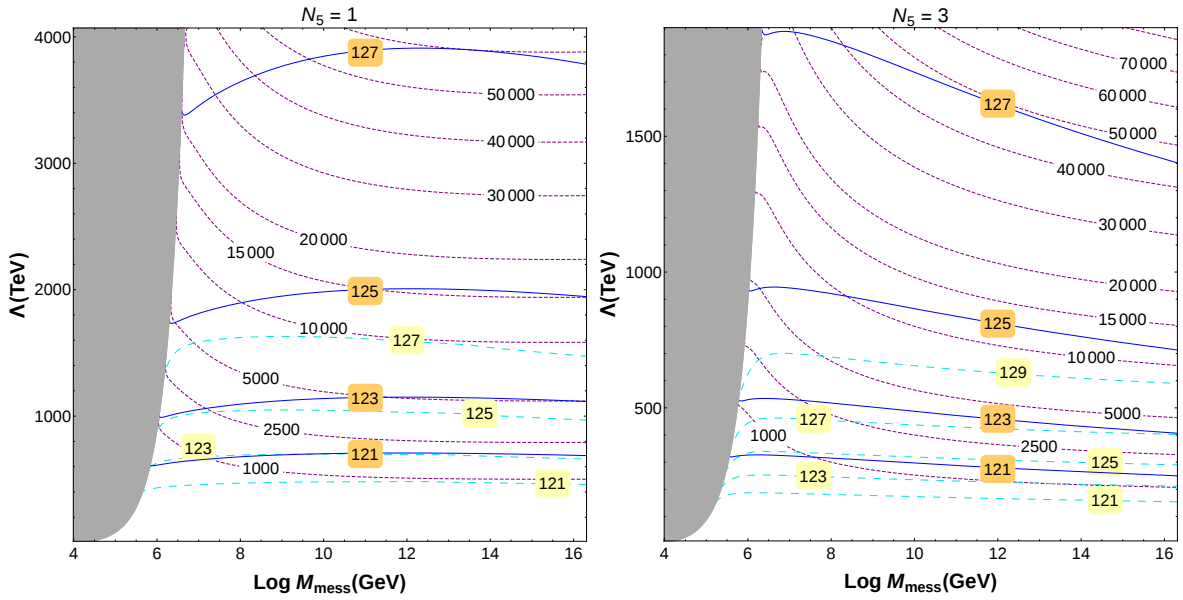

Figure 3.4: Contour lines of constant Δ_Λ (purple lines) and the Higgs mass calculated with `FeynHiggs` (dashed cyan lines) and `SusyHD` (solid blue lines) in the $M_{\rm mess}$–Λ plane, for minimal GMSB and different values of N_5. The unphysical region, $\Lambda \geq M_{\rm mess}$, is shaded in grey.

Then, the possible variations of all those terms arise from those of Λ and are thus correlated. This criterion normally increases the fine-tuning, since a certain variation in $\log\Lambda$ modifies more the value of $\log m^2_{H_u}(\mathrm{LE})$ than the same variation in $\log\Lambda_i$.

Figure 3.6 shows the fine-tuning, Δ in the plane $\lambda - \Lambda$, evaluated according to our criterion for the model defined by the extra term (3.11) and $M_{\rm HE} = M_{\rm mess} = 10^8$ GeV, $N_{10} = 1$ and $\tan\beta = 10$. For small λ, the fine-tuning is dominated by Δ_Λ, while for large λ by Δ_λ; thus the kink in the contour lines. The minimal fine-tuning is about 1500 when m_h is computed with `SusyHD`, and close to 250 when computed with `FeynHiggs`. This represents a certain improvement w.r.t. the minimal GMSB.

In a later paper, Calibbi et al. (CPZ) [210] considered a version of radiatively generated A-terms. More precisely, they considered the following term in the messenger superpotential:

$$\Delta W = \lambda_U Q_3 U_3 \Phi_{H_u} \,, \tag{3.12}$$

where Q_3, U_3 are the third generation of quark superfields and Φ_{H_u} is the SU(2) doublet (included in the messenger superfield Φ) with the same quantum numbers as H_u. Again, a trilinear scalar coupling for the stops is generated at one-loop, see B.2. One can imagine that the λ_U coupling is related in some way to the standard Yukawa couplings, which justifies neglecting similar terms for other superfields. In addition to the trilinear coupling, there appear new contributions to the scalar masses [197, 210] at one-loop and two-loops; see B.2.

Next we re-visit this model in greater detail, to show the obstacles to reduce the fine-tuning in this kind of scenarios. For large enough λ_U (not far from the top Yukawa coupling), the generated A_t-term

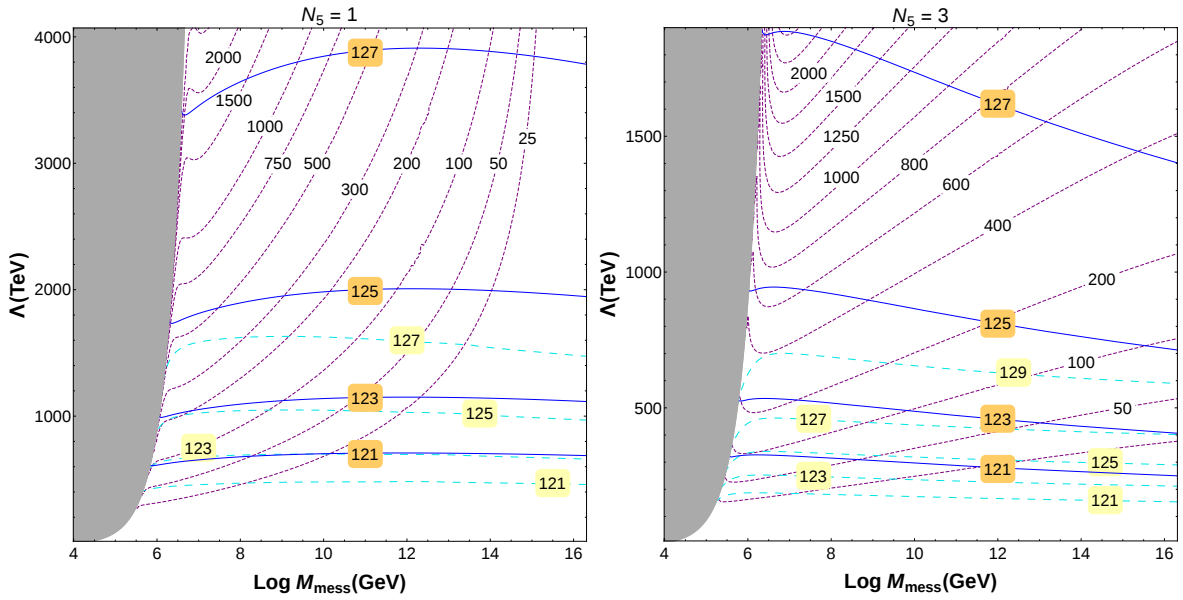

Figure 3.5: Contours of $\Delta_{M_{\rm mess}}$ (purple lines) and the Higgs mass computed with `FeynHiggs` (dashed cyan lines) and `SusyHD` (solid blue lines) in the $M_{\rm mess}$–Λ plane, for minimal GMSB and different choices of N_5. The grey shaded region corresponds to $\Lambda \geq M_{\rm mess}$.

can have the appropriate size at low energy to maximise the threshold correction to the Higgs mass or, in other words, to minimise the magnitude of the stop masses in order to reconcile m_h with the experimental value. According to CPZ, the requirement $m_h > 123$ GeV can be fulfilled for much lighter stops than in the minimal GMSB model. They find that, for $N_5 = 1$, the approximate optimal choice is $\lambda_U \simeq 0.7$, for which the lightest stop can be as light as 400 GeV if the messenger mass is suitably chosen. The second stop, however, is much heavier, close to 2 TeV. Consequently, the Λ scale might be much lower than in the minimal GMSB, which apparently would amount to a substantial reduction in the electroweak fine-tuning. In addition, the rest of the super-particles (squarks, gluinos, etc.) are also closer to the LHC reach since their masses are proportional to Λ. It should be mentioned here that CPZ used `SOFTSUSY` to compute m_h, so, as discussed above, their conclusions are in the optimistic range.

Nevertheless, this scenario has some shortcomings. Due to the new contributions to scalar masses, $m^2_{H_u}$ obtains a negative correction, which can be very important. As a consequence the low-energy (absolute) value of $m^2_{H_u}$ tends to be larger, which implies a more severe electroweak fine-tuning in eq. (2.13). Hence, the reduction of the fine-tuning due to the lighter stops (and thus smaller Λ) is compensated by this effect. Actually, CPZ noted that, in spite of having lighter stops, the value of μ, and thus the fine-tuning, does not decrease appreciably. Besides, compared with the minimal GMSB scenario, the model contains an extra parameter, namely the λ_U coupling. Since we do not know the theoretical connection of this with the other parameters of the model, $\{\Lambda, M_{\rm mess}, \mu, B\}$, its fine-tuning parameter, Δ_{λ_U}, should be computed and considered in eq. (2.14), as we actually did for the Evans and Shih model above. As we will see soon, for large values of λ_U, which CPZ consider interesting for LHC phenomenology, the value of Δ_{λ_U} becomes very important and even larger than Δ_Λ.

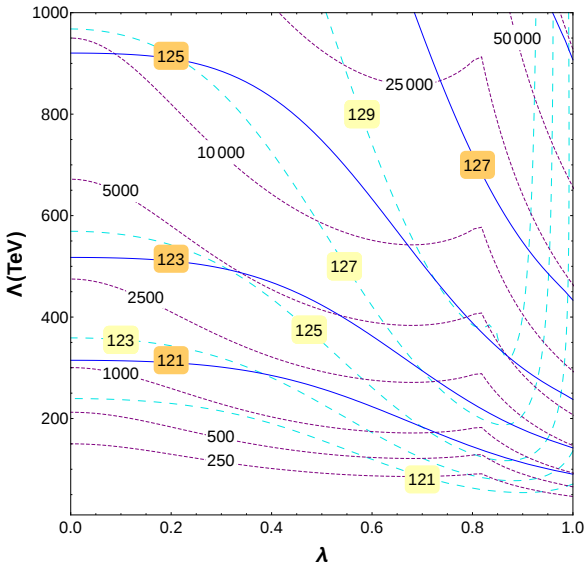

Figure 3.6: Contours of Δ, defined as $\mathrm{Max}\{\Delta_i\}$(purple lines) and the Higgs mass computed with `FeynHiggs` (dashed cyan lines) and `SusyHD` (solid blue lines) in the λ–Λ plane, for the model defined in eq. (3.11), $M_{\rm mess} = 10^8$ GeV and $N_{10} = 1$.

Concerning the stop masses, according to CPZ, the choice $\lambda_U = 0.75$ leads to stops as light as possible. We have checked that for that value of λ_U, stops are lighter than in the minimal GMSB scenario, though the effect is not dramatic. Demanding $m_h > 123$ GeV requires stops above ~ 6 TeV (if m_h is computed with `SusyHD` or ~ 4 TeV with `FeynHiggs`), somewhat smaller than for the minimal GMSB.

Figures 3.7 and 3.8 illustrate some of the previous points. To avoid proliferation of plots, we have focused on the $N_5 = 1$ case, but the results for other values of N_5 are analogous. In addition, we have fixed $\tan\beta = 10$ and $M_{\rm LE} = 10$ TeV. Note that the figures show a "threshold line" close to the $\Lambda \geq M_{\rm mess}$ (grey) region, which cannot be crossed. This virtual line signals when a stop mass-squared becomes negative. Notice here that when Λ approaches $M_{\rm mess}$ the initial values of the soft terms receive important contributions, which are negligible otherwise; see B.2.

Concerning fine-tuning things worsen. Figure 3.7 shows the fine-tuning associated with Λ in the $M_{\rm mess}$–Λ plane for $\lambda_U = 0.25, 0.75$. While for $\lambda_U = 0.25$ the fine-tuning (~ 6000 with `SusyHD`, ~ 2500 with `FeynHiggs`) is only slightly worse than in the minimal GMSB, for $\lambda_U = 0.75$ it becomes more than two times worse. So it does not pay off to go to large values of λ_U, even if the stops become lighter.

Actually, for large λ_U, the fine-tuning associated with λ_U itself becomes even bigger than that associated with Λ. This can be checked in figure 3.8. While for $\lambda_U = 0.25$ the Δ_{λ_U}-parameter is large, but smaller than Δ_Λ, and thus can be ignored; for $\lambda_U = 0.75$ it becomes larger. The situation becomes worse as λ_U is increased.

The previous discussion is well summarised by figure 3.9. In the left panel of figure 3.9, we show contour lines of constant m_h and (averaged) $m_{\tilde{t}}$ in the λ_U–Λ plane for a fixed value of the messenger

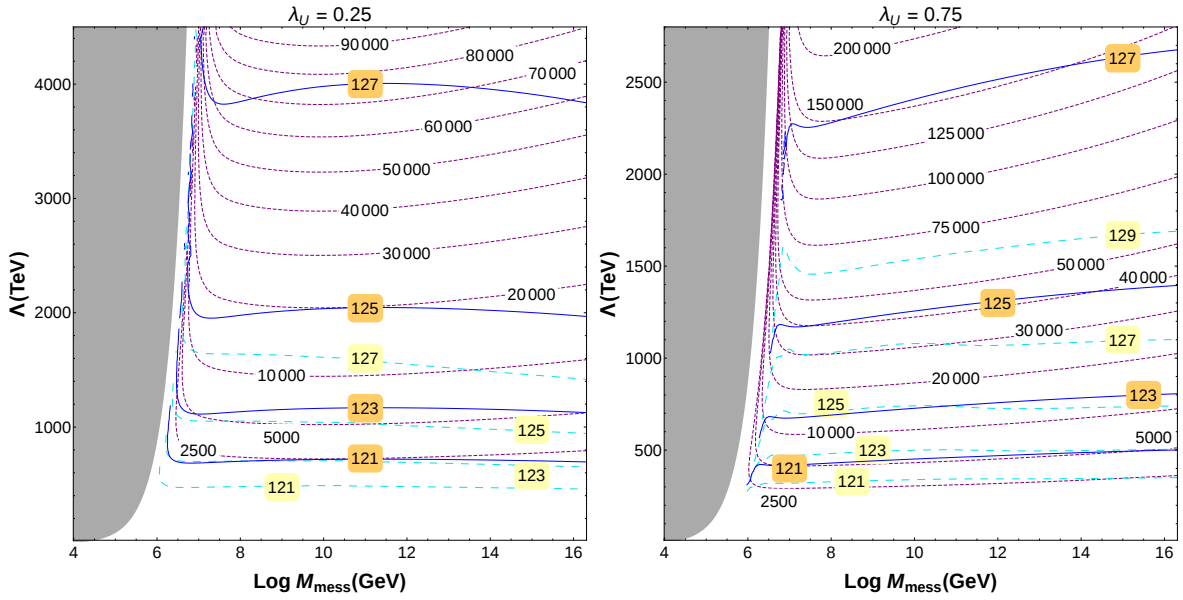

Figure 3.7: Contours of constant Δ_Λ and the Higgs mass calculated with `FeynHiggs` (dashed cyan lines) and `SusyHD` (solid blue lines) in the $M_{\rm mess}$–Λ plane, for the CPZ model and two different choices of λ_U. The grey shaded region corresponds to $\Lambda \geq M_{\rm mess}$.

mass, namely $M_{\rm mess} = 10^8$ GeV (for other choices of $M_{\rm mess}$ the results are essentially equivalent). It can be noted that the stop mass is minimised for $\lambda_U \sim 0.7$, in agreement with CPZ results. The right panel of figure 3.9 shows contour lines of constant fine-tuning, i.e. the Δ_Λ parameter. Clearly, the best choice is $\lambda_U = 0$, i.e. the minimal GMSB scenario. As a matter of fact, for $\lambda_U \gtrsim 0.55$ the fine-tuning associated with λ becomes dominant, i.e. $\Delta_{\lambda_U} > \Delta_\Lambda$, so the situation becomes even worse. On the other hand, notice also that for large λ_U lines are cut. This is due to the (left-handed) slepton masses falling below the present bounds. This imposes an absolute bound on the size of λ_U.

The final conclusion is that, generically, A-terms generated radiatively thanks to the couplings of messengers to the observable fields in the superpotential fail to improve appreciably the fine-tuning of the minimal GMSB model. In some cases they lead to a milder fine-tuning but hardly better than the one per mil level.

3.5 A simple scenario

In this section, we consider a simple GMSB scenario that in principle can yield a fine-tuning as mild as possible. The model is a variation of the idea put forward by Basirnia et al. in ref. [217], namely, the generation of the desired sizeable A_t-term by the exchange of messengers at tree level.

Let us start with the usual GMSB superpotential, eq. (3.1), enhanced with two additional terms,

$$\Delta W = (kX + M_{\rm mess})\Phi_{H_u}\Phi_{H_d} + \lambda Q_3 U_3 \Phi_{H_u} + \lambda' X H_u \Phi_{H_d} \ . \tag{3.13}$$

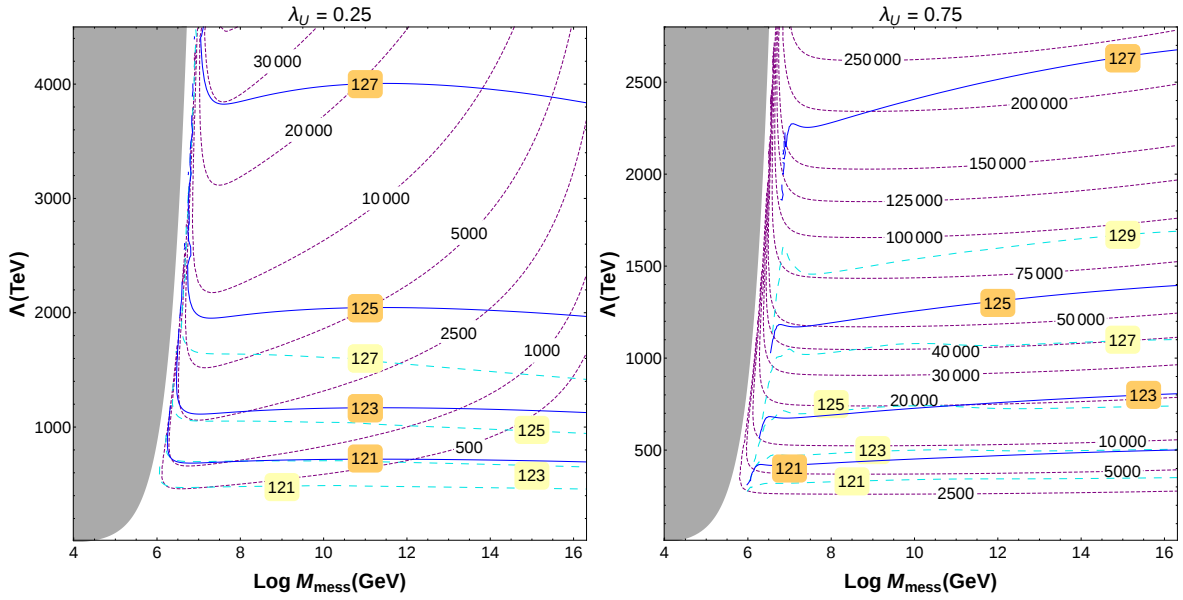

Figure 3.8: Contour lines of Δ_{λ_U} and the Higgs mass computed with `FeynHiggs` (dashed cyan lines) and `SusyHD` (solid blue lines) in the $M_{\rm mess}$–Λ plane for the CPZ model and two different values of λ_U. The unphysical region, $\Lambda \geq M_{\rm mess}$, is shaded in grey.

The term proportional to λ coincides with that used in the CPZ model, but now there is an extra term, proportional to λ', which directly couples the X superfield to the messengers and the standard Higgs fields. As mentioned in section 3.1, we can always re-define the scalar component of X so that $\langle X \rangle = 0$. Now, however, such a re-definition would induce extra terms in W. So, we will assume for simplicity that the X superfield, which couples to H_u and Φ_{H_d} as in eq. (3.13) with no additional terms in W, has a small VEV compared to $M_{\rm mess}$. Then, we can eliminate the heavy messengers using $\frac{\partial W}{\partial \Phi_{H_u}} = \frac{\partial W}{\partial \Phi_{H_d}} = 0$. The resulting effective superpotential reads

$$\Delta W_{\rm eff} \sim -\frac{\lambda \lambda'}{kX + M_{\rm mess}} X Q_3 H_u U_3 \,. \tag{3.14}$$

Expanding in powers of X and replacing it by its scalar component, $\langle X \rangle$, we find a small correction to the standard top Yukawa term, $Y_t \to Y_t - \lambda \lambda' \frac{\langle X \rangle}{M_{\rm mess}}$. Replacing X by its F-component, we obtain a trilinear scalar coupling for the stops, with a coefficient

$$y_t A_t = -\lambda \lambda' \frac{F_X}{M_{\rm mess}} \left[1 + \mathcal{O}(\langle X \rangle / M_{\rm mess})\right] \simeq -\frac{\lambda \lambda'}{k} \Lambda \,. \tag{3.15}$$

Note that the generated A_t-term arises at tree level, so the combination of couplings $\lambda \lambda'/k$ must be small.

The above model is a modification of the model proposed in ref. [217]. The main difference is that the authors of ref. [217] got a sufficiently small A_t by assuming that there was a second spurion, X', with $F_{X'} < F_X$, which was the field coupled as in eq. (3.13) (see their eq. (1.3)). Here we show that, in fact,

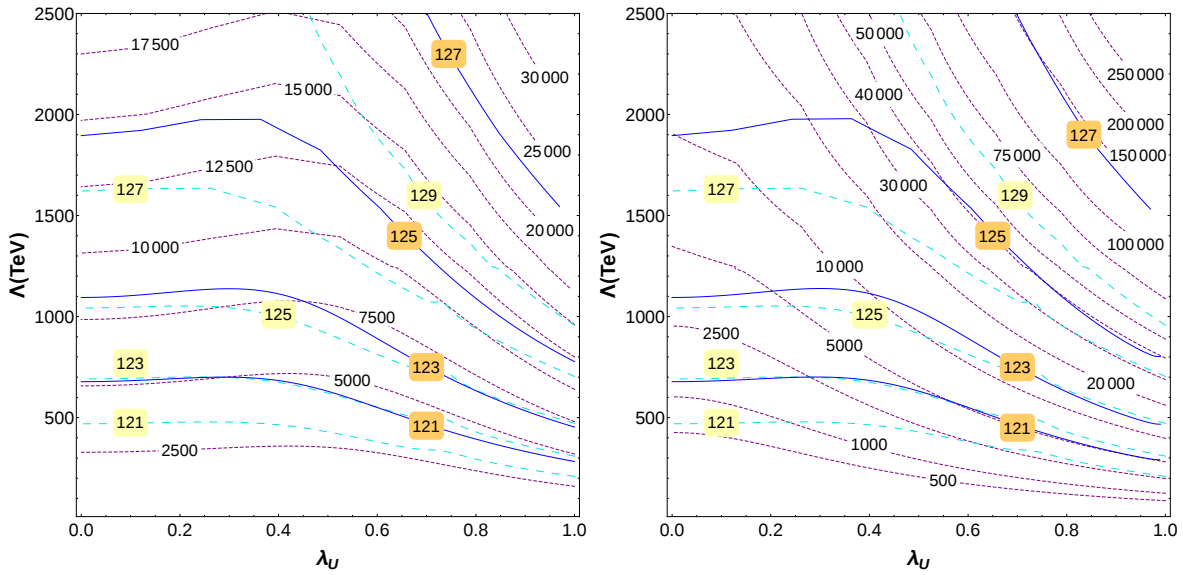

Figure 3.9: Left: contours of constant average stop mass and the Higgs mass calculated with `FeynHiggs` (dashed cyan lines) and `SusyHD` (solid blue lines) in the Λ–λ_U plane for the CPZ model, $M_{\rm mess} = 10^8$ GeV and $N_5 = 1$. Right: contour lines of Δ_Λ and the Higgs mass in the same plane.

this is not necessary. We can live just with one spurion, provided the λ' coupling (which was implicitly assumed to be $\lambda' = 1$ in ref. [217]) is small enough. This represents a conceptual simplification.

Unfortunately, as stressed in ref. [217], after integrating out the Φ_{H_u}, Φ_{H_d} superfields, we not only obtain the modified superpotential eq. (3.14), but also a modified Kähler potential, K. Namely, replacing $\Phi_{H_u} = -\lambda' X H_u / M$ in the canonical K, we find a term

$$\Delta K_{\rm eff} = \frac{|\lambda'|^2}{M^2} |X|^2 |H_u|^2 \,. \tag{3.16}$$

in the effective Kähler potential, which leads to an extra contribution to $m^2_{H_u}$,

$$\delta m^2_{H_u} = -\left|\frac{\lambda' F_X}{M}\right|^2 = -\left|\frac{\lambda' \Lambda}{k}\right|^2 \,. \tag{3.17}$$

Comparing eq. (3.15) with eq. (3.17), we see that it is not possible to arrange the parameters so that $\delta m^2_{H_u}$ is small, since

$$\left|\frac{(y_t A_t)^2}{\delta m^2_{H_u}}\right| = |\lambda|^2 \,. \tag{3.18}$$

In other words, a sizeable $y_t A_t$ implies a sizeable and negative $\delta m^2_{H_u}$. Such a result is a manifestation of the so-called 'little A_t^2/m^2 problem' discussed in [201], i.e. the fact that a large A-term is normally accompanied by a similar or larger sfermion mass-squared. This is bad news for naturalness since the

fine-tuning in Λ is proportional to $|m_{H_u}|^2$, see eq. (3.8). Consequently, for a given value of $y_t A_t$ we should minimise the (negative) size of $\delta m^2_{H_u}$ as much as possible. One obvious way is to consider a large λ, without spoiling the perturbativity regime, $\lambda \leq \mathcal{O}(1)$. In contrast, increasing the number of messengers does not help since there is always a unique combination of them that couples to $Q_3 U_3$ in eq. (3.13). This scenario is illustrated in figure 3.10 for $M_{\rm mess} = 10^8$ GeV, $N_5 = 1$ and $\lambda = 1.5$. We can see that, for a given value of m_h, there is a value of the $\lambda\lambda'/k$ combination that nearly minimises the stop masses and the fine-tuning. Assuming, as usual, a ~ 2 GeV theoretical uncertainty in the determination of m_h, it turns out that the average stop mass can drop to 2.2 TeV while the fine-tuning can be ~ 2500. Comparing with the minimal GMSB for the same messenger mass (figures 3.4 and 3.5), we see that stop masses can be much smaller, though the fine-tuning does not appreciably improve. In fact, it is clearly worse than for the Evans and Shih model of eq. (3.11), see figure 3.6, although it is much better than for the CPZ model.

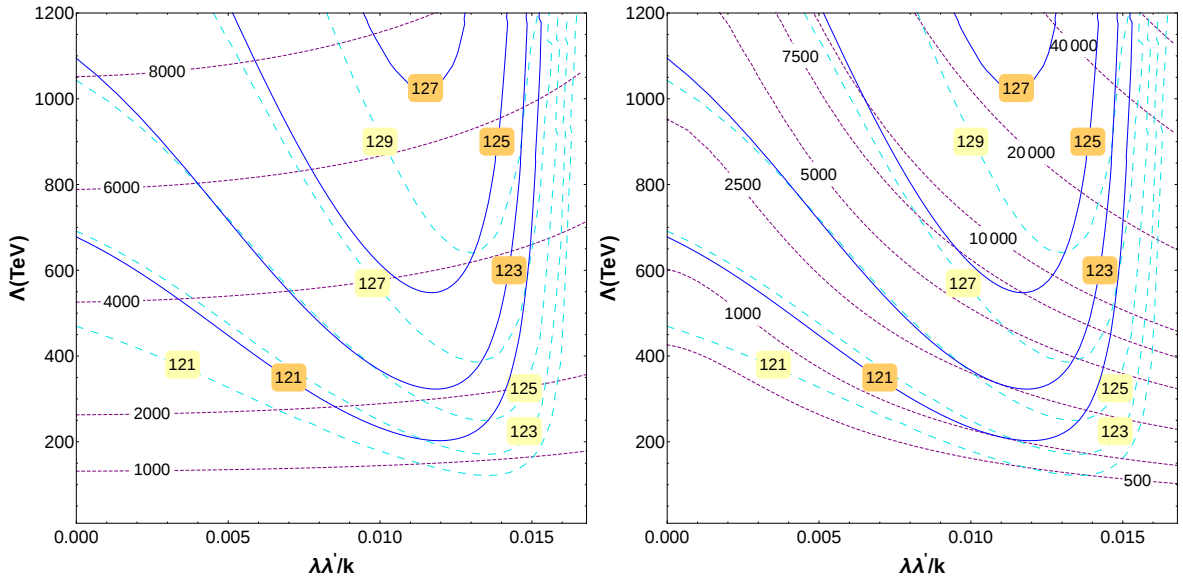

Figure 3.10: Model of eq. (3.13). Left panel: contour lines of the average stop mass and the Higgs mass calculated with `FeynHiggs` (dashed cyan lines) and `SusyHD` (solid blue lines) in the Λ–$\frac{\lambda\lambda'}{k}$ plane for $M_{\rm mess} = 10^8$ GeV, $\lambda = 1.5$ and $N_5 = 1$. Right panel: contours of Δ_Λ and Higgs mass in the same plane.

An alternative, and improved situation occurs when the relevant messengers are not Φ_{H_u}, Φ_{H_d}, but $\Phi_u, \Phi_{\bar{u}}$, with the same quantum numbers as $U_3, \overline{U}_3$ [217]. In this case, the relevant superpotential is similar to that of eq. (3.13),

$$\Delta W = (kX + M_{\rm mess})\Phi_u \Phi_{\bar{u}} + \lambda Q_3 \Phi_u H_u + \lambda' X U_3 \Phi_{\bar{u}} \,, \tag{3.19}$$

and the effective superpotential, after integration of $\Phi_u, \Phi_{\bar{u}}$, reads exactly as that of eq. (3.14). Now, the effective Kähler potential leads to a negative contribution to the singlet squark mass-squared, $\delta m^2_{\tilde{u}_3}$ (instead of $\delta m^2_{H_u}$), with the same size as before, i.e. the r.h.s. of eq. (3.17). This is much less dangerous

than the previous $\delta m^2_{H_u}$. Actually, reducing the size of the stop masses lowers the final absolute value of $m^2_{H_u}$, thus alleviating the fine-tuning.

However, as above, the size of this negative contribution to $\delta m^2_{\tilde{u}_3}$ is limited by the requirement of perturbativity for λ. Actually, we have also to ensure that the VEVs of the coloured scalar fields are vanishing. This implies in particular that the final value of $m^2_{\tilde{u}}$ should be kept positive, which entails an upper bound on A_t, namely

$$|\lambda' F| < m^{(0)}_{\tilde{u}_3} M_{\rm mess} \quad \Rightarrow \quad |y_t A_t| < \lambda m^{(0)}_{\tilde{u}_3} \,, \tag{3.20}$$

where $m^2_{\tilde{u}_3} = (m^{(0)}_{\tilde{u}_3})^2 + \delta m^2_{\tilde{u}_3}$, i.e. $m^{(0)}_{\tilde{u}_3}$ is the standard value of the minimal version of GMSB. We can refine this analysis by studying the square-mass matrix for the $\{\phi_{\bar{u}}, \phi_u, \tilde{u}_3\}$ fields, i.e. before integrating out the messengers. This can be obtained from the scalar potential associated with the superpotential (3.19):

$$M^2_u = \begin{pmatrix} M^2_{\rm mess} & (kF_X)^\dagger & \\ (kF_X) & M^2_{\rm mess} & (\lambda' F_X)^\dagger \\ & (\lambda' F_X) & (m^{(0)}_{\tilde{u}})^2 \end{pmatrix} . \tag{3.21}$$

Stability requires the two order-two minors of the above matrix to be positive. This coincides with the stability conditions eqs. (3.3, 3.4) and (3.20), respectively. In addition, we must demand the determinant to be positive,

$$M^2_{\rm mess} \left[M^2_{\rm mess} (m^{(0)}_{\tilde{u}})^2 - |\lambda' F|^2 \right] - |kF|^2 (m^{(0)}_{\tilde{u}})^2 \; > \; 0 \tag{3.22}$$

This condition becomes relevant if any of the other two conditions are nearly saturated.

Another aspect of this setup is that the messengers cannot belong anymore to the $(5+\bar{5})$, since this does not accommodate an U_3 field. Now, we have to consider copies of $(10+\overline{10})$, although again only one combination of messengers contributes to the above $\lambda Q_3 \Phi_u H_u$ coupling.

The fact that the $(10+\overline{10})$ representation contains pieces with the same quantum numbers as $Q_3, \overline{Q}_3$, say $\Phi_Q, \Phi_{\bar{Q}}$, allows for additional possibilities. In particular, we can add new pieces, $\lambda \Phi_Q U_3 H_u + \lambda' X Q_3 \Phi_{\bar{Q}}$, to the superpotential in eq. (3.19) (for simplicity, we assume that the couplings have the same size as above). Then, after integrating out all the messengers, both $m^2_{\tilde{U}_3}$, $m^2_{\tilde{Q}_3}$ receive the same negative contribution given by the r.h.s. of eq. (3.17). However, now $y_t A_t$ is two times larger than before, so expression (3.18) becomes

$$\left| \frac{(y_t A_t)^2}{\delta m^2_{\tilde{t}}} \right| = 4|\lambda|^2 \,, \tag{3.23}$$

thus improving substantially the $(y_t A_t)^2/\delta m^2_{\tilde{t}}$ ratio. A final possibility, which actually optimises the $(y_t A_t)^2/\delta m^2$ ratio, is to consider messengers in the $(5+\bar{5}) + (10+\overline{10})$. Playing just with a messenger in each representation does not conflict with perturbativity of the gauge couplings for any value of $M_{\rm mess}$.

Then, we can use three messengers in the $\Phi_{H_u}+\Phi_{H_d}$, $\Phi_u+\Phi_{\bar{u}}$ and $\Phi_Q+\Phi_{\bar{Q}}$ representations, coupled as above to generate effective contributions to y_tA_t. Assuming again that the λ, λ' couplings are the same for all of them, we find a 'universal' shift in $\delta m^2_{H_u}=\delta m^2_{\tilde{U}_3}=\delta m^2_{\tilde{Q}_3}$, given by the r.h.s. of eq. (3.17), while the generated y_tA_t term is three times bigger, so

$$\left|\frac{(y_tA_t)^2}{\delta m^2}\right| = 9|\lambda|^2 \,. \tag{3.24}$$

Nevertheless, improving the $(y_tA_t)^2/\delta m^2_{\tilde{t}}$ ratio does not necessarily leads to a milder fine-tuning. As mentioned above, a negative shift in the initial value of $m^2_{H_u}$ increases the fine-tuning, while the same shift in $m^2_{\tilde{u}_3}$ or $m^2_{\tilde{Q}_3}$ reduces it, since these mass-squared terms enter in the RG shift of $m^2_{H_u}$ with negative sign. Thus, the scenarios corresponding to eqs. (3.23) and (3.24) do not improve the fine-tuning with respect to the scenarios with just one messenger $\Phi_u+\Phi_{\bar{u}}$ coupled as in eq. (3.19). For the same reason, the scenario that actually optimises the fine-tuning is that where the messenger that induces the A-term is $\Phi_Q+\Phi_{\bar{Q}}$, rather than $\Phi_u+\Phi_{\bar{u}}$, because $m^2_{\tilde{Q}_3}$ enters the RG shift of $m^2_{H_u}$ with a larger (negative) coefficient than $m^2_{\tilde{u}_3}$ (see chapter 2). Thus, in this optimised model the superpotential reads

$$\Delta W = (kX+M_{\rm mess})\Phi_Q\Phi_{\bar{Q}}+\lambda\Phi_QU_3H_u+\lambda' XQ_3\Phi_{\bar{Q}} \,, \tag{3.25}$$

and the generated y_tA_t, $\delta m^2_{\tilde{Q}_3}$ pieces are given by the r.h.s. of eqs. (3.15) and (3.17). This scenario is illustrated in figure 3.11, for $M_{\rm mess}=10^8$ GeV, $N_{10}=1$ and $\lambda=1.5$. The pattern is similar to the setup of eq. (3.13), illustrated in figure 3.10, but now we can find a substantially milder fine-tuning. Namely, evaluating the Higgs mass with `SusyHD` (`FeynHiggs`), for $m_h>123$ GeV the fine-tuning may drop below 1000 (250). This is even better (though not dramatically) than the optimum model with radiatively generated A-terms identified by Evans and Shih, i.e. that of eq. (3.11), illustrated in figure 3.6; and hence it is an optimal GMSB model concerning fine-tuning (and playing with minimal matter content).

Let us finally mention that in the kind of scenarios discussed in this section, there is an additional fine-tuning source associated with the new parameters, in particular to the combination $\lambda\lambda'/k$, which is proportional to the initial value of y_tA_t. We have checked that this contribution to the fine-tuning is smaller than that associated with Λ.

3.6 Conclusions

Models with gauge-mediated supersymmetry breaking have become one of the most popular supersymmetric scenarios, especially for their prevention of dangerous FCNC effects. Nonetheless, these models typically present a high degree of fine-tuning, due to the initial absence of top trilinear scalar couplings, $A_t(HE)=0$. This renders the threshold correction to the Higgs mass, m_h, far from its maximal value, so that the stop masses must be quite large in order to generate sizeable radiative corrections to m_h, able to reconcile its value with the experimental measurement. Such large stop masses (around 10 TeV)

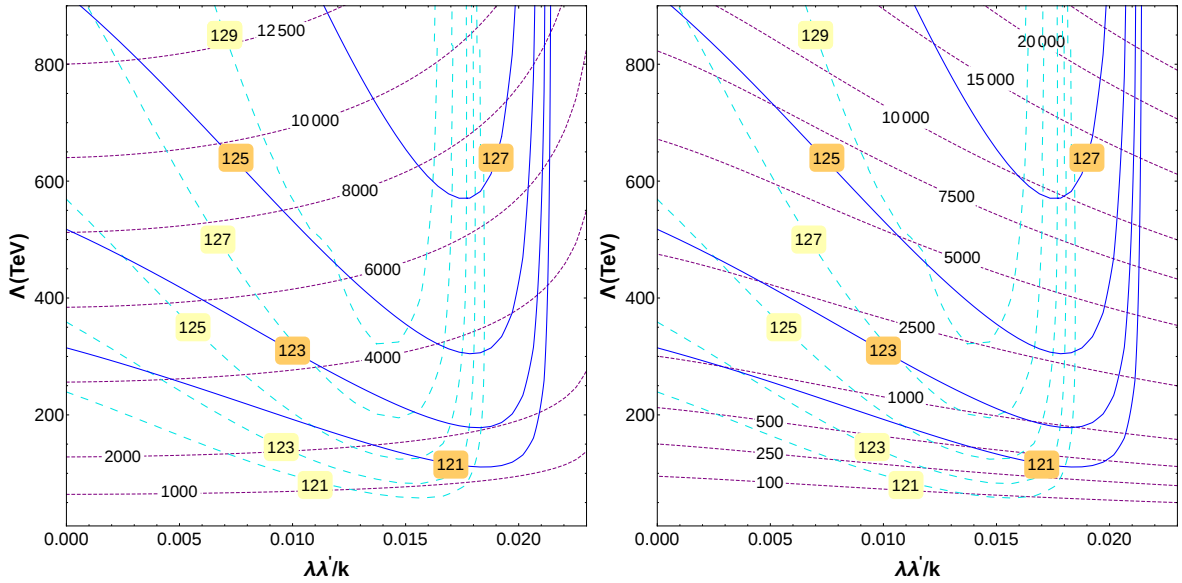

Figure 3.11: The same as figure 3.10, but for the model of eq. (3.25).

imply in turn a large value of $\Lambda \sim F/M_{\rm mess}$ and thus a severe fine-tuning in order to reproduce the right electroweak symmetry breaking scale.

In this chapter, we have carefully evaluated the fine-tuning associated with GMSB, using also the most recent codes for the computation of the Higgs mass in the MSSM, which plays a relevant role in such an evaluation. We show that previous analyses underestimated the fine-tuning of GMSB. The actual tuning is typically of the order a few per ten thousand in the minimal model. Then, we have examined some existing proposals in the literature to improve the situation, incorporating a mechanism to generate the A_t term, while keeping the minimal observable matter content. They always involve non-trivial couplings between the messengers and the MSSM superfields in the superpotential.

We find that, even though the stops can be made lighter, this does not necessarily lead to a better fine-tuning. In particular, in the model proposed by Calibbi et al. [210], an A_t-coupling is generated at one-loop, so that the stops can indeed be lighter than in the minimal version of GMSB. Nevertheless, we show that the fine-tuning becomes actually more severe, essentially due to the additional contributions to the scalar masses (especially $m^2_{H_u}$). The fine-tuning is relaxed, however, for the model with radiatively generated A_t, proposed by Evans and Shih, which was the most favourable scenario from an extensive survey of models of this kind [209].

On the other hand, in the scenario proposed by Basirnia et al. in ref. [217], the A_t-term is generated at tree level and the prospects are generically better. We have explored this scenario and formulated a modified (and conceptually simplified) version which is arguably the optimum GMSB setup (with minimal matter content) concerning the fine-tuning issue. In this model, the fine-tuning can be better than one per mil. As a matter of fact, this is still a severe fine-tuning, but substantially milder than in other versions of GMSB, and of the same order as in other MSSM constructions.

We have also explored the so-called 'little A_t^2/m^2 problem' [201], i.e. the fact that a large A_t-term is normally accompanied by a similar or larger sfermion mass-squared, which typically implies an increase in the fine-tuning. We find the version of GMSB for which this ratio is as large as possible, namely $\mathscr{O}(10)$. However, we show that the model that optimises this ratio does not coincide with the one that has the smallest fine-tuning.

Chapter 4

Naturalness of MSSM dark matter

4.1 Fine-tuning to reproduce the DM relic abundance

In the MSSM, there are several potential sources of fine-tuning, the most notorious being the electroweak (EW) fine-tuning, which generically requires light gluino, light Higgsinos, (not so) light winos and, in many cases, light stops. This fine-tuning can be reasonably quantified by the 'standard' measure [94, 158]:

$$\Delta_i^{(\mathrm{EW})} = \frac{d\log v^2}{d\log\theta_i}\,; \qquad \Delta^{(\mathrm{EW})} \equiv \max\left\{\Delta_i^{(\mathrm{EW})}\right\}, \tag{4.1}$$

where v^2 is the Higgs vacuum expectation value (VEV) and θ_i are the independent (initial) parameters of the model under consideration. Typically $\Delta^{(\mathrm{EW})}$ is dominated by the gluino-mass parameter and its value is $\gtrsim \mathcal{O}(100)$ [144], corresponding to a fine-tuning at the level of $\lesssim 1\%$. There is a vast literature concerning this EW fine-tuning of the MSSM. An important fact is that $\tan\beta$ should be moderately large (say $\tan\beta \gtrsim 6$) in order to reproduce the experimental Higgs mass without the need of gigantic stop masses, which would imply a very severe fine-tuning.

Besides the EW fine-tuning, there is a potential fine-tuning related to the generation of the right amount of dark matter (DM). In some scenarios of supersymmetric dark matter, a delicate balance between a-priori-independent quantities is required, denoting a fine-tuned situation. Here, by contrast, the literature is much less extensive [160, 221–223] and, furthermore, many important mechanisms of supersymmetric dark matter have never been considered from this point of view[1]. The main goal of this chapter is precisely to perform a rigorous study of the fine-tuning associated with the production of MSSM dark matter in all the interesting scenarios. Moreover, we will combine this fine-tuning with that related to the EW scale, to select the MSSM regions that are globally less fine-tuned.

[1] For works studying the effect of DM constraints on the EW fine-tuning, see e.g. [224, 225].

We will focus on the case where the DM particle is a supersymmetric WIMP, namely the lightest state of the neutralino mass matrix,

$$\mathscr{M}_{\chi^0} = \begin{pmatrix} M_1 & 0 & -m_Z s_W c_\beta & m_Z s_W s_\beta \\ 0 & M_2 & m_Z c_W c_\beta & -m_Z c_W s_\beta \\ -m_Z s_W c_\beta & m_Z c_W c_\beta & 0 & -\mu \\ m_Z s_W s_\beta & -m_Z c_W s_\beta & -\mu & 0 \end{pmatrix}, \tag{4.2}$$

which is the 'standard' situation. Of course, the lightest neutralino, χ_1^0, must also be the lightest supersymmetric particle (LSP). In the previous equation, M_1 and M_2 are the (low-energy) bino and wino soft mass parameters, while μ is the mass parameter in the superpotential, which gives mass to Higgsinos. As usual, s_W (c_W) is the sin (cosine) of the weak angle and s_β (c_β) is the sin (cosine) of the $\beta-$angle, defined by the ratio of the two Higgs VEVs, $\tan\beta = \langle H_u\rangle/\langle H_d\rangle$. Generically, χ_1^0 is a combination of bino, wino and Higgsinos, though is usually dominated by one of these species. Certainly, the content of χ_1^0 in each species depends on the particular values of the four parameters that define $\mathscr{M}_{\chi^0}$, i.e. $\{M_1, M_2, \mu, \tan\beta\}$.

The lightest neutralino is a perfect candidate for DM, but, to be successful, it must be produced in the early Universe in the right amount to reproduce the present DM relic density [73]

$$\Omega_{\rm DM}^{\rm (obs)} h^2 = 0.119 \pm 0.012\ . \tag{4.3}$$

We will suppose, throughout this chapter, that the neutralino relic density was produced in the 'standard' thermal way, i.e. under the assumptions that neutralinos were produced thermally thanks to their interactions with other particles in the primordial plasma, and that they decoupled while the Universe was radiation-dominated. Then, their present relic density is given by [226]

$$\Omega_{\rm DM} h^2 = \frac{8.7\times 10^{-11}\ {\rm GeV}^{-2}}{\sqrt{g*}\int_{x_f}^{\infty}\langle\sigma_{\rm ann} v\rangle x^{-2}}\ , \tag{4.4}$$

where the $g*$ parameter accounts for the number of degrees of freedom at freeze-out, $x \equiv m/T$, i.e. temperature over mass, and the subscript f denotes the freeze-out time, $T_f \simeq m/20$. Besides, $\langle\sigma_{\rm ann} v\rangle$ stands for the thermal-averaged annihilation cross section (times the velocity). Thus, in order to reproduce the observed relic density (4.3) the neutralinos must annihilate at early times with a suitable cross section.

From the naturalness point of view, an interesting case occurs when χ_1^0 is close to a pure state. Then, roughly speaking, $\sigma \propto m_{\chi_1^0}^{-2}$ and therefore, in order to reproduce (4.3), there is in principle no need of any fine-arrangement of the parameters in the $\mathscr{M}_{\chi^0}$ matrix; only a particular value of $m_{\chi_1^0}$, i.e. $\sim M_1$, M_2 or μ, depending on the character of χ_1^0. Actually, the case of (close to) pure bino does not work, since its annihilation rate in the early Universe is typically too small for any value of M_1, leading to an overproduction of dark matter, totally inconsistent with eq. (4.3). In contrast, the cases of (essentially)

pure Higgsino or pure wino lead to the correct relic density if their masses are, respectively, $\mu \simeq 1$ TeV or $M_2 \simeq 3$ TeV.[2]

Notice that both cases lead to a rather heavy supersymmetric spectrum, which has two problems. First of all, the expectations to discover supersymmetry at the LHC decrease (actually, for the wino-LSP they vanish). Second, the heavier the spectrum, the more fine-tuned the model with respect to the EW breaking. It is therefore of interest to consider mechanisms that allow for lighter neutralinos, keeping a correct relic density. This can be achieved, provided that χ_1^0 is mostly bino, or at least it possesses a substantial bino-component, and that there is an additional mechanism to increase $\langle\sigma_{\rm ann} v\rangle$. There are three of such mechanisms, which have been extensively studied in the literature:

i) Well-tempered neutralinos. If the parameters of the $\mathscr{M}_{\chi^0}$ matrix are finely chosen, χ_1^0 may be a well-tempered neutralino [167], i.e. an appropriate mixture of bino and Higgsino (or bino, Higgsino and wino), such that it annihilates in the right amount at early times. Since the $\propto M_Z$ off-diagonal entries in $\mathscr{M}_{\chi^0}$ are typically much smaller than M_1, M_2 and μ, a significant mixing requires some of the latter parameters to be near-degenerate.

ii) Funnels. If χ_1^0 is close to a bino, it can annihilate resonantly via $Z-$funnel, Higgs-funnel or $A-$funnel, provided its mass is nearly half of the mass of the funnel-particle.

iii) Co-annihilation. The effective $\langle\sigma_{\rm ann} v\rangle$ increases if χ_1^0 can co-annihilate with other fast-annihilating particle (e.g. a stop, a stau or a gluino). This requires their masses to be nearly-degenerate.

In all the above cases, we can foresee the need of cancellations or delicate balances, and thereby fine-tuning.

The aim of this chapter is to analyse all these possibilities in detail, evaluating the associated fine-tuning. In some cases, this requires to re-visit the concept of fine-tuning itself, because the extrapolation of the 'standard criterion', eq. (4.1), to the relic density is not always appropriate. The chapter is organised as follows. In section 4.2, we will review the different measurements of the fine-tuning. Sections 4.3, 4.4, 4.5 and 4.6 are devoted to the different scenarios for DM within the MSSM. In section 4.7, we make a connection between the fine-tuning in DM and the electroweak fine-tuning. Section 4.8 is devoted to accommodating Higgsino DM in the MSSM and finally our conclusions are presented in section 4.9.

4.2 The fine-tuning measure

In the few places of the literature where the fine-tuning associated with the DM relic density has been considered, the criterion to quantify it has always been the standard measure, i.e. a direct extrapolation

[2] It is not clear at the moment if the pure-wino case is consistent with DM indirect detection [227–229], due to the large uncertainties involved.

of the EW fine-tuning criterion (4.1) replacing v^2 by $\Omega_{\rm DM}$,

$$\Delta_i^{(\rm DM)} = \frac{d\log\Omega_{\rm DM}}{d\log\theta_i}\,; \qquad \Delta^{(\rm DM)} \equiv \max\left\{\Delta_i^{(\rm DM)}\right\}. \tag{4.5}$$

However, behind this 'standard measure' there are implicit assumptions (seldom stated). If these assumptions do not hold, then the standard criterion may be misleading. In the next subsection, we compile those assumptions, and later we will show instances where those conditions are not fulfilled and therefore the standard criterion is not applicable. As we will see in the following sections, these instances are actually realised in several cases of DM production, which requires to improve the criterion to quantify the fine-tuning.

4.2.1 Assumptions behind the standard fine-tuning criterion

Let us now analyse the statistical meaning of the standard fine-tuning criterion, eq. (4.1). For the sake of simplicity, we will consider a single and representative $\theta-$parameter, e.g. that producing the maximum Δ (usually θ is a soft mass or the $\mu-$parameter),

$$\Delta_\theta = \frac{\partial\log v^2}{\partial\log\theta}\,. \tag{4.6}$$

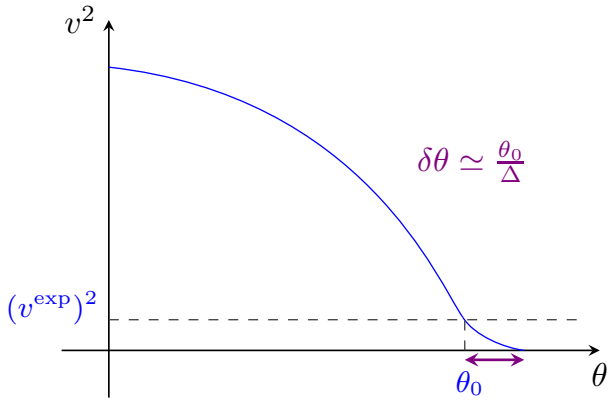

Figure 4.1: Schematic representation of the statistical interpretation of the standard fine-tuning criterion as the (inverse of the) $p-$value, $\Delta^{-1} = \delta\theta/\theta_0$.

As it is known, the issue of the value of v^2 is that it receives contributions of the size of the soft squared-masses, which are typically $\mathcal{O}(100)$ times larger; thus a somewhat artificial cancellation among these contributions is required. Since for non-tuned values of the soft terms (represented by θ), v^2 tends to be too large, we can estimate the small range of θ for which v^2 is abnormally small, say $v^2 \lesssim (v^{\rm exp})^2$. Expanding $v^2(\theta)$ at first order around the value θ^0, which gives $(v^{\rm exp})^2$, $v^2(\theta_0+\delta\theta) \simeq v^2(\theta_0) + (\partial v^2(\theta)/\partial\theta)_{\theta_0}\,\delta\theta$, we find that only for a small neighbourhood $\delta\theta \simeq \theta^0/\Delta_\theta$

around this point, v^2 is equal or smaller than the experimental value (see figure 4.1). Therefore, if we assume that θ could reasonably have taken any value of the order of magnitude of θ^0, then only for a small fraction $\sim \left|\delta\theta/\theta^0\right| \simeq \Delta_\theta^{-1}$ of the θ values we obtain $v^2 \lesssim (v^{\rm exp})^2$; this is the rough probabilistic meaning of Δ_θ (see ref. [97] and section 2.2.1 for further details). Consequently, Δ can be interpreted as the inverse of the p-value to obtain v^2 equal to the observed value or even smaller,

$$p-\text{value} \simeq \left|\frac{\delta\theta}{\theta_0}\right| \equiv \Delta^{-1} \ . \tag{4.7}$$

Then, we can summarise the implicit assumptions behind the standard fine-tuning criterion, eq. (4.1):

1. The possible values of a $\theta-$parameter are distributed, with approximately flat probability, in the $\sim [0,\theta^0]$ range (flat prior in the Bayesian language). Note that, in fact, this represents two assumptions.

2. The expansion of $v^2(\theta)$ at first order captures its behaviour in the neighbourhood of interest.

If any of these assumptions is not fulfilled, then the standard criterion has to be re-visited. Before showing some typical examples where this can happen, let us add some comments on the above conditions.

The assumed range for θ does not need to be $[0,\theta_0]$, any range of the same length, e.g. $[\theta_0/2, 3\theta_0/2]$, works equally well. The idea is that the range for θ should be of the same order than its actual value, θ_0, so that the latter is a typical value. It could be argued that in the upper half of the previous alternative range, i.e. $[\theta_0, 3\theta_0/2]$ it happens that $v^2 \leq (v^{\rm exp})^2$, simply because $v^2 = 0$ for most of it. Then the $p-$value would be $\simeq 1/2$. Nevertheless, the region where v^2 is strictly vanishing should not be counted since it does not represent any extreme case but simply the case where the Higgs mass-squared parameter is positive. An equivalent way to take this fact into account is to directly define the $p-$value for the mass parameter itself, m^2, instead of v^2 (both are related by $v^2 = -m^2/\lambda$). Then, we evaluate the probability of having $|m^2| \leq |m^{\rm exp}|^2$, giving a similar result as eq. (4.7).

The previous discussion illustrates the fact that there is always an $\sim \mathcal{O}(1)$ factor of arbitrariness for the fine-tuning measure. E.g. choosing the range of θ two times longer than the previous one increases Δ_θ by a factor 2.

It is also worth mentioning that the standard fine-tuning criterion is also valid for alternative choices of the prior and range of θ. E.g., if we assume that θ has a logarithmic prior, i.e. its a-priori probability distribution is flat in the logarithm, $\mathscr{P}(\theta) \propto 1/\theta$, then a similar argument leads to the same eq. (4.7), provided that the range of θ satisfies $\log|\theta^{\rm max}/\theta^{\rm min}| = 1$.

Let us finally mention that the previous discussion about the statistical meaning of the fine-tuning can be expressed in Bayesian terms, following a Bayesian analysis of the probability distribution in the parameter space, see refs. [114, 157].

4.2.2 Examples

The EW fine-tuning stemming from the artificial cancellation between different contributions in order to yield a small enough v^2, does reasonably fulfil conditions 1 and 2 of the previous subsection. In other words, in the MSSM the dependence of v^2 on the relevant soft terms and the $\mu-$parameter goes as in figure 4.1 or behaves in a similar manner. So the standard criterion to quantify the EW fine-tuning is sound.

Now, let us suppose that the fine-tuned quantity, say F, has a different dependence on θ. Figures 4.2 and 4.3 show two instances in which this happens in distinct ways. In figure 4.2, the hypothetical F-quantity acquires its experimentally observed value $F^{(\mathrm{obs})}$ for some value θ_0. However, there is no value of θ for which F vanishes. Hence, the region of $\delta\theta$ for which $F \leq F^{(\mathrm{obs})}$ cannot be approximated by $\delta\theta \simeq \theta_0/\Delta_\theta$. The actual $\delta\theta$ region is narrower and thus the actual $p-$value is smaller and the fine-tuning is more severe. This example also illustrates another potential departure from the conditions 1 and 2 stated in the previous subsection. Obviously, if the value of θ_0 that reproduces $F^{(\mathrm{obs})}$ lies *very* close to the minimum of the $F(\theta)$ function, then the fine-tuning is enormous, since essentially the $\delta\theta$ region for which $F \leq F^{(\mathrm{obs})}$ shrinks to a point. Nevertheless, a blind application of the standard criterion would lead to $\Delta \to \infty$. Evidently, the problem is that in this case θ_0 would be a stationary point and thereby it would be no longer justified to truncate the expansion at first order (condition 2 in the previous subsection). An important lesson is that sensitivity is not always equivalent to fine-tuning, and sometimes the measure of sensitivity, which is what the standard criterion provides, does not reflect the actual degree of fine-tuning. As we will see, when the relic density reaches the observed value thanks to the annihilation of neutralinos through Z, Higgs or A funnels, Ω_{DM} has a dependence on the MSSM parameters similar to that of figure 4.2.

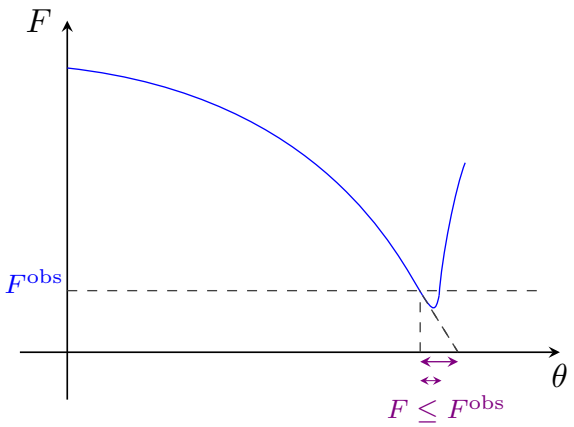

Figure 4.2: A hypothetical case where the standard criterion (see figure 4.1) underestimates the severity of the fine-tuning.

Figure 4.3 shows another example in which the assumptions for the applicability of the standard fine-tuning criterion do not hold. In this case, the truncation of $F(\theta)$ at first order is not good enough to evaluate the region $\delta\theta_0$ for which $F \leq F^{(\mathrm{obs})}$. Here, the linear approximation leads to an underestimation

of $\delta\theta_0$, so that the actual $p-$value is larger and the fine-tuning is less severe than that obtained from the standard criterion. As we will see, the example of figure 4.3 describes schematically the dependence of $\Omega_{\rm DM}$ on the MSSM parameters when the DM is wiped out through co-annihilations.

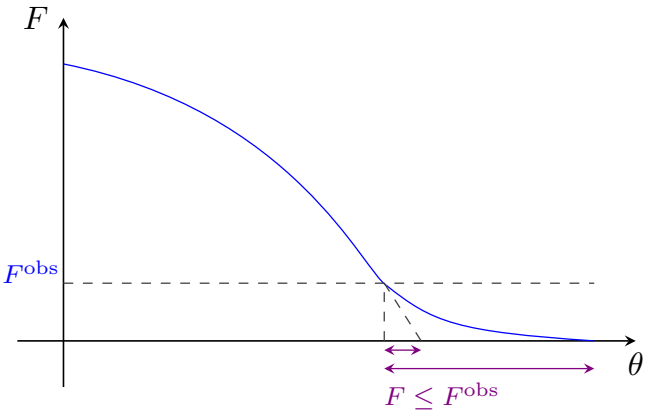

Figure 4.3: A hypothetical case where the standard criterion (see figure 4.1) overestimates the severity of the fine-tuning.

4.3 Well tempered bino-Higgsino

Consider first the well-tempered Higgsino/bino, i.e. the case in which the lightest neutralino is a combination of bino and Higgsino. Obviously, this scenario includes the pure-Higgsino case as a particular and important limit (recall that, in contrast, the pure-bino limit is not viable unless additional mechanisms for DM annihilation are present). As mentioned in the introduction, the appeal of this setup is that it enables cases where the LSP is lighter than in the pure-Higgsino case, since the annihilation of LSPs becomes reduced thanks to the bino component. On the other hand, the possibility to find DM in (spin-independent) direct detection experiments through the neutralino elastic scattering off quarks mediated by a Higgs boson, is also higher, due to the Higgsino-bino-Higgs coupling. Indeed, present bounds on direct detection are able to exclude a large portion of the bino-Higgsino parameter space [221, 230]. However, it still remains as an interesting scenario, with relevant implications for the LHC and DM direct detection searches. It is also an illustrative example of the subtleties involved in the calculation of the DM fine-tuning.

From the four parameters that define the neutralino mass matrix, eq. (4.2), the most relevant ones here are M_1 and μ. M_2 plays a negligible role, unless it happens to be quite degenerate with M_1 and μ, in which case the neutral and charged wino would contribute to DM co-annihilation processes. This would correspond to the bino/wino/Higgsino scenario, to be analysed in the next subsection. Consequently, for the bino-Higgsino analysis, M_2 can be made large enough for winos to be ignored. In addition, as stated in the introduction, we need $\tan\beta$ at least moderately large, say $\tan\beta \gtrsim 6$, in order to maximise the tree-level Higgs mass ($m_h^{\rm tree} \leq M_Z$). In this way, we avoid the necessity of large radiative corrections

to increase m_h up to its experimental value, which would require enormous stop masses and thereby an extremely large EW fine-tuning. Since the aim of this chapter is to explore as less fine-tuned as possible supersymmetric DM, we will ignore the small $\tan\beta$ regime. On the other hand, in the large-$\tan\beta$ regime the precise value of $\tan\beta$ is not very important, because it hardly affects the numerical values of the $\mathscr{M}_{\chi^0}$ entries. In conclusion, concerning the potential fine-tuning to arrange the correct DM relic density, $\tan\beta$ can be safely ignored.

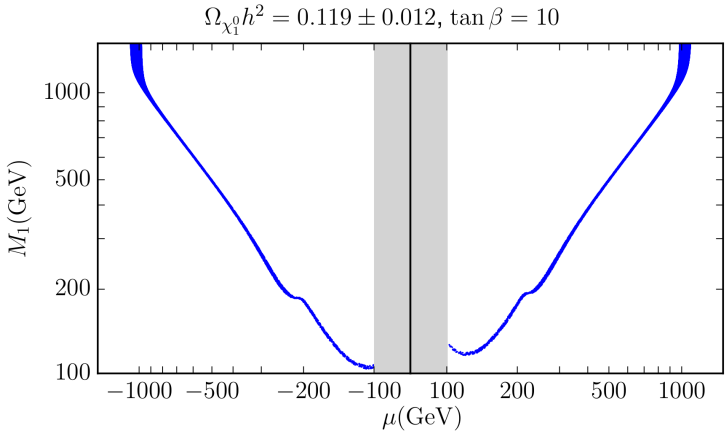

Figure 4.4: Region of the $\mu - M_1$ plane that leads to the observed DM relic density, $\Omega_{\chi_1^0}h^2 = 0.119 \pm 0.012$, in a well-tempered bino-Higgsino scenario (blue bands). The grey band is excluded by LEP limits on charginos.

Figure 4.4 shows in blue the region in the $\mu - M_1$ plane where $\Omega_{\chi_1^0}h^2 = 0.119 \pm 0.012$. It is located close to the $|\mu| = M_1$ lines, something required in order to yield a non-trivial bino-Higgsino mixture. The calculation has been performed using `SOFTSUSY-3.6.2` [219] to compute the mass spectrum, `micrOMEGAs-4.1.8` [231, 232] for the relic density and direct detection cross section, and `MultiNest-3.9` [233–235] to efficiently explore the parameter space. The current LUX exclusion line [236] and the preliminary LUX 2016 limit [237] for the two signs of μ are presented in figure 4.5, showing the impressive power of present and future experiments of DM direct detection to exclude large regions of the parameter space. In fact, the (non-visible) XENON 1T and LZ projected sensitivities lie below the horizontal axes, so that they will potentially probe the whole scenario [238–240].

Let us now consider the DM fine-tuning issue. From figure 4.4, it is clear that a certain fine-tuning is required for the viability of the model, since the (low-energy) values of $|\mu|$ and M_1 must be quite degenerate. In the absence of a theoretical argument to justify such coincidence, this clearly represents a fine-tuning.

Before attempting to quantify it, let us mention an interesting and fortunate fact. The degree of naturalness of a physical scenario must be evaluated by examining the behaviour of the fine-tuned quantities with respect to the independent parameters of the theory, see e.g. the standard measure of eq. (4.1). Here, 'independent' means that there is no known theoretical connection between them (or no connection based on some specific model is assumed). For the present case, the relevant independent

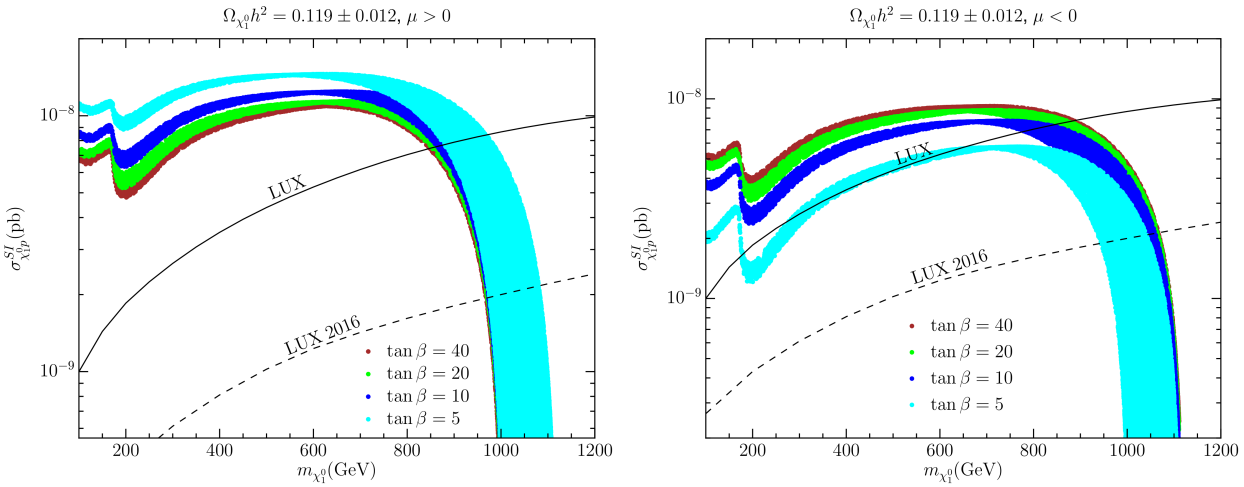

Figure 4.5: Spin-independent neutralino-proton cross section for the bino-Higgsino scenario for $\mu > 0$ (left) and $\mu < 0$ (right) and different values of $\tan\beta$. The current exclusion line and the preliminary 2016 limit from LUX (assuming that the neutralino is entirely made of bino-Higgsinos) are shown as solid and dashed lines, respectively. The XENON 1T and LZ projected sensitivities lie below the horizontal axes.

parameters are the initial (high-energy) values of the soft parameters and μ. E.g. $\tan\beta$ is a derived parameter, which depends on the initial ones in a complicated way. Nevertheless, as mentioned above, the dependence of $\mathscr{M}_{\chi^0}$ on $\tan\beta$ is very weak, so we can ignore its impact on the fine-tuning. Now, the fortunate fact is that the remaining three relevant (low-energy) parameters, involved in $\mathscr{M}_{\chi^0}$, namely M_1, M_2 and μ, are essentially in one-to-one multiplicative correspondence with the three initial (high-energy) parameters,

$$\begin{aligned} M_i|_{LE} &= c_{M_i}\, M_i|_{HE}\,, \quad i = 1,2, \\ \mu|_{LE} &= c_\mu\, \mu|_{HE}\,, \end{aligned} \tag{4.8}$$

where the HE (LE) subscript denotes high- (low-) energy, and the values of the $c-$coefficients depend on the value of the HE scale (see chapter 2). However, for fine-tuning purposes the particular values of the c's, and thus the choice of the HE scale, are irrelevant. E.g. for the standard fine-tuning measure, eq. (4.5), the logarithmic derivatives are the same evaluated with respect to the HE or the LE parameters. This fact simplifies life considerably and allows to use just with the low-energy parameters, producing results on $\Delta^{(\mathrm{DM})}$ which are pretty general, in particular $\Delta^{(\mathrm{DM})}$ is essentially independent of the HE scale and the values of the remaining MSSM parameters, which is remarkable. Incidentally, this is not the case for the EW fine-tuning, where a specific analysis must be performed for each model.

Let us now compute the DM fine-tuning. Before relying on the standard measure, eq. (4.5), it is convenient to test if the conditions 1 and 2 listed in subsection 4.2.1 are fulfilled. In other words, we should check the dependence of $\Omega_{\chi_1^0}$ on the μ and M_1 parameters (the only relevant ones for this

scenario). Since the tuning is precisely between these two parameters, it is enough to consider one of them, say M_1.[3] Figure 4.6 shows such dependence for a fixed value of μ.

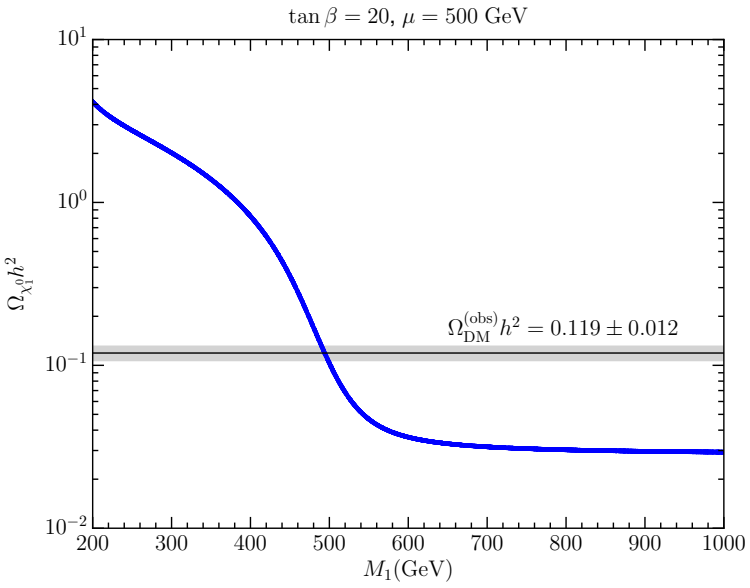

Figure 4.6: $\Omega_{\chi_1^0}h^2$ vs M_1 in the well-tempered bino-Higgsino scenario for fixed values of μ and $\tan\beta$.

As expected, only for a small interval of M_1, $\Omega_{\chi_1^0}$ is consistent with the observed value. Nevertheless, concerning the fine-tuning, the important issue is that, *typically*, $\Omega_{\chi_1^0}$ is much larger or much smaller than $\Omega_{\rm DM}^{\rm (obs)}$. It requires a tuning between M_1 and μ for $\Omega_{\chi_1^0}$ to be in the vicinity of the observed value. Now, if we consider that the range of M_1 is $[0, M_1^{(0)}]$, where $M_1^{(0)}$ is the value that reproduces $\Omega_{\rm DM}^{\rm (obs)}$, then the standard measure of eq. (4.5) and its interpretation in terms of $p-$value, i.e. the probability of obtaining $\Omega_{\chi_1^0} \leq \Omega_{\rm DM}^{\rm (obs)}$, is justified. However, changing the limits of the range to e.g. $[M_1^{(0)}/2,\ 3M_1^{(0)}/2]$ jeopardises the $p-$value interpretation, because there is a large interval of M_1 for which $\Omega_{\chi_1^0} \leq \Omega_{\rm DM}^{\rm (obs)}$. A way out to this difficulty is to change the definition of the fine-tuned quantity. Instead of $\Omega_{\chi_1^0}$, we can use the mixing angle, θ, between the bino and the Higgsino. More precisely, upon diagonalization of $\mathscr{M}_{\chi^0}$, given by eq. (4.2), we find

$$|\tan 2\theta| \simeq \frac{\sqrt{2}\, s_W M_Z}{||\mu| - |M_1||} \,. \tag{4.9}$$

It is worth noting that θ is a physical quantity, in direct correspondence with $\Omega_{\chi_1^0}$, which could have been experimentally measured before $\Omega_{\rm DM}^{\rm (obs)}$. If $\tan 2\theta$ is large, this clearly denotes a fine-tuning between M_1 and μ in eq. (4.9). In terms of $\tan 2\theta$ the $p-$value interpretation of the fine-tuning is much more transparent and robust than before: it is the probability of obtaining $|\tan 2\theta| \geq |\tan 2\theta^{\rm (obs)}|$. Assuming,

[3] This has the advantage of avoiding interference with the EW fine-tuning, for which μ is a very relevant parameter, unlike M_1.

as usual, a flat prior for M_1 in the region of interest, such $p-$value is simply

$$p-\text{value} \;=\; \frac{2(|\mu|-|M_1|)}{|M_1|}\,, \tag{4.10}$$

independent of the position of the M_1-range limits.

Figure 4.7 shows the fine-tuning calculated with the standard criterion eq. (4.5) and that estimated by the inverse of the $p-$value, eq. (4.10).[4] Needless to say, a $(p-\text{value})^{-1} = \mathcal{O}(1)$ is completely normal for a non-fine-tuned quantity, so fine-tunings below 5 or even 10 are not significant.

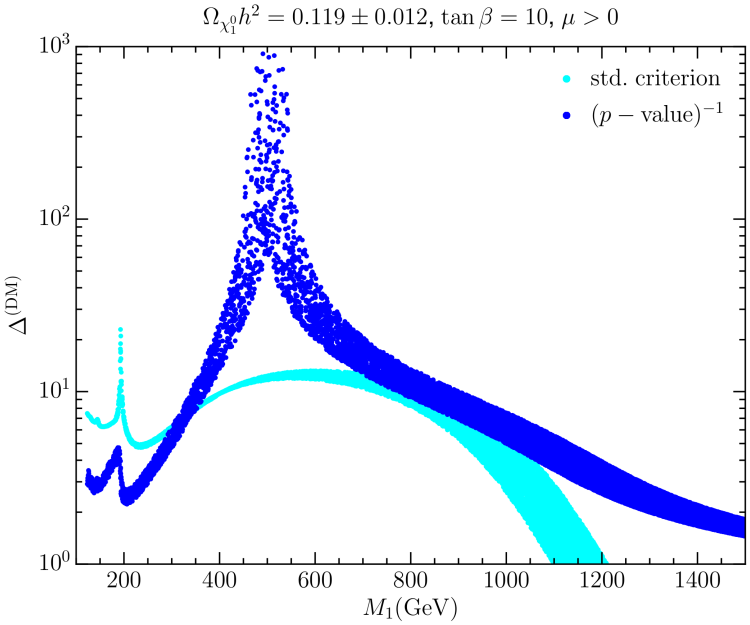

Figure 4.7: Fine-tuning in the well-tempered bino-Higgsino scenario for $\mu > 0$, calculated using the 'standard criterion' [see eq. (4.5)] (cyan band) and using the $p-$value criterion [i.e., the inverse of the $p-$value evaluated as in eq. (4.10)] (blue band). The width of the bands corresponds to the uncertainty in the relic density, $\Omega_{\chi_1^0}h^2 = 0.119 \pm 0.012$.

Qualitatively both criteria give similar results. In particular, the region around $M_1 = 500-600$ GeV is the most fine-tuned, since it requires $\mu = M_1$ with more precision (it corresponds to maximal bino-Higgsino mixing angle). This can also be seen at naked eye in figure 4.4, by examining the width of the $\Omega_{\chi_1^0}h^2 = 0.119 \pm 0.012$ (blue) band, which narrows in that region. Quantitatively, the fine-tuning estimated by the $p-$value criterion is in general more severe and, in our opinion, more reliable for the above-discussed reasons. Interestingly, for the $M_1 \gtrsim 950$ GeV region, which is allowed by LUX, see figure 4.5, the tuning is rather small, even non-significant. This includes, of course, the $M_1 > \mu \simeq 1$ TeV region, for which the lightest neutralino is essentially a Higgsino. Actually, in this limit the precise value

[4] Let us note the funny fact that if we had applied the standard fine-tuning criterion to the physical quantity $\tan 2\theta$ instead of $\Omega_{\chi_1^0}$, i.e. $\Delta = d\log\tan 2\theta / d\log M_1$, the result would have become essentially equivalent to the inverse of the $p-$value, eq. (4.10). This shows that the standard criterion is not always robust under changes in the definition of the fine-tuned quantity. However, starting directly with the $p-$value criterion is much more trustworthy.

of M_1 is irrelevant, and the dependence of $\Omega_{\chi_1^0}$ on μ, namely $\Omega_{\chi_1^0} \propto \mu^2$, does not entail any fine-tuning, as expected, see the discussion in section 4.1.

4.4 Well-tempered bino-wino(-Higgsino)

By inspection of the $\mathscr{M}_{\chi^0}$ mass matrix, eq. (4.2), it is clear that a substantial bino-wino mixing requires a not too-large μ. Thus, assuming again moderate or large $\tan\beta$, this scenario has three relevant parameters, M_1, M_2 and μ. Furthermore, the Higgsino is also mixed, so that the scenario really becomes well-tempered bino-wino-Higgsino.

However, there is a special and physically relevant limit, where things become simpler. Namely, for large enough μ, the mixing between bino and wino (and Higgsino) is small. In that regime, provided M_1 and M_2 are nearly-degenerate, the neutralino annihilation is dominated by co-annihilation with winos (more precisely, by wino-annihilation provided these are in thermal equilibrium with the lightest neutralino) [167] and is almost independent of the value of μ. All this is illustrated in figure 4.8, which shows the region in the $M_1 - M_2$ plane where $\Omega_{\chi_1^0}h^2 = 0.119 \pm 0.012$ for three different values of μ and the two signs of M_2. For $|\mu| \gg |M_1|, |M_2|$ the solution is close to the straight band $|M_1| \simeq |M_2|$ and is quite independent of μ (the larger μ, the more independent the solution). This scenario can still be called well-tempered bino-wino, even though χ_1^0 is mostly bino.

In this figure, the $|\mu| \simeq |M_1| \ll |M_2|$ regions (nearly vertical segments of the coloured bands) are also visible. They correspond to the bino-Higgsino solution (analysed in the previous section), and are quite independent of the value of $|M_2|$. Likewise, the $|\mu| \sim |M_1| \sim |M_2|$ regions (short, curved parts of the bands) correspond to the bino-wino-Higgsino case, to be discussed later.

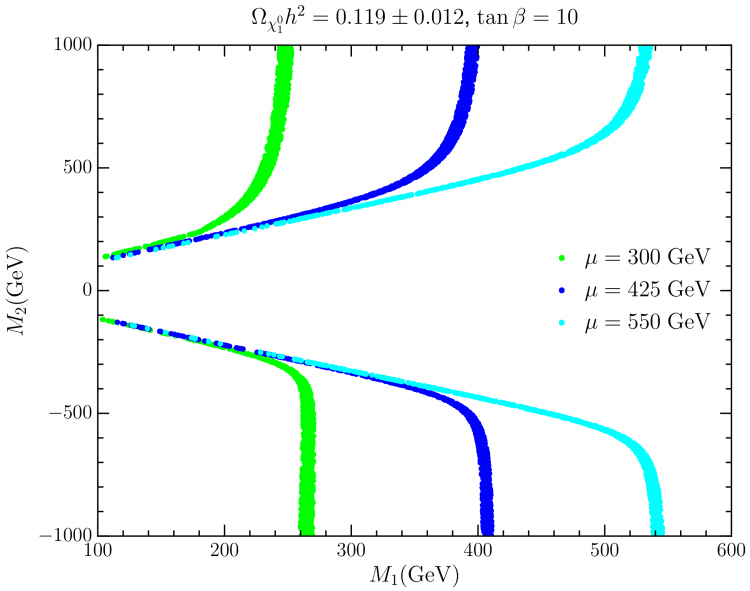

Figure 4.8: Region of the $M_1 - M_2$ plane that leads to the observed DM relic density, $\Omega_{\chi_1^0}h^2 = 0.119 \pm 0.012$, for three different values of μ in a well-tempered neutralino scenario.

For the fine-tuning discussion of the bino-wino scenario, it is useful to consider some analytical approximations. Note that, since this is a co-annihilation scenario, the averaged annihilation cross-section $\langle\sigma_{\rm ann} v\rangle$ in eq. (4.4) must be replaced by [167]

$$\langle\sigma_{\rm eff} v\rangle = \frac{\sum_{i,j=1}^{N} w_i w_j \sigma_{ij} x^{-n}}{(\sum_{i=1}^{N} w_i^2)^2} \ , \quad w_i = \left(\frac{m_i}{m_1}\right)^{3/2} e^{-x\left(\frac{m_i}{m_1}-1\right)} \ , \tag{4.11}$$

where N is the number of co-annihilating species (in this case the bino and the three winos), m_1 is the lowest mass (in this case $\sim M_1$) and the $ij \to$ SM SM annihilation-cross-sections are parametrized as the dominant term in the velocity- (or equivalently x-) expansion

$$\langle\sigma_{ij} v\rangle \simeq \sigma_{ij} x^{-n} \ . \tag{4.12}$$

Under these circumstances the neutralino relic abundance is mostly determined by the $\tilde{W}$ annihilation processes, whose cross sections go as $\sim g^4/M_2$. Plugging numerical factors we arrive to a good approximate expression for the relic density [167],

$$\Omega_{\chi_1^0} h^2 \simeq 0.13 \left(\frac{M_2}{2.5\ \text{TeV}}\right)^2 \frac{1}{R_{\tilde{W}}} \ , \tag{4.13}$$

where

$$R_{\tilde{W}} = \int_0^1 dy \left[1 + \frac{1}{3}\left(\frac{M_1}{M_2}\right)^{3/2} e^{\frac{x_f}{y}\left(\frac{M_2}{M_1}-1\right)}\right]^{-2} \simeq \left(\frac{3}{4}\right)^2 e^{-\xi_{\tilde{W}} x_f \left(\frac{M_2}{M_1}-1\right)} \ , \tag{4.14}$$

with $\xi_{\tilde{W}} \simeq 1.7$. Recalling that $x_f \sim 20$, the previous equations (4.13, 4.14) show a strong sensitivity of $\Omega_{\chi_1^0}$ to M_1. This is illustrated in figure 4.9, which shows $\Omega_{\chi_1^0} h^2$ vs. M_1, using the complete numerical evaluation performed with `micrOMEGAs`, for fixed values of M_2 and $\tan\beta$. The value of μ is quite irrelevant provided is large enough ($\mu = 1.5$ TeV in the figure).

From eqs. (4.13, 4.14) and figure 4.9, we could foresee that the standard criterion will point to a severe fine-tuning. On the other hand, it should be noticed that the application of the standard recipe eq. (4.5) to eqs.(4.13, 4.14) leads to a value of the fine-tuning, Δ, that is essentially independent of the mass difference $\Delta m = ||M_2| - |M_1||$, as $\Omega_{\chi_1^0}$ is dominated by the Boltzmann (exponential) factor in a substantial range of M_1-values. This is counter-intuitive, since logically the fine-tuning should be more severe when Δm is required to be smaller. Figure 4.9 (right panel), which shows the dependence of $\Omega_{\chi_1^0} h^2$ on M_1 in a linear scale, clarifies the connection of the standard fine-tuning measure to the $p-$value in this case. Evidently, the exponential shape leads to an over-estimation of the fine-tuning when this is calculated with the standard criterion, compare figure 4.9 (right panel) to figure 4.3. Again, we find that the simple '$p-$value–like measure', $\Delta m/M_1$, offers a more sensible and robust description of the fine-tuning, as it happened in the bino-Higgsino case analysed in section 4.3.

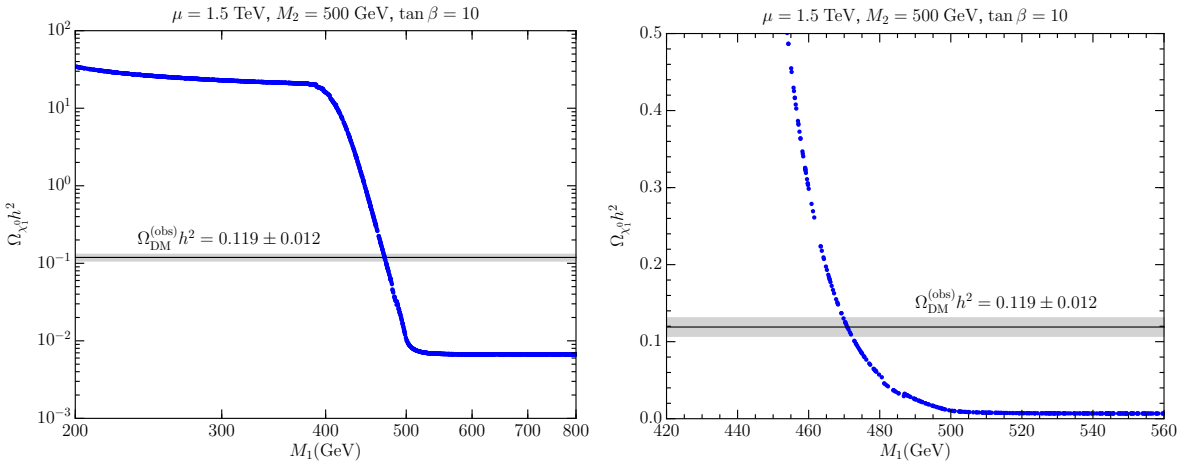

Figure 4.9: $\Omega_{\chi_1^0}h^2$ vs M_1 in the well-tempered bino-wino scenario for fixed $\mu = 1.5$ TeV, $M_2 = 500$ GeV and $\tan\beta = 10$. Left (right) panel shows the relic abundance in logarithmic (linear) units.

Figure 4.10 shows the performance of both criteria. For each value of M_1, the corresponding M_2 is chosen so that the observed relic density (4.3) is fulfilled (recall that the value of μ is large and fairly irrelevant). Both M_1 and M_2 are defined at the $Q = M_1$ scale, and their values are close to the physical masses, $m_{\chi_1^0}$ and $m_{\chi_2^0}, m_{\chi_1^\pm}$, respectively. As discussed above, the standard criterion leads to an almost flat fine-tuning, independently of M_1 and Δm. The $p-$value criterion, however, varies considerably with M_1, showing a rather mild fine-tuning when the neutralino is light. The reason is that the heavier the wino, the less efficient its annihilation. Hence, in order to reproduce the relic density, the Boltzmann penalty in the co-annihilation process must be lessened, which requires a smaller $\Delta m/M_1$, and thus a higher fine-tuning.

Interestingly, the fine-tuning (evaluated with the $p-$value criterion) is milder when $|\mu|$ approaches the value of $|M_1|$ or $|M_2|$. This is due to the fact that as $|\mu|$ decreases the mixing between bino and wino increases. Then, the neutralino annihilation does not only occur through wino co-annihilation, as explained above, but also through direct $\chi_1^0\chi_1^0 \to$ SM SM, $\chi_1^0\chi_1^\pm \to$ SM SM processes, thanks to the non-negligible wino component of the neutralino. Since the resulting annihilation is now more efficient, $|M_1|$ does not need to be that close to $|M_2|$. Consequently, the $p-$value is larger (and the fine-tuning less severe). This effect is illustrated in figure 4.11, which displays the upper part of figure 4.8 (positive M_1/M_2 plane), but explicitly showing the percentage of $\chi_1^0\chi_1^0 \to$ SM SM annihilation.

The situation depicted above connects with the bino-wino-Higgsino case, which occurs when the three relevant parameters, μ, M_1 and M_2, have similar absolute values (curved segments of the bands in figure 4.11). Intuitively, this case requires a more severe fine-tuning, as it requires a 'conspiracy' between three (a priori) independent parameters. It is therefore disfavoured from the point of view of naturalness, which is the main concern of this chapter. We can try to estimate the related $p-$value. Assuming that μ is a given value, the separate $p-$values associated with the tuning of M_1 and M_2 are of

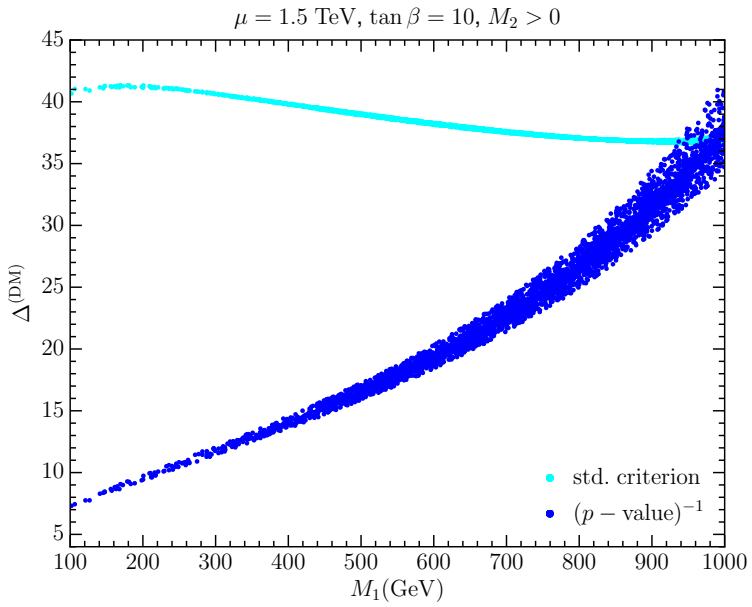

Figure 4.10: Fine-tuning in the well-tempered bino-wino scenario for $\mu = 1.5$ TeV, $\tan\beta = 10$, calculated using the 'standard criterion' [see eq. (4.5)] (cyan band) and using the $p-$value criterion, i.e. $(\Delta m/M_1)^{-1}$ (blue band). The width of the bands corresponds to the uncertainty in the relic density, $\Omega_{\chi_1^0}h^2 = 0.119 \pm 0.012$.

order

$$\sim \left|\frac{|\mu| - |M_1|}{M_1}\right|, \left|\frac{|\mu| - |M_2|}{M_2}\right|, \tag{4.15}$$

respectively. They should be combined multiplicatively. It is easy to check from figure 4.11 that this leads to a fine-tuning which is typically an $\mathcal{O}(1-10)$ factor more severe than the tuning in the regions related to well tempered bino-Higgsino or bino-wino, as expected.

4.5 Funnels

When the LSP can resonantly annihilate in the $s-$channel through an intermediate boson, say F, and $m_{\chi_1^0} \simeq m_F/2$, the annihilation cross-section increases enormously. In this way, scenarios of almost pure bino, which normally lead to excessive relic density, can be rescued. The funnel particle, F, can be the Z-boson, the ordinary Higgs boson, h, and the pseudoscalar, A. Note that for the first two cases χ_1^0 must be rather light, which implies, as a matter of fact, that it should be nearly pure bino; otherwise, either M_2 or μ would be necessarily close to $m_Z/2$ or $m_h/2$, thus leading to charginos below the LEP limit, $M_{\chi^\pm} \gtrsim 100$ GeV. For the $A-$funnel case, it is desirable that χ_1^0 be mostly bino as well, otherwise its mass should be very large. Notice here that, without the help of any funnel, the annihilation cross section of pure Higgsinos or pure winos is already quite efficient, which requires them to be rather heavy ($\simeq 1$ TeV and $\simeq 3$ TeV respectively) in order to reproduce the correct relic density. If, in addition, there

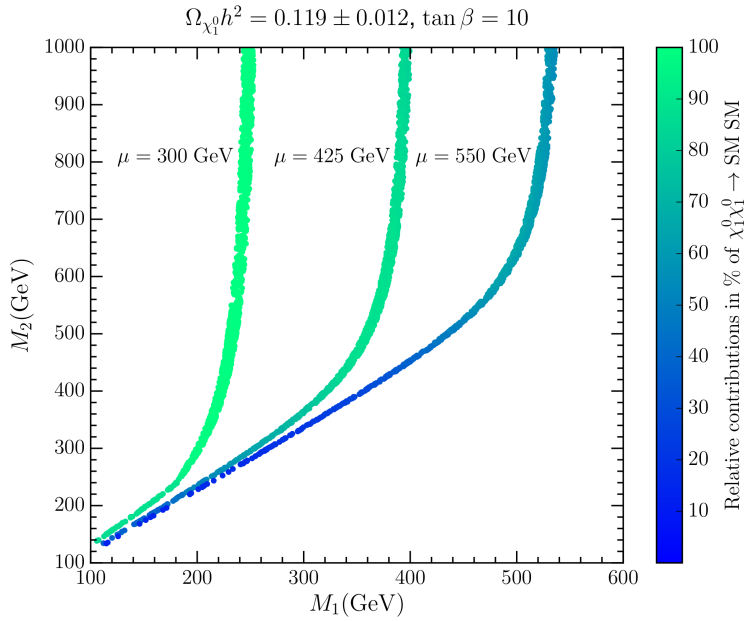

Figure 4.11: As figure 4.8, zoomed on the positive region of the $M_1 - M_2$ plane. The colour code denotes the percentage of $\chi_1^0\chi_1^0 \to$ SM SM annihilation (the remaining DM annihilation proceeds mainly via co-annihilation with winos).

is a channel of resonant annihilation (funnel), then their masses should be even larger, which would imply a heavier supersymmetric spectrum, and thus a more severe EW fine-tuning.

Let us first consider the $A-$funnel, i.e. the resonant annihilation through the A pseudoscalar

$$\chi_1^0\chi_1^0 \to A \to SM\ SM, \tag{4.16}$$

where $SM\ SM = b\bar{b}, gg$, etc. Note that, for this process to take place, χ_1^0 must have a non-vanishing component of Higgsino, so that the $\chi_1^0 - \chi_1^0 - A$ vertex is in fact $\tilde{B} - \tilde{H}^0 - A$. Consequently, the larger the Higgsino component of χ_1^0 (and thereby the smaller μ), the more efficient the annihilation. Another point to keep in mind is that, even if M_1 is below the resonant value, i.e. $m_A/2 - M_1 > \Gamma_A$, there can still be resonant annihilations, thanks to the thermal agitation in the early Universe, for some collisions the kinetic energy of the neutralinos can be large enough to reach $s \simeq m_A/2$. Of course, this amounts to a 'Boltzmann penalty' for the averaged cross section. On the other hand, if $M_1 > m_A/2$, resonant annihilations are not possible. Then, the relic density, eq. (4.4), as a function of M_1 shows a characteristic asymmetric dependence on M_1 in the resonance-region.

All this is illustrated in figure 4.12 for $m_A = 800$ GeV. Note that 'far' from the resonant point the dependence of $\Omega_{\chi_1^0}$ on M_1 has an exponential shape due to the above-mentioned Boltzmann penalty. Thus we can expect that, similarly to what happened for the bino-wino co-annihilation scenario (section 4.4), the standard criterion for the fine-tuning is not suitable here and typically overestimates the real fine-tuning. Nevertheless, when M_1 approaches the resonant point, we expect the opposite (recall the

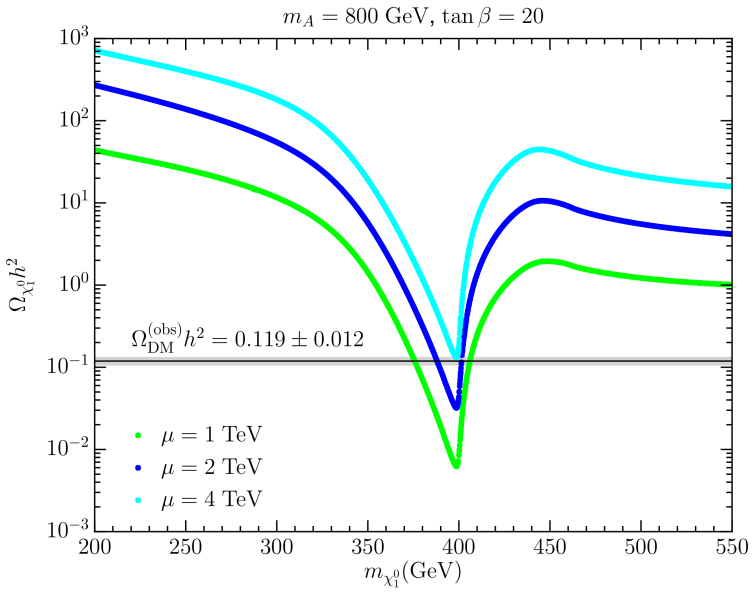

Figure 4.12: $\Omega_{\chi_1^0}h^2$ vs M_1 in the $A-$funnel scenario for $m_A = 800$ GeV, $\tan\beta = 20$ and three (positive) values of μ. The grey band denotes the observed relic abundance.

discussion around figure 4.2). In the limiting case, in which the physical region, $\Omega_{\chi_1^0} \simeq \Omega_{\rm DM}^{\rm (obs)}$, is close to the minimum of the curve (this occurs for $\mu \simeq 4000$ GeV in the example of figure 4.12), then the standard criterion indicates no fine-tuning at all; however this is obviously the most fine-tuned case!

In contrast, the $p-$value criterion is very transparent and easy to apply. Let us call $M_1^{(0)}$ the value of M_1 that, for given m_A and μ, leads to $\Omega_{\chi_1^0} = \Omega_{\rm DM}^{\rm (obs)}$. Then, only in the narrow range $M_1 \in [M_1^{(0)}, M_1^{(0)} + \Delta m]$, with $\Delta m \simeq |m_A/2 - |M_1^{(0)}||$, the relic density will be equal or smaller than the observed value, as it is clear from figure 4.12. Therefore, the $p-$value is (once more) simply $\Delta m/|M_1^{(0)}|$.

Figure 4.13 illustrates the previous discussion, showing the fine-tuning calculated with the standard criterion, eq. (4.5), and that estimated as the inverse of the $p-$value, eq. (4.10), for $m_A = 800$ GeV. For each value of M_1, the corresponding $\mu > 0$ is chosen so that the observed relic density (4.3) is fulfilled (recall that the value of μ determines the amount of Higgsino mixing).

It is also worth-mentioning that this scenario is quite safe with respect to the current DM direct detection bounds because the elastic scattering cross section does not benefit from any resonant enhancement. This is shown in figure 4.14 for three different values of m_A.

Let us finally mention that for $|M_1| \lesssim \frac{3}{4}(m_A/2)$ the enhancement due to the resonant annihilation is lost, but the relic density can still be reproduced if μ (and/or M_2) are close enough to M_1 for the scenario to become a well-tempered neutralino case. In that case, the fine-tuning is due to this well-tempered character and has been analysed in sections 4.3 and 4.4.

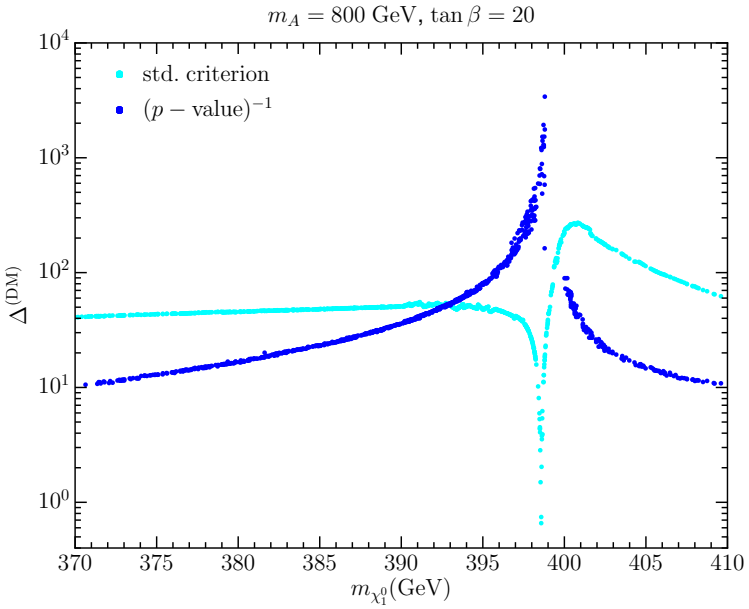

Figure 4.13: Fine-tuning in the $A-$funnel scenario for $m_A = 800$ GeV and $\tan\beta = 20$, calculated using the 'standard criterion' [see eq. (4.5)] (cyan band) and using the $p-$value criterion, i.e. $(|m_A/2 - |M_1||/|M_1|)^{-1}$ (blue band). For each value of M_1, the corresponding (positive) μ is chosen so that $\Omega_{\text{DM}}^{(\text{obs})}$ is reproduced.

Now, we turn to the $h-$ and $Z-$funnels

$$\chi_1^0\chi_1^0 \to h \to SM\ SM, \tag{4.17}$$

$$\chi_1^0\chi_1^0 \to Z \to SM\ SM. \tag{4.18}$$

Similarly to the $A-$funnel case, these channels require χ_1^0 to have a non-vanishing Higgsino component, so that the $\chi_1^0 - \chi_1^0 - h$ ($\chi_1^0 - \chi_1^0 - Z$) vertex has the $\tilde{B} - \tilde{H}^0 - h$ ($\tilde{H}^0 - \tilde{H}^0 - Z$) structure[5]. Thus, again, the larger the Higgsino component of χ_1^0 (and thus the smaller μ), the more efficient the annihilation. This effect is stronger for the $Z-$funnel, as it involves the Higgsino component in the two incoming neutralinos. All this is illustrated in figure 4.15, which shows the dependence of $\Omega_{\chi_1^0}$ vs M_1 for three different values of μ.

Regarding the fine-tuning issue, as for the $A-$funnel case, we expect that typically, the standard criterion overestimates the fine-tuning, except when the physical region, $\Omega_{\chi_1^0} \simeq \Omega_{\text{DM}}^{(\text{obs})}$, is close to a stationary point. Looking at figure 4.15, there are now three stationary points, corresponding to the two minima at $m_{\chi_1^0} \simeq m_h/2, M_Z/2$ and to the maximum between both. For the very same reasons as for the $A-$channel, we find that a more robust and reliable measure of the fine-tuning is provided by

[5]For the $h-$funnel $\sigma_{\text{ann}} \propto |N_{11}N_{14}|^2$, while for the $Z-$funnel $\sigma_{\text{ann}} \propto |N_{11}N_{13} - N_{11}N_{14}|^4$, with N being the neutralino mass matrix.

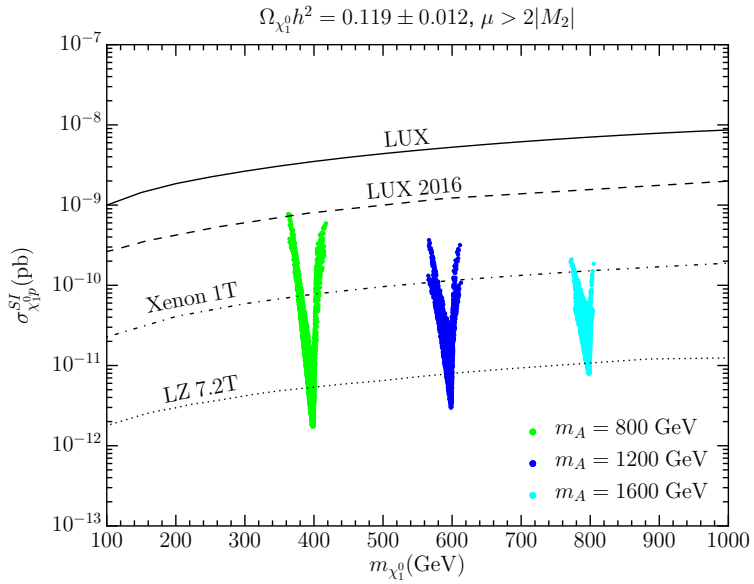

Figure 4.14: Spin-independent neutralino-proton cross section in the $A-$funnel scenario for $m_A = 800$ GeV. The solid and dashed black lines denote the current LUX upper limit and the preliminary LUX 2016 bound, respectively. The XENON 1T (dash-dotted line) and LZ (dotted line) projected sensitivities are also depicted.

the $p-$value $\simeq \Delta m/|M_1|$, where Δm is the length of the M_1-range where the relic density is equal or smaller than the observed value[6].

Figure 4.16 (left panel), which is similar to figure 4.13 but for the $h-$ and $Z-$funnels, illustrates the previous discussion. Again, for each value of M_1, the corresponding $\mu > 0$ is chosen so that the observed relic density (4.3) is reproduced. As argued above, the standard criterion overestimates (non-dramatically) the fine-tuning in most of the M_1-range. However, around the three stationary points (in particular the two resonant points), it underestimates the fine-tuning dramatically. Indeed, apart from the resonant points, the fine-tuning (estimated with the $p-$value criterion) is quite mild ($\lesssim 10$). Note from figure 4.15 that for 150 GeV $\lesssim \mu \lesssim$ 450 GeV both the $h-$funnel and the $Z-$funnel can successfully reproduce a relic density equal to the observed size, or even smaller, if M_1 is positive and has the appropriate value. Thus, the two $p-$values should be added, implying a less severe fine-tuning. The results are shown in figure 4.16 (right panel). Notice that in this way the peak associated with the $Z-$funnel region is blown-up. This occurs because, for a given value of (positive) μ, the possibility of $Z-$funnel annihilation is always accompanied by the possibility of $h-$funnel annihilation, but not the other way round, see figure 4.15. For $\mu < 0$ the results are similar, but in that case the blown-up peak corresponds to the $h-$funnel for analogous reasons. The bottom line is that, apart from the peaks very close to the resonant points, the $h-$ and $Z-$funnels show very mild or non-significant fine-tuning.

[6] Around the Higgs-resonance $\Delta m \simeq |m_h/2 - m_{\chi_1^0}|$, while around the $Z-$resonance $\Delta m \simeq 2|m_Z/2 - m_{\chi_1^0}|$, due to the larger width of the $Z-$boson. This can be appreciated in figure 4.15.

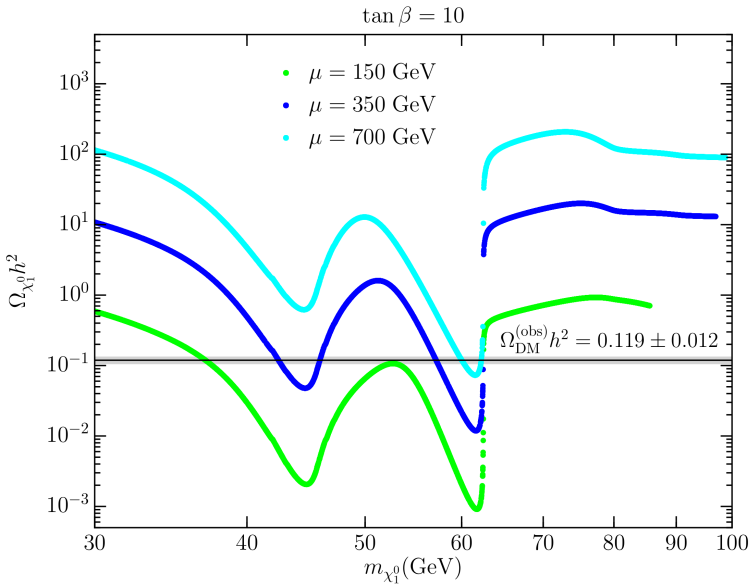

Figure 4.15: $\Omega_{\chi_1^0}h^2$ vs M_1 in the region of $h-$ and $Z-$funnels for $\tan\beta = 10$ and three (positive) values of μ. The grey band denotes the observed relic abundance.

4.6 Annihilation and Co-annihilation

Co-annihilation occurs when one or several particles with masses close to the LSP annihilate efficiently. In that case, the relic density is still given by eq. (4.4), but with the, effective, averaged annihilation cross-section, $\langle\sigma_{\rm eff}v\rangle$, given by eq. (4.11). Once more, this mechanism is only useful if the LSP is essentially a bino, which is the instance where the LSP does not annihilate efficiently enough at early times.

Due to the Boltzmann factor in eq. (4.11), $\langle\sigma_{\rm eff}v\rangle$, and thus $\Omega_{\chi_1^0}$, is exponentially sensitive to the mass gap, Δm, between the neutralino and its neighbouring particles. Hence, the most important dependence on M_1 goes, qualitatively, as

$$\Omega_{\chi_1^0} \sim e^{-\xi x_f\left(\frac{\Delta m}{M_1}\right)} , \tag{4.19}$$

where $x_f \simeq 20$ and ξ is typically $\mathcal{O}(1)$. Some particularly important possibilities for the co-annihilating particles are the gluino, the stop and the stau (beside Higgsinos and winos, analysed in previous sections). The above exponential dependence makes the standard criterion of fine-tuning to be quite severe in all cases,

$$\Delta_{M_1} = \left|\frac{\partial \log \Omega_{\chi_1^0}}{\partial \log M_1}\right| \simeq \xi x_f \frac{\tilde{m}}{M_1} = \mathcal{O}(1)\times 20 , \tag{4.20}$$

where $\tilde{m}$ is the mass of the co-annihilating particle. The puzzling, and suspicious, fact is that this estimation of the tuning does *not* depend on the mass difference $\tilde{m} - M_1$. It is essentially constant

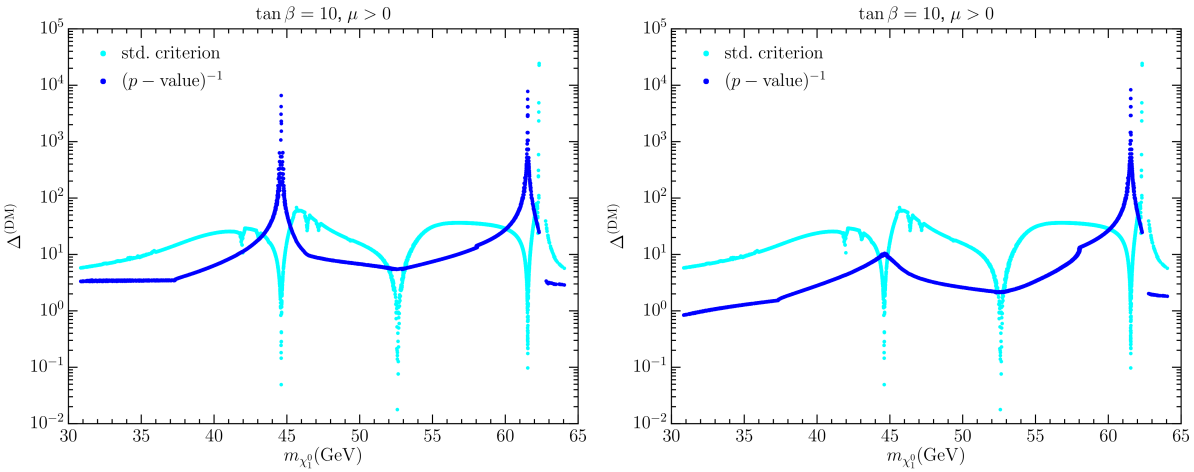

Figure 4.16: Left panel: Fine-tuning in the region of $h-$ and $Z-$funnels for $\tan\beta = 10$, calculated using the 'standard criterion' [see eq. (4.5)] (cyan band) and using the $p-$value criterion, as explained in the text (blue band). Right panel: The same but adding up the $p-$values corresponding to the $h-$ and $Z-$funnels, when the value of μ allows for both possibilities (see text).

independently of how precisely M_1 should be close to $\tilde{m}$. Certainly, this is due to the fact that the standard criterion measures sensitivity rather than fine-tuning, and these are not always equivalent.

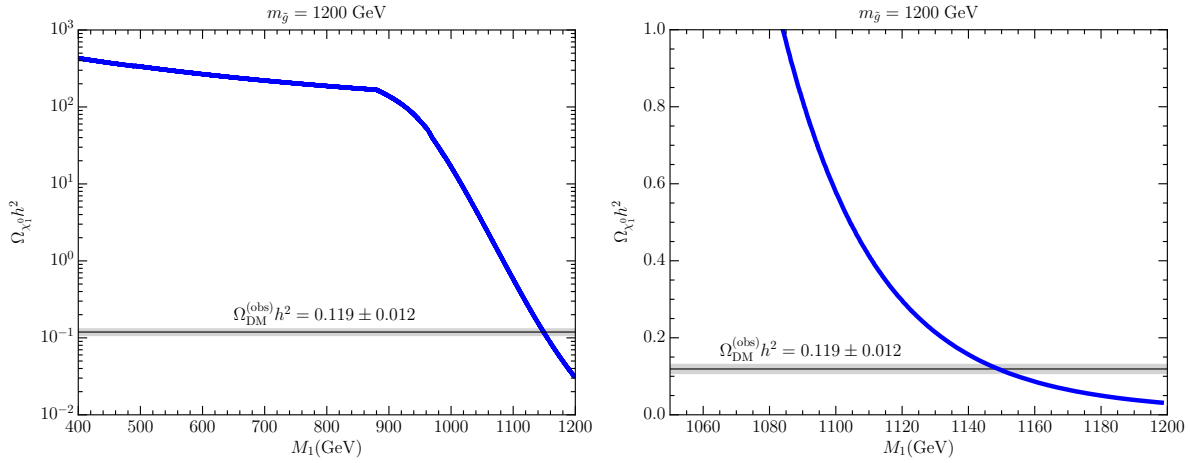

Figure 4.17: $\Omega_{\chi_1^0}h^2$ vs M_1 in the gluino co-annihilation scenario for fixed $m_{\tilde{g}} = 1200$ GeV. The lightest neutralino is essentially bino. Left (right) panel shows the dependence in logarithmic (linear) units.

In order to illustrate these aspects, let us consider the case of gluino co-annihilation. Figure 4.17 (left panel) shows $\Omega_{\chi_1^0}$ vs M_1 for $m_{\tilde{g}} = 1200$ GeV. The exponential dependence on M_1 in the co-annihilation region has been zoomed in linear scale in the right panel. Now, comparing this figure to figure 4.3, it is clear that the standard criterion leads to an overestimation of the fine-tuning, since the truncation of $\Omega_{\chi_1^0}(M_1)$ at first order around the physical point is not good enough to describe the whole region where

$\Omega_{\chi_1^0} \leq \Omega_{\rm DM}^{\rm (obs)}$. Once again a more sensible measure is given by the $p-$value,

$$p-\text{value} \simeq \frac{\Delta m}{|M_1|} \,. \tag{4.21}$$

Figure 4.18 shows the fine-tuning calculated with the standard criterion eq. (4.5) and that estimated as the inverse of the $p-$value eq. (4.21) for gluino co-annihilation. For each value of M_1, the corresponding $m_{\tilde{g}}$ is chosen so that the observed relic abundance (4.3) is reproduced. As expected, the standard criterion clearly overestimates the fine-tuning and is suspiciously independent of M_1. On the contrary, the $p-$value criterion shows a less severe tuning, especially for $M_1 \lesssim 500$ GeV, where it becomes almost irrelevant. The increase in this fine-tuning with M_1 occurs because the heavier the gluino, the less efficient becomes its annihilation, and this must be compensated by a more precise gluino-bino degeneracy.

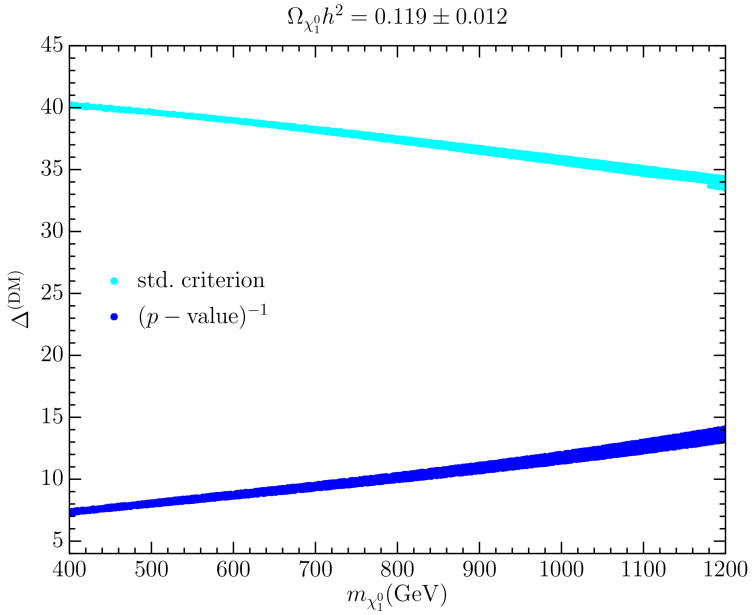

Figure 4.18: Fine-tuning in the gluino co-annihilation scenario, calculated using the 'standard criterion' [see eq. (4.5)] (cyan band) and using the $p-$value criterion, i.e. $(\Delta m/M_1)^{-1}$ (blue band). The $m_{\tilde{g}}$ value is chosen so that the observed relic density, $\Omega_{\chi_1^0}h^2 = 0.119 \pm 0.012$, is always reproduced. The lightest neutralino is essentially bino.

Other co-annihilation cases, as the mentioned above, show a similar pattern.

4.7 Connection to the electroweak fine-tuning

The DM fine-tuning must be combined with that related to the EW scale, since both affect the same theoretical scenario, namely the MSSM. We recall here that the EW fine-tuning is reasonably well esti-

mated by the 'standard measure', $\Delta^{(\mathrm{EW})} = \max\{\partial m_h^2/\partial\theta_i\}$ [7], where θ_i are the independent parameters of the model. As discussed in section 4.2 [see eq. (4.7)], this measure can be interpreted as the $p-$value associated with the small size of the EW scale. In sections 4.3–4.6, we have evaluated the analogous $p-$value to reproduce $\Omega_{\mathrm{DM}}^{(\mathrm{obs})}$. The main (computational) difference with the EW fine-tuning is that in this case the 'standard measure' of the fine-tuning is not a reliable estimation of the $p-$value, so the latter has to be evaluated in a more direct way, as we have done. Typically, the EW fine-tuning is $\gtrsim \mathscr{O}(100)$, i.e. it is $\mathscr{O}(10)$ times more severe than of the the DM relic abundance, though the latter can be extremely larger at special places, see e.g. figures. 4.7, 4.13 and 4.16. On the other hand, due to their common statistical interpretation (as $p-$values), it is clear that both fine-tunings should be multiplicatively combined. A subtle aspect here is that the EW and DM fine-tunings arise from cancellations between the same set of parameters.

This issue was analysed in ref. [165], appendix A[8]. The idea is that when we compute the fine-tuning in a quantity, say Ω_{DM}, we are free to vary the input θ_i's only in a way that all the potential constraints (in this case the EW scale) are fulfilled. Denoting, for simplicity, $(\Delta_{\mathrm{EW}})_i$, $(\Delta_{\mathrm{DM}})_i$ the EW and DM fine-tunings (i.e. the inverse $p-$values) with respect to the θ_i parameters, and $G(\theta_i) = 0$ the EW condition, we should project $\vec{\Delta}_{\mathrm{DM}}$ into the subspace orthogonal to the $G(\theta_i) = 0$ hypersurface in the $\{\log\theta_i\}$ space. In other words, we have to re-define the DM fine-tuning as

$$\vec{\Delta}_{\mathrm{DM}} \to \vec{\Delta}_{\mathrm{DM}} - \frac{1}{|\vec{\Delta}G|^2}(\vec{\Delta}_{\mathrm{DM}}\cdot\vec{\Delta}G)\vec{\Delta}G\,, \tag{4.22}$$

where $\overrightarrow{\Delta G} \equiv \{\partial G/\partial\log\theta_i\} \propto \vec{\Delta}_{\mathrm{EW}}$.

From this discussion, it is clear that only the parameters that contribute substantially to both the EW and DM fine-tunings are to play a relevant role in the previous projection. In this sense, the EW fine-tuning is dominated by the initial values of $m_{\tilde{t}}^2, M_3$ and μ parameters (see chapter 2), while the DM fine-tuning is dominated by M_1, and, depending on the annihilation mechanism, by μ, M_2, m_A or $m_{\chi'}$, where χ' is a possible co-annihilating particle (gluino, stop, etc.). Consequently, only the DM fine-tuning associated with μ or $m_{\chi'}$ is subject to be lowered by the non-trivial 'interference' with that of the EW scale. The conclusion is that the DM fine-tuning with respect to M_1 (which was computed in previous subsections) is always representative of the total DM fine-tuning and does not need to be corrected by the projection onto the subspace satisfying the EW condition.

As discussed in section 4.3, the DM fine-tuning is quite independent of the details of the MSSM scenario (whether it is CMSSM, NUHM, etc., or the value of the high-energy scale, M_{HE}). In this respect, it is a very robust feature of the MSSM. This fortunate circumstance does not occur for the EW fine-tuning: $\Delta^{(\mathrm{EW})}$ is much more model-dependent, since it depends on the initial values of $M_3, m_{\tilde{t}}$, etc., and on the correlations between them (e.g. whether or not there is a universal scalar mass). It also depends on M_{HE}. Concerning this point, we can presume that $M_{HE} = M_X$, because a lower value for

[7] This expression is equivalent to the expression (4.6), once the radiative corrections to the Higgs effective potential are taken into account (see chapter 2).

[8] The same prescriptions were independently found in later references [160, 221].

M_{HE} would typically lead to a very light gravitino[9] ($m_{3/2} \sim (M_{\rm HE}/M_{\rm P})m_0$), which would then play the role of the LSP, instead of the lightest neutralino, as assumed in this chapter. In any case, it is clear that for every scenario for which the DM fine-tuning has been computed in sections 4.3–4.6, there is not a unique value of $\Delta^{(\rm EW)}$; the latter depends on the details of the high-energy theory.

Nevertheless, instead of $\Delta^{(\rm EW)}$ we can consider $\Delta^{(\rm EW)}_{\rm min}$, i.e. the minimal EW fine-tuning. Normally $\Delta^{(\rm EW)}$ is dominated by the M_3-contribution or by the $\mu-$contribution[10]. So we could just set $m_{\tilde{g}}$ at its experimental lower bound, ~ 1.3 TeV [242], which amounts to $M_3 \simeq 0.59$ TeV. This gives $\Delta^{(\rm EW)}_{M_3} = \mathcal{O}(100)$ (see chapter 2), independently of the DM scenario, provided it can accommodate such light gluino. However, this is not always the case, e.g., as mentioned in the introduction, for pure-wino DM (which does not entail DM fine-tuning), $M_{\chi^0_1} \sim m_{\tilde{W}} \simeq 3$ TeV. This necessarily implies a heavy gluino, $m_{\tilde{g}} > 3$ TeV and, in turn, a much larger EW fine-tuning, near $\mathcal{O}(1000)$ (notice here that, parametrically, $\Delta^{(\rm EW)}_{M_3} \propto M_3^2 \propto m_{\tilde{g}}^2$). If the gaugino masses are unified at high energy, the EW tuning is even larger, since $m_{\tilde{g}} \simeq 2.8 m_{\tilde{W}}$ (see chapter 2). Other DM scenarios that may demand a heavy gluino are co-annihilation (with a particle different from gluino), $A-$funnel or well-tempered bino-wino-Higgsino, whenever $M_{\chi^0_1} \gtrsim 1.3$ TeV. In contrast, if the co-annihilation is with a gluino, this can be substantially lighter than 1.3 TeV, because it would be quite degenerate with the LSP, and thus invisible at the LHC. Hence, the latter scenario would reduce $\Delta^{(\rm EW)}_{M_3}$! Actually, from figure 4.18, we see that co-annihilation with a light gluino could improve both the DM and the EW fine-tunings.

Regarding the $\mu-$contribution, this is $\Delta^{(\rm EW)}_{\mu} \simeq (2\mu/m_h)^2$ (for further details see chapter 2), so for large enough μ, $\Delta^{(\rm EW)}$ becomes dominated by $\Delta^{(\rm EW)}_{\mu}$. More precisely, this happens for $\mu \gtrsim (1/2.3)m_{\tilde{g}}$, in particular for $\mu \gtrsim 570$ GeV if $m_{\tilde{g}}$ is close to its 1.3 TeV lower bound [242]. Consequently, the above-mentioned DM scenarios that implied a large $\Delta^{(\rm EW)}_{M_3}$, imply also an even larger $\Delta^{(\rm EW)}_{\mu}$. It is also worth mentioning that for pure Higgsino DM (which does not amount to DM fine-tuning), $M_{\chi^0_1} \sim \mu \simeq 1$ TeV, implying $\Delta^{(\rm EW)}_{\mu} \gtrsim \mathcal{O}(200)$.

From the previous discussion, it is clear that $\Delta^{(\rm DM)}$ should be kept as small as possible, preferably compatible with a non-fine-tuned situation, otherwise the combined fine-tuning will be above several thousands. This can be achieved in an obvious way if the DM is pure Higgsino or pure wino. Nonetheless, as mentioned, in the latter case the EW fine-tuning raises to $\gtrsim \mathcal{O}(1000)$ (for pure Higgsino it also grows but in a much milder way). Other cases that essentially imply no (or very mild) DM fine-tuning are: well-tempered bino-Higgsino (if $M_{\chi^0_1}$ is not around 500 GeV); Higgs, Z and A funnels when $M_{\chi^0_1}$ is not too close to (half) the resonance mass; and co-annihilation scenarios when $M_{\chi^0_1}$ is rather light, i.e. $\lesssim$ 500 GeV.

Finally, in all the cases we have to ensure that *i)* the value of $m^2_{H_u}$ at LE has the right size ($\sim \mu^2$) to enable the correct EW breaking, and *ii)* the physical Higgs mass, $m_h \simeq 125$ GeV, is reproduced. Both facts have to do with the values of $m^2_{\tilde{t}_L}$, $m^2_{\tilde{t}_R}$, A_t, and $m^2_{H_u}$ at HE. In general, it will be possible to

[9] The gravitino could be heavier than this naive expectation in theories with extra dimensions, where gravity is stronger, see e.g. ref. [241].

[10] We are not considering here an (unknown) hypothetical scenario where all the soft terms and μ are theoretically correlated in such fortunate way that their contributions to m^2_h nearly cancel, so that there is no fine-tuning!

arrange these parameters so that (in combination with $M_3 \simeq 1.3$ TeV) they implement *i)* and *ii)* without significantly affecting the value of $\Delta^{(\mathrm{EW})}$. However, if there are theoretical correlations between the initial soft terms, the *i)* and *ii)* conditions may imply further constraints on the theory and thereby an increase in $\Delta^{(\mathrm{EW})}$. Next, we illustrate this point by considering the case of pure Higgsino DM (one of the preferred scenarios from the above discussion) when the theory is some kind of constrained MSSM.

4.8 Accommodating Higgsino DM in the MSSM

If the LSP is close to a pure Higgsino (with mass $\simeq \mu \simeq 1$ TeV), the rest of the supersymmetric particles must be heavier, which imposes conditions on HE parameters. Assuming $M_{\mathrm{HE}} = M_{\mathrm{X}}$ in what follows, in section 2.3.3 we have found

$$\begin{aligned} m_{\tilde{g}} &\simeq 2.22 M_3 > 1 \text{ TeV} , \\ m_{\tilde{W}} &\simeq 0.8 M_2 > 1 \text{ TeV} , \\ m_{\tilde{B}} &\simeq 0.43 M_1 > 1 \text{ TeV} , \end{aligned} \tag{4.23}$$

where M_i are the gaugino masses at the HE scale. If these are unified, $M_1 = M_2 = M_3 \equiv M_{1/2}$, then from the last equation

$$M_{1/2} \gtrsim 2.3 \text{ TeV} , \tag{4.24}$$

implying

$$m_{\tilde{g}} > 5.16 \text{ TeV} . \tag{4.25}$$

This large value of $M_{1/2}$ implies a huge EW fine-tuning, see eq. (4.29) below. Other supersymmetric masses are also forced to be very large, e.g. the average stop mass, $m_{\tilde{t}}^2 \equiv \frac{1}{2}(m_{\tilde{t}_1}^2 + m_{\tilde{t}_2}^2)$, according to section 2.3.3

$$\overline{m}_{\tilde{t}}^2 \simeq \frac{1}{2}(5.945 M_3^2 + 0.679 m_{\tilde{t}_L}^2 + 0.611 m_{\tilde{t}_R}^2 + 0.182 M_2^2 - 0.307 m_{H_u}^2 \cdots) + m_t^2 . \tag{4.26}$$

Therefore, assuming gaugino unification leads to $m_{\tilde{t}} \gtrsim 4$ TeV. Similarly, using the formulae derived in chapter 2, we find $m_{\tilde{L}} \gtrsim 1.5$ TeV. The singlet sleptons are much less constrained, but they are forced anyhow to live above 1 TeV so that the Higgsino plays the LSP role. All the previous relations are much less restrictive if we give up gaugino unification or considers lower values of M_{HE}, though the latter possibility is disfavoured if the LSP is not the gravitino.

One can consider now the EW minimization condition, which, at (moderately) large $\tan\beta$, reads

$$-\frac{m_h^2}{2} = \mu^2 + m_{H_u}^2 , \tag{4.27}$$

with all quantities defined at LE, in particular (see table A.1)

$$\begin{aligned} m_{H_u}^2\big|_{LE} &= -1.6M_3^2 + 0.63m_{H_u}^2 - 0.37m_{\tilde{t}_L}^2 - 0.29m_{\tilde{t}_R}^2 \\ &\quad +0.28A_tM_3 + 0.2M_2^2 - 0.13M_2M_3 - 0.11A_t^2 + \cdots , \end{aligned} \tag{4.28}$$

where the variables in the r.h.s. are at HE. Notice from eq. (4.27) that for $|\mu| \simeq 1$ TeV, $m_{H_u}^2 \simeq -|\mu|^2 \simeq -1$ TeV^2, which is an additional constraint. In fact, in the popular constrained-MSSM (CMSSM), it seems impossible to satisfy this constraint with all the supersymmetric masses higher than 1 TeV. Note that for the CMSSM, the contributions from $m_{H_u}^2$, $m_{\tilde{t}_L}^2$ and $m_{\tilde{t}_R}^2$ almost cancel in eq. (4.28), which is the well-known focus-point behaviour. Then, it is almost impossible to compensate the huge negative contribution coming from M_3^2 (recall that in the CMSSM $M_3 = M_{1/2} \simeq 2.3$ TeV, due to gaugino unification). Using a very large A_t with the appropriate sign does not help since the negative contribution from A_t^2 would dominate. Incidentally, pure wino DM is also unattainable, because whenever there is gaugino unification, the bino is lighter than the wino, so the latter cannot be the LSP.

Therefore, we have to go beyond the CMSSM. The non-universal-Higgs-Mass model (NUHM) is like the CMSSM, but allowing the soft Higgs masses, $m_{H_u}^2, m_{H_d}^2$ to be different from the other scalar masses at HE (a usual choice is $m_{H_u}^2 = m_{H_d}^2$). Then, if $m_{H_u}^2$ is large enough at HE, we can achieve $m_{H_u}^2(LE) \simeq -1$ TeV^2 in eq. (4.28). This implies that the extra Higgs states are quite heavy (if the $m_{H_u}^2 = m_{H_d}^2$ condition is imposed). The whole spectrum seems beyond the LHC. In addition, the model presents a high EW fine-tuning:

$$\Delta_{M_{1/2}}^{(\mathrm{EW})} = \left|\frac{d\log m_h^2}{d\log M_{1/2}}\right| \simeq \left|-4\frac{M_{1/2}^2}{m_h^2}\left(-1.6+0.2-0.13+0.14\frac{A_t}{M_{1/2}}+\cdots\right)\right| \simeq 2000\,. \tag{4.29}$$

Another possibility is to start with non-universal gaugino masses. This is a much more flexible scenario and, in principle, it does not seem difficult in this case to achieve the LSP condition for the Higgsino and the correct EW breaking with supersymmetric masses (in particular gluino masses) not far from their experimental lower bounds.

4.9 Conclusions

One of the most celebrated bonuses of supersymmetric theories is the presence of stable WIMPs, which are natural candidates for dark matter (DM). In the MSSM, such role is usually played by the lightest supersymmetric particle (LSP), which is typically the lightest neutralino. However, when we go into the details, it turns out that in most scenarios some kind of tuning is needed in order to obtain Ω_{DM} of the right magnitude. This fine-tuning is worrisome since it has to be combined with the ubiquitous electroweak (EW) fine-tuning problem, i.e. the delicate balance between soft terms required to reproduce the smallness of the EW scale.

Taking into account that the original motivation for low-energy SUSY was to solve the hierarchy problem, which is, in fact, the EW fine-tuning problem of the SM, it is logical to demand SUSY scenarios to be as natural as possible. In this sense, there exists a vast literature examining the EW fine-tuning problem, but little concerning that of the DM relic density.

In this chapter, we have studied this problem in an, as much as possible, exhaustive and rigorous way. We have considered the MSSM framework, assuming that the LSP is the lightest neutralino, χ_1^0, and explored various possible scenarios. These include different masses and compositions of χ_1^0, which are completely defined by the parameters involved in the neutralino mass matrix ($M_1, M_2, \mu, \tan\beta$), as well as different mechanisms for neutralino annihilation in the early Universe (well-tempering, funnels and co-annihilation scenarios). We have also discussed the statistical meaning of the fine-tuning and how it should be computed for the DM relic abundance, and combined with the EW fine-tuning. It turns out that the 'standard fine-tuning measure', $\Delta = d\log\Omega_{\rm DM}/d\log\theta$ is not appropriate in most of the cases, and we have to evaluate the $p-$value associated with the smallness of $\Omega_{\rm DM}$, which, actually, amounts normally to a simpler computation. A fortunate fact is that the relevant (low-energy) parameters, involved in the neutralino mass matrix are essentially in one-to-one multiplicative correspondence with the initial (high-energy) parameters. This allows to compute the fine-tuning directly on the low-energy parameters with full generality. In consequence, the DM fine-tuning is quite independent of the details of the MSSM scenario (whether it is CMSSM, NUHM, etc., or the value of the high-energy scale). In this sense, it is a very robust feature of the MSSM. In contrast, the EW fine-tuning is much more model-dependent.

Concerning the results, the fine-tuning related just to the DM relic abundance is negligible or very mild in a number of scenarios. More precisely, when χ_1^0 is essentially a pure Higgsino or a pure wino there is no fine-tuning associated with the DM relic density. Other cases that essentially imply no (or very mild) DM fine-tuning are: well-tempered bino-Higgsino (if $M_{\chi_1^0}$ is not around 500 GeV); Higgs, Z and A funnels when $M_{\chi_1^0}$ is not too close to (half) the resonance mass; and co-annihilation scenarios when $M_{\chi_1^0}$ is rather light, i.e. $\lesssim$ 500 GeV.

Nevertheless, this is not the end of the story, as the DM fine-tuning must be combined with that of the EW scale. Modulo some subtleties discussed in this chapter, both fine-tunings should be essentially multiplicatively combined. Thus, we should demand $\Delta^{(\rm EW)}$ to be as mild as possible. Normally $\Delta^{(\rm EW)}$ is dominated by the M_3-contribution or by the $\mu-$contribution. So we could just set $m_{\tilde{g}}$ at its experimental lower bound, ~ 1.3 TeV, which leads to $\Delta^{(\rm EW)} = \mathcal{O}(100)$, independently of the DM scenario, provided it can accommodate such light gluino (see chapter 2). However, this is not always the case. E.g. for pure-wino DM (which does not entail DM fine-tuning), $M_{\chi_1^0} \sim m_{\tilde{W}} \simeq 3$ TeV. This necessarily implies a heavier gluino and, in turn, a much larger EW fine-tuning, near $\mathcal{O}(1000)$. By contrast, if the co-annihilation is with a gluino, the latter can be substantially lighter than 1.3 TeV, since it would be invisible at the LHC. Hence, the latter scenario would reduce $\Delta^{(\rm EW)}$!

As a final remark, naturalness is a reasonable guide to look for plausible supersymmetric scenarios. In this regard, a strong emphasis has been put on the EW fine-tuning, but the DM fine-tuning is also very important, as shown in this chapter, especially when it is combined with that of the EW scale. Needless

to say, this aspect should be taken into account when we explore ‘Natural SUSY’ scenarios and their possible signatures at the LHC and in DM detection experiments.

Chapter 5

Case study: Low-mass neutralino dark matter in supergravity scenarios

Weakly-interacting massive particles (WIMPs) are a very appealing kind of candidates to solve the dark matter (DM) problem, since generally they would be thermally produced in the correct amount in the early Universe. Among them, light WIMPs have received much attention in the last years in view of some direct [243–249] and indirect [250–264] detection experiments which might be seeing hints pointing towards a light DM particle.

However, these potential signals are being challenged by the null observations of other experiments. Several collaborations for DM direct detection have been able to place important constraints generally excluding the DM interpretation of these signals under certain assumptions. The most stringent bounds come from LUX [236, 265–267], PandaX-II [268], XENON [269–271], CDMS [272, 273], SIMPLE [274], KIMS [275], CRESST [276], a combination of CDMS and EDELWEISS data [277] and SuperCDMS [278, 279]. Furthermore, indirect detection experiments also provide an important constraint for low mass DM. Probably, the most important constraint for light WIMPs comes from the non detection of dwarf spheroidal galaxies (dSphs) in gamma rays by the Fermi-LAT collaboration [280, 281]. Although, under certain assumptions on the Milky Way DM profile, the Galactic centre provides a very stringent constraint as well [282]. The dSph limits exclude WIMPs with a thermal cross section (3×10^{-26} cm^3/s) up to masses around 100 GeV. Moreover, the DM interpretation of the potential hints from the Galactic centre [250–264] are seriously challenged by this analysis.

On the theoretical side, there have been efforts in constructing well motivated theoretical models to explain the direct detection potential signals. In this context, neutralino DM in Supersymmetric theories is one of the best motivated candidates. Light neutralino DM has been studied in the most appealing realisations of Supersymmetry (SUSY) at the Electroweak (EW) scale such as the Minimal Supersymmetric Standard Model (MSSM) [224, 283–293], the Next-to-MSSM (NMSSM) [8, 285, 287, 294–301], and some minimal extensions of the NMSSM [5, 6, 8, 302]. Furthermore, some regions of the parameter space of these models are still viable in light of the most recent experimental constraints [5, 6, 8, 290–293, 300, 301].

Nevertheless, an important question that still remains unanswered is whether or not these *effective* Supersymmetric models can have a viable origin from a Supergravity (SUGRA) theory defined at the Grand Unification Theory (GUT) scale. This is an interesting question since a conventional way of understanding the source of the soft supersymmetry-breaking terms is the breaking of Supergravity at a high energy scale. Moreover, by identifying the structure of the boundary conditions at the GUT scale, we could understand and quantify the degree of non-universality that is needed for having viable light neutralino DM, and hence providing a more accurate idea about the naturalness of these scenarios. The aim of this chapter is thus analysing if solutions with low-mass neutralinos in the MSSM can be achieved from a theory defined at the GUT scale and how natural these solutions are. We show that obtaining light neutralinos which are viable dark matter candidates is actually possible from the point of view of SUGRA theories with soft terms defined at the GUT scale. Furthermore, we have determined the important role of non-universalities in the structures of the soft parameters and discussed the possibility of discovering these solutions by means of the LHC and indirect detection experiments.

Another important issue that concerns MSSM scenarios is naturalness. Since the original motivation for SUSY models was precisely to avoid the huge fine-tuning associated with the hierarchy problem, we have performed a precise calculation of all the potential sources of fine-tuning in the MSSM. We have considered not only the contribution arising from the electroweak symmetry breaking condition, but also those required to reproduce different experimental and observational results such as the Higgs mass and the DM relic abundance. Lastly, we have estimated the total amount of fine-tuning present in those solutions allowed by the experimental data.

This chapter is organised as follows. In section 5.1, we summarise the conditions under which very light neutralinos can be viable dark matter candidates in the MSSM with parameters defined at the EW scale. Then, in section 5.2, we investigate whether these conditions can also be obtained from a high-energy description of the theory. We analyse a general Supergravity model and investigate the choices of non-universal gaugino and scalar masses that can produce viable neutralinos with very light masses without violating any experimental constraint. We also study the phenomenology of these scenarios in the context of direct and indirect DM searches. Besides, in this section we study the constraints coming from the LHC data, namely, from searches involving direct EW production of charginos, selectrons and smuons. In section 5.3, we summarise and calculate each of the contributions to the fine-tuning present in these scenarios, as well as the total amount of fine-tuning. Finally, the conclusions are left for section 5.4.

5.1 Low-mass neutralinos in the effective MSSM

Several studies [283–293, 303] have shown that a low-mass neutralino in the MSSM is a viable, albeit very fine-tuned, DM candidate. All the analyses performed after the Higgs boson discovery at the LHC consider the soft supersymmetry-breaking terms as input parameters defined at the SUSY scale. This is a framework often referred to as *effective* MSSM [283], which exhibits a large flexibility since it does

not incorporate any correlation among these parameters (although simplifying arguments are usually made).

In order for the neutralinos, $\tilde{\chi}_1^0$, to be viable DM candidates they have to reproduce the correct value for their thermal abundance, $\Omega_{\tilde{\chi}_1^0}h^2$, which is actually non trivial in the MSSM, in particular when they are light. In the MSSM, within the regions of the parameter space where neutralinos are lighter than 50 GeV, there exist three dominant ways in which light neutralinos can annihilate efficiently. The first annihilation mechanism involves the exchange of CP-odd Higgses, the second involves the exchange of a Z boson and, finally, the correct relic density can also be achieved through the t-channel exchange of sleptons.

For neutralinos lighter than approximately 25 GeV, the first mechanism is the most efficient one and the relic density condition is fulfilled if m_{A^0} is around $100-150$ GeV and $\tan\beta$ is $6-14$ [283, 284, 286]. Since the CP-odd Higgs mass and $\tan\beta$ parameters control the mass scale of the Higgs sector, the requirement of such light m_{A^0} pushes the entire Higgs sector masses around this value. This scenario, known as *intense coupling regime* [304], is very restricted by ATLAS and CMS searches for neutral and charged scalars decaying into τ-leptons [305, 306]. These unsuccessful searches have allowed to place stringent constraints on this scenario, almost ruling out this possibility. As previously mentioned, another possibility for neutralinos to account for the observed relic abundance occurs when they annihilate through the exchange of the Z boson while satisfying the resonant condition, $m_{\tilde{\chi}_1^0} \approx M_Z/2$. However, this possibility restricts the mass of neutralinos to be in a few GeV range around the resonance and thus, it does not allow to obtain neutralinos far below this region.

The annihilation through the exchange of sleptons, $\tilde{l}$, occurs in a t-channel diagram with a leptonic final state. This process is sufficiently efficient when the mediator is light enough. In ref. [287], this option was investigated concluding that the sleptons must lie just above the LEP limit, $\mathcal{O}(90)$ GeV, in order for the annihilation to be high, and hence, to fulfil the relic density constraint. In this scenario, the requirement of a relatively light CP-odd Higgs boson is not longer necessary which makes easier to evade all the collider constraints [285], and to yield neutralinos as light as 15 GeV [289–291]. Other works have pointed out the possibility that neutralinos could also be as light as 6 GeV if one sbottom is very light, with a mass splitting between them of a few GeV profiting from coannihilations[1] [288]. In view of the foregoing, hereafter we will focus only on this scenario.

The slepton exchange mechanism benefits especially from the presence of light staus, namely, their right-handed (RH) component [289]. This occurs specifically, due to an enhancement of the coupling of bino-like neutralinos to this component with respect to that of the left-handed (LH) component. The

[1] This scenario was motivated by the potential hints seen in direct detection experiments. Such a light sbottom increases considerably the elastic scattering cross section of neutralinos off protons and neutrons.

neutralino coupling to staus can be written as follows [290, 307]:

$$
\begin{aligned}
g_{\tilde{\chi}_1^0\tilde{\tau}_1\tau_{LH}} &= \sqrt{\frac{2}{v_u^2+v_d^2}}\left(m_Z\cos\theta_\tau(N_{11}s_W+N_{12}c_W)-N_{13}m_\tau\frac{\sin\theta_\tau}{\cos\beta}\right),\\
g_{\tilde{\chi}_1^0\tilde{\tau}_1\tau_{RH}} &= -\sqrt{\frac{2}{v_u^2+v_d^2}}\left(2m_Z\sin\theta_\tau N_{11}s_W-N_{13}m_\tau\frac{\cos\theta_\tau}{\cos\beta}\right),
\end{aligned}
\tag{5.1}
$$

where N_{1i} is the i-th component of the lightest neutralino in the basis $(\widetilde{B},\widetilde{W}^3,\widetilde{H}_d^0,\widetilde{H}_u^0)$, $v_{u,d}$ are the vacuum expectation values (VEVs) of the up and down Higgses, respectively, and finally $\cos\theta_\tau$ is the stau mixing. Since light neutralinos have to be mostly bino-like, $N_{11}\approx 1$, in order to avoid the constraints from the Z invisible decay, the coupling to the lightest RH stau in this case is higher than the corresponding coupling to the LH component. Therefore, the annihilation cross section of neutralinos through this mechanism will be increased due to the presence of a RH stau with a mass around 90 GeV, as close as possible to its lower experimental bound.

The most stringent limits on slepton masses come from LEP [308]. These sparticles were constrained to have masses $m_{\tilde{e}} > 100$ GeV, $m_{\tilde{\mu}} > 99$ GeV, $m_{\tilde{\tau}_1} > 80.5$ GeV and $m_{\tilde{\nu}} > 43$ GeV. Notice that the actual limits depend on the neutralino mass, which is assumed to be the LSP to extract these bounds. Thus, we will incorporate this dependence in our results. Furthermore, using LHC data is also possible to constrain the mass of the sleptons, namely through the searches for direct production of selectrons and smuons [309, 310].

Other constraints on SUSY particles might also affect the scenario considered along this chapter. For the first two generation of squarks, inclusive searches constrain their mass to be above 608 GeV, which holds for a compressed scenario [311]. For specific scenarios such as mass degeneracy in these families, this constraint can be as high as 1.5 TeV [312]. Consequently, in our analysis we will impose that the first two generation of squarks must be heavier than 1.5 TeV, which is a conservative choice. For the third generation of squarks and the gluino masses, no restriction will be implemented, since as we will see in section 5.2.3, we will analyse these cases separately.

Finally, low-energy observables are known to constrain severely SUSY theories, and namely, they can play an important role in this scenario. We will impose the recent measurement of the branching ratio of the $B_s\to\mu^+\mu^-$ process by the LHCb [313] and CMS [314] collaborations, which collectively yields $1.5\times10^{-9} < \mathrm{BR}(B_s\to\mu^+\mu^-) < 4.3\times10^{-9}$ at 95% CL [315]. This branching ratio is strongly dependent on the Higgs sector of the model, and more specifically, on the CP-odd Higgs mass and $\tan\beta$. In SUSY theories the contributions to the flavour changing decay process $b\to s\gamma$ can be very important. We will take the experimental measurement of this observable at 2σ, which requires the range $2.89\times10^{-4} < \mathrm{BR}(b\to s\gamma) < 4.21\times10^{-4}$, which takes into account theoretical and experimental uncertainties added in quadrature [316–320]. It is also known that there exists a discrepancy between the measured values of the muon anomalous magnetic moment, a_μ, and the SM prediction, that can be interpreted as a hint of SUSY. Although, we have not included this observable as a constraint in our analysis, we will comment on the prediction of a_μ for the solutions found in this chapter.

5.2 Low-mass neutralinos in SUGRA theories

As usual, the SUGRA model presented in this chapter is defined in terms of the soft supersymmetry-breaking parameters, which comprise mass parameters for the scalars and gauginos, as well as trilinear parameters associated with the Yukawa couplings. Successful Radiative Electroweak Symmetry Breaking (REWSB) is achieved by imposing the following boundary condition on the μ parameter at the EW scale,

$$\mu^2 = \frac{m_{H_d}^2 - m_{H_u}^2 \tan^2\beta}{\tan^2\beta - 1} - \frac{1}{2}M_Z^2, \tag{5.2}$$

in terms of the Higgs soft mass parameters. The ratio of the Higgs VEVs, $\tan\beta$, will hereafter be considered as a free parameter.

In general, the soft SUSY breaking terms arising from a large class of string scenarios, namely symmetric orbifold constructions, present a certain degree of non universality [321–323]. Furthermore, within some realisation of type I string models is possible to obtain non universal gaugino masses, A-terms and scalar masses [324]. This motivates us to consider a general scenario in which some of the soft terms can be different from each other. Moreover, it is known that in the minimal SUGRA scenario of the MSSM light neutralinos ($m_{\tilde{\chi}_1^0} \lesssim 50$ GeV) are not allowed in light of experimental constraints such as the chargino mass constraint and the Higgs mass measurement [325, 326]. Due to this fact, the first crucial step to find scenarios comprising light neutralinos is to allow departures from the universal scenario in the gaugino sector which allow the lightest neutralino to be dominated by the bino component. Bino-like neutralinos are obtained by lowering $|M_1|$ with respect to $|M_2|$ and $|\mu|$. These two parameters, M_2 and μ, are involved in the chargino mass matrix, and thus, LEP constraint rules out the region of the parameter space in which $|M_2|, |\mu| \lesssim 100$ GeV. From this condition, it follows that bino-like neutralinos require $|M_1| \lesssim 100$ GeV and then $m_{\tilde{\chi}_1^0} \simeq |M_1|$ at the EW scale. We will keep a universal relation between M_2 and M_3 at the GUT scale. In what follows, to differentiate between parameters evaluated at the GUT and EW scales, unless otherwise specified, we denote the latter with the upper index EW.

Let us start defining the soft masses and trilinear parameters at the GUT scale. We will consider a gaugino sector parametrized by

$$M_1, M_2 = M_3\,. \tag{5.3}$$

Regarding the scalar sector, we will allow departures from universality in the Higgs soft masses, which in light of eq. (5.2) control the μ parameter at the EW scale. This has a profound impact on the phenomenology of the solutions at the EW scale since μ determines the Higgsino component of the lightest neutralino and therefore the DM phenomenology [327]. In consequence, we have used as input parameters,

$$m_{H_d}, m_{H_u}\,. \tag{5.4}$$

As mentioned in the previous section, the relic density constraint requires slepton masses close to the LEP limit, namely, a RH stau mass around 90 GeV at the EW scale. For this reason, we have considered non-universalities in the slepton soft masses, which at high energy are described by the

Parameter	Range
M_1	$[-110, 110]$
$M_2 = M_3$	$[-1000, 1000]$
$\tan\beta$	$[1.5, 60]$
A_U	$[-7000, 7000]$
A_D	0
A_E	$[-7000, 7000]$
m_{H_u}	$[1, 7000]$
m_{H_d}	$[1, 7000]$
$m_{\tilde{L}_2} = m_{\tilde{L}_1}$	$[0, 7000]$
$m_{\tilde{L}_3}$	$[0, 7000]$
$m_{\tilde{E}_2} = m_{\tilde{E}_1}$	$[0, 7000]$
$m_{\tilde{E}_3}$	$[1, 7000]$
$m_{\tilde{Q}_{1,2,3}} = m_{\tilde{U}_{1,2,3}} = m_{\tilde{D}_{1,2,3}}$	$[0, 7000]$

Table 5.1: Input parameters for the scan defined at the GUT scale. Masses and trilinear parameters are given in GeV.

following parameters,

$$m_{\tilde{L}_3}, m_{\tilde{E}_3}, m_{\tilde{L}_2} = m_{\tilde{L}_1}, m_{\tilde{E}_2} = m_{\tilde{E}_1}\,. \tag{5.5}$$

Since the LHC limits on the slepton masses are especially stringent for the first and second generations, we have taken the soft masses of these two generations as degenerated, while the third generation parameters are free to vary independently.

For the squarks soft masses, we have assumed universality so that they are given at the GUT scale by just one free parameter,

$$m_{\tilde{Q}_{1,2,3}} = m_{\tilde{U}_{1,2,3}} = m_{\tilde{D}_{1,2,3}} = m_{\tilde{Q}}\,. \tag{5.6}$$

Finally, the three trilinear parameters A_U, A_D and A_E are considered family independent. Particularly important is the top trilinear, A_U, which controls the Higgs mass and affects very strongly the BR($B_s \to \mu^+\mu^-$) [328]. The slepton trilinear term, A_E, might play an important role through the stau mixing. For the down type squarks, we have chosen $A_D = 0$. This parameter controls the mixing of the down sector and might modify radiative corrections to the Higgs mass at large $\tan\beta$, which would result in an increase of the Higgs mass[329]. This could be important to achieve a Higgs mass around 125 GeV. However, the large $\tan\beta$ regime is disfavoured by flavour constraints, and thus we would expect that this choice does not have an impact on the scenarios investigated throughout this chapter[2]. Therefore, we have considered the following trilinear parameters as inputs,

$$A_U, A_D = 0, A_E\,. \tag{5.7}$$

[2]Notice that some flavour constraints such as BR($B_s \to \mu^+\mu^-$) scale as $1/m_{A^0}^4$ and hence could be also avoided for large pseudoscalar masses.

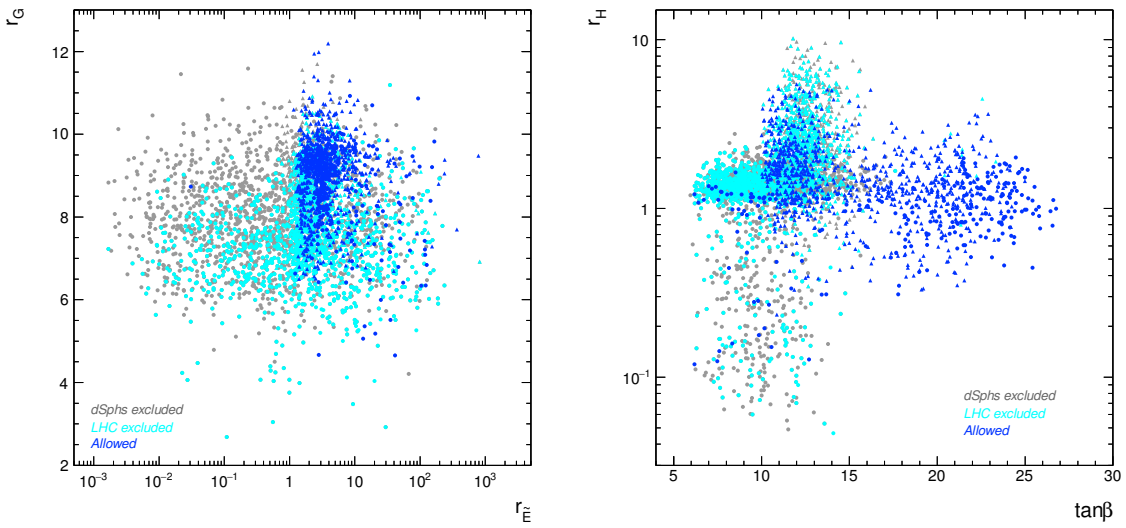

Figure 5.1: Universality patterns in the scalar and gaugino sectors. All points fulfil the experimental constraints from the Higgs sector, LEP limits on new particles, relic density and direct detection searches. Points excluded by dSph bounds for a $\tau^+\tau^-$ final state are shown in grey, solutions excluded by LHC searches for sparticles in cyan and points fulfilling all the experimental constraints are shown in blue. Circle points (◯) correspond to solutions with $M_1 > 0$, $M_2 > 0$ and $A_U < 0$, whereas triangles (△) represent those with $M_1 < 0$, $M_2 < 0$ and $A_U > 0$.

Following these criteria, we have performed a scan over the MSSM parameter space where the aforesaid input parameters are varied according to Table 5.1. In order to efficiently explore the 12-th dimensional parameter space considered, we have used `MultiNest 3.10` [233–235]. To that end, we have built a likelihood function, whose parameters are the neutralino relic density consistent with latest Planck results [330], $m_{H_1^0}$, BR$(B_s \to \mu^+\mu^-)$, and BR$(b \to s\gamma)$, calculated with `micrOMEGAs 4.3` [232, 331], and taken as Gaussian probability distribution functions around the measured values with 2σ deviations. This likelihood function is used to generate MCMC and to find regions of the parameter space that maximise the likelihood. Using `MultiNest` allows us to scan the parameter space of the model more efficiently, since relatively few evaluations are needed to converge to regions of maximum likelihood. Let us clarify at this point that a statistical approach to the problem presented here is out of the scope of this chapter. Our aim is to provide an answer to whether or not light neutralinos can be obtained from a general SUGRA scenario, not how statistically favoured are these scenarios in light of the current experimental data. Other constrains such as those coming from direct and indirect DM searches have been included once the solutions have been found and thus, they are not used to generate the MCMC. To evolve from the GUT scale down to the EW scale the input parameters, we have used `SoftSUSY 3.7.2` [219]. All collider constraints, including those from LEP, Tevatron and the LHC, have been implemented using the interfaces available in the `micrOMEGAs 4.3` code to different tools [331]. More specifically, the constraints on the Higgs sector were implemented through the codes

`HiggsBounds` [332, 333], `HiggsSignals` [334] and `Lilith` [335], LEP limits were imposed through the functions provided by `micrOMEGAs 4.3`, and finally LHC constraints on SUSY particles have been calculated with `SModelS` [336, 337].

For convenience, let us define the ratios,

$$r_G \equiv \frac{M_2}{M_1}, \qquad r_H \equiv \frac{m_{H_d}}{m_{H_u}}, \qquad r_{\tilde{E}} \equiv \frac{m_{\tilde{E}_3}}{m_{\tilde{E}_2}}, \tag{5.8}$$

which measure the departure from universality in the gaugino, Higgs and slepton sectors, respectively. In figure 5.1, we show the values of these ratios for all the solutions found fulfilling the experimental constraints from the Higgs sector, LEP limits on new particles, relic density and direct DM searches. Points excluded by Pass 8 data from dSphs are displayed in grey, those excluded by LHC searches for SUSY particles are shown in cyan and the solutions that fulfil all the experimental constrains in blue. Finally, circular shaped points (◯) correspond to solutions in which $M_1 > 0$, $M_2 > 0$ and $A_U < 0$, whereas triangle shaped points (△) represent those with $M_1 < 0$, $M_2 < 0$ and $A_U > 0$.

In the left panel of figure 5.1, we have plotted r_G versus $r_{\tilde{E}}$. As it can be seen, all viable points exhibit a precise relation between gaugino masses, $2.5 \lesssim r_G \lesssim 12$. As stated above, the chargino mass is proportional to M_2^{EW}, and it is restricted by LEP null searches as a function of the neutralino masses which results in $r_G > 1$ (the universal value). On top of that, our choice $M_2 = M_3$ yields $M_2^{EW} \simeq 3M_3^{EW}$, and thus the lower bound on the gluino mass forbids M_2 below ~ 250 GeV (see figure 5.2). All this together is translated into values of $r_G \gtrsim 2.5$. On the other hand, the ratio of slepton soft masses, $r_{\tilde{E}}$, is much less constrained. The relic density constraint, which prefers a light RH stau, favours $m_{\tilde{E}_3}$ to be below the LEP constraint[3] and hence it is found close to the lower edge of the scan range (see figure 5.2). On top of this, the values of $m_{\tilde{E}_2} = m_{\tilde{E}_1}$ are affected by the ATLAS bound on the first and second generation of sleptons which clearly generates $r_{\tilde{E}} < 1$. However, since we are allowing A_E to be a free parameter[4], the slepton masses can be deeply influenced by it, rendering into a less constrained $r_{\tilde{E}}$ ratio.

In the right panel of figure 5.1, r_H is plotted versus $\tan\beta$, with the same colour code as the left panel. In this plane, we can see that the relation between the Higgs soft masses is, in general, surprisingly close to the universal value. The values of $\tan\beta$ found are in the range 6-27, which is mainly a consequence of the Higgs mass bound because in this range the maximal mixing scenario is reached.

Let us comment that when universal relations between the soft parameters at the GUT scale are taken, it is has been pointed out that the SM-like Higgs mass requires $|A_U/m_{\tilde{Q}}| > 2$ [338]. Unlike this, we have obtained points with the correct Higgs mass with $|A_U/m_{\tilde{Q}}| < 2$ due to the flexibility provided by assuming non universality. For the slepton sector, we have found that in general our solutions accumulate around $|A_E/m_{\tilde{E}_3}| \approx 5$, but they can reach very high values when the soft mass $m_{\tilde{E}_3} < 10$ GeV and $|A_E|$ is at the TeV scale.

In figure 5.2, the spectrum of soft masses at the GUT scale is shown. Notably, we observe that low-mass neutralinos require a definite type of spectrum. Most of the allowed solutions comprise soft

[3] The running of this parameter is positive [41].

[4] Remind that this parameter is taken as family independent.

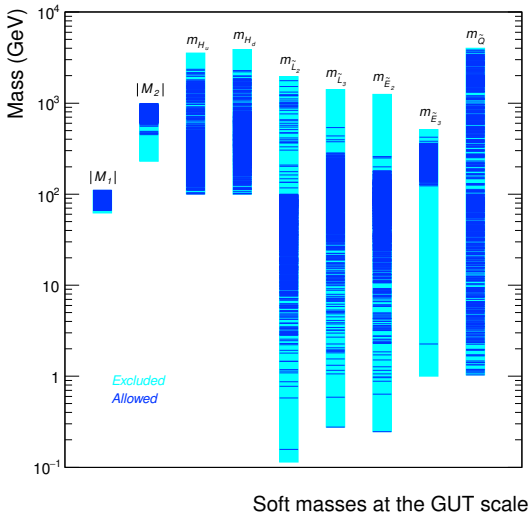

Figure 5.2: Spectrum of the soft masses at the GUT scale. Regions shaded in blue correspond to the points fulfilling all the experimental constrains, solutions excluded by LHC searches for sparticles and dSph bounds are shaded in cyan.

masses at the GUT scale in the range of 10 GeV and 1 TeV, being lighter, in general, the soft masses corresponding to the slepton sector. This translates, at the EW scale, into spectra that can be taken as representative of these scenarios, as it can be observed in figure 5.3. More specifically, these scenarios comprise a gap between the EW sector, represented by the sleptons and the lightest neutralino, and the coloured sector which is sited at the TeV scale as a consequence of the LHC null searches. As we will see later, this kind of scenarios can be explored at the LHC by means of searches involving EW direct production.

Finally, the presence of relatively light smuons, charginos and neutralinos, as well as large values of $\tan\beta$, produce sizeable SUSY contributions to the muon anomalous magnetic moment. From e^+e^- data, the SUSY contribution to this observable is constrained to be $10.1\times10^{-10} < a_\mu^{SUSY} < 42.1\times10^{-10}$ at 2σ. However, tau data favour a slightly smaller discrepancy, $2.9\times10^{-10} < a_\mu^{SUSY} < 36.1\times10^{-10}$ at 2σ [339], while a more recent update using the Hidden Local Symmetry model leads to $16.5\times10^{-10} < a_\mu^{SUSY} < 48.6\times10^{-10}$ at 2σ [340]. We have checked that most of the solutions found satisfying all the experimental constraints cluster around $a_\mu^{SUSY} \approx 20\times10^{-10}$, in great agreement with all the mentioned data sets. Only a subset of these solutions fall well below 10^{-10}, but these are still within the 2σ lower bounds. This is a consequence that arises from the presence of a light EW sector in the allowed solutions (see figure 5.3).

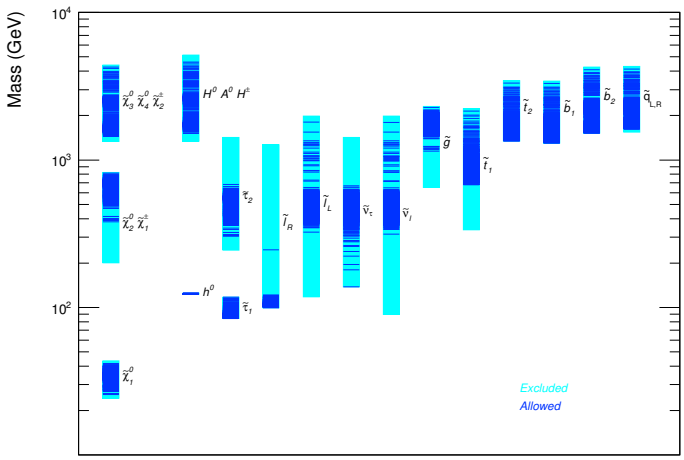

Figure 5.3: Spectrum of physical masses. Colour code as in figure 5.2.

5.2.1 Direct detection

Direct DM searches are based on the elastic scattering of DM off nuclei inside a detector. For any WIMP candidate, the WIMP-nucleus elastic cross section depends, at the microscopic level, on the WIMP-quark interaction strength. For the MSSM neutralino (and in general for any Majorana fermion, neglecting momentum and velocity suppressed operators, the effective Lagrangian describing this interaction reads

$$L_{eff} = \sum_{q_i} \alpha_{q_i} \bar{\chi}\chi\bar{q}_i q_i + \xi_{q_i} \bar{\chi}\gamma_5\gamma_\mu\chi\bar{q}_i\gamma_5\gamma^\mu q_i \,, \tag{5.9}$$

where the sum runs over the six quarks, and the coefficients α_{q_i} and ξ_{q_i} can be found in refs. [342, 343]. The first term in eq. (5.9) corresponds to the scalar interactions, which contribute to the spin-independent (SI) interactions, and the latter, the axial-vector interactions, contribute to the spin-dependent (SD) interactions.

For the SI interactions, the neutralino-nucleon cross section can be written as

$$\sigma^{SI}_{p,n} = \frac{4\mu^2_{p,n}}{\pi} f^2_{p,n} \,, \tag{5.10}$$

where $\mu_{p,n}$ is the neutralino-nucleon reduced mass and p,n stand for protons and neutrons, respectively[5]. These parameters can be further decomposed as,

$$\frac{f_{p,n}}{m_{p,n}} = \sum_{q_i} f^{p,n}_{q_i} \frac{\alpha_{q_i}}{m_{q_i}} \,, \tag{5.11}$$

[5]Notice that the same can be done for the SD interactions. For instance see ref. [344].

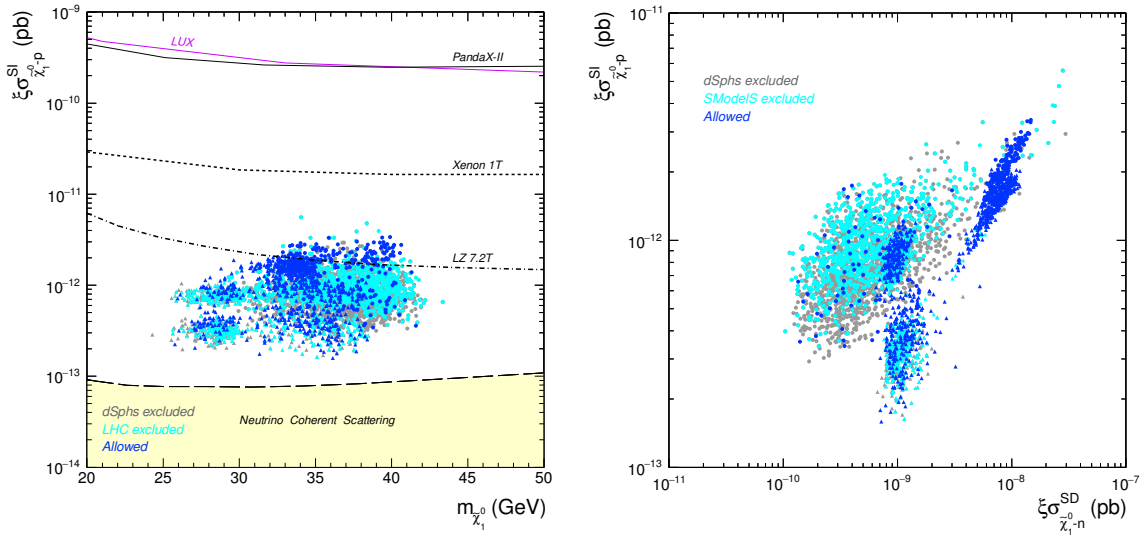

Figure 5.4: Left: Theoretical predictions for $\xi\sigma^{SI}_{\tilde{\chi}^0_1-p}$ as a function of the neutralino mass using the same colour code as in figure 5.1. As a reference, we have included the current constraints from LUX (solid violet line) and PandaX-II (solid black line), and the future prospects of LZ(dot-dashed line) and Xenon 1T (dashed line). In addition, the irreducible neutrino background is shown as a yellow region at the bottom of the plot [341]. Right: Spin independent cross section off protons, $\xi\sigma^{SI}_{\tilde{\chi}^0_1-p}$, as a function of the spin dependent cross section off neutrons, $\xi\sigma^{SD}_{\tilde{\chi}^0_1-n}$. The colour code is as in the left panel.

where m_{q_i} is the corresponding quark mass. The parameter α_{q_i} represents the effective coupling of neutralinos to quarks, and it must be calculated for the elastic scattering of neutralinos off quarks mediated by CP-even Higgs bosons and squarks [342]. The $f^{p,n}_{q_i}$ terms parametrize the quark content of the nucleon for either protons and neutrons. These quantities depend on the light quark mass ratios (m_u/m_d and m_s/m_d), the pion sigma term $\sigma_{\pi N}$, and the operator $\sigma_s = m_s\langle p|\bar{s}s|p\rangle$ [343]. For our calculations, we have used the values from the latest version of the `micrOMEGAs` code [331]. Nevertheless, it is important to remark that these parameters are extracted using lattice QCD calculations, and hence, are subject to important uncertainties that can affect the elastic scattering cross section [345]. It is also worth mentioning that for SD interactions the uncertainties related to the calculation of the SD structure functions can lead to important differences in the theoretical predictions of the differential event rate of the elastic scattering of neutralinos off a nucleus as well [346].

In figure 5.4 (left panel), the SI elastic scattering cross section of the lightest neutralino off protons, $\xi\sigma^{SI}_{\tilde{\chi}^0_1-p}$, is shown versus the lightest neutralino mass. The fractional density, $\xi = \min[1, \Omega_{\tilde{\chi}^0_1}h^2/0.11]$, is included to account for the reduction in the direct detection rate in the cases where the neutralino only contributes to a fraction of the total DM density, assuming that it is present in the DM halo in the same proportion as in the Universe[6]. Unfortunately, from the experimental point of view, the SI cross

[6]The use of ξ in this case is not very important since most of the solutions found do not present a relic abundance below 0.1.

sections predicted for these scenarios are remarkably small, even out of the reach of future experiments like Xenon 1T [239] (dashed line), only LZ [240] (dot-dashed line) could probe a small fraction of our results. However, there would be a chance to detect them via direct detection experiments since these solutions are above the so-called irreducible neutrino background [341]. The bino-like nature of the lightest neutralino, $N_{11}^2 \approx 1$, resulting from $M_1 \ll M_2, \mu$, decreases the coupling to the scalar Higgs, which is proportional to the Higgsino components, N_{13} and N_{14}. The remaining contribution to the cross section arises from the squark s-channel exchange. The cross section corresponding to this interaction is proportional to

$$\sigma^{SI}_{\tilde{\chi}_1^0 - p} \propto \frac{|N_{11}|^4}{m_{\tilde{q}}^4}\,, \tag{5.12}$$

and hence, the LHC bounds on the squark masses are translated into a strong decrease of this cross section.

In figure 5.4 (right panel), we show the SI cross section off protons versus the SD cross section off neutrons[7]. As it can be seen, the SD cross section predictions found for these solutions are very small, and in general would not contribute to the differential event rate more than the SI contribution. The main contribution to the SD cross section comes from the t-channel Z boson exchange, but the coupling of neutralinos to the Z boson is proportional to the Higgsino mixing. Therefore, this cross section is suppressed as well.

It is worth noting that predictions for direct detection cross sections are a consequence of the REWSB boundary condition of eq. (5.2). All the solutions experimentally allowed entail values of μ at the TeV scale, which along with the fact that low-mass neutralinos have a relatively low value of M_1, pose a difficult challenge for direct DM searches. This is, indeed, the main difference with solutions found in refs. [287, 290] with soft parameters at the EW scale. The amount of the Higgsino component found in these solutions increases substantially the cross sections through the t-channel Higgs exchange.

5.2.2 Indirect detection

As already stated, the predictions of these scenarios for direct DM searches are strongly influenced by the μ parameter value, and hence are very low, out of the reach of the current experiments. Nonetheless, it is known that thermal relics generally predict annihilation cross sections in DM haloes that lie in the ballpark of the current searches, especially for light DM candidates. Since in the scenarios presented here neutralinos are thermally produced in the early Universe, indirect detection experiments might provide a hopeful window to probe these scenarios.

To estimate the thermally averaged cross section, usually an expansion in powers of $x \equiv T/m$ is employed. In this approximation, the annihilation cross section times the relative velocity can be written as $\langle \sigma v \rangle \simeq a + 6bx$, which holds for non-relativistic particles at the freeze-out temperature as long as there are not s-channel resonances and thresholds for new final states. In the case studied here, this

[7] Xe-based experiments are mostly sensitive to the neutron component of the SD cross section.

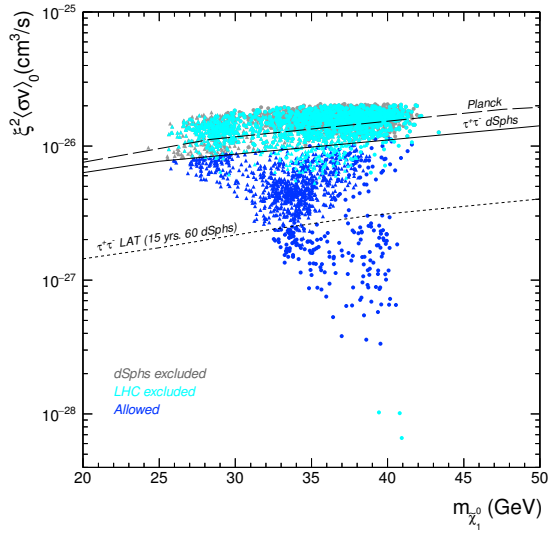

Figure 5.5: Thermally averaged neutralino annihilation cross section in the Galactic halo, $\xi^2\langle\sigma v\rangle_0$, as a function of the neutralino mass. The solid line corresponds to the upper bound on $\langle\sigma v\rangle$ derived from an analysis of dSph galaxies for pure $\tau^-\tau^+$ using the Pass 8 reprocessed data set. The dotted line corresponds to the expected sensitivity of the LAT experiment [347], and the dashed line stands for the Planck limits [73]. The colour code is as in figure 5.1.

approximation can be safely used, at least to extract interesting features about expected values[8]. In the limit of vanishing stau mixing, the a and b parameters can be written as follows [290]

$$\begin{aligned} a &= \frac{m^2_{\tilde{\chi}^0_1}}{8\pi}\left[\frac{g_{\tilde{\chi}^0_1\tilde{\tau}_1\tau_R}\, g_{\tilde{\chi}^0_1\tilde{\tau}_1\tau_L}}{(m^2_{\tilde{\tau}^0_1}+m^2_{\tilde{\chi}^0_1})}\right]^2, \\ b &\approx \frac{m^2_{\tilde{\chi}^0_1}}{48\pi}\left[\frac{(g^4_{\tilde{\chi}^0_1\tilde{\tau}_1\tau_R}+g^4_{\tilde{\chi}^0_1\tilde{\tau}_1\tau_L})(m^4_{\tilde{\tau}^0_1}+m^4_{\tilde{\chi}^0_1})}{(m^2_{\tilde{\tau}^0_1}+m^2_{\tilde{\chi}^0_1})^4}\right]. \end{aligned} \tag{5.13}$$

On the one hand, in this limit the a parameter, known as the s-wave contribution, is proportional to the Higgsino mixing, and thus it can be neglected. On the other hand, the b parameter, known as the p-wave contribution, is going to dominate the cross section. However, a cross section dominated by the p-wave term is temperature suppressed, by a factor T/m. This means that, when the temperature decreases the annihilation cross section decreases as well. Therefore, the annihilation in DM haloes is suppressed relative to that of the early Universe and a lower gamma ray flux is expected (with respect to the canonical cross section, $3\times10^{-26}\mathrm{cm}^3/\mathrm{s}$).

In figure 5.5, the theoretical predictions for the thermally averaged cross section of neutralinos in the Galactic halo, $\xi^2\langle\sigma v\rangle_0$, as a function of its mass are depicted. The fractional density is included squared because the annihilations of neutralinos in the halo depend on its density squared. The main annihilation

[8] Our results make use of the whole numerical calculation provided by `micrOMEGAs`.

channel is driven by the exchange of a light RH stau which yields a pair of τ-leptons in the final state. In order to compare our findings with current limits, we have also included those from dSph galaxies by Fermi-LAT collaboration (solid line) for a $\tau^+\tau^-$ final state [281] and the Planck bounds (dashed line) [73]. Despite of the suppressed cross sections respect to the thermal value, we can observe that the recent Pass 8 data from Fermi-LAT collaboration is starting to probe these scenarios. Interestingly, the scenarios unconstrained by Pass 8 could be tested in the near future provided that the Fermi-LAT experiment accumulates more exposure [347] (dotted line). We see that the prospects are very promising for these scenarios. Most of the solutions corresponding to $M_1 < 0$ and $M_2 < 0$ (triangles) will be probed by the LAT experiment, and only a small subset of solutions, those with cross sections below 2×10^{-27} cm^3/s approximately, will remain hidden.

5.2.3 LHC searches for SUSY particles

Many of the points entailing light neutralinos are ruled out by LHC searches for SUSY particles. Even though, some solutions are excluded by direct production of gluinos [78] and stops [348], the most restricting channels are those involving the electroweak production of sleptons, charginos and chargino-neutralino par production. Namely, two opposite sign leptons and missing transverse energy E_T^{miss} final states through the processes $pp \to \tilde{\chi}^{\pm}\tilde{\chi}^{\mp} \to l\tilde{l}\nu\tilde{\nu} \to \tilde{\chi}_1^0\tilde{\chi}_1^0 l\nu$ and $pp \to \tilde{l}\tilde{l} \to \tilde{\chi}_1^0\tilde{\chi}_1^0 ll$ entailing chargino and slepton pair production, and three leptons and missing transverse energy E_T^{miss} final states through the processes $pp \to \tilde{\chi}^{\pm}\tilde{\chi}_2^0 \to l\tilde{l}l\tilde{\nu} \to \tilde{\chi}_1^0\tilde{\chi}_1^0 l\nu$ and $pp \to \tilde{\chi}^{\pm}\tilde{\chi}_2^0 \to l\tilde{l}\nu\tilde{l} \to \tilde{\chi}_1^0\tilde{\chi}_1^0 ll$ involving chargino-neutralino production [309, 310]. The former being the most constraining of these two LHC searches.

As previously mentioned, we have calculated the LHC bounds from SUSY particle searches with `SModelS`. In figure 5.6, we show the solutions excluded by dilepton (violet) and trilepton (green) searches, whereas solutions ruled out by gluino and stop limits are displayed in cyan. Grey points are excluded by Femi-LAT dSph upper limits, illustrating the complementarity between indirect detection experiments and collider searches, and finally the solutions fulfilling all the experimental constraints are shown in blue. It is worth remarking that there are points ruled out by more than one channel, mainly by dilepton and trilepton final states, in those cases we have represented only the most constraining channel. As expected, most of our excluded results are ruled out by right-handed slepton pair production (see upper-right panel of figure 5.6), in particular by ATLAS results. Note that we have depicted the ATLAS (black lines) and CMS (light-blue lines) bounds at 95% CL as a reference, since they depend on the production cross section, and in the chargino production bound $m_{\tilde{l}} = m_{\tilde{\nu}} = (m_{\tilde{\chi}_1^0} + m_{\tilde{\chi}_1^{\pm}})/2$ is also assumed.

The latest ATLAS [349] and CMS [350] results at 13 TeV on electroweak production of SUSY particles in multilepton final states have not being incorporated in our results, since they do not include slepton pair production, which is the most restrictive process for the scenarios analysed here. Other LHC bounds that can potentially probe part of our allowed solutions are the most recent searches for gluino pair production from ATLAS [351] and CMS [352], and direct stop pair production from CMS [353].

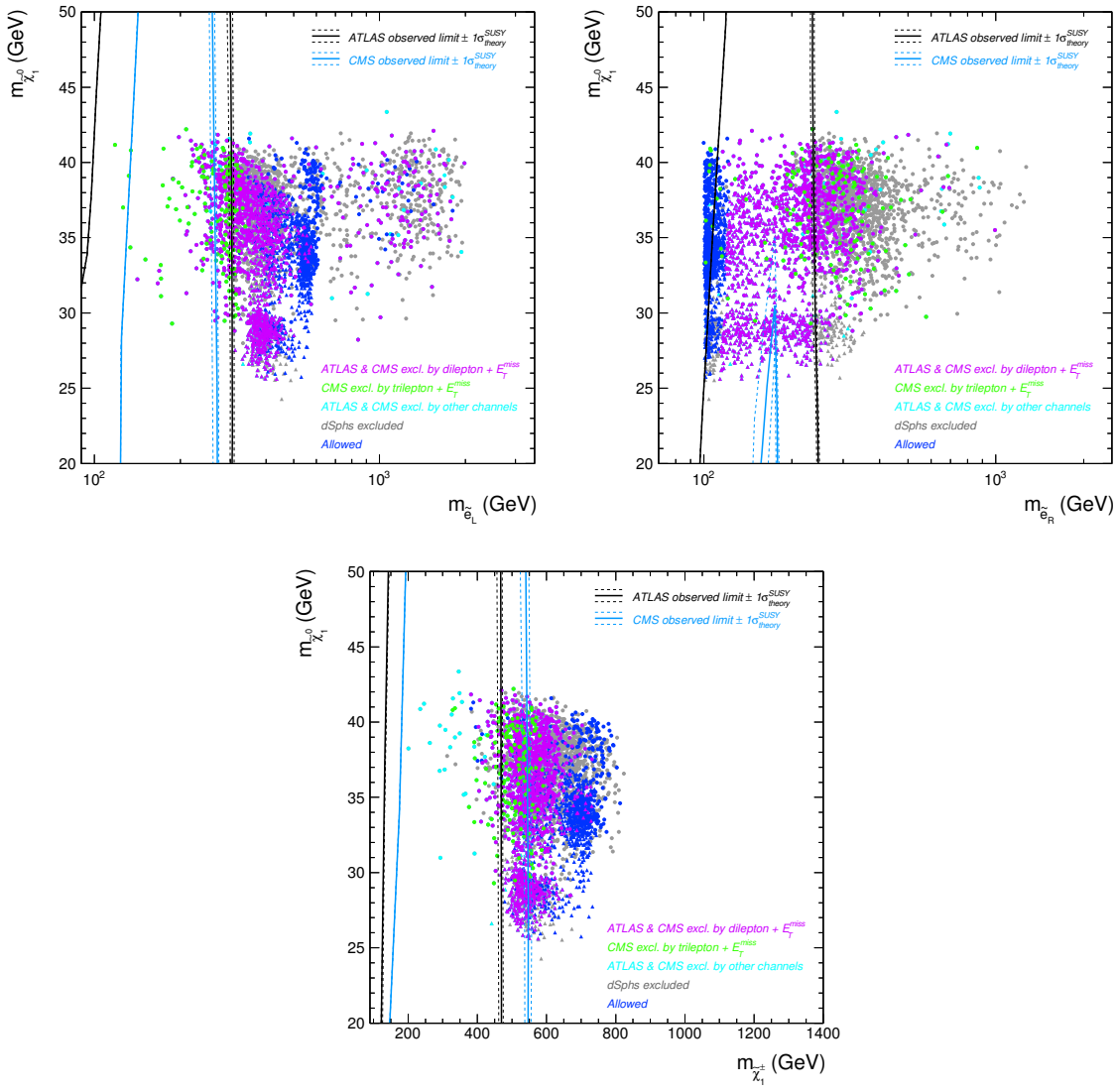

Figure 5.6: LHC searches for direct slepton and chargino par production. Violet points denote solutions excluded by ATLAS and CMS dilepton searches, green points are ruled out by CMS trilepton searches, whereas cyan points are excluded by ATLAS and CMS gluino and stop bounds. Solutions excluded by Fermi-LAT bounds from dSphs are shown in grey and finally allowed solutions are depicted in blue. As a reference, we include the 95% CL ATLAS (black lines) and CMS (light-blue lines) limits on pure left-handed slepton pair production (upper left panel), right-handed slepton pair production (upper right panel) and chargino par production (bottom panel).

Regarding future colliders, currently, there are no prospects for improving the limits on the direct production of sleptons, charginos and chargino - neutralino at the high luminosity LHC (HL-LHC), when sleptons are not so heavy. These are the most constraining channels for the scenarios we have studied. Nonetheless, we expect that some of our solutions could be probed by direct gluino, top and

sbottom pair production at the HL-LHC [354–356]. On the other hand, linear colliders such as the ILC and CLIC can shed light on the scenarios studied here by the direct production of sleptons, charginos and neutralinos, provided they have sufficiently large centre of mass energy, they might either measure very precisely their mass, spin and couplings or push harder the LEP constraints [357–360].

5.3 Naturalness of SUGRA scenarios

Being the original motivation for low-energy SUSY to solve the hierarchy problem, i.e. the delicate balance between the soft terms required to reproduce the smallness of the EW scale, it is interesting to check the degree of naturalness of our solutions in the SUGRA model considered here. In consequence, we must analyse all the potential sources of fine-tuning that could affect these scenarios in order to obtain a total estimation of the degree of fine-tuning of our allowed solutions.

5.3.1 Electroweak fine-tuning

Let us start by the most important source of fine-tuning and, in fact, the most extensively studied in the literature, that induced to reproduce the electroweak scale. In what follows, we summarise the origin and the method to measure the EW fine-tuning in the MSSM, and then, we compute it for the solutions that fulfil all the experimental constraints discussed in the previous sections.

Since we have solutions of the parameter space with not too large $\tan\beta (\lesssim 10)$, we will employ the following expression to the electroweak fine-tuning instead of eq. 2.13

$$-\frac{m_h^2}{2} = \mu^2(LE) - \frac{m_{H_d}^2(LE) - m_{H_u}^2(LE)\tan^2\beta}{\tan^2\beta - 1} \,. \tag{5.14}$$

Notice that the terms on the r.h.s of eq. (5.14) have to be evaluated at the low-energy scale. Then, the standard fine-tuning measure reads

$$\begin{aligned} \Delta_{\theta_i}^{(\mathrm{EW})} &= \frac{\theta_i}{m_h^2}\frac{\partial m_h^2}{\partial \theta_i} = -2\frac{\theta_i}{m_h^2}\frac{\partial}{\partial \theta_i}\left(\mu^2(LE) - \frac{m_{H_d}^2(LE) - m_{H_u}^2(LE)\tan^2\beta}{\tan^2\beta - 1}\right) , \\ \Delta^{(\mathrm{EW})} &\equiv \mathrm{Max}\left|\Delta_{\theta_i}^{(\mathrm{EW})}\right| , \end{aligned} \tag{5.15}$$

where θ_i is an independent parameter of the model under consideration and $\Delta_{\theta_i}^{(\mathrm{EW})}$ is the fine-tuning associated with it. Typically, $\{\theta_i\}$ are the initial (high-energy) values of the soft terms and the μ parameter.

In order to use the standard measure of the fine-tuning, eq. (5.15), it is necessary to write the r.h.s of the minimization equation (5.14) as a function of the initial (input) parameters of the model. This, in turn, implies to write the low-energy (LE)[9] values of μ^2, $m_{H_u}^2$ and $m_{H_d}^2$ in terms of the initial, GUT

[9] We recall that the low-energy scale is the scale at which we set the SUSY threshold and the supersymmetric spectrum is computed, taken here as the average stop mass.

scale parameters, which are related through the renormalization group equations (RGEs). Fortunately, dimensional and analytical consistency dictates the form of such dependence,

$$\begin{aligned} m^2_{H_u}(LE) &= c_{M_3^2} M_3^2 + c_{M_2^2} M_2^2 + c_{M_1^2} M_1^2 + c_{A_U^2} A_U^2 + c_{A_U M_3} A_U M_3 + c_{M_3 M_2} M_3 M_2 + \cdots \\ &\quad \cdots + c_{m^2_{H_u}} m^2_{H_u} + c_{m^2_{Q_3}} m^2_{Q_3} + c_{m^2_{U_3}} m^2_{U_3} + \cdots , \qquad (5.16) \\ m^2_{H_d}(LE) &= c_{m^2_{H_d}} m^2_{H_d} + c_{M_2^2} M_2^2 + \cdots , \qquad (5.17) \\ \mu(LE) &= c_\mu \mu , \qquad (5.18) \end{aligned}$$

where the terms on the r.h.s are the soft terms at the GUT scale. The numerical coefficients, $c_{M_3^2}, c_{M_2^2}, \ldots$ are obtained by fitting the result of the numerical integration of the RGEs to eqs. (5.16, 5.17, 5.18), a task that was performed following the prescription described in chapter 2, this is, considering the different threshold scales involved and two-loop RGEs. First, we have performed the integration of the SM and MSSM RGEs between the corresponding scales with `SARAH 4.9.1` [163] (see chapter 2 for further details). Then, we have calculated the coefficients for a generic MSSM, i.e. a model with the following initial parameters

$$\Theta_i = \left\{ \mu, M_1, M_2, M_3, A_U, A_D, A_E, m^2_{H_u}, m^2_{H_d}, m^2_{U_3}, m^2_{Q_3}, \cdots \right\} . \qquad (5.19)$$

Next, we have determined the coefficients of eqs. (5.16) and (5.17) for the model analysed here, applying the relations among the initial parameters indicated in section 5.2. Finally, we have evaluated $\Delta^{(\mathrm{EW})}_{\theta_i}$ for our set of initial parameters, namely

$$\Theta_i = \left\{ \mu, M_1, M_2, A_U, A_E, m^2_{H_u}, m^2_{H_d}, m^2_Q, m^2_{L_2}, m^2_{L_3}, m^2_{E_2}, m^2_{E_3} \right\} , \qquad (5.20)$$

by using eqs. (5.16) - (5.18) in (5.15) and determined $\Delta^{(\mathrm{EW})}$.

The EW fine-tuning for the points that fulfil all the experimental data are shown in figure 5.7. In all cases, the main source of fine-tuning is the μ parameter, which at the LE scale lies in the range $\sim [1500, 4500]$ GeV. Remarkably, more than 50% of our solutions have $\Delta^{(\mathrm{EW})}$ at the percent level,[10] corresponding to those with lower $\mu(LE)$, since

$$\Delta^{(\mathrm{EW})}_\mu = \frac{\mu}{m_h^2} \frac{\partial m_h^2}{\partial \mu} = -4 c_\mu^2 \frac{\mu^2}{m_h^2} = -4 \left(\frac{\mu(LE)}{m_h} \right)^2 . \qquad (5.21)$$

Nevertheless, in the MSSM, there are other implicit potential fine-tunings that have to be taken into account when evaluating the global degree of naturalness. They stem from the need of having a physical Higgs mass consistent with $m_h^{(\mathrm{exp})} \simeq 125$ GeV and from the requirement of a large value of $\tan\beta$. Regarding the latter, moderately large values of $\tan\beta$ generically require a small value of $B\mu$ at low energy, a fact which entails a cancellation between the initial value and the radiative contribution

[10] An $\Delta^{(\mathrm{EW})} \gtrsim \mathcal{O}(100)$ corresponds to a fine-tuning at a level $\lesssim 1\%$.

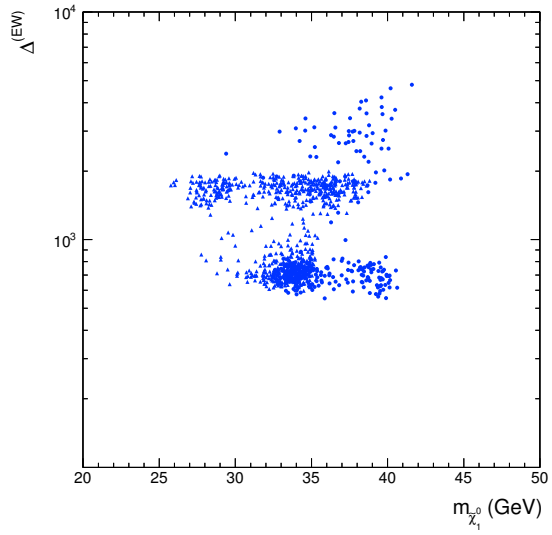

Figure 5.7: Electroweak fine-tuning as a function of the neutralino mass for all the experimentally allowed solutions discussed in the previous sections.

from the RGE running. Using eq. (2.68), we have verified that there is no fine-tuning associated with the values of $\tan\beta$ in our allowed solutions.

5.3.2 Fine-tuning to obtain the experimental Higgs mass

As mentioned in section 2.1.3, in the MSSM radiative corrections to the Higgs mass are needed to reconcile it with the experimental value, see eq. 2.9. If the X_t-contribution that arises from the threshold corrections were not present heavy stops would be needed (of about 3 TeV once higher order corrections are included) for large $\tan\beta$ (and much heavier as $\tan\beta$ decreases [153, 154]). However, taking X_t close to the 'maximal' value also entails a certain degree of tuning depending on how close to such value it is required to be. As stated in chapter 2, the precision needed depends, in turn, on the values of $\tan\beta$ and the stop masses.

To illustrate this potential fine-tuning, we have let $A_t(LE)$ vary freely for four of our allowed solutions with different average stop masses in figure 5.8. Three of them correspond to points of the parameter space with $A_U < 0$ and $\overline{m}_{\tilde{t}} = 1$ TeV, 1.5 TeV and 2 TeV, and the other case to $A_U > 0$ and $\overline{m}_{\tilde{t}} = 1.25$ TeV. The shaded regions and solid lines denote the X_t range for which $m_h \geq m_h^{(\mathrm{exp})}$. Dashed lines show that, in fact, there are four possible values of X_t for which m_h lies in the interval, $m_h^{(\mathrm{exp})} = 125 \pm 2$ GeV (the uncertainty is mainly due to the theoretical calculation)[11]. Note that for $\overline{m}_{\tilde{t}} \sim 1$ TeV and $X_t < 0$ (solid violet line), we require an almost precise value of $A_t(LE)$, around

[11] Notice that the Higgs mass computation vary according to the code used, which could affect our fine-tuning estimation (see for instance chapter 3). For this reason, we have assumed a 2 GeV uncertainty on m_h.

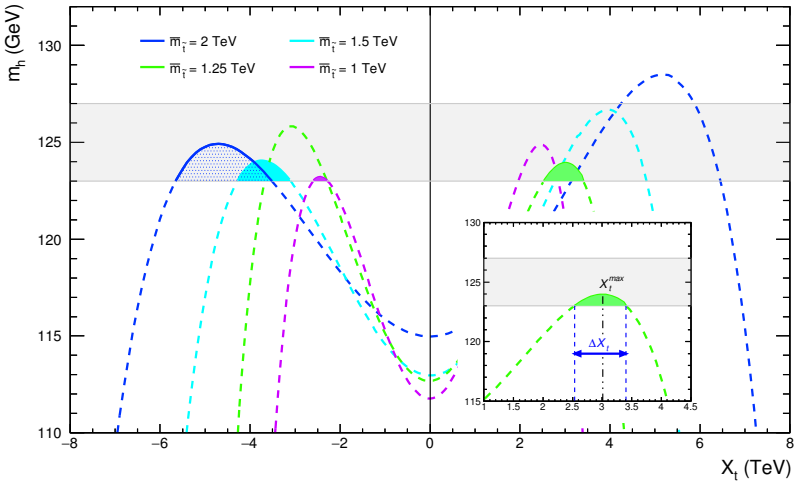

Figure 5.8: The Higgs mass as a function of X_t for different average stop masses for four of our allowed solutions, three of them with $A_U < 0$ and $\overline{m}_{\tilde{t}} = 1$ TeV, 1.5 TeV and 2 TeV, and one with $A_U > 0$ and $\overline{m}_{\tilde{t}} = 1.25$ TeV. The grey band denotes the uncertainty on the Higgs mass, $m_h^{(\exp)} = 125 \pm 2$ GeV. Solid lines and shaded regions correspond to the range of variation in $A_t(LE)$ to achieve the experimental Higgs mass. Dashed lines are drawn for completeness to show that there are four possible X_t values to obtain a Higgs mass within the theoretical uncertainty. The inset plot illustrates the criterion to determine the p-value measure of the fine-tuning to obtain $m_h^{(\exp)}$ for the solution with $A_U > 0$ and $\overline{m}_{\tilde{t}} = 1.25$ TeV.

~ -2.5 TeV to achieve $m_h^{(\exp)}$ (see the small shaded violet region)[12]. On the contrary, for $\overline{m}_{\tilde{t}} \gtrsim 1.25$ TeV (see shaded green, cyan and blue regions), no accurate arrangement is needed since a broad range of X_t values is allowed, e.g. for $\overline{m}_{\tilde{t}} \simeq 1.25$ TeV, $A_t(LE)$ could take values in the range $\simeq 3 \pm 0.5$ TeV.

The aforementioned fine-tuning is independent of that required to obtain the correct electroweak scale; therefore, as stated in section 2.5.1 if both tunings are present we must properly combine them. From figure 5.8, we can infer that some of our solutions could undergo this tuning. Consequently, we have to quantify it, with a method that has a similar statistical meaning as the measure used for the EW fine-tuning[13]. We have adopted the criterion described in section 2.5.1, which states that the fine-tuning is well estimated by the $p-$value of obtaining $m_h \geq m_h^{(\exp)}$. Then, the fine-tuning is evaluated as the inverse of the p-value. Note here that $X_t \simeq A_t(LE)$ is a low-energy quantity and thus a prior on it can not be defined. Strictly speaking, the prior should be assumed on the initial, GUT scale parameters that determine the value of $A_t(LE)$, (i.e. A_U and M_2, since for the model analysed here $A_t(LE) \simeq c_{M_2} M_2 + c_{A_U} A_U$), in a similar way to the previous section.

The criterion adopted here for the p-value measure is as follows. Assuming a flat prior on A_U and M_2, we have obtained a range of X_t values that yield different Higgs masses, similar to those of figure 5.8.

[12] Remind that we are in a moderately large $\tan\beta$ regime (see figure 5.1, right-hand panel), then we can approximate $X_t = A_t(LE) - \mu(LE)\cot\beta \simeq A_t(LE)$.

[13] Recall that the value of $\Delta^{(\mathrm{EW})}$ can be interpreted as the inverse of the p-value to obtain $m_h^2 \lesssim m_h^{2\ (\exp)}$.

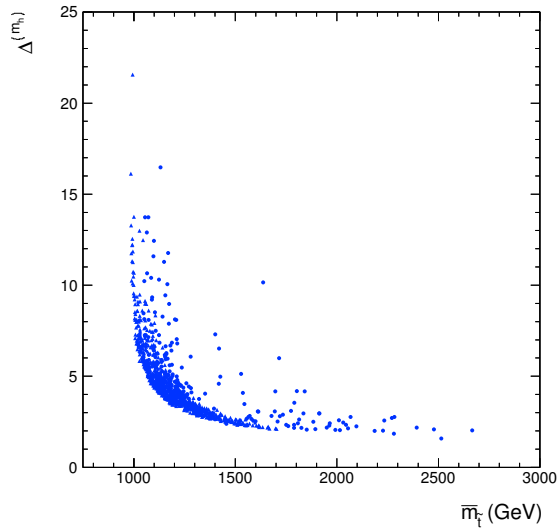

Figure 5.9: Fine-tuning to obtain the experimental Higgs mass as a function of the average stop mass, for the solutions that fulfil all the experimental constraints.

Next, we have determined the X_t interval, ΔX_t, for which we reach the minimum Higgs mass within the 2 GeV uncertainty considered throughout this chapter. Finally, we have computed the X_t value that maximises m_h in this interval, X_t^{max} (see inset plot in figure 5.8), and evaluated the p-value as

$$p-\text{value} = \left| \frac{\Delta X_t}{X_t^{max}} \right| . \tag{5.22}$$

Following this method, we have calculated the fine-tuning to achieve the measured Higgs mass. In figure 5.9, we show our results as a function of the average stop mass. Notice that for $\overline{m}_{\tilde{t}} \gtrsim 1200$ GeV, $(p-\text{value})^{-1}$ is $\mathcal{O}(1)$, this means that in this $\overline{m}_{\tilde{t}}$ range, and taking into account the two previously described sources of fine-tuning, the only important contribution is that associated with the electroweak scale. On the other hand, for solutions with $\overline{m}_{\tilde{t}} \lesssim 1200$ GeV, even though they exhibit a mild fine-tuning to obtain $m_h^{(\text{exp})}$, their total fine-tuning will grow more than one order of magnitude, when combined with $\Delta^{(\text{EW})}$. Indeed, these points correspond to solutions with $\Delta^{(\text{EW})}$ at the percent level, leading to a total fine-tuning at the per-mil level or even worse in a few cases.

5.3.3 Fine-tuning to reproduce the DM relic abundance

Besides the fine-tunings described above, there is another potential source of fine-tuning related to the generation of the right amount of DM in the Universe, since a delicate balance between a-priori-independent quantities might be required in order to reproduce it. In such a case, we should combine this fine-tuning with that of the EW scale and, if it exists, with that to match the measured Higgs mass, to select the regions of the parameter space that are globally less fine-tuned.

The light neutralinos analysed in this chapter, are bino-like, specifically they are bino-Higgsino, which requires a certain degree of well-tempering that could entail a fine-tuning. As argued in section 4.2, the 'standard measure' of the fine-tuning, is not appropriate for this kind of scenarios, and we have to evaluate the p-value associated with the smallness of $\Omega_{\rm DM}$. Therefore, we can estimate $\Delta^{(\rm DM)}$ with the inverse of the p-value, i.e. for a bino-Higgsino admixture, from eq. 4.10 we obtain

$$\Delta^{(\rm DM)} = (p-\text{value})^{-1} = \frac{|M_1|}{2|\mu - |M_1||} \,. \tag{5.23}$$

From this expression, we conclude that there is no tuning needed, since $\mu \gg |M_1|$ and consequently $\Delta^{(\rm DM)} \ll 1$.

Nonetheless, the scenarios analysed throughout this chapter not only depend on the well-tempered bino-Higgsino, but as we have seen previously, they also rely heavily on the presence of light RH-like staus. This is due to the fact that the relic density is produced mainly by neutralino annihilation into $\tau^+\tau^-$ through stau exchange. The existence of this final state is controlled by $m_{\tilde{\tau}_1}$, which should be large enough to avoid the LEP limit and sufficiently small to provide the dominant annihilation channel. Therefore, we once again adopt a p-value criterion, which has been proved to be a sensible measure of $\Delta^{(\rm DM)}$ in chapter. 4, based on this observable. For a given solution of the parameter space with the lightest stau mass, $m^0_{\tilde{\tau}_1}$, the p-value reads

$$p-\text{value} = \frac{\Delta m_{\tilde{\tau}_1}}{m^0_{\tilde{\tau}_1}} \,, \tag{5.24}$$

where $\Delta m_{\tilde{\tau}_1}$ is the $m_{\tilde{\tau}_1}$ interval for which $\Omega_{\tilde{\chi}^0_1} h^2 \leq \Omega^{(\rm obs)}_{\rm DM} h^2$ and the main annihilation final state in the early Universe is $\tau^+\tau^-$. Figure 5.10 highlights the use of this criterion for one of our allowed solutions. We can observe how the LEP bound shrinks significantly the value of $\Delta m_{\tilde{\tau}_1}$, which otherwise would lead to a mild fine-tuning. The upper limit on the stau mass is given by requiring the correct relic abundance and the channel mediated by $\tilde{\tau}_1$ being the dominant annihilation final state.

To apply this measure to our data, we have to assume a flat prior on the initial GUT scale parameters, that play a role in the determination of $m_{\tilde{\tau}_1}$, and $\tan\beta$ in a similar way as in the previous fine-tuning computations. Accordingly, the parameters that should be selected are those that will determine $m^2_{E_3}(LE)$, $m^2_{L_3}(LE)$, $A_\tau(LE)$ and $\mu(LE)$. To be more concrete, the subset of initial parameters we should considered for this calculation are[14]

$$\Theta_i = \left\{\mu, M_1, M_2, A_E, m^2_{L_3}, m^2_{E_3}, \tan\beta\right\}. \tag{5.25}$$

Let us at this point to comment on the subtleties that we must take into account to proceed correctly. On the one hand, notice that μ is not a free parameter of our scan but it is the result of the REWSB, for this reason we need to enlarge the set of θ_i parameters in eq.(5.25) to consider those that will impact on the value of $\mu(LE)$. It is worth mentioning that in the SUGRA scenarios investigated here, M_2 will

[14] Note that $m^2_{L_3}(LE) \simeq c_{m^2_{L_3}} m^2_{L_3} + c_{M_2^2} M_2^2$, $m^2_{E_3}(LE) \simeq c_{m^2_{E_3}} m^2_{E_3} + c_{M_1^2} M_1^2$ and $A_\tau(LE) \simeq c_{A_E} A_E + c_{M_2} M_2 + c_{M_1} M_1$.

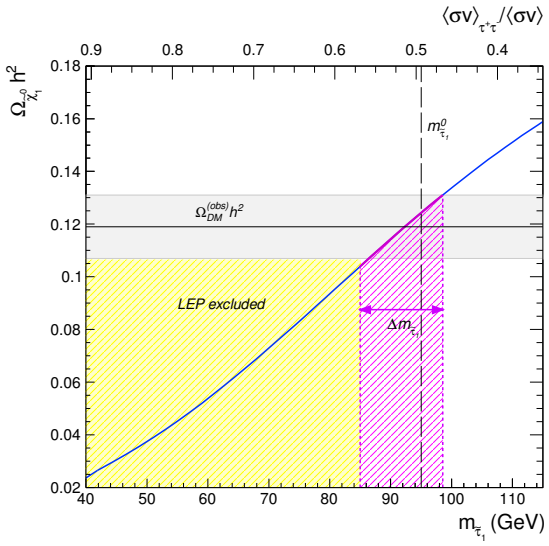

Figure 5.10: Relic density versus the lightest stau mass and the p-value criterion to estimate the fine-tuning to reproduce the DM relic density. The grey band stands for $\Omega_{DM}^{(\mathrm{obs})}h^2 = 0.119 \pm 0.012$ and the yellow region is excluded by the LEP bound on the stau mass.

affect both $\mu(LE)$ and $m_{L_3}^2(LE)$. On the other hand, when computing the fine-tuning in a quantity, say Ω_{DM}, without taking into account all the potential constraints (in this case that of the EW scale, being $G(\theta_i) = 0$ the EW condition), the constrained $\Delta^{(\mathrm{DM})}$ must be calculated projecting the unconstrained quantity $\vec{\Delta}^{(\mathrm{DM})}$ into the subspace orthogonal to the $G(\theta_i) = 0$ hypersurface in the $\{\log\theta_i\}$ space. In other words, we have to re-define the $\vec{\Delta}^{(\mathrm{DM})}$ as

$$\vec{\Delta}^{(\mathrm{DM})} \to \vec{\Delta}^{(\mathrm{DM})} - \frac{1}{|\vec{\Delta}G|^2}(\vec{\Delta}^{(\mathrm{DM})}\cdot\vec{\Delta}G)\vec{\Delta}G\,, \tag{5.26}$$

where $\overrightarrow{\Delta G} \equiv \{\partial G/\partial\log\theta_i\} \propto \vec{\Delta}^{(\mathrm{EW})}$. This issue was first noted in ref. [165], and subsequently in refs. [160, 221] and section 4.7. In light of this, we have calculated the p-value subject to there exist electroweak symmetry breaking and a valid MSSM mass spectrum for the following parameters,

$$\Theta_i = \left\{M_1, M_2, A_E, m_{L_3}^2, m_{\tilde{E}_3}^2, m_{H_u}^2, m_{H_d}^2, A_U, m_Q^2, \tan\beta\right\}. \tag{5.27}$$

We have evaluated then the fine-tuning to reproduce the DM relic abundance, $\Delta^{(\mathrm{DM})}$, as follows

$$\Delta_{\theta_i}^{(\mathrm{DM})} = (p-\mathrm{value})_{\theta_i}^{-1}\,, \qquad \Delta^{(\mathrm{DM})} \equiv \mathrm{Max}\,\left|\Delta_{\theta_i}^{(\mathrm{DM})}\right|\,. \tag{5.28}$$

In figure 5.11, we present our results for $\Delta^{(\mathrm{DM})}$ as a function of $m_{\tilde{\tau}_1}$. Note that the DM fine-tuning spans several orders of magnitude. There are a few points with $(p-\mathrm{value})^{-1} \lesssim 10$, this is, with no significant DM tuning. As expected, the vast majority of solutions have a $\Delta^{(\mathrm{DM})}$ above the sub-percent

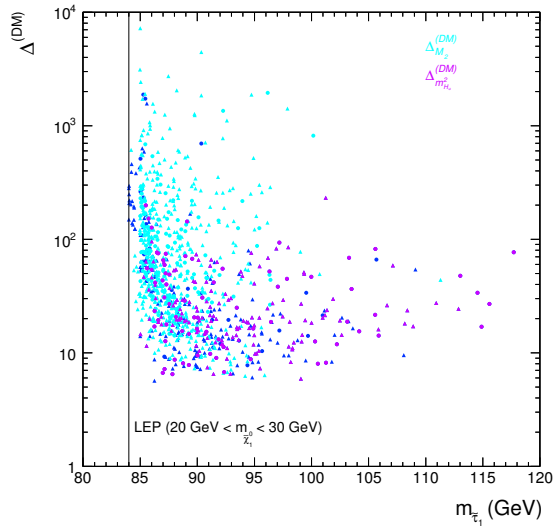

Figure 5.11: Fine-tuning to obtain $\Omega_{\tilde{\chi}_1^0}h^2 \leq \Omega_{\rm DM}^{\rm (obs)}h^2$ as a function of $m_{\tilde{\tau}_1}$ for the solutions that fulfil all the experimental constrains. The black solid line denotes the LEP bound for 20 GeV $< m_{\tilde{\chi}_1^0} <$ 30 GeV. Cyan points represent solutions with $\Delta^{(\rm DM)} = \Delta^{(\rm DM)}_{M_2}$, violet points depict solutions with $\Delta^{(\rm DM)} = \Delta^{(\rm DM)}_{m^2_{H_u}}$, whereas solutions with other main sources of $\Delta^{(\rm DM)}$ are displayed in blue.

level or even as severe as the per-mil level. This is caused by the LEP limit that bounds $m_{\tilde{\tau}_1}$ from below depending on the neutralino mass, and hence shrinking considerably the $m_{\tilde{\tau}_1}$ interval for which $\Omega_{\tilde{\chi}_1^0}h^2 \leq \Omega_{\rm DM}^{\rm (obs)}h^2$, as mentioned before.

We observe that, for a given $m_{\tilde{\tau}_1}$, $\Delta^{(\rm DM)}$ can take a broad range of values as well. This occurs because we are calculating $\Delta^{(\rm DM)}$ subject to fulfil all the potential constraints. In consequence, when any θ_i parameter in eq. (5.27) is varied to determine $\Delta m_{\tilde{\tau}_1}$, we must ensure, at each step as mentioned before, that there exist electroweak symmetry breaking and a valid MSSM mass spectrum. This is well highlighted by the fact that the main source of $\Delta^{(\rm DM)}$ is M_2 (see cyan points in figure 5.11), which turns out to be the leading contribution to the running of $m^2_{H_u}$ and the squark soft masses, and the next-to-leading contribution to the running of the left-handed slepton soft masses.[15] As a result, M_2 is the main parameter to constrain $\Delta m_{\tilde{\tau}_1}$ through the EW symmetry breaking condition and a valid physical mass spectrum, aside from the LEP limit and the DM relic density. Other parameters that have a significant impact on $\Delta^{(\rm DM)}$ are $m^2_{H_u}$ (violet points), A_U, m^2_Q and M_1(blue points).

5.3.4 Total estimation of the fine-tuning

Even if $\Delta^{(\rm DM)}$ alone could seem less severe than $\Delta^{(\rm EW)}$ for most of our solutions, we should combine $\Delta^{(\rm DM)}$ with the tunings calculated in the previous sections in order to obtain a total fine-tuning measure.

[15] We remind the reader that we have considered $M_2 = M_3$.

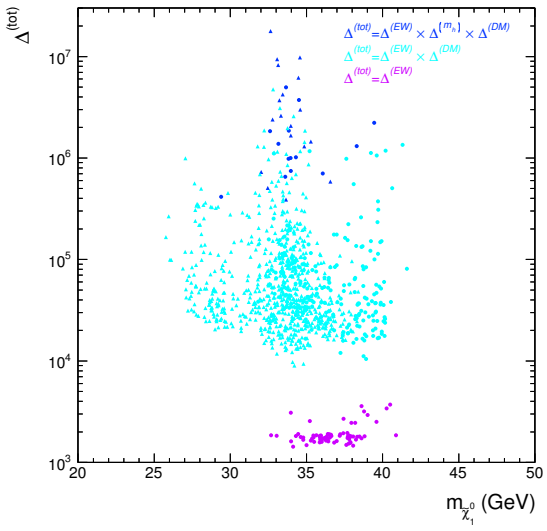

Figure 5.12: Total fine-tuning as a function of the lightest neutralino mass for the allowed solutions considering all the relevant sources of fine-tuning. Solutions that suffer from the three fine-tunings analysed here are shown in blue ($\Delta^{(\mathrm{tot})} = \Delta^{(\mathrm{EW})} \times \Delta^{(m_h)} \times \Delta^{(\mathrm{DM})}$), points that exhibit only EW and DM tunings are depicted in cyan ($\Delta^{(\mathrm{tot})} = \Delta^{(\mathrm{EW})} \times \Delta^{(\mathrm{DM})}$) and finally solutions with only $\Delta^{(\mathrm{EW})}$ are shown in violet.

Due to their common statistical interpretation (as p-values), these quantities should be multiplicatively combined. As already pointed out, we have computed $\Delta^{(\mathrm{DM})}$ considering that all constraints are fulfilled, so that we are allowed to directly combine $\Delta^{(\mathrm{DM})}$ with the other fine-tunings without any redefinition of this quantity.

In figure 5.12, we show the total estimation of the fine-tuning, $\Delta^{(\mathrm{tot})}$, for the solutions that fulfil all the experimental constraints. Points in blue undergo the three kinds of fine-tuning computed along this section, points in cyan have $\Delta^{(\mathrm{tot})} = \Delta^{(\mathrm{EW})} \times \Delta^{(\mathrm{DM})}$, while those in violet only suffer from $\Delta^{(\mathrm{EW})}$. The latter are the least fine-tuned of our solutions, with $\Delta^{(\mathrm{tot})}$ at the per-mil level.

Summarising, we have addressed the naturalness issue taking into account all the potential sources of fine-tuning in the MSSM. We have found that the electroweak fine-tuning and that associated with the DM relic abundance are the main factors that contribute to the total fine-tuning of the model analysed here. Adopting a p-value measure to quantify all the different kinds of fine-tuning, it turns out that our results are severely tuned, with the minimum $\Delta^{(\mathrm{tot})}$ of $\mathscr{O}(10^3)$ that corresponds to the solutions that only undergo electroweak fine-tuning and have neutralino masses above 32 GeV. Solutions featuring lighter neutralinos are even more fine-tuned with $\Delta^{(\mathrm{tot})} > \mathscr{O}(10^4)$. Finally, let us remark that this would have gone unnoticed, if we have only considered the EW fine-tuning (compare figures 5.7 and 5.12).

5.4 Conclusions

In this chapter, we have presented the conditions in the SUSY soft terms for a general supergravity theory to contain light neutralinos ($m_{\tilde{\chi}_1^0} \lesssim 40$ GeV). We have explored a 12-th dimensional parameter space in order to find these solutions while fulfilling all current experimental constraints from LHC, LEP, low energy observables, direct and indirect dark matter searches. More specifically, we have applied the bounds on the Higgs mass and couplings from the LHC, which are known to be very stringent in the MSSM, and the constraints on the squarks and slepton masses from the LHC. From LEP, we have taken into account the neutralino mass dependent lower bound on slepton and chargino masses. Finally, we have used the latest determinations on the rare decays $\text{BR}(B_s \to \mu^+\mu^-)$ and $\text{BR}(b \to s\gamma)$.

The spectrum of solutions found exhibit a definite pattern in the gaugino sector at the GUT scale, $4 \lesssim M_2/M_1 \lesssim 12$, with $M_2 = M_3$, highlighting that light neutralinos require a *very* non universal scenario in this sector in order to fulfil the experimental constraints. This is a consequence of the LHC bounds on squarks and sleptons and of the maximisation of the bino component of the lightest neutralino. The third generation trilinear, A_U, and $\tan\beta$ parameters are very constrained by the Higgs boson properties which gives rise to a similar conclusion to that found in the universal case. The pattern of the slepton soft masses is, in general, very irregular but in most cases it lies below the TeV scale. Finally, we have found the ratio between the two Higgs soft masses, m_{H_u} and m_{H_d}, remarkably close to one, and hence light neutralino scenarios do not require large deviations from universality in the Higgs sector.

The phenomenology associated with these light neutralinos is somewhat different to previous studies of the MSSM defined at the EW scale. The difference lies in the values of the μ parameter which, in the scenarios found here, are above the TeV scale. Therefore, the elastic scattering cross section (both SI and SD) of neutralinos off protons and neutrons are far below the current sensitivities of the experiments, but generally above the neutrino floor. On the other hand, the annihilation cross section of neutralinos in the halo, in spite of being below the thermal value for an *s*-wave annihilator, it is in the ballpark of the Fermi-LAT searches using the most recent Pass 8 reprocessed data from dSphs. The accumulation of higher exposure would be a key piece to explore these models. Hence, we can conclude that a hint in favour of these scenarios, regarding DM searches, would be the detection of a gamma ray source from dSphs, while no signal would appear in direct detection experiments, at least in the near future.

The complementarity between the LHC and DM searches is, in these cases, remarkably important. We have shown that it would be possible to probe these scenarios with searches for direct production of sleptons and charginos at the LHC. Some of the solutions found in the reach of the LHC, would be really challenging for both direct and indirect detection of DM, highlighting the importance of combining the different new physics search techniques. All in all, one might expect that future runs could shed light on the survival, or even discovery, of the scenarios presented in this chapter.

Finally, we have analysed the naturalness of the solutions allowed by the experimental data, quantifying all the possible sources of tuning in the MSSM. First of all, we have calculated the electroweak fine-tuning which despite being controlled by the TeV scale μ parameter can be as low as the percent level. Nevertheless, solutions with $\overline{m}_{\tilde{t}}$ around 1 TeV are also subject to a tuning to match the measured

Higgs mass, which is independent of that needed to reproduce the EW scale. A very mild tuning when considered separately, but it should be combined with the other sources of fine-tuning. There is also another delicate balance required by the scenarios investigated here, that needed to obtain the correct DM relic abundance, which relies heavily on the lightest RH-like stau mass and that could be of the same order as the EW fine-tuning or even greater due to the LEP bound. When we combine all these tunings, the final picture is a severely fine-tuned scenario with the least tuned solutions at the per-mil level, i.e. $\mathscr{O}(0.1\%)$, which are those that only undergo EW fine-tuning and have neutralino masses above 32 GeV. Lighter neutralinos exhibit an even worse fine-tuning, $< \mathscr{O}(0.01\%)$. These findings highlight the importance of taking into account all the potential fine-tunings of a model when looking for regions of the parameter space with as natural as possible SUSY scenarios.

Chapter 6

Conclusions

Historically, naturalness principles have been an important motivation for some conceptual progress in fundamental physics. However, there exists no formal definition of the term 'natural', which could be subject to ambiguities and misconceptions, that certainly lead to scepticism regarding naturalness.

In particle physics, the hierarchy problem has been the driver of BSM model proposals that intend to solve or at least alleviate the electroweak fine-tuning of the SM, i.e. its sensitivity to high energy scales. For decades, supersymmetry has been the leading paradigm of new physics, since besides tackling the SM quadratic divergences, it features gauge coupling unification and provide a weakly interacting candidate for dark matter. Nevertheless, current experimental results, in particular the null searches for weak scale SUSY at the LHC, seem to have forced this kind of models into fine-tuned regions of their parameter space, according to the 'standard' Natural SUSY scenario. Then, it appears that we have exchanged the quadratic instability of the SM for the EW fine-tuning of the MSSM, although, of course the degree of fine-tuning of the latter is much lower than that of the former.

In the light of these facts, in chapter 2 we have revisited the 'standard' Natural SUSY scenario within the MSSM framework and introduced several improvements in the EW fine-tuning computation which include, among others, the mixing of the soft term contributions to the tuning to obtain the right EW scale and the dependence on the low- and high-energy scales. Then, we have applied the outlined method to specific MSSM scenarios, defined at any high-energy (HE) scale, and derived a complete set of fine-tuning bounds. Contrary to what was expected, we have shown that Natural SUSY does indeed *not* demand light stops. Actually, an average stop mass below 800 GeV is disfavoured, due to an additional fine-tuning required to reproduce the Higgs mass, though one of the stops might be very light. Concerning phenomenology, the most stringent upper bound from naturalness is that of the gluino mass, which typically sets the current level of fine-tuning at $\mathcal{O}(1\%)$. However, this result presents a strong dependence on the HE scale. E.g. if the latter is 10^7 GeV, the level of fine-tuning is $\sim$ four times less severe than that if $M_{\rm HE} \simeq M_X$. Finally, the most robust result of Natural SUSY is by far that Higgsinos should be rather light, certainly below 700 GeV for a fine-tuning of $\mathcal{O}(1\%)$ or milder. Incidentally, this upper bound is not far from $\simeq 1$ TeV, that is the value required if dark matter is made only of Higgsinos.

In chapter 3, we have employed the method developed in chapter 2 to gauge-mediated supersymmetry breaking (GMSB) models in order to find the setup with minimal matter content that is less fine-tuned. As expected, we find that the EW fine-tuning of the minimal model is severe, worse than the per mil level. One of the main reasons is the fact that the trilinear terms, in particular, that associated to the top, A_t, are initially zero. Then, we have examined some existing proposals in the literature to generate $A_t(HE) \neq 0$ in this context. This forces the stops to be heavy to generate sizeable enough radiative corrections to the Higgs mass. We have found that, although the stops can be made lighter, usually the tuning does not improve (it may be even worse, due to the large value of $m^2_{H_u}$ at low-energy), with some exceptions, which involve the generation of $A_t(HE)$ at one-loop or tree level. We have investigated both possibilities and even propose a conceptually simplified version of the latter; which is arguably the optimum GMSB setup (with minimal matter content), concerning the naturalness issue. The resulting fine-tuning is better than one per mil, still severe but similar to other MSSM constructions. In addition, we have explored the so-called 'little A_t^2/m^2 problem', i.e. the fact that a large A_t-term is normally accompanied by a similar or larger sfermion mass, which typically implies an increase in the fine-tuning. More precisely, we have found the version of GMSB for which this ratio is optimised, which, nevertheless, does not minimise the fine-tuning.

Aiming to formulate a general naturalness criterion for the MSSM, we have identified other potential sources of fine-tuning in this framework, that include the tuning of $B\mu$ (at low-energy) to achieve the large $\tan\beta$ regime and that of the threshold correction to match the measured Higgs mass. These tunings should be avoided, otherwise they must be combined with that of the EW scale, which may give rise to a gigantic global degree of fine-tuning. On the other hand, if the dark matter particle is a WIMP, a well-motivated candidate for DM in the MSSM is the lightest neutralino. To that end, the observed thermal relic abundance must be fulfilled, which could lead to other delicate balances in the MSSM. We have studied all these potential tunings in detail in chapters 2 and 4, quantifying them with a p-value like criterion that allows us, if it is the case, to combine them multiplicatively with the EW fine-tuning in order to obtain a global measure of the fine-tuning, since the criterion to evaluate the latter also admits a p-value interpretation.

Regarding the tuning to obtain the correct DM relic density, as mentioned above, we have assumed that the lightest supersymmetric particle is the lightest neutralino. We have investigated the various possibilities for its mass and composition as well as different mechanisms for neutralino annihilation in the early Universe (well-tempering, funnels and co-annihilation scenarios), looked for precise cancellations in each of them that could yield a fine-tuned relic abundance, and proposed a proper way to quantify this potential tuning and combined it with that of the EWSB scale.

Thus, we have outlined the tunings that must be considered when looking for as natural as possible MSSM scenarios and formulated a proper measure to quantify them. Afterwards, we have applied these prescriptions and measures to a specific MSSM model in chapter 5, namely low-mass neutralinos in supergravity featuring light sleptons at low-energy that mediate neutralino annihilation. First, we have studied the phenomenology of this model, regardless of its naturalness, identifying the optimal choices of non-universalities in the soft supersymmetry-breaking parameters for both, gauginos and

scalars, in order to avoid the stringent experimental constraints from the LHC and DM searches. We have shown that light neutralinos, with a mass as low as 25 GeV, are viable in supergravity scenarios if the gaugino mass parameters at high-energy are very non universal, while the scalar masses can remain of the same order. These scenarios typically predict a very small cross section of neutralinos off protons and neutrons, thereby being very challenging for direct detection experiments. However, a potential detection of smuons and selectrons at the LHC, together with a hypothetical discovery of a gamma-ray signal from neutralino annihilations in dwarf spheroidal galaxies could shed light on this kind of scenarios. Next, we have investigated the naturalness of the configurations of the parameter space of this model that fulfil all the experimental constraints, taking into account the potential sources of tuning studied in the preceding chapters. Furthermore, we have stated a p-value criterion to measure the tuning to reproduce the correct DM relic abundance for this specific annihilation channel, that was not studied in chapter 4. Besides the electroweak fine-tuning, we have found that the tuning to reproduce the observed DM relic abundance and that required to match the measured Higgs mass can also be important when estimating the total degree of naturalness. Lastly, we have concluded that this kind of scenarios are severely fine-tuned with the least tuned solutions at the per-mil level, which would have gone unnoticed, if we have only considered the EW fine-tuning.

The previous result highlights the importance of a naturalness criterion that could guide current and future experimental analyses, as well as searches for new particles and interactions, that help us to gain further insight into the mechanism behind the electroweak symmetry breaking and the true nature of the dark matter particle.

As a final remark, the naturalness criterion presented in this dissertation can be extended to other supersymmetric models beyond the minimal setup and even other scenarios of new physics, taking into account the distinctive features of each of them.

Conclusiones

Históricamente, los principios de naturalidad han sido una motivación importante en algunos avances conceptuales en física fundamental. Sin embargo, no existe una definición formal del término 'natural', el cual puede estar sujeto a ambigüedades y confusiones, lo que sin duda alguna conduce al escepticismo hacia el concepto de naturalidad.

En la física de partículas, el problema de las jerarquías ha sido el motor de propuestas de modelos de física más allá del modelo estándar (ME) que intentan resolver o por lo menos aliviar el fine-tuning electrodébil del ME, esto es su sensibilidad a las escalas de alta energía. Durante décadas la supersimetría (SUSY) ha sido el principal paradigma de los modelos de nueva física, ya que además de abordar el problema de las divergencias cuadráticas del ME, proporciona acoplos gauge unificados y un candidato a materia oscura débilmente interactuante. Sin embargo, los resultados experimentales actuales, en particular los resultados nulos del LHC en la búsqueda de SUSY a la escala electrodébil, habrían hecho retroceder esta clase de modelos hacia regiones de su espacio de parámetros que requieren de ajustes precisos. según el escenario estándar de Natural SUSY. Pareciera entonces que hemos intercambiado la inestabilidad cuadrática del ME por el fine-tuning electrodébil del modelo estándar supersimétrico mínimo (MSSM), aunque por supuesto el grado de ajuste fino de este último es muy inferior al del primero.

A la luz de estos hechos, en el capítulo 2 hemos revisado el escenario estándar de Natural SUSY dentro del marco del MSSM e introducido varias mejoras en el cálculo del fine-tuning elecrodébil, las cuales incluyen, entre otras, la mezcla de las contribuciones de los términos soft al ajuste para obtener la escala electrodébil correcta y la dependencia de las escalas de baja y alta energía. Posteriormente, hemos aplicado el método descrito a escenarios específicos en el MSSM, definidos a cualquier escala de alta energía, y derivado un conjunto completo de límites de naturalidad. Contrariamente a lo esperado, hemos mostrado que Natural SUSY no exige stops ligeros. Una masa promedio de los stops de 800 GeV está en realidad desfavorecida, debido a un fine-tuning adicional requerido para reproducir la masa del Higgs, aunque uno de los stops podría ser muy ligero. Con respecto a la fenomenología, el límite más restrictivo desde el punto de vista de la naturalidad es el de la masa del gluino, que típicamente determina el nivel actual de fine-tuning al $\mathcal{O}(1\%)$. Sin embargo, este resultado es fuertemente dependiente de la escala de alta energía. Por ejemplo, si ésta es 10^7 GeV, el nivel del ajuste fino requerido es aproximadamente cuatro veces menos severo que si $M_{\rm HE} \simeq M_X$. Por último, el resultado más sólido de Natural SUSY es que los Higgsinos deben ser bastante ligeros, ciertamente por debajo de los 700 GeV para obtener un

fine-tuning de $\mathcal{O}(1\%)$ o aún más leve. Accidentalmente, este límite no está lejos de $\simeq 1$ TeV, que es el valor requerido si la materia oscura está compuesta solo de Higgsinos.

En el capítulo 3, hemos empleado el método desarrollado en el capítulo 2 a modelos con rompimiento de supersimetría por mediación gauge (GMSB), con la finalidad de encontrar el modelo con mínimo contenido de materia que posea el menor fine-tuning. Como estaba previsto, el fine-tuning del modelo mínimo es severo, peor que el uno por mil. Una de las razones más importantes para ello es el hecho de que los terminos trilineales, en particular el asociado al top, A_t, son inicialmente cero. Esto obliga a que los stops sean pesados para poder así generar correcciones radiativas lo suficientemente grandes a la masa del Higgs. A continuación, hemos analizado algunas de las propuestas en la literatura para generar $A_t(HE) \neq 0$ en este contexto ($HE \equiv$ alta energía). Hemos encontrado que aunque los stops pueden ser ligeros, generalmente el grado de ajuste no mejora (puede ser incluso peor, debido al gran valor de $m^2_{H_u}$ a baja energía), salvo algunas excepciones en las que se genera $A_t(HE)$ a un loop o a nivel árbol. Hemos analizado ambas posibilidades e incluso propuesto una versión simplificada de la última, que es, podría decirse, el modelo de GMSB (con el mínimo contenido de materia) óptimo desde el punto de vista del problema de la naturalidad. El fine-tuning resultante es mejor que el tanto por mil, aún severo pero comparable a otros modelos en el MSSM. Además, hemos explorado el así llamado "problema del cociente A_t^2/m^2 pequeño", es decir, el hecho de que un término A_t grande viene normalmente acompañado de una masa grande de lo sfermiones, lo que usualmente implica un incremento en el fine-tuning. Concretamente, hemos encontrado la versión de GMSB en la cual este cociente es el óptimo, la que, sin embargo no coincide con la del fine-tuning mínimo.

Con el objetivo de formular un criterio de naturalidad general para el MSSM, hemos identificado otras fuentes potenciales de ajustes de precisión en este marco de trabajo, que incluyen el ajuste de $B\mu$ (a baja energía) para conseguir que $\tan\beta$ sea grande y el de la corrección finita de umbral a la masa del Higgs. Estos ajustes finos deben ser evitados, pues de lo contrario deben ser combinados con el fine-tuning electrodébil pudiendo dar lugar a fine-tunings totales enormes. Por otro lado, si la partícula de materia oscura es débilmente interactuante, un buen candidato en el MSSM es el neutralino más ligero. Para ello, debe cumplir con la abundancia térmica observada de materia oscura, lo que puede conducir a otros ajustes finos en el MSSM. En los capítulos 2 y 4, hemos estudiado en detalle todos estos posibles fine-tunings cuantificándolos con criterios basados en el p-value, lo que permite, dado el caso, combinarlos multiplicativamente con el fine-tuning electrodébil, puesto que el criterio para evaluar este último admite una interpretación en términos del p-value.

Con respecto al ajuste para obtener la densidad reliquia de materia oscura correcta, como mencionamos antes, hemos asumido que la partícula supersimétrica más ligera es el neutralino más ligero. Hemos estudiado las diferentes posibilidades de masa y composición, así como diferentes mecanismos de aniquilación en el Universo temprano (atemperamiento, resonancias y co-aniquilación), buscando posibles cancelaciones precisas de los parámetros iniciales en cada una de ellas que conduzcan a un ajuste fino para reproducir la abundancia de materia oscura. A continuación, hemos propuesto una forma adecuada de cuantificarlo y combinarlo con el de la escala electrodébil.

De esta manera, hemos descrito los ajustes precisos más importantes que deben ser considerados en la búsqueda de escenarios en el MSSM tan naturales como sea posible y formulado una manera apropiada de cuantificarlos. Después, hemos aplicado estas prescripciones y medidas a un modelo particular del MSSM en el capítulo 5, específicamente neutralinos de baja masa en supergravedad que presentan sleptones ligeros a baja energía, los que sirven de mediadores en la aniquilación de los neutralinos. En primer lugar, hemos estudiado la fenomenología de este modelo, sin tomar en cuenta su naturalidad, identificando las opciones óptimas de no universalidad en los parámetros de rompimiento suave de la supersimetría, tanto para gauginos como para escalares, que permiten evitar los límites experimentales más rigurosos de las búsquedas de materia oscura y las del LHC. Hemos demostrado que neutralinos con masas tan bajas como 25 GeV son viables en escenarios de supergravedad si los parámetros de masa de los gauginos a alta energía son muy no universales, mientras que las masas de los escalares pueden permanecer del mismo orden. Estos escenarios predicen típicamente secciones eficaces neutralino-protón neutralino-neutrón muy pequeñas, siendo así muy exigentes para los experimentos de detección directa. Sin embargo, una deteccíon potencial de smuones y/o selectrones en el LHC, junto con un descubrimiento hipotético de una señal de rayos gamma proveniente de la aniquilación de neutralinos en galaxias enanas esferoidales, podrían arrojar luz sobre esta clase de escenarios. Posteriormente, hemos investigado la naturalidad de las configuraciones del espacio de parámetros de este modelo que cumplen todos los límites experimentales, teniendo en cuenta todas las fuentes potenciales de ajustes finos estudiadas en los capítulos precedentes. Además, hemos enunciado un criterio basado en el p-value para medir el fine-tuning asociado a la densidad reliquia de materia oscura correcta para este canal de aniquilación específico, que no fue estudiado en el capítulo 4. Además del fine-tuning electrodébil, hemos encontrado que el ajuste para reproducir la abundancia de materia oscura observada y el requerido para conseguir la masa del Higgs pueden también ser importantes al estimar el grado total de naturalidad. Por último, hemos concluido que esta clase de escenarios tienen un fine-tuning severo, con las soluciones con menos ajustes precisos en el orden del tanto per mil, lo que hubiera pasado desapercibido si solamente hubiéramos considerado el fine-tuning electrodébil.

El resultado previo resalta la importancia de un criterio de naturalidad que pueda servir de guía a análisis experimentales presentes y futuros, así como a las búsquedas de nuevas partículas e interacciones, que nos ayuden a obtener más información sobre el mecanismo detrás del rompimiento de la simetría electrodébil y la verdadera naturaleza de la materia oscura.

Como comentario final, el criterio de naturalidad presentado en esta tesis puede ser extendido a otros modelos supersimétricos más allá de la versión mínima, e incluso a otros escenarios de nueva física, teniendo en cuenta las peculiaridades de cada uno de ellos.

References

[1] J. A. Casas, J. M. Moreno, S. Robles, K. Rolbiecki and B. Zaldívar, *What is a Natural SUSY scenario?*, *JHEP* **06** (2015) 070, [1407.6966]. (Cited on page vii.)

[2] J. A. Casas, J. M. Moreno, S. Robles and K. Rolbiecki, *Reducing the fine-tuning of gauge-mediated SUSY breaking*, *Eur. Phys. J.* **C76** (2016) 450, [1602.06892]. (Cited on page vii.)

[3] M. E. Cabrera, J. A. Casas, A. Delgado, S. Robles and R. Ruiz de Austri, *Naturalness of MSSM dark matter*, *JHEP* **08** (2016) 058, [1604.02102]. (Cited on page vii.)

[4] M. Peiró and S. Robles, *Low-mass neutralino dark matter in supergravity scenarios: phenomenology and naturalness*, *JCAP* **1705** (2017) 010, [1612.00460]. (Cited on page vii.)

[5] D. G. Cerdeño, M. Peiró and S. Robles, *Low-mass right-handed sneutrino dark matter: SuperCDMS and LUX constraints and the Galactic Centre gamma-ray excess*, *JCAP* **1408** (2014) 005, [1404.2572]. (Cited on pages vii and 87.)

[6] D. G. Cerdeño, M. Peiró and S. Robles, *Fits to the Fermi-LAT GeV excess with RH sneutrino dark matter: implications for direct and indirect dark matter searches and the LHC*, *Phys. Rev.* **D91** (2015) 123530, [1501.01296]. (Cited on pages vii and 87.)

[7] C. Marcos, M. Peiró and S. Robles, *On the importance of direct detection combined limits for spin independent and spin dependent dark matter interactions*, *JCAP* **1603** (2016) 019, [1507.08625]. (Cited on page vii.)

[8] D. G. Cerdeño, M. Peiró and S. Robles, *Enhanced lines and box-shaped features in the gamma-ray spectrum from annihilating dark matter in the NMSSM*, *JCAP* **1604** (2016) 011, [1507.08974]. (Cited on pages vii and 87.)

[9] S. L. Glashow, *Partial Symmetries of Weak Interactions*, *Nucl. Phys.* **22** (1961) 579–588. (Cited on page 1.)

[10] S. Weinberg, *A Model of Leptons*, *Phys. Rev. Lett.* **19** (1967) 1264–1266. (Cited on page 1.)

[11] A. Salam, *Weak and Electromagnetic Interactions*, *Conf. Proc.* **C680519** (1968) 367–377. (Cited on page 1.)

[12] ATLAS collaboration, G. Aad et al., *Observation of a new particle in the search for the Standard Model Higgs boson with the ATLAS detector at the LHC*, *Phys.Lett.* **B716** (2012) 1–29, [1207.7214]. (Cited on pages 1 and 6.)

[13] CMS collaboration, S. Chatrchyan et al., *Observation of a new boson at a mass of 125 GeV with the CMS experiment at the LHC*, *Phys.Lett.* **B716** (2012) 30–61, [1207.7235]. (Cited on pages 1 and 6.)

[14] ATLAS collaboration, G. Aad et al., *Measurements of Higgs boson production and couplings in diboson final states with the ATLAS detector at the LHC*, *Phys. Lett.* **B726** (2013) 88–119, [1307.1427]. (Cited on page 1.)

[15] CMS collaboration, S. Chatrchyan et al., *Observation of a new boson with mass near 125 GeV in pp collisions at $\sqrt{s}$ = 7 and 8 TeV*, *JHEP* **06** (2013) 081, [1303.4571]. (Cited on page 1.)

[16] K. G. Wilson, *The Renormalization Group and Strong Interactions*, *Phys. Rev.* **D3** (1971) 1818. (Cited on page 1.)

[17] S. Weinberg, *Implications of Dynamical Symmetry Breaking*, *Phys. Rev.* **D13** (1976) 974–996. (Cited on page 1.)

[18] S. Weinberg, *Implications of Dynamical Symmetry Breaking: An Addendum*, *Phys. Rev.* **D19** (1979) 1277–1280. (Cited on page 1.)

[19] E. Gildener, *Gauge Symmetry Hierarchies*, *Phys. Rev.* **D14** (1976) 1667. (Cited on page 1.)

[20] L. Susskind, *Dynamics of Spontaneous Symmetry Breaking in the Weinberg-Salam Theory*, *Phys. Rev.* **D20** (1979) 2619–2625. (Cited on page 1.)

[21] G. 't Hooft, *Naturalness, chiral symmetry, and spontaneous chiral symmetry breaking*, *NATO Sci. Ser. B* **59** (1980) 135–157. (Cited on page 1.)

[22] P. W. Higgs, *Broken symmetries, massless particles and gauge fields*, *Phys. Lett.* **12** (1964) 132–133. (Cited on page 1.)

[23] P. W. Higgs, *Broken Symmetries and the Masses of Gauge Bosons*, *Phys. Rev. Lett.* **13** (1964) 508–509. (Cited on page 1.)

[24] F. Englert and R. Brout, *Broken Symmetry and the Mass of Gauge Vector Mesons*, *Phys. Rev. Lett.* **13** (1964) 321–323. (Cited on page 1.)

[25] G. S. Guralnik, C. R. Hagen and T. W. B. Kibble, *Global Conservation Laws and Massless Particles*, *Phys. Rev. Lett.* **13** (1964) 585–587. (Cited on page 1.)

[26] P. W. Higgs, *Spontaneous Symmetry Breakdown without Massless Bosons*, *Phys. Rev.* **145** (1966) 1156–1163. (Cited on page 1.)

[27] T. W. B. Kibble, *Symmetry breaking in nonAbelian gauge theories*, *Phys. Rev.* **155** (1967) 1554–1561. (Cited on page 1.)

[28] ATLAS collaboration, G. Aad et al., *Measurement of the Higgs boson mass from the $H \to \gamma\gamma$ and $H \to ZZ^* \to 4\ell$ channels with the ATLAS detector using 25 fb^{-1} of pp collision data*, *Phys. Rev.* **D90** (2014) 052004, [1406.3827]. (Cited on pages 1 and 6.)

[29] CMS collaboration, *Precise determination of the mass of the Higgs boson and studies of the compatibility*, CMS-PAS-HIG-14-009, 2014. (Cited on pages 1 and 6.)

[30] ATLAS, CMS collaboration, G. Aad et al., *Combined Measurement of the Higgs Boson Mass in pp Collisions at $\sqrt{s} = 7$ and 8 TeV with the ATLAS and CMS Experiments*, *Phys. Rev. Lett.* **114** (2015) 191803, [1503.07589]. (Cited on pages 1 and 6.)

[31] PARTICLE DATA GROUP collaboration, C. Patrignani et al., *Review of Particle Physics*, *Chin. Phys.* **C40** (2016) 100001. (Cited on page 1.)

[32] R. Kitano and Y. Nomura, *Supersymmetry, naturalness, and signatures at the LHC*, *Phys.Rev.* **D73** (2006) 095004, [hep-ph/0602096]. (Cited on pages 2, 6, and 7.)

[33] L. J. Hall and Y. Nomura, *Evidence for the Multiverse in the Standard Model and Beyond*, *Phys. Rev.* **D78** (2008) 035001, [0712.2454]. (Cited on page 2.)

[34] J. Wess and B. Zumino, *Supergauge Transformations in Four-Dimensions*, *Nucl. Phys.* **B70** (1974) 39–50. (Cited on page 2.)

[35] J. Wess and B. Zumino, *A Lagrangian Model Invariant Under Supergauge Transformations*, *Phys. Lett.* **49B** (1974) 52. (Cited on page 2.)

[36] P. Fayet, *Spontaneously Broken Supersymmetric Theories of Weak, Electromagnetic and Strong Interactions*, *Phys. Lett.* **69B** (1977) 489. (Cited on page 2.)

[37] P. Fayet, *Weak Interactions of a Light Gravitino: A Lower Limit on the Gravitino Mass from the Decay psi —> Gravitino anti-Photino*, *Phys. Lett.* **B84** (1979) 421–426. (Cited on page 2.)

[38] P. Fayet, *Scattering Cross-Sections of the Photino and the Goldstino (Gravitino) on Matter*, *Phys. Lett.* **B86** (1979) 272–278. (Cited on page 2.)

[39] H. P. Nilles, *Supersymmetry, Supergravity and Particle Physics*, *Phys. Rept.* **110** (1984) 1–162. (Cited on page 2.)

[40] H. E. Haber and G. L. Kane, *The Search for Supersymmetry: Probing Physics Beyond the Standard Model*, *Phys. Rept.* **117** (1985) 75–263. (Cited on page 2.)

[41] S. P. Martin, *A Supersymmetry primer*, hep-ph/9709356. (Cited on pages 2, 28, and 94.)

[42] D. B. Kaplan and H. Georgi, *SU(2) x U(1) Breaking by Vacuum Misalignment*, *Phys. Lett.* **B136** (1984) 183–186. (Cited on page 2.)

[43] D. B. Kaplan, H. Georgi and S. Dimopoulos, *Composite Higgs Scalars*, *Phys. Lett.* **B136** (1984) 187–190. (Cited on page 2.)

[44] T. Banks, *Constraints on SU(2) x U(1) breaking by vacuum misalignment*, *Nucl. Phys.* **B243** (1984) 125–130. (Cited on page 2.)

[45] H. Georgi, D. B. Kaplan and P. Galison, *Calculation of the Composite Higgs Mass*, *Phys. Lett.* **B143** (1984) 152–154. (Cited on page 2.)

[46] H. Georgi and D. B. Kaplan, *Composite Higgs and Custodial SU(2)*, *Phys. Lett.* **B145** (1984) 216–220. (Cited on page 2.)

[47] M. J. Dugan, H. Georgi and D. B. Kaplan, *Anatomy of a Composite Higgs Model*, *Nucl. Phys.* **B254** (1985) 299–326. (Cited on page 2.)

[48] L. Randall and R. Sundrum, *A Large mass hierarchy from a small extra dimension*, *Phys. Rev. Lett.* **83** (1999) 3370–3373, [hep-ph/9905221]. (Cited on page 2.)

[49] P. W. Graham, D. E. Kaplan and S. Rajendran, *Cosmological Relaxation of the Electroweak Scale*, *Phys. Rev. Lett.* **115** (2015) 221801, [1504.07551]. (Cited on page 2.)

[50] J. R. Espinosa, C. Grojean, G. Panico, A. Pomarol, O. Pujolàs and G. Servant, *Cosmological Higgs-Axion Interplay for a Naturally Small Electroweak Scale*, *Phys. Rev. Lett.* **115** (2015) 251803, [1506.09217]. (Cited on page 2.)

[51] G. F. Giudice and M. McCullough, *A Clockwork Theory*, *JHEP* **02** (2017) 036, [1610.07962]. (Cited on page 2.)

[52] L. Maiani, *Vector bosons and Higgs bosons in the Weinberg-Salam theory of weak and electromagnetic interactions*, in *Proc. of the Summer School on Particle Physics, Gif-sur-Yvette, 3-7 Sep 1979, IN_2P_3, Paris, France* (M. e. a. Davier, ed.), 1979. (Cited on page 3.)

[53] M. J. G. Veltman, *The Infrared - Ultraviolet Connection*, *Acta Phys. Polon.* **B12** (1981) 437. (Cited on page 3.)

[54] E. Witten, *Dynamical Breaking of Supersymmetry*, *Nucl. Phys.* **B188** (1981) 513. (Cited on page 3.)

[55] R. K. Kaul, *Gauge Hierarchy in a Supersymmetric Model*, *Phys. Lett.* **B109** (1982) 19–24. (Cited on page 3.)

[56] R. K. Kaul, *Supersymmetric Solution of Gauge Hierarchy Problem*, *Pramana* **19** (1982) 183. (Cited on page 3.)

[57] L. Susskind, *The gauge hierarchy problem, technicolor, supersymmetry, and all that.*, *Phys. Rept.* **104** (1984) 181–193. (Cited on page 3.)

[58] F. Zwicky, *Die Rotverschiebung von extragalaktischen Nebeln*, *Helv. Phys. Acta* **6** (1933) 110–127. (Cited on page 4.)

[59] V. C. Rubin and J. Ford, W. Kent, *Rotation of the Andromeda Nebula from a Spectroscopic Survey of Emission Regions*, *Astrophys.J.* **159** (1970) 379–403. (Cited on page 4.)

[60] V. Rubin, N. Thonnard and J. Ford, W.K., *Rotational properties of 21 SC galaxies with a large range of luminosities and radii, from NGC 4605 /R = 4kpc/ to UGC 2885 /R = 122 kpc/*, *Astrophys.J.* **238** (1980) 471. (Cited on page 4.)

[61] A. Bosma, *21-cm line studies of spiral galaxies. 2. The distribution and kinematics of neutral hydrogen in spiral galaxies of various morphological types.*, *Astron. J.* **86** (1981) 1825. (Cited on page 4.)

[62] V. Trimble, *Existence and Nature of Dark Matter in the Universe*, *Ann.Rev.Astron.Astrophys.* **25** (1987) 425–472. (Cited on page 4.)

[63] J. A. Tyson, G. P. Kochanski and I. P. Dell'Antonio, *Detailed mass map of CL0024+1654 from strong lensing*, *Astrophys.J.* **498** (1998) L107, [astro-ph/9801193]. (Cited on page 4.)

[64] Supernova Search Team collaboration, A. G. Riess et al., *Observational evidence from supernovae for an accelerating universe and a cosmological constant*, *Astron.J.* **116** (1998) 1009–1038, [astro-ph/9805201]. (Cited on page 4.)

[65] Supernova Cosmology Project collaboration, S. Perlmutter et al., *Measurements of Omega and Lambda from 42 high redshift supernovae*, *Astrophys.J.* **517** (1999) 565–586, [astro-ph/9812133]. (Cited on page 4.)

[66] A. D. Lewis, D. A. Buote and J. T. Stocke, *Chandra observations of Abell 2029: The Dark Matter Profile Down to below 0.01 R(VIR) in an unusually relaxed cluster*, *Astrophys.J.* **586** (2003) 135–142, [astro-ph/0209205]. (Cited on page 4.)

[67] S. Allen, A. Fabian, R. Schmidt and H. Ebeling, *Cosmological constraints from the local x-ray luminosity function of the most x-ray luminous galaxy clusters*, *Mon.Not.Roy.Astron.Soc.* **342** (2003) 287, [astro-ph/0208394]. (Cited on page 4.)

[68] R. B. Metcalf, L. A. Moustakas, A. J. Bunker and I. R. Parry, *Spectroscopic gravitational lensing and limits on the dark matter substructure in Q2237+0305*, *Astrophys.J.* **607** (2004) 43–59, [astro-ph/0309738]. (Cited on page 4.)

[69] D. Clowe, M. Bradac, A. H. Gonzalez, M. Markevitch, S. W. Randall et al., *A direct empirical proof of the existence of dark matter*, *Astrophys.J.* **648** (2006) L109–L113, [astro-ph/0608407]. (Cited on page 4.)

[70] WMAP collaboration, G. Hinshaw et al., *Nine-Year Wilkinson Microwave Anisotropy Probe (WMAP) Observations: Cosmological Parameter Results*, 1212.5226. (Cited on page 4.)

[71] PARTICLE DATA GROUP collaboration, J. Beringer et al., *Review of particle physics, "Big Bang nucleosynthesis"*, *Phys. Rev. D* **86** (Jul, 2012) 010001. (Cited on page 4.)

[72] J. P. Dietrich, N. Werner, D. Clowe, A. Finoguenov, T. Kitching et al., *A filament of dark matter between two clusters of galaxies*, *Nature* (2012) , [1207.0809]. (Cited on page 4.)

[73] PLANCK collaboration, P. A. R. Ade et al., *Planck 2015 results. XIII. Cosmological parameters*, *Astron. Astrophys.* **594** (2016) A13, [1502.01589]. (Cited on pages 4, 60, 99, and 100.)

[74] ATLAS collaboration, G. Aad et al., *Search for supersymmetry at $\sqrt{s}$=8 TeV in final states with jets and two same-sign leptons or three leptons with the ATLAS detector*, *JHEP* **06** (2014) 035, [1404.2500]. (Cited on page 5.)

[75] ATLAS collaboration, G. Aad et al., *Search for squarks and gluinos with the ATLAS detector in final states with jets and missing transverse momentum using $\sqrt{s} = 8$ TeV proton–proton collision data*, *JHEP* **09** (2014) 176, [1405.7875]. (Cited on page 5.)

[76] ATLAS collaboration, G. Aad et al., *Search for direct pair production of the top squark in all-hadronic final states in proton-proton collisions at $\sqrt{s} = 8$ TeV with the ATLAS detector*, *JHEP* **09** (2014) 015, [1406.1122]. (Cited on page 5.)

[77] ATLAS collaboration, *A general search for new phenomena with the ATLAS detector in pp collisions at $\sqrt{s} = 8$ TeV*, ATLAS-CONF-2014-006, Mar, 2014. (Cited on page 5.)

[78] CMS collaboration, S. Chatrchyan et al., *Search for supersymmetry in pp collisions at $\sqrt{s}$=8 TeV in events with a single lepton, large jet multiplicity, and multiple b jets*, *Phys.Lett.* **B733** (2014) 328–353, [1311.4937]. (Cited on pages 5 and 100.)

[79] CMS collaboration, S. Chatrchyan et al., *Search for top-squark pair production in the single-lepton final state in pp collisions at $\sqrt{s}$ = 8 TeV*, *Eur.Phys.J.* **C73** (2013) 2677, [1308.1586]. (Cited on page 5.)

[80] CMS collaboration, S. Chatrchyan et al., *Search for new physics in the multijet and missing transverse momentum final state in proton-proton collisions at $\sqrt{s}$= 8 TeV*, *JHEP* **1406** (2014) 055, [1402.4770]. (Cited on page 5.)

[81] CMS collaboration, *Phenomenological MSSM interpretation of the CMS 7 and 8 TeV results*, CMS-PAS-SUS-13-020, 2014. (Cited on page 5.)

[82] ATLAS collaboration, G. Aad et al., *Search for top squark pair production in final states with one isolated lepton, jets, and missing transverse momentum in $\sqrt{s}$ =8 TeV pp collisions with the ATLAS detector*, *JHEP* **11** (2014) 118, [1407.0583]. (Cited on page 5.)

[83] K. Rolbiecki and K. Sakurai, *Light stops emerging in WW cross section measurements?*, *JHEP* **1309** (2013) 004, [1303.5696]. (Cited on page 5.)

[84] J. S. Kim, K. Rolbiecki, K. Sakurai and J. Tattersall, *'Stop' that ambulance! New physics at the LHC?*, *JHEP* **12** (2014) 010, [1406.0858]. (Cited on page 5.)

[85] D. Curtin, P. Meade and P.-J. Tien, *Natural SUSY in Plain Sight*, *Phys. Rev.* **D90** (2014) 115012, [1406.0848]. (Cited on page 5.)

[86] ATLAS collaboration, *Search for strong production of supersymmetric particles in final states with missing transverse momentum and at least three b-jets using 20.1 fb^{-1} of pp collisions at $\sqrt{s} = 8$ TeV with the ATLAS Detector*, ATLAS-CONF-2013-061, Jun, 2013. (Cited on page 5.)

[87] ALEPH collaboration, A. Heister et al., *Search for charginos nearly mass degenerate with the lightest neutralino in e^+e^- collisions at center-of-mass energies up to 209-GeV*, *Phys.Lett.* **B533** (2002) 223–236, [hep-ex/0203020]. (Cited on page 6.)

[88] OPAL collaboration, G. Abbiendi et al., *Search for nearly mass degenerate charginos and neutralinos at LEP*, *Eur.Phys.J.* **C29** (2003) 479–489, [hep-ex/0210043]. (Cited on page 6.)

[89] J. L. Feng, P. Kant, S. Profumo and D. Sanford, *Three-Loop Corrections to the Higgs Boson Mass and Implications for Supersymmetry at the LHC*, *Phys.Rev.Lett.* **111** (2013) 131802, [1306.2318]. (Cited on page 6.)

[90] T. Hahn, S. Heinemeyer, W. Hollik, H. Rzehak and G. Weiglein, *High-Precision Predictions for the Light CP -Even Higgs Boson Mass of the Minimal Supersymmetric Standard Model*, *Phys. Rev. Lett.* **112** (2014) 141801, [1312.4937]. (Cited on pages 6, 31, and 43.)

[91] R. Harlander, P. Kant, L. Mihaila and M. Steinhauser, *Higgs boson mass in supersymmetry to three loops*, *Phys.Rev.Lett.* **100** (2008) 191602, [0803.0672]. (Cited on page 6.)

[92] ATLAS collaboration, *Updated coupling measurements of the Higgs boson with the ATLAS detector using up to 25 fb^{-1} of proton-proton collision data*, ATLAS-CONF-2014-009, Mar, 2014. (Cited on page 6.)

[93] A. Dobado, M. J. Herrero and S. Penaranda, *The Higgs sector of the MSSM in the decoupling limit*, *Eur.Phys.J.* **C17** (2000) 487–500, [hep-ph/0002134]. (Cited on page 6.)

[94] R. Barbieri and G. Giudice, *Upper Bounds on Supersymmetric Particle Masses*, *Nucl.Phys.* **B306** (1988) 63. (Cited on pages 6, 12, and 59.)

[95] B. de Carlos and J. Casas, *One loop analysis of the electroweak breaking in supersymmetric models and the fine tuning problem*, *Phys.Lett.* **B309** (1993) 320–328, [hep-ph/9303291]. (Cited on pages 6 and 11.)

[96] G. W. Anderson and D. J. Castano, *Measures of fine tuning*, *Phys.Lett.* **B347** (1995) 300–308, [hep-ph/9409419]. (Cited on page 6.)

[97] P. Ciafaloni and A. Strumia, *Naturalness upper bounds on gauge mediated soft terms*, *Nucl.Phys.* **B494** (1997) 41–53, [hep-ph/9611204]. (Cited on pages 6, 12, 46, and 63.)

[98] G. Bhattacharyya and A. Romanino, *Naturalness constraints on gauge mediated supersymmetry breaking models*, *Phys.Rev.* **D55** (1997) 7015–7019, [hep-ph/9611243]. (Cited on page 6.)

[99] P. H. Chankowski, J. R. Ellis and S. Pokorski, *The Fine tuning price of LEP*, *Phys.Lett.* **B423** (1998) 327–336, [hep-ph/9712234]. (Cited on page 6.)

[100] R. Barbieri and A. Strumia, *About the fine tuning price of LEP*, *Phys.Lett.* **B433** (1998) 63–66, [hep-ph/9801353]. (Cited on page 6.)

[101] G. L. Kane and S. King, *Naturalness implications of LEP results*, *Phys.Lett.* **B451** (1999) 113–122, [hep-ph/9810374]. (Cited on page 6.)

[102] L. Giusti, A. Romanino and A. Strumia, *Natural ranges of supersymmetric signals*, *Nucl.Phys.* **B550** (1999) 3–31, [hep-ph/9811386]. (Cited on page 6.)

[103] M. Bastero-Gil, G. L. Kane and S. King, *Fine tuning constraints on supergravity models*, *Phys.Lett.* **B474** (2000) 103–112, [hep-ph/9910506]. (Cited on page 6.)

[104] K. L. Chan, U. Chattopadhyay and P. Nath, *Naturalness, weak scale supersymmetry and the prospect for the observation of supersymmetry at the Tevatron and at the CERN LHC*, *Phys.Rev.* **D58** (1998) 096004, [hep-ph/9710473]. (Cited on pages 6 and 8.)

[105] Z. Chacko, Y. Nomura and D. Tucker-Smith, *A Minimally fine-tuned supersymmetric standard model*, *Nucl.Phys.* **B725** (2005) 207–250, [hep-ph/0504095]. (Cited on page 6.)

[106] K. Choi, K. S. Jeong, T. Kobayashi and K.-i. Okumura, *Little SUSY hierarchy in mixed modulus-anomaly mediation*, *Phys.Lett.* **B633** (2006) 355–361, [hep-ph/0508029]. (Cited on page 6.)

[107] Y. Nomura and B. Tweedie, *The Supersymmetric fine-tuning problem and TeV-scale exotic scalars*, *Phys.Rev.* **D72** (2005) 015006, [hep-ph/0504246]. (Cited on page 6.)

[108] R. Kitano and Y. Nomura, *A Solution to the supersymmetric fine-tuning problem within the MSSM*, *Phys.Lett.* **B631** (2005) 58–67, [hep-ph/0509039]. (Cited on page 6.)

[109] Y. Nomura, D. Poland and B. Tweedie, *Minimally fine-tuned supersymmetric standard models with intermediate-scale supersymmetry breaking*, *Nucl.Phys.* **B745** (2006) 29–48, [hep-ph/0509243]. (Cited on page 6.)

[110] O. Lebedev, H. P. Nilles and M. Ratz, *A Note on fine-tuning in mirage mediation*, in *CP Violation and the Flavour Puzzle: Symposium in Honour of Gustavo C. Branco. GustavoFest 2005, Lisbon, Portugal, July 2005*, pp. 211–221, 2005. hep-ph/0511320. (Cited on page 6.)

[111] B. Allanach, *Naturalness priors and fits to the constrained minimal supersymmetric standard model*, *Phys.Lett.* **B635** (2006) 123–130, [hep-ph/0601089]. (Cited on page 6.)

[112] M. Perelstein and C. Spethmann, *A Collider signature of the supersymmetric golden region*, *JHEP* **0704** (2007) 070, [hep-ph/0702038]. (Cited on page 6.)

[113] B. C. Allanach, K. Cranmer, C. G. Lester and A. M. Weber, *Natural priors, CMSSM fits and LHC weather forecasts*, *JHEP* **0708** (2007) 023, [0705.0487]. (Cited on page 6.)

[114] M. Cabrera, J. Casas and R. Ruiz de Austri, *Bayesian approach and Naturalness in MSSM analyses for the LHC*, *JHEP* **0903** (2009) 075, [0812.0536]. (Cited on pages 6, 14, and 63.)

[115] S. Cassel, D. Ghilencea and G. Ross, *Fine tuning as an indication of physics beyond the MSSM*, *Nucl.Phys.* **B825** (2010) 203–221, [0903.1115]. (Cited on page 6.)

[116] T. Kobayashi, Y. Nakai and R. Takahashi, *Fine Tuning in General Gauge Mediation*, *JHEP* **1001** (2010) 003, [0910.3477]. (Cited on page 6.)

[117] P. Lodone, *Naturalness bounds in extensions of the MSSM without a light Higgs boson*, *JHEP* **1005** (2010) 068, [1004.1271]. (Cited on page 6.)

[118] M. Asano, H. D. Kim, R. Kitano and Y. Shimizu, *Natural Supersymmetry at the LHC*, *JHEP* **1012** (2010) 019, [1010.0692]. (Cited on page 6.)

[119] S. Cassel, D. Ghilencea, S. Kraml, A. Lessa and G. Ross, *Fine-tuning implications for complementary dark matter and LHC SUSY searches*, *JHEP* **1105** (2011) 120, [1101.4664]. (Cited on page 6.)

[120] G. Giudice and R. Rattazzi, *Living Dangerously with Low-Energy Supersymmetry*, *Nucl.Phys.* **B757** (2006) 19–46, [hep-ph/0606105]. (Cited on page 6.)

[121] R. Barbieri and D. Pappadopulo, *S-particles at their naturalness limits*, *JHEP* **0910** (2009) 061, [0906.4546]. (Cited on page 6.)

[122] J. L. Feng, K. T. Matchev and T. Moroi, *Multi - TeV scalars are natural in minimal supergravity*, *Phys.Rev.Lett.* **84** (2000) 2322–2325, [hep-ph/9908309]. (Cited on pages 6 and 8.)

[123] J. L. Feng, K. T. Matchev and T. Moroi, *Focus points and naturalness in supersymmetry*, *Phys.Rev.* **D61** (2000) 075005, [hep-ph/9909334]. (Cited on pages 6 and 8.)

[124] A. Romanino and A. Strumia, *Are heavy scalars natural in minimal supergravity?*, *Phys.Lett.* **B487** (2000) 165–170, [hep-ph/9912301]. (Cited on page 6.)

[125] D. Horton and G. Ross, *Naturalness and Focus Points with Non-Universal Gaugino Masses*, *Nucl.Phys.* **B830** (2010) 221–247, [0908.0857]. (Cited on page 6.)

[126] A. Strumia, *The Fine-tuning price of the early LHC*, *JHEP* **1104** (2011) 073, [1101.2195]. (Cited on page 6.)

[127] S. Akula, M. Liu, P. Nath and G. Peim, *Naturalness, Supersymmetry and Implications for LHC and Dark Matter*, *Phys.Lett.* **B709** (2012) 192–199, [1111.4589]. (Cited on page 6.)

[128] S. Antusch, L. Calibbi, V. Maurer, M. Monaco and M. Spinrath, *Naturalness of the Non-Universal MSSM in the Light of the Recent Higgs Results*, *JHEP* **1301** (2013) 187, [1207.7236]. (Cited on pages 6 and 21.)

[129] S. P. Martin, *Non-universal gaugino masses and semi-natural supersymmetry in view of the Higgs boson discovery*, *Phys.Rev.* **D89** (2014) 035011, [1312.0582]. (Cited on pages 6 and 21.)

[130] J. A. Evans, Y. Kats, D. Shih and M. J. Strassler, *Toward Full LHC Coverage of Natural Supersymmetry*, *JHEP* **07** (2014) 101, [1310.5758]. (Cited on page 6.)

[131] E. Hardy, *Is Natural SUSY Natural?*, *JHEP* **1310** (2013) 133, [1306.1534]. (Cited on page 6.)

[132] H. Baer, V. Barger and M. Padeffke-Kirkland, *Electroweak versus high scale finetuning in the 19-parameter SUGRA model*, *Phys.Rev.* **D88** (2013) 055026, [1304.6732]. (Cited on page 6.)

[133] A. Arvanitaki, M. Baryakhtar, X. Huang, K. van Tilburg and G. Villadoro, *The Last Vestiges of Naturalness*, *JHEP* **1403** (2014) 022, [1309.3568]. (Cited on page 6.)

[134] A. Kaminska, G. G. Ross and K. Schmidt-Hoberg, *Non-universal gaugino masses and fine tuning implications for SUSY searches in the MSSM and the GNMSSM*, *JHEP* **1311** (2013) 209, [1308.4168]. (Cited on pages 6 and 21.)

[135] H. Baer, V. Barger, D. Mickelson and M. Padeffke-Kirkland, *SUSY models under siege: LHC constraints and electroweak fine-tuning*, *Phys.Rev.* **D89** (2014) 115019, [1404.2277]. (Cited on page 6.)

[136] K. J. Bae, H. Baer, V. Barger, D. Mickelson and M. Savoy, *Implications of naturalness for the heavy Higgs bosons of supersymmetry*, *Phys. Rev.* **D90** (2014) 075010, [1407.3853]. (Cited on page 6.)

[137] M. Chakraborti, U. Chattopadhyay, A. Choudhury, A. Datta and S. Poddar, *The Electroweak Sector of the pMSSM in the Light of LHC - 8 TeV and Other Data*, *JHEP* **1407** (2014) 019, [1404.4841]. (Cited on page 6.)

[138] A. Mustafayev and X. Tata, *Supersymmetry, Naturalness, and Light Higgsinos*, *Indian J. Phys.* **88** (2014) 991–1004, [1404.1386]. (Cited on page 6.)

[139] A. Fowlie, *CMSSM, naturalness and the "fine-tuning price" of the Very Large Hadron Collider*, *Phys. Rev.* **D90** (2014) 015010, [1403.3407]. (Cited on page 6.)

[140] N. Craig, *The State of Supersymmetry after Run I of the LHC*, in *Beyond the Standard Model after the first run of the LHC Arcetri, Florence, Italy, May 20-July 12, 2013*, 2013. 1309.0528. (Cited on page 6.)

[141] I. Antoniadis, E. M. Babalic and D. M. Ghilencea, *Naturalness in low-scale SUSY models and "non-linear" MSSM*, *Eur. Phys. J.* **C74** (2014) 3050, [1405.4314]. (Cited on page 6.)

[142] K. Kowalska, L. Roszkowski, E. M. Sessolo and S. Trojanowski, *Low fine tuning in the MSSM with higgsino dark matter and unification constraints*, *JHEP* **1404** (2014) 166, [1402.1328]. (Cited on pages 6 and 22.)

[143] A. Delgado, M. Quiros and C. Wagner, *General Focus Point in the MSSM*, *JHEP* **1404** (2014) 093, [1402.1735]. (Cited on pages 6 and 22.)

[144] M. Papucci, J. T. Ruderman and A. Weiler, *Natural SUSY Endures*, *JHEP* **1209** (2012) 035, [1110.6926]. (Cited on pages 6, 7, 8, 14, and 59.)

[145] J. L. Feng, *Naturalness and the Status of Supersymmetry*, *Ann.Rev.Nucl.Part.Sci.* **63** (2013) 351–382, [1302.6587]. (Cited on pages 8, 12, 18, and 20.)

[146] C. Ford, D. Jones, P. Stephenson and M. Einhorn, *The Effective potential and the renormalization group*, *Nucl.Phys.* **B395** (1993) 17–34, [hep-lat/9210033]. (Cited on page 8.)

[147] M. Bando, T. Kugo, N. Maekawa and H. Nakano, *Improving the effective potential*, *Phys.Lett.* **B301** (1993) 83–89, [hep-ph/9210228]. (Cited on page 8.)

[148] M. Bando, T. Kugo, N. Maekawa and H. Nakano, *Improving the effective potential: Multimass scale case*, *Prog.Theor.Phys.* **90** (1993) 405–418, [hep-ph/9210229]. (Cited on page 8.)

[149] M. Einhorn and D. Jones, *Scale Fixing by Dimensional Transmutation: Supersymmetric Unified Models and the Renormalization Group*, *Nucl.Phys.* **B211** (1983) 29. (Cited on page 8.)

[150] J. Casas, J. Espinosa, M. Quiros and A. Riotto, *The Lightest Higgs boson mass in the minimal supersymmetric standard model*, *Nucl.Phys.* **B436** (1995) 3–29, [hep-ph/9407389]. (Cited on page 9.)

[151] M. S. Carena, J. Espinosa, M. Quiros and C. Wagner, *Analytical expressions for radiatively corrected Higgs masses and couplings in the MSSM*, *Phys.Lett.* **B355** (1995) 209–221, [hep-ph/9504316]. (Cited on page 9.)

[152] H. E. Haber, R. Hempfling and A. H. Hoang, *Approximating the radiatively corrected Higgs mass in the minimal supersymmetric model*, *Z.Phys.* **C75** (1997) 539–554, [hep-ph/9609331]. (Cited on page 9.)

[153] M. Cabrera, J. Casas and A. Delgado, *Upper Bounds on Superpartner Masses from Upper Bounds on the Higgs Boson Mass*, *Phys.Rev.Lett.* **108** (2012) 021802, [1108.3867]. (Cited on pages 10, 11, and 104.)

[154] G. F. Giudice and A. Strumia, *Probing High-Scale and Split Supersymmetry with Higgs Mass Measurements*, *Nucl.Phys.* **B858** (2012) 63–83, [1108.6077]. (Cited on pages 10, 11, and 104.)

[155] A. E. Nelson and L. Randall, *Naturally large tan BETA*, *Phys.Lett.* **B316** (1993) 516–520, [hep-ph/9308277]. (Cited on page 10.)

[156] L. J. Hall, R. Rattazzi and U. Sarid, *The Top quark mass in supersymmetric SO(10) unification*, *Phys.Rev.* **D50** (1994) 7048–7065, [hep-ph/9306309]. (Cited on page 10.)

[157] M. E. Cabrera, J. A. Casas and R. Ruiz d Austri, *MSSM Forecast for the LHC*, *JHEP* **1005** (2010) 043, [0911.4686]. (Cited on pages 10, 14, and 63.)

[158] J. R. Ellis, K. Enqvist, D. V. Nanopoulos and F. Zwirner, *Observables in Low-Energy Superstring Models*, *Mod.Phys.Lett.* **A1** (1986) 57. (Cited on pages 12 and 59.)

[159] D. Ghilencea and G. Ross, *The fine-tuning cost of the likelihood in SUSY models*, *Nucl.Phys.* **B868** (2013) 65–74, [1208.0837]. (Cited on page 14.)

[160] S. Fichet, *Quantified naturalness from Bayesian statistics*, *Phys.Rev.* **D86** (2012) 125029, [1204.4940]. (Cited on pages 14, 59, 81, and 108.)

[161] H. Abe, T. Kobayashi and Y. Omura, *Relaxed fine-tuning in models with non-universal gaugino masses*, *Phys.Rev.* **D76** (2007) 015002, [hep-ph/0703044]. (Cited on page 16.)

[162] S. P. Martin, *Compressed supersymmetry and natural neutralino dark matter from top squark-mediated annihilation to top quarks*, *Phys.Rev.* **D75** (2007) 115005, [hep-ph/0703097]. (Cited on page 16.)

[163] F. Staub, *SARAH 4: A tool for (not only SUSY) model builders*, *Comput.Phys.Commun.* **185** (2014) 1773–1790, [1309.7223]. (Cited on pages 16 and 103.)

[164] S. P. Martin and M. T. Vaughn, *Regularization dependence of running couplings in softly broken supersymmetry*, *Phys.Lett.* **B318** (1993) 331–337, [hep-ph/9308222]. (Cited on page 22.)

[165] J. A. Casas, J. R. Espinosa and I. Hidalgo, *Implications for new physics from fine-tuning arguments. II. Little Higgs models*, *JHEP* **0503** (2005) 038, [hep-ph/0502066]. (Cited on pages 23, 46, 81, and 108.)

[166] J. Alcaraz, *Beyond the SM searches: 'LHC14' prospects*, Talk given at LCH France 2013, Annecy. (Cited on page 25.)

[167] N. Arkani-Hamed, A. Delgado and G. Giudice, *The Well-tempered neutralino*, *Nucl.Phys.* **B741** (2006) 108–130, [hep-ph/0601041]. (Cited on pages 25, 61, 70, and 71.)

[168] M. Cahill-Rowley, R. Cotta, A. Drlica-Wagner, S. Funk, J. Hewett, A. Ismail et al., *Complementarity of dark matter searches in the phenomenological MSSM*, *Phys. Rev.* **D91** (2015) 055011, [1405.6716]. (Cited on page 25.)

[169] A. Brignole, J. Casas, J. Espinosa and I. Navarro, *Low scale supersymmetry breaking: Effective description, electroweak breaking and phenomenology*, *Nucl.Phys.* **B666** (2003) 105–143, [hep-ph/0301121]. (Cited on page 25.)

[170] J. Casas, J. Espinosa and I. Hidalgo, *The MSSM fine tuning problem: A Way out*, *JHEP* **0401** (2004) 008, [hep-ph/0310137]. (Cited on page 25.)

[171] M. Dine, N. Seiberg and S. Thomas, *Higgs physics as a window beyond the MSSM (BMSSM)*, *Phys.Rev.* **D76** (2007) 095004, [0707.0005]. (Cited on page 25.)

[172] L. Randall and R. Sundrum, *Out of this world supersymmetry breaking*, *Nucl.Phys.* **B557** (1999) 79–118, [hep-th/9810155]. (Cited on page 29.)

[173] V. S. Kaplunovsky and J. Louis, *Model independent analysis of soft terms in effective supergravity and in string theory*, *Phys.Lett.* **B306** (1993) 269–275, [hep-th/9303040]. (Cited on page 29.)

[174] M. Frank, T. Hahn, S. Heinemeyer, W. Hollik, H. Rzehak et al., *The Higgs Boson Masses and Mixings of the Complex MSSM in the Feynman-Diagrammatic Approach*, *JHEP* **0702** (2007) 047, [hep-ph/0611326]. (Cited on pages 31 and 43.)

[175] G. Degrassi, S. Heinemeyer, W. Hollik, P. Slavich and G. Weiglein, *Towards high precision predictions for the MSSM Higgs sector*, *Eur.Phys.J.* **C28** (2003) 133–143, [hep-ph/0212020]. (Cited on pages 31 and 43.)

[176] S. Heinemeyer, W. Hollik and G. Weiglein, *The Masses of the neutral CP - even Higgs bosons in the MSSM: Accurate analysis at the two loop level*, *Eur.Phys.J.* **C9** (1999) 343–366, [hep-ph/9812472]. (Cited on pages 31 and 43.)

[177] S. Heinemeyer, W. Hollik and G. Weiglein, *FeynHiggs: A Program for the calculation of the masses of the neutral CP even Higgs bosons in the MSSM*, *Comput.Phys.Commun.* **124** (2000) 76–89, [hep-ph/9812320]. (Cited on pages 31 and 43.)

[178] M. Dine, W. Fischler and M. Srednicki, *Supersymmetric Technicolor*, *Nucl. Phys.* **B189** (1981) 575–593. (Cited on page 39.)

[179] S. Dimopoulos and S. Raby, *Supercolor*, *Nucl. Phys.* **B192** (1981) 353. (Cited on page 39.)

[180] M. Dine and W. Fischler, *A Phenomenological Model of Particle Physics Based on Supersymmetry*, *Phys. Lett.* **B110** (1982) 227. (Cited on page 39.)

[181] M. Dine and M. Srednicki, *More Supersymmetric Technicolor*, *Nucl. Phys.* **B202** (1982) 238. (Cited on page 39.)

[182] M. Dine and W. Fischler, *A Supersymmetric GUT*, *Nucl. Phys.* **B204** (1982) 346. (Cited on page 39.)

[183] L. Alvarez-Gaume, M. Claudson and M. B. Wise, *Low-Energy Supersymmetry*, *Nucl. Phys.* **B207** (1982) 96. (Cited on page 39.)

[184] C. R. Nappi and B. A. Ovrut, *Supersymmetric Extension of the SU(3) x SU(2) x U(1) Model*, *Phys. Lett.* **B113** (1982) 175. (Cited on page 39.)

[185] S. Dimopoulos and S. Raby, *Geometric Hierarchy*, *Nucl. Phys.* **B219** (1983) 479. (Cited on page 39.)

[186] M. Dine and A. E. Nelson, *Dynamical supersymmetry breaking at low-energies*, *Phys. Rev.* **D48** (1993) 1277–1287, [hep-ph/9303230]. (Cited on page 39.)

[187] M. Dine, A. E. Nelson and Y. Shirman, *Low-energy dynamical supersymmetry breaking simplified*, *Phys. Rev.* **D51** (1995) 1362–1370, [hep-ph/9408384]. (Cited on page 39.)

[188] M. Dine, A. E. Nelson, Y. Nir and Y. Shirman, *New tools for low-energy dynamical supersymmetry breaking*, *Phys. Rev.* **D53** (1996) 2658–2669, [hep-ph/9507378]. (Cited on page 39.)

[189] S. Dimopoulos, G. F. Giudice and A. Pomarol, *Dark matter in theories of gauge mediated supersymmetry breaking*, *Phys. Lett.* **B389** (1996) 37–42, [hep-ph/9607225]. (Cited on pages 40 and 153.)

[190] S. P. Martin, *Generalized messengers of supersymmetry breaking and the sparticle mass spectrum*, *Phys. Rev.* **D55** (1997) 3177–3187, [hep-ph/9608224]. (Cited on pages 40 and 153.)

[191] E. Poppitz and S. P. Trivedi, *Some remarks on gauge mediated supersymmetry breaking*, *Phys. Lett.* **B401** (1997) 38–46, [hep-ph/9703246]. (Cited on pages 40 and 153.)

[192] M. Dine, Y. Nir and Y. Shirman, *Variations on minimal gauge mediated supersymmetry breaking*, *Phys. Rev.* **D55** (1997) 1501–1508, [hep-ph/9607397]. (Cited on page 41.)

[193] G. F. Giudice and R. Rattazzi, *Extracting supersymmetry breaking effects from wave function renormalization*, *Nucl. Phys.* **B511** (1998) 25–44, [hep-ph/9706540]. (Cited on page 41.)

[194] Z. Chacko and E. Ponton, *Yukawa deflected gauge mediation*, *Phys. Rev.* **D66** (2002) 095004, [hep-ph/0112190]. (Cited on pages 41 and 45.)

[195] Z. Chacko, E. Katz and E. Perazzi, *Yukawa deflected gauge mediation in four dimensions*, *Phys. Rev.* **D66** (2002) 095012, [hep-ph/0203080]. (Cited on pages 41 and 45.)

[196] Y. Shadmi and P. Z. Szabo, *Flavored Gauge-Mediation*, *JHEP* **06** (2012) 124, [1103.0292]. (Cited on pages 41 and 45.)

[197] J. L. Evans, M. Ibe and T. T. Yanagida, *Relatively Heavy Higgs Boson in More Generic Gauge Mediation*, *Phys. Lett.* **B705** (2011) 342–348, [1107.3006]. (Cited on pages 41, 45, 47, and 154.)

[198] T. Jelinski, J. Pawelczyk and K. Turzynski, *On Low-Energy Predictions of Unification Models Inspired by F-theory*, *Phys. Lett.* **B711** (2012) 307–312, [1111.6492]. (Cited on pages 41 and 45.)

[199] J. L. Evans, M. Ibe, S. Shirai and T. T. Yanagida, *A 125GeV Higgs Boson and Muon g-2 in More Generic Gauge Mediation*, *Phys. Rev.* **D85** (2012) 095004, [1201.2611]. (Cited on pages 41, 45, and 154.)

[200] Z. Kang, T. Li, T. Liu, C. Tong and J. M. Yang, *A Heavy SM-like Higgs and a Light Stop from Yukawa-Deflected Gauge Mediation*, *Phys. Rev.* **D86** (2012) 095020, [1203.2336]. (Cited on page 41.)

[201] N. Craig, S. Knapen, D. Shih and Y. Zhao, *A Complete Model of Low-Scale Gauge Mediation*, *JHEP* **03** (2013) 154, [1206.4086]. (Cited on pages 41, 45, 52, and 57.)

[202] A. Albaid and K. S. Babu, *Higgs boson of mass 125 GeV in GMSB models with messenger-matter mixing*, *Phys. Rev.* **D88** (2013) 055007, [1207.1014]. (Cited on pages 41 and 45.)

[203] M. Abdullah, I. Galon, Y. Shadmi and Y. Shirman, *Flavored Gauge Mediation, A Heavy Higgs, and Supersymmetric Alignment*, *JHEP* **06** (2013) 057, [1209.4904]. (Cited on pages 41 and 45.)

[204] M. J. Perez, P. Ramond and J. Zhang, *Mixing supersymmetry and family symmetry breakings*, *Phys. Rev.* **D87** (2013) 035021, [1209.6071]. (Cited on pages 41 and 45.)

[205] M. Endo, K. Hamaguchi, S. Iwamoto and N. Yokozaki, *Vacuum Stability Bound on Extended GMSB Models*, *JHEP* **06** (2012) 060, [1202.2751]. (Cited on pages 41 and 45.)

[206] H. D. Kim, D. Y. Mo and M.-S. Seo, *Neutrino Assisted Gauge Mediation*, *Eur. Phys. J.* **C73** (2013) 2449, [1211.6479]. (Cited on page 41.)

[207] P. Byakti and T. S. Ray, *Burgeoning the Higgs mass to 125 GeV through messenger-matter interactions in GMSB models*, *JHEP* **05** (2013) 055, [1301.7605]. (Cited on page 41.)

[208] N. Craig, S. Knapen and D. Shih, *General Messenger Higgs Mediation*, *JHEP* **08** (2013) 118, [1302.2642]. (Cited on page 41.)

[209] J. A. Evans and D. Shih, *Surveying Extended GMSB Models with m_h=125 GeV*, *JHEP* **08** (2013) 093, [1303.0228]. (Cited on pages 41, 45, 46, and 56.)

[210] L. Calibbi, P. Paradisi and R. Ziegler, *Gauge Mediation beyond Minimal Flavor Violation*, *JHEP* **06** (2013) 052, [1304.1453]. (Cited on pages 41, 45, 47, and 56.)

[211] T. Jeliński, *On messengers couplings in extended GMSB models*, *JHEP* **09** (2013) 107, [1305.6277]. (Cited on page 41.)

[212] I. Galon, G. Perez and Y. Shadmi, *Non-Degenerate Squarks from Flavored Gauge Mediation*, *JHEP* **09** (2013) 117, [1306.6631]. (Cited on page 41.)

[213] W. Fischler and W. Tangarife, *Vector-like Fields, Messenger Mixing and the Higgs mass in Gauge Mediation*, *JHEP* **05** (2014) 151, [1310.6369]. (Cited on page 41.)

[214] S. Knapen and D. Shih, *Higgs Mediation with Strong Hidden Sector Dynamics*, *JHEP* **08** (2014) 136, [1311.7107]. (Cited on page 41.)

[215] R. Ding, T. Li, F. Staub and B. Zhu, *Focus Point Supersymmetry in Extended Gauge Mediation*, *JHEP* **03** (2014) 130, [1312.5407]. (Cited on page 41.)

[216] L. Calibbi, P. Paradisi and R. Ziegler, *Lepton Flavor Violation in Flavored Gauge Mediation*, *Eur. Phys. J.* **C74** (2014) 3211, [1408.0754]. (Cited on page 41.)

[217] A. Basirnia, D. Egana-Ugrinovic, S. Knapen and D. Shih, *125 GeV Higgs from Tree-Level A-terms*, *JHEP* **06** (2015) 144, [1501.00997]. (Cited on pages 41, 50, 51, 52, 53, and 56.)

[218] J. P. Vega and G. Villadoro, *SusyHD: Higgs mass Determination in Supersymmetry*, *JHEP* **07** (2015) 159, [1504.05200]. (Cited on pages 43 and 46.)

[219] B. C. Allanach, *SOFTSUSY: a program for calculating supersymmetric spectra*, *Comput. Phys. Commun.* **143** (2002) 305–331, [hep-ph/0104145]. (Cited on pages 46, 66, and 93.)

[220] E. Bagnaschi, G. F. Giudice, P. Slavich and A. Strumia, *Higgs Mass and Unnatural Supersymmetry*, *JHEP* **09** (2014) 092, [1407.4081]. (Cited on page 46.)

[221] C. Cheung, L. J. Hall, D. Pinner and J. T. Ruderman, *Prospects and Blind Spots for Neutralino Dark Matter*, *JHEP* **05** (2013) 100, [1211.4873]. (Cited on pages 46, 59, 65, 81, and 108.)

[222] P. Grothaus, M. Lindner and Y. Takanishi, *Naturalness of Neutralino Dark Matter*, *JHEP* **07** (2013) 094, [1207.4434]. (Cited on page 59.)

[223] T. Cohen and J. G. Wacker, *Here be Dragons: The Unexplored Continents of the CMSSM*, *JHEP* **09** (2013) 061, [1305.2914]. (Cited on page 59.)

[224] C. Boehm, P. S. B. Dev, A. Mazumdar and E. Pukartas, *Naturalness of Light Neutralino Dark Matter in pMSSM after LHC, XENON100 and Planck Data*, *JHEP* **06** (2013) 113, [1303.5386]. (Cited on pages 59 and 87.)

[225] D. Barducci, A. Belyaev, A. K. M. Bharucha, W. Porod and V. Sanz, *Uncovering Natural Supersymmetry via the interplay between the LHC and Direct Dark Matter Detection*, *JHEP* **07** (2015) 066, [1504.02472]. (Cited on page 59.)

[226] P. Gondolo and G. Gelmini, *Cosmic abundances of stable particles: Improved analysis*, *Nucl. Phys.* **B360** (1991) 145–179. (Cited on page 60.)

[227] T. Cohen, M. Lisanti, A. Pierce and T. R. Slatyer, *Wino Dark Matter Under Siege*, *JCAP* **1310** (2013) 061, [1307.4082]. (Cited on page 61.)

[228] J. Fan and M. Reece, *In Wino Veritas? Indirect Searches Shed Light on Neutralino Dark Matter*, *JHEP* **1310** (2013) 124, [1307.4400]. (Cited on page 61.)

[229] A. Hryczuk, I. Cholis, R. Iengo, M. Tavakoli and P. Ullio, *Indirect Detection Analysis: Wino Dark Matter Case Study*, *JCAP* **1407** (2014) 031, [1401.6212]. (Cited on page 61.)

[230] A. Crivellin, M. Hoferichter, M. Procura and L. C. Tunstall, *Light stops, blind spots, and isospin violation in the MSSM*, *JHEP* **07** (2015) 129, [1503.03478]. (Cited on page 65.)

[231] G. Bélanger, F. Boudjema, A. Pukhov and A. Semenov, *micrOMEGAs4.1: two dark matter candidates*, *Comput. Phys. Commun.* **192** (2015) 322–329, [1407.6129]. (Cited on page 66.)

[232] G. Belanger, F. Boudjema, A. Pukhov and A. Semenov, *micrOMEGAs_3: A program for calculating dark matter observables*, *Comput. Phys. Commun.* **185** (2014) 960–985, [1305.0237]. (Cited on pages 66 and 93.)

[233] F. Feroz and M. P. Hobson, *Multimodal nested sampling: an efficient and robust alternative to MCMC methods for astronomical data analysis*, *Mon. Not. Roy. Astron. Soc.* **384** (2008) 449, [0704.3704]. (Cited on pages 66 and 93.)

[234] F. Feroz, M. P. Hobson and M. Bridges, *MultiNest: an efficient and robust Bayesian inference tool for cosmology and particle physics*, *Mon. Not. Roy. Astron. Soc.* **398** (2009) 1601–1614, [0809.3437]. (Cited on pages 66 and 93.)

[235] F. Feroz, M. P. Hobson, E. Cameron and A. N. Pettitt, *Importance Nested Sampling and the MultiNest Algorithm*, 1306.2144. (Cited on pages 66 and 93.)

[236] LUX collaboration, D. S. Akerib et al., *Improved Limits on Scattering of Weakly Interacting Massive Particles from Reanalysis of 2013 LUX Data*, *Phys. Rev. Lett.* **116** (2016) 161301, [1512.03506]. (Cited on pages 66 and 87.)

[237] LUX collaboration, A. Manalaysay, *Dark-matter results from 332 new live days of lux data*, in *Identification of Dark Matter 2016*, The University of Sheffield, Sheffield, U.K., July, 2016. (Cited on page 66.)

[238] XENON1T collaboration, E. Aprile, *The XENON1T Dark Matter Search Experiment*, *Springer Proc. Phys.* **148** (2013) 93–96, [1206.6288]. (Cited on page 66.)

[239] XENON collaboration, E. Aprile et al., *Physics reach of the XENON1T dark matter experiment*, *JCAP* **1604** (2016) 027, [1512.07501]. (Cited on pages 66 and 98.)

[240] P. Cushman et al., *Working Group Report: WIMP Dark Matter Direct Detection*, in *Proceedings, 2013 Community Summer Study on the Future of U.S. Particle Physics: Snowmass on the Mississippi (CSS2013): Minneapolis, MN, USA, July 29-August 6, 2013*, 2013. 1310.8327. (Cited on pages 66 and 98.)

[241] I. Antoniadis, C. Muñoz and M. Quiros, *Dynamical supersymmetry breaking with a large internal dimension*, *Nucl. Phys.* **B397** (1993) 515–538, [hep-ph/9211309]. (Cited on page 82.)

[242] ATLAS collaboration, G. Aad et al., *Search for strong production of supersymmetric particles in final states with missing transverse momentum and at least three b-jets at $\sqrt{s}$= 8 TeV proton-proton collisions with the ATLAS detector*, *JHEP* **10** (2014) 024, [1407.0600]. (Cited on page 82.)

[243] R. Bernabei et al., *Dark matter search*, *Riv. Nuovo Cim.* **26N1** (2003) 1–73, [astro-ph/0307403]. (Cited on page 87.)

[244] DAMA collaboration, R. Bernabei et al., *First results from DAMA/LIBRA and the combined results with DAMA/NaI*, *Eur. Phys. J.* **C56** (2008) 333–355, [0804.2741]. (Cited on page 87.)

[245] CoGeNT collaboration, C. E. Aalseth et al., *Results from a Search for Light-Mass Dark Matter with a P-type Point Contact Germanium Detector*, *Phys. Rev. Lett.* **106** (2011) 131301, [1002.4703]. (Cited on page 87.)

[246] G. Angloher et al., *Results from 730 kg days of the CRESST-II Dark Matter Search*, *Eur. Phys. J.* **C72** (2012) 1971, [1109.0702]. (Cited on page 87.)

[247] C. E. Aalseth et al., *Search for an Annual Modulation in a P-type Point Contact Germanium Dark Matter Detector*, *Phys. Rev. Lett.* **107** (2011) 141301, [1106.0650]. (Cited on page 87.)

[248] CDMS collaboration, R. Agnese et al., *Silicon Detector Dark Matter Results from the Final Exposure of CDMS II*, *Phys. Rev. Lett.* **111** (2013) 251301, [1304.4279]. (Cited on page 87.)

[249] C. E. Aalseth et al., *Maximum Likelihood Signal Extraction Method Applied to 3.4 years of CoGeNT Data*, 1401.6234. (Cited on page 87.)

[250] Fermi-LAT collaboration, V. Vitale and A. Morselli, *Indirect Search for Dark Matter from the center of the Milky Way with the Fermi-Large Area Telescope*, in *Fermi gamma-ray space telescope. Proceedings, 2nd Fermi Symposium, Washington, USA, November 2-5, 2009*, 2009. 0912.3828. (Cited on page 87.)

[251] L. Goodenough and D. Hooper, *Possible Evidence For Dark Matter Annihilation In The Inner Milky Way From The Fermi Gamma Ray Space Telescope*, 0910.2998. (Cited on page 87.)

[252] D. Hooper and L. Goodenough, *Dark Matter Annihilation in The Galactic Center As Seen by the Fermi Gamma Ray Space Telescope*, *Phys. Lett.* **B697** (2011) 412–428, [1010.2752]. (Cited on page 87.)

[253] D. Hooper and T. Linden, *On The Origin Of The Gamma Rays From The Galactic Center*, *Phys. Rev.* **D84** (2011) 123005, [1110.0006]. (Cited on page 87.)

[254] K. N. Abazajian and M. Kaplinghat, *Detection of a Gamma-Ray Source in the Galactic Center Consistent with Extended Emission from Dark Matter Annihilation and Concentrated Astrophysical Emission*, *Phys. Rev.* **D86** (2012) 083511, [1207.6047]. (Cited on page 87.)

[255] C. Gordon and O. Macias, *Dark Matter and Pulsar Model Constraints from Galactic Center Fermi-LAT Gamma Ray Observations*, *Phys. Rev.* **D88** (2013) 083521, [1306.5725]. (Cited on page 87.)

[256] O. Macias and C. Gordon, *Contribution of cosmic rays interacting with molecular clouds to the Galactic Center gamma-ray excess*, *Phys. Rev.* **D89** (2014) 063515, [1312.6671]. (Cited on page 87.)

[257] K. N. Abazajian, N. Canac, S. Horiuchi and M. Kaplinghat, *Astrophysical and Dark Matter Interpretations of Extended Gamma-Ray Emission from the Galactic Center*, *Phys. Rev.* **D90** (2014) 023526, [1402.4090]. (Cited on page 87.)

[258] T. Daylan, D. P. Finkbeiner, D. Hooper, T. Linden, S. K. N. Portillo, N. L. Rodd et al., *The characterization of the gamma-ray signal from the central Milky Way: A case for annihilating dark matter*, *Phys. Dark Univ.* **12** (2016) 1–23, [1402.6703]. (Cited on page 87.)

[259] FERMI-LAT collaboration, M. Ajello et al., *Fermi-LAT Observations of High-Energy γ-Ray Emission Toward the Galactic Center*, *Astrophys. J.* **819** (2016) 44, [1511.02938]. (Cited on page 87.)

[260] F. Calore, I. Cholis and C. Weniger, *Background Model Systematics for the Fermi GeV Excess*, *JCAP* **1503** (2015) 038, [1409.0042]. (Cited on page 87.)

[261] F. Calore, I. Cholis, C. McCabe and C. Weniger, *A Tale of Tails: Dark Matter Interpretations of the Fermi GeV Excess in Light of Background Model Systematics*, *Phys. Rev.* **D91** (2015) 063003, [1411.4647]. (Cited on page 87.)

[262] F. Calore, I. Cholis and C. Weniger, *The GeV Excess Shining Through: Background Systematics for the Inner Galaxy Analysis*, in *5th International Fermi Symposium Nagoya, Japan, October 20-24, 2014*, 2015. 1502.02805. (Cited on page 87.)

[263] FERMI-LAT collaboration, T. A. Porter and S. Murgia, *Observations of High-Energy Gamma-Ray Emission Toward the Galactic Centre with the Fermi Large Area Telescope*, *PoS* **ICRC2015** (2016) 815, [1507.04688]. (Cited on page 87.)

[264] T. Linden, N. L. Rodd, B. R. Safdi and T. R. Slatyer, *High-energy tail of the Galactic Center gamma-ray excess*, *Phys. Rev.* **D94** (2016) 103013, [1604.01026]. (Cited on page 87.)

[265] LUX collaboration, D. S. Akerib et al., *First results from the LUX dark matter experiment at the Sanford Underground Research Facility*, *Phys. Rev. Lett.* **112** (2014) 091303, [1310.8214]. (Cited on page 87.)

[266] LUX collaboration, D. S. Akerib et al., *Results on the Spin-Dependent Scattering of Weakly Interacting Massive Particles on Nucleons from the Run 3 Data of the LUX Experiment*, *Phys. Rev. Lett.* **116** (2016) 161302, [1602.03489]. (Cited on page 87.)

[267] LUX collaboration, D. S. Akerib et al., *Results from a search for dark matter in the complete LUX exposure*, *Phys. Rev. Lett.* **118** (2017) 021303, [1608.07648]. (Cited on page 87.)

[268] PANDAX-II collaboration, A. Tan et al., *Dark Matter Results from First 98.7 Days of Data from the PandaX-II Experiment*, *Phys. Rev. Lett.* **117** (2016) 121303, [1607.07400]. (Cited on page 87.)

[269] XENON10 collaboration, J. Angle et al., *A search for light dark matter in XENON10 data*, *Phys. Rev. Lett.* **107** (2011) 051301, [1104.3088]. (Cited on page 87.)

[270] XENON100 collaboration, E. Aprile et al., *Dark Matter Results from 225 Live Days of XENON100 Data*, *Phys. Rev. Lett.* **109** (2012) 181301, [1207.5988]. (Cited on page 87.)

[271] XENON100 collaboration, E. Aprile et al., *Limits on spin-dependent WIMP-nucleon cross sections from 225 live days of XENON100 data*, *Phys. Rev. Lett.* **111** (2013) 021301, [1301.6620]. (Cited on page 87.)

[272] CDMS-II collaboration, Z. Ahmed et al., *Dark Matter Search Results from the CDMS II Experiment*, *Science* **327** (2010) 1619–1621, [0912.3592]. (Cited on page 87.)

[273] SUPERCDMS collaboration, R. Agnese et al., *Search for Low-Mass Weakly Interacting Massive Particles Using Voltage-Assisted Calorimetric Ionization Detection in the SuperCDMS Experiment*, *Phys. Rev. Lett.* **112** (2014) 041302, [1309.3259]. (Cited on page 87.)

[274] M. Felizardo et al., *Final Analysis and Results of the Phase II SIMPLE Dark Matter Search*, *Phys. Rev. Lett.* **108** (2012) 201302, [1106.3014]. (Cited on page 87.)

[275] S. C. Kim et al., *New Limits on Interactions between Weakly Interacting Massive Particles and Nucleons Obtained with CsI(Tl) Crystal Detectors*, *Phys. Rev. Lett.* **108** (2012) 181301, [1204.2646]. (Cited on page 87.)

[276] CRESST collaboration, G. Angloher et al., *Results on light dark matter particles with a low-threshold CRESST-II detector*, *Eur. Phys. J.* **C76** (2016) 25, [1509.01515]. (Cited on page 87.)

[277] CDMS, EDELWEISS collaboration, Z. Ahmed et al., *Combined Limits on WIMPs from the CDMS and EDELWEISS Experiments*, *Phys. Rev.* **D84** (2011) 011102, [1105.3377]. (Cited on page 87.)

[278] SUPERCDMS collaboration, R. Agnese et al., *Search for Low-Mass Weakly Interacting Massive Particles with SuperCDMS*, *Phys. Rev. Lett.* **112** (2014) 241302, [1402.7137]. (Cited on page 87.)

[279] SUPERCDMS collaboration, R. Agnese et al., *New Results from the Search for Low-Mass Weakly Interacting Massive Particles with the CDMS Low Ionization Threshold Experiment*, *Phys. Rev. Lett.* **116** (2016) 071301, [1509.02448]. (Cited on page 87.)

[280] FERMI-LAT collaboration, M. Ackermann et al., *Dark matter constraints from observations of 25 Milky Way satellite galaxies with the Fermi Large Area Telescope*, *Phys. Rev.* **D89** (2014) 042001, [1310.0828]. (Cited on page 87.)

[281] FERMI-LAT collaboration, M. Ackermann et al., *Searching for Dark Matter Annihilation from Milky Way Dwarf Spheroidal Galaxies with Six Years of Fermi Large Area Telescope Data*, *Phys. Rev. Lett.* **115** (2015) 231301, [1503.02641]. (Cited on pages 87 and 100.)

[282] G. A. Gómez-Vargas, M. A. Sánchez-Conde, J.-H. Huh, M. Peiró, F. Prada, A. Morselli et al., *Constraints on WIMP annihilation for contracted dark matterin the inner Galaxy with the Fermi-LAT*, *JCAP* **1310** (2013) 029, [1308.3515]. (Cited on page 87.)

[283] A. Bottino, N. Fornengo and S. Scopel, *Light relic neutralinos*, *Phys. Rev.* **D67** (2003) 063519, [hep-ph/0212379]. (Cited on pages 87, 88, and 89.)

[284] N. Fornengo, S. Scopel and A. Bottino, *Discussing direct search of dark matter particles in the Minimal Supersymmetric extension of the Standard Model with light neutralinos*, *Phys. Rev.* **D83** (2011) 015001, [1011.4743]. (Cited on pages 87, 88, and 89.)

[285] D. Albornoz Vasquez, G. Belanger, C. Boehm, A. Pukhov and J. Silk, *Can neutralinos in the MSSM and NMSSM scenarios still be light?*, *Phys. Rev.* **D82** (2010) 115027, [1009.4380]. (Cited on pages 87, 88, and 89.)

[286] A. Bottino, N. Fornengo and S. Scopel, *Phenomenology of light neutralinos in view of recent results at the CERN Large Hadron Collider*, *Phys. Rev.* **D85** (2012) 095013, [1112.5666]. (Cited on pages 87, 88, and 89.)

[287] D. Albornoz Vasquez, G. Belanger and C. Boehm, *Revisiting light neutralino scenarios in the MSSM*, *Phys. Rev.* **D84** (2011) 095015, [1108.1338]. (Cited on pages 87, 88, 89, and 98.)

[288] A. Arbey, M. Battaglia and F. Mahmoudi, *Light Neutralino Dark Matter in the pMSSM: Implications of LEP, LHC and Dark Matter Searches on SUSY Particle Spectra*, *Eur. Phys. J.* **C72** (2012) 2169, [1205.2557]. (Cited on pages 87, 88, and 89.)

[289] G. Belanger, S. Biswas, C. Boehm and B. Mukhopadhyaya, *Light Neutralino Dark Matter in the MSSM and Its Implication for LHC Searches for Staus*, *JHEP* **12** (2012) 076, [1206.5404]. (Cited on pages 87, 88, and 89.)

[290] A. Pierce, N. R. Shah and K. Freese, *Neutralino Dark Matter with Light Staus*, 1309.7351. (Cited on pages 87, 88, 89, 90, 98, and 99.)

[291] G. Bélanger, G. Drieu La Rochelle, B. Dumont, R. M. Godbole, S. Kraml and S. Kulkarni, *LHC constraints on light neutralino dark matter in the MSSM*, *Phys. Lett.* **B726** (2013) 773–780, [1308.3735]. (Cited on pages 87, 88, and 89.)

[292] K. Hagiwara, S. Mukhopadhyay and J. Nakamura, *10 GeV neutralino dark matter and light stau in the MSSM*, *Phys. Rev.* **D89** (2014) 015023, [1308.6738]. (Cited on pages 87 and 88.)

[293] L. Calibbi, J. M. Lindert, T. Ota and Y. Takanishi, *Cornering light Neutralino Dark Matter at the LHC*, *JHEP* **10** (2013) 132, [1307.4119]. (Cited on pages 87 and 88.)

[294] J. F. Gunion, D. Hooper and B. McElrath, *Light neutralino dark matter in the NMSSM*, *Phys. Rev.* **D73** (2006) 015011, [hep-ph/0509024]. (Cited on page 87.)

[295] D. Das and U. Ellwanger, *Light dark matter in the NMSSM: upper bounds on direct detection cross sections*, *JHEP* **09** (2010) 085, [1007.1151]. (Cited on page 87.)

[296] J.-J. Cao, K.-i. Hikasa, W. Wang, J. M. Yang, K.-i. Hikasa, W.-Y. Wang et al., *Light dark matter in NMSSM and implication on Higgs phenomenology*, *Phys. Lett.* **B703** (2011) 292–297, [1104.1754]. (Cited on page 87.)

[297] M. Carena, N. R. Shah and C. E. M. Wagner, *Light Dark Matter and the Electroweak Phase Transition in the NMSSM*, *Phys. Rev.* **D85** (2012) 036003, [1110.4378]. (Cited on page 87.)

[298] D. Albornoz Vasquez, G. Belanger and C. Boehm, *Astrophysical limits on light NMSSM neutralinos*, *Phys. Rev.* **D84** (2011) 095008, [1107.1614]. (Cited on page 87.)

[299] D. E. Lopez-Fogliani, *Light Higgs and neutralino dark matter in the NMSSM*, *J. Phys. Conf. Ser.* **384** (2012) 012014. (Cited on page 87.)

[300] J. Kozaczuk and S. Profumo, *Light NMSSM neutralino dark matter in the wake of CDMS II and a 126 GeV Higgs boson*, *Phys. Rev.* **D89** (2014) 095012, [1308.5705]. (Cited on page 87.)

[301] T. Han, Z. Liu and S. Su, *Light Neutralino Dark Matter: Direct/Indirect Detection and Collider Searches*, *JHEP* **08** (2014) 093, [1406.1181]. (Cited on page 87.)

[302] D. G. Cerdeño, J.-H. Huh, M. Peiró and O. Seto, *Very light right-handed sneutrino dark matter in the NMSSM*, *JCAP* **1111** (2011) 027, [1108.0978]. (Cited on page 87.)

[303] S. Scopel, N. Fornengo and A. Bottino, *Embedding the 125 GeV Higgs boson measured at the LHC in an effective MSSM: Possible implications for neutralino dark matter*, *Phys. Rev.* **D88** (2013) 023506, [1304.5353]. (Cited on page 88.)

[304] E. Boos, A. Djouadi, M. Muhlleitner and A. Vologdin, *The MSSM Higgs bosons in the intense coupling regime*, *Phys. Rev.* **D66** (2002) 055004, [hep-ph/0205160]. (Cited on page 89.)

[305] CMS collaboration, *Higgs to tau tau (MSSM) (HCP)*, CMS-PAS-HIG-12-050, 2012. (Cited on page 89.)

[306] ATLAS collaboration, G. Aad et al., *Search for charged Higgs bosons decaying via $H^+ \to \tau\nu$ in top quark pair events using pp collision data at $\sqrt{s} = 7$ TeV with the ATLAS detector*, *JHEP* **06** (2012) 039, [1204.2760]. (Cited on page 89.)

[307] J. Rosiek, *Complete set of Feynman rules for the MSSM: Erratum*, hep-ph/9511250. (Cited on page 90.)

[308] ALEPH, DELPHI, L3 AND OPAL collaboration, *Combined LEP Selectron/Smuon/Stau Results, 183-208 GeV*, note LEPSUSYWG/04-01.1, LEP2 SUSY Working Group, 2004. (Cited on page 90.)

[309] ATLAS collaboration, G. Aad et al., *Search for direct production of charginos, neutralinos and sleptons in final states with two leptons and missing transverse momentum in pp collisions at $\sqrt{s} = 8$ TeV with the ATLAS detector*, *JHEP* **05** (2014) 071, [1403.5294]. (Cited on pages 90 and 100.)

[310] CMS collaboration, V. Khachatryan et al., *Searches for electroweak production of charginos, neutralinos, and sleptons decaying to leptons and W, Z, and Higgs bosons in pp collisions at 8 TeV*, *Eur. Phys. J.* **C74** (2014) 3036, [1405.7570]. (Cited on pages 90 and 100.)

[311] ATLAS collaboration, M. Aaboud et al., *Search for new phenomena in final states with an energetic jet and large missing transverse momentum in pp collisions at $\sqrt{s} = 13$ TeV using the ATLAS detector*, *Phys. Rev.* **D94** (2016) 032005, [1604.07773]. (Cited on page 90.)

[312] ATLAS collaboration, *Search for squarks and gluinos in final states with jets and missing transverse momentum using 36 fb^{-1} of $\sqrt{s} = 13$ TeV pp collision data with the ATLAS detector*, ATLAS-CONF-2017-022, Apr, 2017. (Cited on page 90.)

[313] LHCB collaboration, R. Aaij et al., *Measurement of the $B_s^0 \to \mu^+\mu^-$ branching fraction and search for $B^0 \to \mu^+\mu^-$ decays at the LHCb experiment*, *Phys. Rev. Lett.* **111** (2013) 101805, [1307.5024]. (Cited on page 90.)

[314] CMS collaboration, S. Chatrchyan et al., *Measurement of the B(s) to mu+ mu- branching fraction and search for B0 to mu+ mu- with the CMS Experiment*, *Phys. Rev. Lett.* **111** (2013) 101804, [1307.5025]. (Cited on page 90.)

[315] M. Galanti, *Measurement of $\mathscr{B}(B_s^0 \to \mu^+\mu^-)$ and search for $B^0 \to \mu^+\mu^-$ with CMS*, Collider Cross Talk, 2013. (Cited on page 90.)

[316] M. Ciuchini, G. Degrassi, P. Gambino and G. F. Giudice, *Next-to-leading QCD corrections to B —> X(s) gamma in supersymmetry*, *Nucl. Phys.* **B534** (1998) 3–20, [hep-ph/9806308]. (Cited on page 90.)

[317] G. D'Ambrosio, G. F. Giudice, G. Isidori and A. Strumia, *Minimal flavor violation: An Effective field theory approach*, *Nucl. Phys.* **B645** (2002) 155–187, [hep-ph/0207036]. (Cited on page 90.)

[318] M. Misiak et al., *Estimate of $\mathscr{B}(\bar{B} \to X_s\gamma)$ at $O(\alpha_s^2)$*, *Phys. Rev. Lett.* **98** (2007) 022002, [hep-ph/0609232]. (Cited on page 90.)

[319] M. Misiak and M. Steinhauser, *NNLO QCD corrections to the anti-B —> X(s) gamma matrix elements using interpolation in m(c)*, *Nucl. Phys.* **B764** (2007) 62–82, [hep-ph/0609241]. (Cited on page 90.)

[320] HEAVY FLAVOR AVERAGING GROUP collaboration, Y. Amhis et al., *Averages of B-Hadron, C-Hadron, and tau-lepton properties as of early 2012*, 1207.1158. (Cited on page 90.)

[321] B. de Carlos, J. A. Casas and C. Muñoz, *Soft SUSY breaking terms in stringy scenarios: computation and phenomenological viability*, *Phys. Lett.* **B299** (1993) 234–246, [hep-ph/9211266]. (Cited on page 91.)

[322] A. Brignole, L. E. Ibañez and C. Muñoz, *Towards a theory of soft terms for the supersymmetric Standard Model*, *Nucl. Phys.* **B422** (1994) 125–171, [hep-ph/9308271]. (Cited on page 91.)

[323] H. Baer, M. A. Diaz, P. Quintana and X. Tata, *Impact of physical principles at very high-energy scales on the superparticle mass spectrum*, *JHEP* **04** (2000) 016, [hep-ph/0002245]. (Cited on page 91.)

[324] S. Khalil, T. Kobayashi and O. Vives, *EDM free supersymmetric CP violation with nonuniversal soft terms*, *Nucl. Phys.* **B580** (2000) 275–288, [hep-ph/0003086]. (Cited on page 91.)

[325] J. Ellis and K. A. Olive, *Revisiting the Higgs Mass and Dark Matter in the CMSSM*, *Eur. Phys. J.* **C72** (2012) 2005, [1202.3262]. (Cited on page 91.)

[326] H. Baer, V. Barger and A. Mustafayev, *Neutralino dark matter in mSUGRA/CMSSM with a 125 GeV light Higgs scalar*, *JHEP* **05** (2012) 091, [1202.4038]. (Cited on page 91.)

[327] D. G. Cerdeño and C. Muñoz, *Neutralino dark matter in supergravity theories with non-universal scalar and gaugino masses*, *JHEP* **10** (2004) 015, [hep-ph/0405057]. (Cited on page 91.)

[328] S. Baek, D. G. Cerdeño, Y. G. Kim, P. Ko and C. Muñoz, *Direct detection of neutralino dark matter in supergravity*, *JHEP* **06** (2005) 017, [hep-ph/0505019]. (Cited on page 92.)

[329] M. Carena, S. Gori, N. R. Shah and C. E. M. Wagner, *A 125 GeV SM-like Higgs in the MSSM and the $\gamma\gamma$ rate*, *JHEP* **03** (2012) 014, [1112.3336]. (Cited on page 92.)

[330] PLANCK collaboration, P. A. R. Ade et al., *Planck 2013 results. XVI. Cosmological parameters*, *Astron. Astrophys.* **571** (2014) A16, [1303.5076]. (Cited on page 93.)

[331] D. Barducci, G. Belanger, J. Bernon, F. Boudjema, J. Da Silva, S. Kraml et al., *Collider limits on new physics within micrOMEGAs*, 1606.03834. (Cited on pages 93 and 97.)

[332] P. Bechtle, O. Brein, S. Heinemeyer, G. Weiglein and K. E. Williams, *HiggsBounds: Confronting Arbitrary Higgs Sectors with Exclusion Bounds from LEP and the Tevatron*, *Comput. Phys. Commun.* **181** (2010) 138–167, [0811.4169]. (Cited on page 94.)

[333] P. Bechtle, O. Brein, S. Heinemeyer, O. Stål, T. Stefaniak, G. Weiglein et al., HiggsBounds – 4*: Improved Tests of Extended Higgs Sectors against Exclusion Bounds from LEP, the Tevatron and the LHC*, *Eur. Phys. J.* **C74** (2014) 2693, [1311.0055]. (Cited on page 94.)

[334] P. Bechtle, S. Heinemeyer, O. Stål, T. Stefaniak and G. Weiglein, *HiggsSignals: Confronting arbitrary Higgs sectors with measurements at the Tevatron and the LHC*, *Eur. Phys. J.* **C74** (2014) 2711, [1305.1933]. (Cited on page 94.)

[335] J. Bernon and B. Dumont, *Lilith: a tool for constraining new physics from Higgs measurements*, *Eur. Phys. J.* **C75** (2015) 440, [1502.04138]. (Cited on page 94.)

[336] S. Kraml, S. Kulkarni, U. Laa, A. Lessa, W. Magerl, D. Proschofsky-Spindler et al., *SModelS: a tool for interpreting simplified-model results from the LHC and its application to supersymmetry*, *Eur. Phys. J.* **C74** (2014) 2868, [1312.4175]. (Cited on page 94.)

[337] S. Kraml, S. Kulkarni, U. Laa, A. Lessa, V. Magerl, W. Magerl et al., *SModelS v1.0: a short user guide*, 1412.1745. (Cited on page 94.)

[338] L. Aparicio, D. G. Cerdeño and L. E. Ibañez, *A 119-125 GeV Higgs from a string derived slice of the CMSSM*, *JHEP* **04** (2012) 126, [1202.0822]. (Cited on page 94.)

[339] M. Davier, A. Hoecker, B. Malaescu and Z. Zhang, *Reevaluation of the Hadronic Contributions to the Muon g-2 and to alpha(MZ)*, *Eur. Phys. J.* **C71** (2011) 1515, [1010.4180]. (Cited on page 95.)

[340] M. Benayoun, P. David, L. DelBuono and F. Jegerlehner, *An Update of the HLS Estimate of the Muon g-2*, *Eur. Phys. J.* **C73** (2013) 2453, [1210.7184]. (Cited on page 95.)

[341] J. Billard, L. Strigari and E. Figueroa-Feliciano, *Implication of neutrino backgrounds on the reach of next generation dark matter direct detection experiments*, *Phys. Rev.* **D89** (2014) 023524, [1307.5458]. (Cited on pages 97 and 98.)

[342] G. Jungman, M. Kamionkowski and K. Griest, *Supersymmetric dark matter*, *Phys. Rept.* **267** (1996) 195–373, [hep-ph/9506380]. (Cited on pages 96 and 97.)

[343] G. Belanger, F. Boudjema, A. Pukhov and A. Semenov, *Dark matter direct detection rate in a generic model with micrOMEGAs 2.2*, *Comput. Phys. Commun.* **180** (2009) 747–767, [0803.2360]. (Cited on pages 96 and 97.)

[344] D. G. Cerdeño et al., *Complementarity of dark matter direct detection: the role of bolometric targets*, *JCAP* **1307** (2013) 028, [1304.1758]. (Cited on page 96.)

[345] J. R. Ellis, K. A. Olive and C. Savage, *Hadronic Uncertainties in the Elastic Scattering of Supersymmetric Dark Matter*, *Phys. Rev.* **D77** (2008) 065026, [0801.3656]. (Cited on page 97.)

[346] D. G. Cerdeño, M. Fornasa, J. H. Huh and M. Peiró, *Nuclear uncertainties in the spin-dependent structure functions for direct dark matter detection*, *Phys. Rev.* **D87** (2013) 023512, [1208.6426]. (Cited on page 97.)

[347] FERMI-LAT collaboration, E. Charles et al., *Sensitivity Projections for Dark Matter Searches with the Fermi Large Area Telescope*, *Phys. Rept.* **636** (2016) 1–46, [1605.02016]. (Cited on pages 99 and 100.)

[348] ATLAS collaboration, *Search for direct production of the top squark in the all-hadronic ttbar + etmiss final state in 21 fb-1 of p-pcollisions at sqrt(s)=8 TeV with the ATLAS detector*, ATLAS-CONF-2013-024, Mar, 2013. (Cited on page 100.)

[349] ATLAS collaboration, *Search for supersymmetry with two and three leptons and missing transverse momentum in the final state at* $\sqrt{s} = 13$ *TeV with the ATLAS detector*, ATLAS-CONF-2016-096, Sep, 2016. (Cited on page 100.)

[350] CMS collaboration, *Search for electroweak SUSY production in multilepton final states in pp collisions at sqrt(s)=13 TeV with 12.9/fb*, CMS-PAS-SUS-16-024, 2016. (Cited on page 100.)

[351] ATLAS collaboration, *Search for pair production of gluinos decaying via top or bottom squarks in events with b-jets and large missing transverse momentum in pp collisions at* $\sqrt{s} = 13$ *TeV with the ATLAS detector*, ATLAS-CONF-2016-052, Aug, 2016. (Cited on page 100.)

[352] CMS collaboration, *Search for supersymmetry in events with jets and missing transverse momentum in proton-proton collisions at 13 TeV*, CMS-PAS-SUS-16-014, 2016. (Cited on page 100.)

[353] CMS collaboration, *Search for direct top squark pair production in the fully hadronic final state in proton-proton collisions at sqrt(s) = 13 TeV corresponding to an integrated luminosity of 12.9/fb*, CMS-PAS-SUS-16-029, 2016. (Cited on page 100.)

[354] CMS collaboration, *Study of the Discovery Reach in Searches for Supersymmetry at CMS with 3000/fb*, CMS-PAS-FTR-13-014, 2013. (Cited on page 102.)

[355] ATLAS collaboration, *Prospects for benchmark Supersymmetry searches at the high luminosity LHC with the ATLAS Detector*, ATL-PHYS-PUB-2013-011, Sep, 2013. (Cited on page 102.)

[356] ATLAS collaboration, *Search for Supersymmetry at the high luminosity LHC with the ATLAS experiment*, ATL-PHYS-PUB-2014-010, Jul, 2014. (Cited on page 102.)

[357] L. Linssen, A. Miyamoto, M. Stanitzki and H. Weerts, *Physics and Detectors at CLIC: CLIC Conceptual Design Report*, 1202.5940. (Cited on page 102.)

[358] H. Baer, M. Berggren, J. List, M. M. Nojiri, M. Perelstein, A. Pierce et al., *Physics Case for the ILC Project: Perspective from Beyond the Standard Model*, in *Proceedings, Community Summer Study 2013: Snowmass on the Mississippi (CSS2013): Minneapolis, MN, USA, July 29-August 6, 2013*, 2013. 1307.5248. (Cited on page 102.)

[359] A. Arbey et al., *Physics at the e+ e- Linear Collider*, *Eur. Phys. J.* **C75** (2015) 371, [1504.01726]. (Cited on page 102.)

[360] CLICDP, CLIC collaboration, M. J. Boland et al., *Updated baseline for a staged Compact Linear Collider*, 1608.07537. (Cited on page 102.)

[361] T. Jelinski and J. Gluza, *Analytical two-loop soft mass terms of sfermions in Extended GMSB models*, *Phys. Lett.* **B751** (2015) 541–547, [1505.07443]. (Cited on page 154.)

Appendix A

Low-energy running coefficients at 2 loops

We compile in this appendix the coefficients of the functional forms that exactly fit the low-energy (LE) parameters in terms of the high-energy (HE) ones. Namely, for dimension-two parameters, say $\mathscr{M}^2$

$$\begin{aligned}\mathscr{M}^2(LE) &= c_{M_3^2}M_3^2 + c_{M_2^2}M_2^2 + c_{M_1^2}M_1^2 + c_{A_t^2}A_t^2 + c_{A_tM_3}A_tM_3 + c_{M_3M_2}M_3M_2 + \cdots \\ &\quad \cdots + c_{m_{H_u}^2}m_{H_u}^2 + c_{m_{Q_3}^2}m_{Q_3}^2 + c_{m_{U_3}^2}m_{U_3}^2 + \cdots ,\end{aligned} \tag{A.1}$$

where the r.h.s. parameters are understood at the HE scale. Similarly, for dimension-one parameters, say $\mathscr{M}$, we have

$$\mathscr{M}(LE) = c_{M_3}M_3 + c_{M_2}M_2 + c_{M_1}M_1 + c_{A_t}A_t + \cdots \tag{A.2}$$

In tables A.1–A.7 we list the values of the above $c-$coefficients for each LE soft term and for the LE $\mu-$parameter. These values correspond to the choice $M_{\rm HE} = M_X$, $M_{\rm LE} = 1$ TeV and $\tan\beta = 10$.

The dependence on $\tan\beta$ is very small provided $5 \lesssim \tan\beta \lesssim 30$. If $\tan\beta \lesssim 5$ the top Yukawa coupling becomes larger, affecting the entire set of RGEs. Likewise, for larger values of $\tan\beta \gtrsim 30$ the effect of the bottom and tau Yukawa couplings start to be non-negligible. Notice however $\tan\beta \lesssim 5$ implies extremely heavy stops, so that the radiative correction to the Higgs mass is large enough to reproduce $m_h \simeq 125$ GeV. This amounts to an enormous fine-tuning. Analogously, for $\tan\beta \gtrsim 30$ the tuning required to get large $\tan\beta$ usually raises the global fine-tuning up to unreasonable levels, see section 2.1.3.

The dependence of the $c-$coefficients on $M_{\rm LE}$ is logarithmic and can be well approximated by

$$c_i(M_{\rm LE}) \simeq c_i(1\ \ {\rm TeV}) + b_i \ln\frac{M_{\rm LE}}{1\ \ {\rm TeV}}\ . \tag{A.3}$$

The value of the b_i coefficients is also given in Tables A.1–A.7 .

Finally, the dependence of the $c-$coefficients (and $b_{M_3^2}$) on $M_{\rm HE}$ is shown in figures A.1, A.2, A.3, A.4 and A.5.

	$m^2_{H_u}(M_{\rm LE})$		$m^2_{H_d}(M_{\rm LE})$	
HE	c_i	b_i	c_i	b_i
M_3^2	-1.603	0.381	-0.056	0.016
$m^2_{H_u}$	0.631	0.019	0.025	-0.001
$m^2_{Q_3}$	-0.367	0.018	0.015	–
$m^2_{U_3}$	-0.290	0.017	-0.051	0.001
$A_t M_3$	0.285	-0.024	-0.002	0.001
M_2^2	0.203	0.006	0.410	-0.016
$M_2 M_3$	-0.134	0.021	-0.016	0.003
A_t^2	-0.109	-0.006	–	–
$A_t M_2$	0.068	–	-0.002	–
$m^2_{U_{1,2}}$	0.054	-0.001	-0.052	0.001
$m^2_{H_d}$	0.026	-0.001	0.961	0.001
$m^2_{E_{1,2}}$	-0.026	0.001	0.025	-0.001
$m^2_{E_3}$	-0.026	0.001	0.023	-0.001
$m^2_{L_{1,2}}$	0.025	-0.001	-0.027	0.001
$m^2_{L_3}$	0.025	-0.001	-0.029	0.001
$m^2_{Q_{1,2}}$	-0.025	–	0.024	–
$m^2_{D_{1,2}}$	-0.025	–	0.026	-0.001
$m^2_{D_3}$	-0.024	–	0.016	–
$M_1 M_3$	-0.020	0.002	-0.001	–
$A_t M_1$	0.012	–	–	–
M_1^2	0.006	0.002	0.033	–
$M_1 M_2$	-0.005	–	-0.001	–
$A_b M_3$	-0.002	–	0.022	-0.005
A_b^2	0.001	–	-0.009	0.001
$A_b M_2$	–	–	0.006	-0.001
A_τ^2	–	–	-0.003	–
$A_\tau M_2$	–	–	0.002	–
$A_b A_t$	–	–	0.001	–
$A_\tau M_1$	–	–	0.001	–

Table A.1: c_i and b_i coefficients for the Higgs boson squared soft masses derived for $\tan\beta = 10$, where '–' stands for HE parameters with $c_i, b_i < 0.001$. $M_{\rm LE}$ is set at 1 TeV. For further details see eqs. (A.1–A.3).

	$m^2_{Q_3}(M_{\rm LE})$		$m^2_{U_3}(M_{\rm LE})$		$m^2_{D_3}(M_{\rm LE})$	
HE	c_i	b_i	c_i	b_i	c_i	b_i
M_3^2	3.191	−0.563	2.754	−0.462	3.678	−0.672
$m^2_{Q_3}$	0.871	0.007	−0.192	0.013	−0.029	0.002
M_2^2	0.333	−0.008	−0.151	0.017	−0.010	0.002
$m^2_{H_u}$	−0.118	0.006	−0.189	0.011	−0.015	–
$m^2_{U_3}$	−0.095	0.005	0.706	0.011	0.032	–
M_2M_3	−0.084	0.015	−0.100	0.018	−0.026	0.007
A_tM_3	0.072	−0.003	0.159	−0.010	−0.010	0.003
A_t^2	−0.034	−0.002	−0.070	−0.004	0.001	–
A_tM_2	0.020	–	0.047	–	−0.001	–
$m^2_{Q_{1,2}}$	−0.017	0.001	0.030	–	−0.025	0.002
$m^2_{D_3}$	−0.015	0.001	0.032	–	0.973	0.001
$m^2_{U_{1,2}}$	0.014	–	−0.073	0.002	0.031	–
$m^2_{D_{1,2}}$	−0.012	0.001	0.032	–	−0.021	0.001
M_1M_3	−0.009	0.001	−0.018	0.002	−0.004	0.001
$m^2_{E_{1,2,3}}$	−0.009	–	0.034	−0.001	−0.017	–
$m^2_{L_{1,2,3}}$	0.008	–	−0.034	0.001	0.017	–
A_bM_3	0.006	−0.001	−0.001	–	0.014	−0.003
M_1^2	−0.006	0.001	0.041	0.001	0.014	–
$m^2_{H_d}$	0.005	–	−0.034	0.001	0.011	–
A_tM_1	0.004	–	0.007	–	–	–
A_b^2	−0.003	–	–	–	−0.006	0.001
M_1M_2	−0.002	–	−0.003	–	–	–
A_bM_2	0.002	–	–	–	0.004	−0.001
A_bA_t	0.001	–	–	–	0.001	–

Table A.2: As table A.1, for the squared soft masses of the third family squarks.

	$m^2_{Q_1}(M_{\rm LE})$		$m^2_{U_1}(M_{\rm LE})$		$m^2_{D_1}(M_{\rm LE})$	
HE	c_i	b_i	c_i	b_i	c_i	b_i
M_3^2	3.672	−0.674	3.702	−0.680	3.708	−0.681
$m^2_{Q_1}$	0.982	0.001	0.028	–	−0.025	0.002
M_2^2	0.403	−0.015	−0.005	0.001	−0.005	0.001
M_2M_3	−0.046	0.009	−0.022	0.006	−0.021	0.006
$m^2_{Q_2}$	−0.018	0.001	0.028	–	−0.025	0.002
$m^2_{Q_3}$	−0.017	0.001	0.029	–	−0.023	0.001
$m^2_{U_3}$	0.015	–	−0.072	0.002	0.032	–
$m^2_{U_1}$	0.014	–	0.927	0.002	0.031	–
$m^2_{U_2}$	0.014	–	−0.073	0.002	0.031	–
$m^2_{D_2}$	−0.012	0.001	0.031	–	−0.021	0.001
$m^2_{D_1}$	−0.012	0.001	0.031	–	0.979	0.001
$m^2_{D_3}$	−0.012	0.001	0.031	–	−0.021	0.001
$m^2_{E_{1,2,3}}$	−0.009	–	0.034	−0.001	−0.017	–
A_tM_3	−0.008	0.002	−0.008	0.002	−0.008	0.002
$m^2_{H_u}$	−0.008	–	0.035	−0.001	−0.016	–
$m^2_{H_d}$	0.008	–	−0.034	0.001	0.017	–
$m^2_{L_{1,2,3}}$	0.008	–	−0.034	0.001	0.017	–
M_1M_3	−0.003	0.001	−0.006	0.001	−0.004	0.001
M_1^2	0.003	–	0.059	−0.001	0.014	–
A_tM_2	−0.001	–	–	–	–	–
A_t^2	0.001	–	0.001	–	–	–

Table A.3: As table A.1, for the squared soft masses of the first family squarks. Second generation squarks are degenerated with the first family.

	$m^2_{L_3}(M_{\rm LE})$		$m^2_{E_3}(M_{\rm LE})$		$m^2_{L_1}(M_{\rm LE})$		$m^2_{E_1}(M_{\rm LE})$	
HE	c_i	b_i	c_i	b_i	c_i	b_i	c_i	b_i
$m^2_{L_3}$	0.971	0.001	0.045	−0.001	−0.027	0.001	0.051	−0.001
M_2^2	0.416	−0.017	−0.004	–	0.418	−0.018	–	–
$m^2_{U_{1,2}}$	−0.052	0.001	0.104	−0.002	−0.052	0.001	0.104	−0.002
$m^2_{U_3}$	−0.051	0.001	0.103	−0.002	−0.051	0.001	0.103	−0.002
M_1^2	0.034	–	0.136	−0.002	0.034	–	0.137	−0.002
$m^2_{H_d}$	−0.029	0.001	0.045	−0.001	−0.026	0.001	0.051	−0.001
$m^2_{L_1}$	−0.027	0.001	0.051	−0.001	0.973	0.001	0.051	−0.001
$m^2_{L_2}$	−0.027	0.001	0.051	−0.001	−0.027	0.001	0.051	−0.001
$m^2_{D_{1,2,3}}$	0.026	−0.001	−0.052	0.001	0.026	−0.001	−0.052	0.001
$m^2_{E_1}$	0.025	−0.001	−0.052	0.001	0.025	−0.001	0.948	0.001
$m^2_{E_2}$	0.025	−0.001	−0.052	0.001	0.025	−0.001	−0.052	0.001
$m^2_{H_u}$	0.025	–	−0.051	0.001	0.025	–	−0.051	0.001
$m^2_{Q_3}$	0.024	–	−0.052	0.001	0.024	–	−0.052	0.001
$m^2_{Q_{1,2}}$	0.024	–	−0.053	0.001	0.024	–	−0.053	0.001
$m^2_{E_3}$	0.023	−0.001	0.942	0.001	0.025	−0.001	−0.052	0.001
M_2M_3	−0.009	0.001	0.001	–	−0.009	0.001	0.001	–
M_3^2	−0.007	0.001	−0.001	–	−0.007	0.001	−0.001	–
A_τ^2	−0.003	–	−0.006	–	–	–	–	–
$A_\tau M_2$	0.002	–	0.003	–	–	–	–	–
$A_t M_2$	−0.001	–	–	–	−0.001	–	–	–
M_1M_2	−0.001	–	−0.001	–	−0.001	–	–	–
$A_\tau M_1$	0.001	–	0.001	–	–	–	–	–
M_1M_3	–	–	−0.002	–	–	–	−0.002	–
$A_t M_3$	–	–	−0.001	–	–	–	−0.001	–

Table A.4: As table A.1, for the squared soft masses of the third and first family sleptons. Second generation sleptons are degenerated with the first family.

	$M_3(M_{\rm LE})$		$M_2(M_{\rm LE})$		$M_1(M_{\rm LE})$	
HE	c_i	b_i	c_i	b_i	c_i	b_i
M_3	2.224	−0.160	−0.024	0.004	−0.009	0.001
M_2	−0.009	0.001	0.806	0.011	−0.001	–
A_t	−0.003	–	−0.002	–	−0.001	–
M_1	−0.001	–	–	–	0.431	0.012

Table A.5: As table A.1, for the gaugino masses.

	$A_t(M_{\rm LE})$		$A_b(M_{\rm LE})$		$A_\tau(M_{\rm LE})$	
HE	c_i	b_i	c_i	b_i	c_i	b_i
M_3	-1.438	0.148	-2.129	0.277	0.017	-0.003
A_t	0.325	0.035	-0.106	0.005	0.001	–
M_2	-0.237	-0.005	-0.413	0.016	-0.460	0.022
M_1	-0.032	-0.002	-0.030	–	-0.145	0.003
A_b	-0.002	–	0.981	0.002	-0.010	0.001
A_τ	–	–	-0.003	–	0.988	–

Table A.6: As table A.1, for the trilinear scalar couplings.

	$\mu(M_{\rm LE})$	
HE	c_i	b_i
μ	1.002	0.013

	$B\mu(M_{\rm LE})$	
HE	c_i	b_i
$B\mu$	1.002	0.013
$M_3\mu$	0.456	-0.080
$M_2\mu$	-0.354	0.004
$A_t\mu$	-0.343	0.013
$M_1\mu$	-0.030	-0.001
$A_b\mu$	-0.009	0.001
$A_\tau\mu$	-0.003	–

Table A.7: Left, c_i and b_i coefficients for the $\mu-$parameter. Right, c_i and b_i coefficients for $B\mu$.

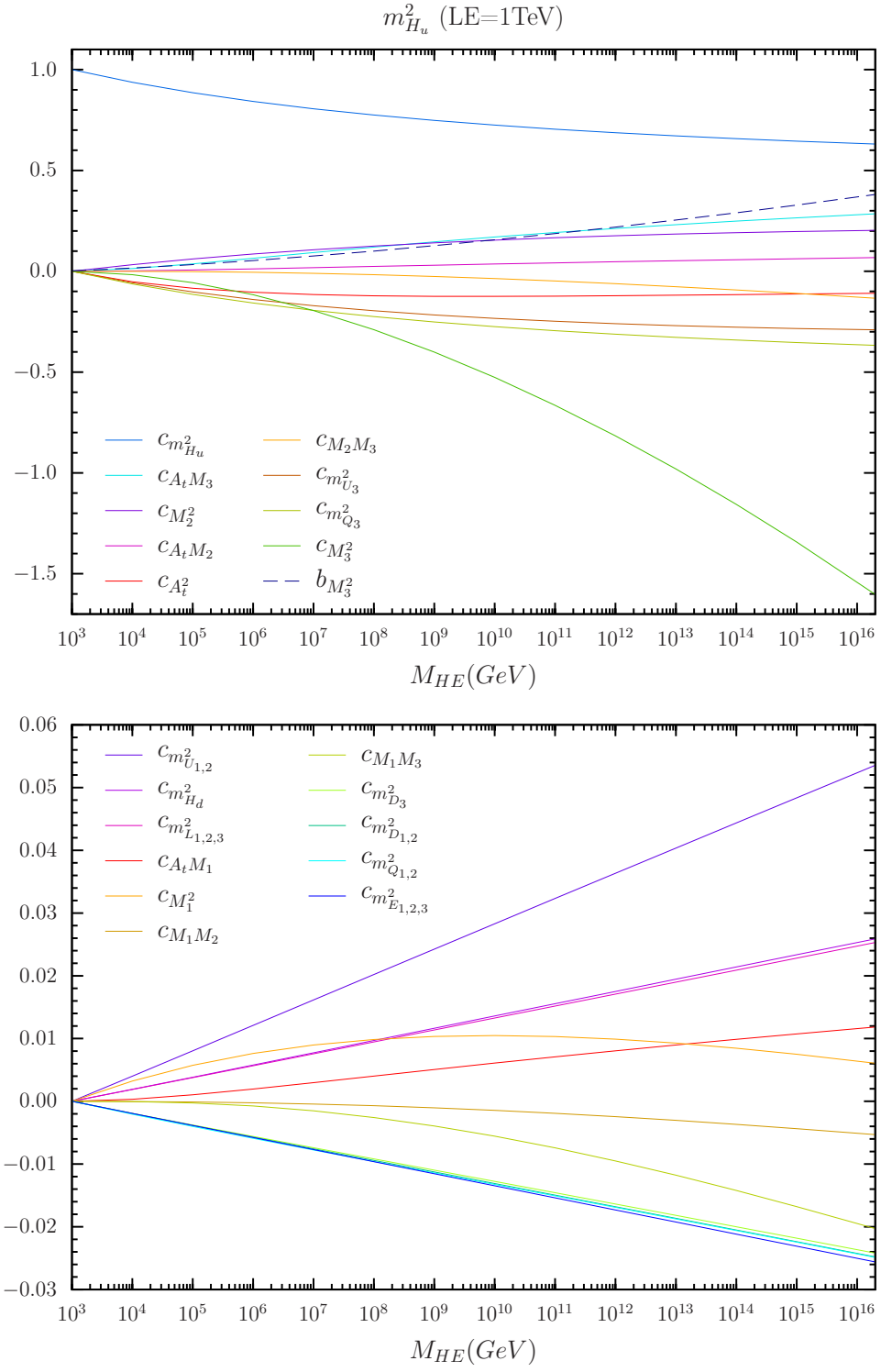

Figure A.1: $m^2_{H_u}(M_{\rm LE})$ coefficients dependence on the HE scale, for $M_{\rm LE} = 1\,\text{TeV}$ and $\tan\beta = 10$. For further details, see eqs. (A.1–A.3).

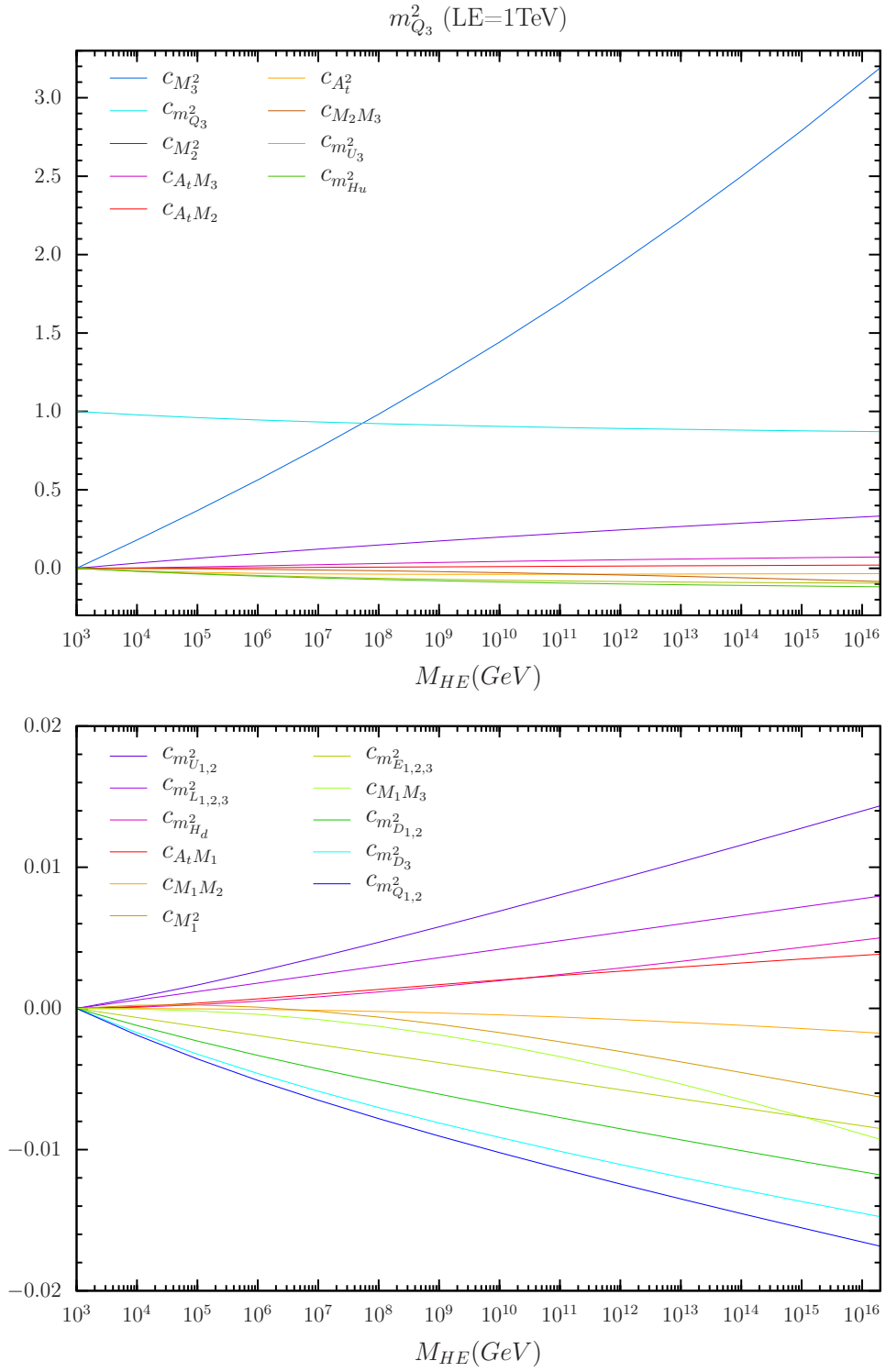

Figure A.2: As Figure A.1, for $m^2_{Q_3}(M_{\rm LE})$.

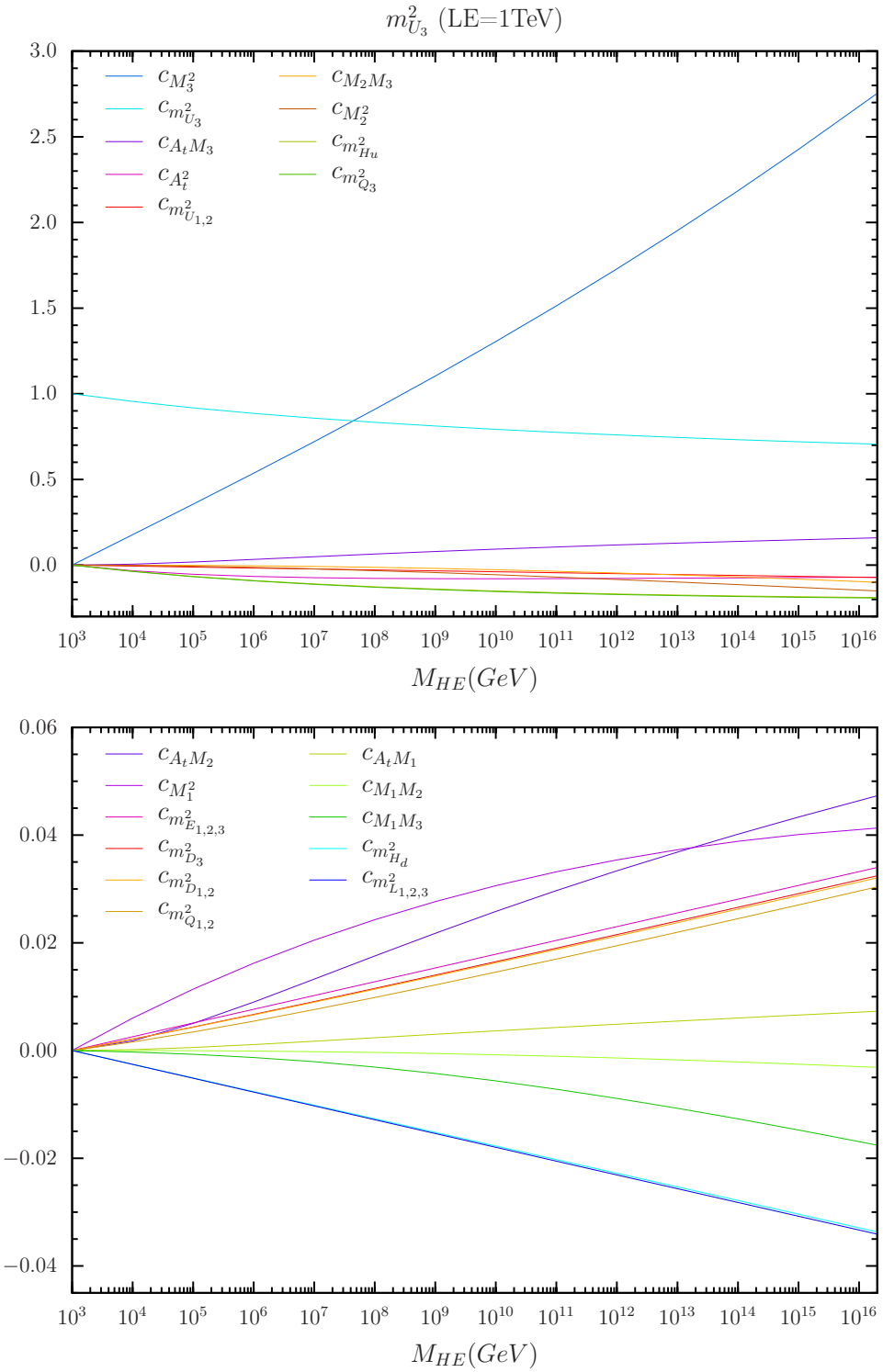

Figure A.3: As Figure A.1, for $m^2_{U_3}(M_{\rm LE})$.

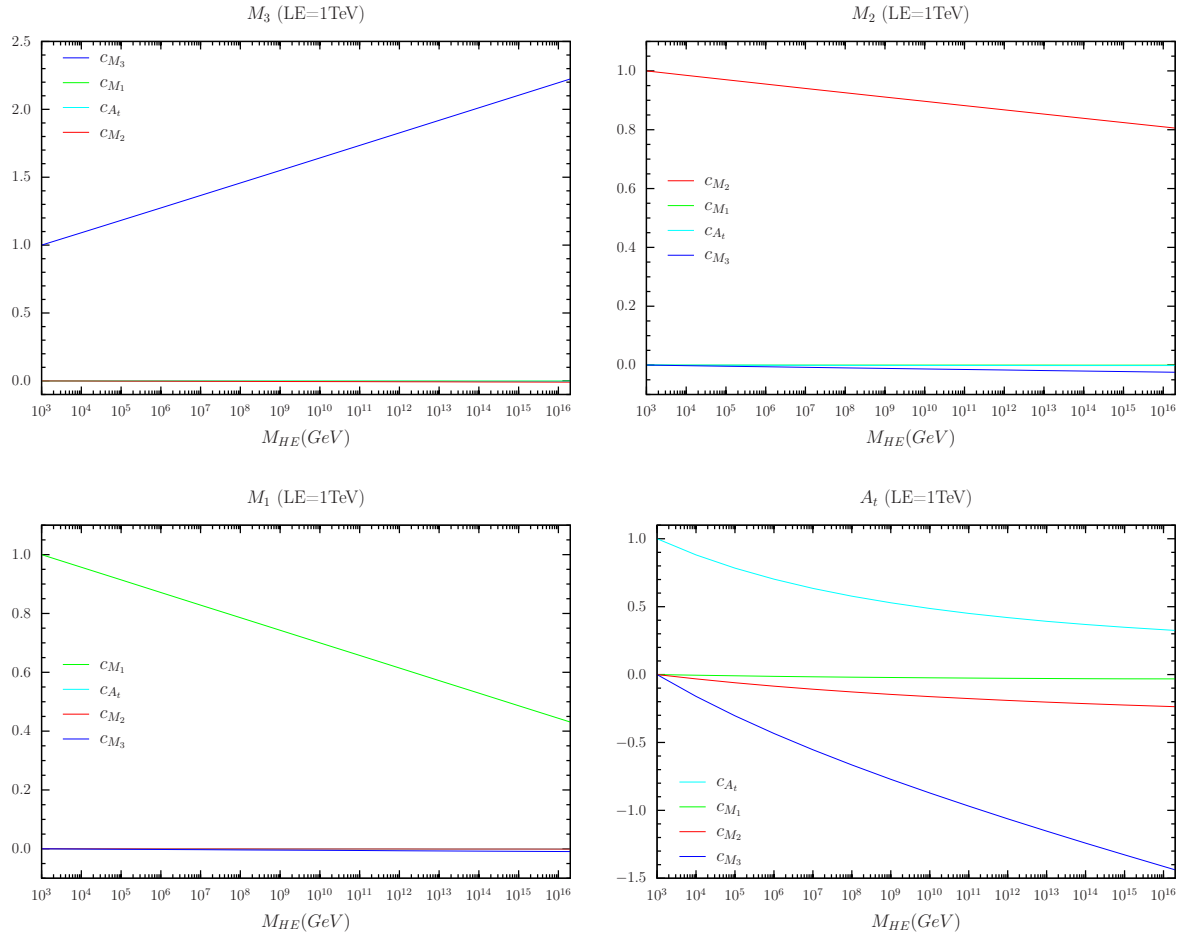

Figure A.4: Left to right, top to bottom: As Figure. A.1, for $M_3(M_{\rm LE})$, $M_2(M_{\rm LE})$, $M_1(M_{\rm LE})$ and $A_t(M_{\rm LE})$.

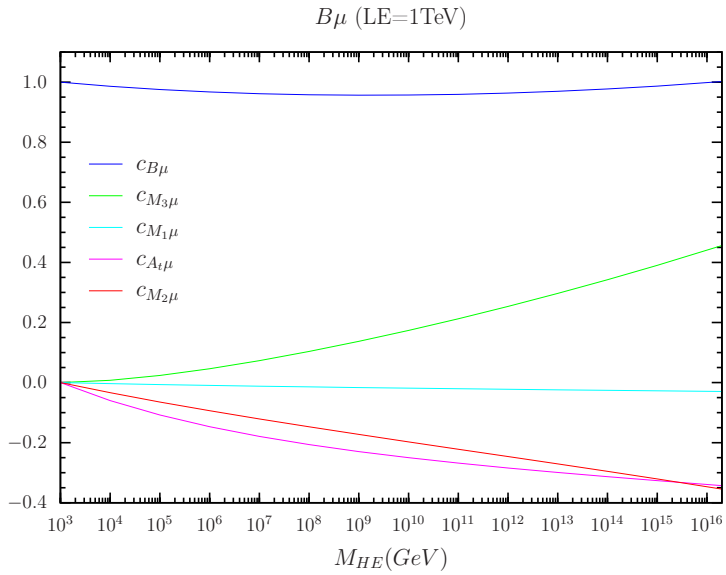

Figure A.5: As Figure A.1, for $B\mu$.

Appendix B

GMSB high-energy spectrum

B.1 Minimal GMSB

In the minimal GMSB, gauginos acquire their mass at one loop. Computing the corresponding Feynman diagrams, the gaugino masses are [189–191]:

$$M_i = \frac{\alpha_i}{4\pi}\Lambda N_5 g(x) \qquad (i=1,2,3)\ , \tag{B.1}$$

where $\alpha_i = g_i^2/4\pi$ are the usual gauge couplings of $SU(3)_c \times SU(2) \times U(1)_Y$ at the messenger scale, x has been defined in eq. (3.4), and

$$g(x) = \frac{1}{x^2}\left[(1+x)\log(1+x)+(1-x)\log(1-x)\right]\ , \tag{B.2}$$

$$g(x) \simeq 1+\frac{x^2}{6}+\frac{x^4}{15}+\frac{x^6}{28}+\mathscr{O}(x^8)\ . \tag{B.3}$$

On the other hand, the scalar masses arise from two-loop diagrams. Calculation of these graphs gives:

$$m_{\tilde{f}}^2 = 2\Lambda^2 N_5 \sum_{i=1}^{3} C_i^{\tilde{f}} \left(\frac{\alpha_i}{4\pi}\right)^2 f(x)\ , \tag{B.4}$$

where C_i are the corresponding quadratic Casimir operators [$C_N = (N^2-1)/(2N)$ for $SU(N)$] and

$$f(x) = \frac{1+x}{x^2}\left[\log(1+x) - 2\mathrm{Li}_2\left(\frac{x}{1+x}\right)+\frac{1}{2}\mathrm{Li}_2\left(\frac{2x}{1+x}\right)\right] + (x\to -x)\ , \tag{B.5}$$

$$f(x) \simeq 1+\frac{x^2}{36}-\frac{11x^4}{450}-\frac{319x^6}{11760}+\mathscr{O}(x^8)\ , \tag{B.6}$$

where Li_2 is the dilogarithm (Spence's function).

B.2 Models with radiatively generated A-terms

In these models, the presence of cubic operators in the superpotential, involving MSSM and messenger superfields, leads to trilinear couplings generated at one-loop level [197, 199]. For the Evans and Shih model of eq. (3.11) the stop trilinear coupling reads

$$A_t = -\frac{5\Lambda}{16\pi^2}\lambda^2 j(x), \tag{B.7}$$

where

$$j(x) = \frac{1}{2x}\log\left(\frac{1+x}{1-x}\right), \tag{B.8}$$

$$j(x) \simeq 1+\frac{x^2}{3}+\frac{x^4}{5}+\frac{x^6}{7}+\mathcal{O}(x^8). \tag{B.9}$$

In addition, the following contributions to the scalar soft masses appear at one loop:

$$\delta m^2_{U_3} = -\frac{\Lambda^2}{48\pi^2}\lambda^2 x^2 h(x), \tag{B.10}$$

$$\delta m^2_{H_u} = -\frac{\Lambda^2}{32\pi^2}\lambda^2 x^2 h(x), \tag{B.11}$$

where

$$h(x) = \frac{3}{x^4}\left[(x-2)\log(1-x)-(2+x)\log(1+x)\right], \tag{B.12}$$

$$h(x) \simeq 1+\frac{4x^2}{5}+\frac{9x^4}{14}+\frac{8x^6}{15}+\mathcal{O}(x^8). \tag{B.13}$$

There are also two-loop contributions to the soft scalar masses that read

$$\delta m^2_{Q_3} = -\frac{5\Lambda^2}{256\pi^4}\lambda^2 y_t^2 f_{h,2}(x), \tag{B.14}$$

$$\delta m^2_{U_3} = \frac{\Lambda^2}{128\pi^4}\lambda^2\left[6\lambda^2+2y_t^2-\frac{13}{15}g_1^2-3g_2^2-\frac{16}{3}g_3^2\right]f_{h,2}(x), \tag{B.15}$$

$$\delta m^2_{H_u} = \frac{\Lambda^2}{128\pi^4}\lambda^2\left[9\lambda^2+3y_t^2-\frac{13}{10}g_1^2-\frac{9}{2}g_2^2-8g_3^2\right]f_{h,2}(x), \tag{B.16}$$

where y_t is the top Yukawa coupling, evaluated at $M_{\rm mess}$, and $f_{h,2}(x)$ can be found in ref. [361].

Regarding the CPZ model of eq. (3.12), the trilinear couplings for the stop and the sbottom read

$$A_t = -\frac{3\Lambda}{16\pi^2}|\lambda_U|^2 y_t j(x), \tag{B.17}$$

$$A_b = -\frac{\Lambda}{16\pi^2}|\lambda_U|^2 y_b j(x), \tag{B.18}$$

where y_t and y_b are the top and bottom Yukawa couplings, respectively, evaluated at $M_{\rm mess}$.

There are also one-loop contributions to the sfermions masses, given by

$$\delta m^2_{Q_3} = -\frac{\Lambda^2}{96\pi^2}|\lambda_U|^2 x^2 h(x) \,, \tag{B.19}$$

$$\delta m^2_{U_3} = -\frac{\Lambda^2}{48\pi^2}|\lambda_U|^2 x^2 h(x) \,, \tag{B.20}$$

Finally, the two-loop contributions to the soft scalar masses for $x \ll 1$ read

$$\delta m^2_{Q_3} = \frac{\Lambda^2}{256\pi^4}|\lambda_U|^2 \left[6|\lambda_U|^2 + 6y_t^2 - \frac{13}{15}g_1^2 - 3g_2^2 - \frac{16}{3}g_3^2\right] \,, \tag{B.21}$$

$$\delta m^2_{U_3} = \frac{\Lambda^2}{128\pi^4}|\lambda_U|^2 \left[6|\lambda_U|^2 + 6y_t^2 + y_b^2 - \frac{13}{15}g_1^2 - 3g_2^2 - \frac{16}{3}g_3^2\right] \,, \tag{B.22}$$

$$\delta m^2_{D_3} = -\frac{\Lambda^2}{128\pi^4}|\lambda_U|^2 y_b^2 \,, \tag{B.23}$$

$$\delta m^2_{H_u} = -\frac{9\Lambda^2}{256\pi^4}|\lambda_U|^2 y_t^2 \,, \tag{B.24}$$

$$\delta m^2_{H_d} = -\frac{3\Lambda^2}{256\pi^4}|\lambda_U|^2 y_b^2 \,. \tag{B.25}$$